THE DEVELOPMENT AND INVESTIGATION OF A NOVEL PULSATILE HEART ASSIST DEVICE

AHMAD ZAHRAN BIN MD KHUDZARI

Doctor of Philosophy

ASTON UNIVERSITY

SEPTEMBER 2012

ASTON UNIVERSITY

THE DEVELOPMENT AND INVESTIGATION OF A NOVEL HEART ASSIST DEVICE

AHMAD ZAHRAN BIN MD KHUDZARI

Doctor of Philosophy

2012

SUMMARY

Cardiovascular diseases (CVD) contributed to almost 30% of worldwide mortality; with heart failure being one class of CVD. One popular and widely available treatment for heart failure is the intra-aortic balloon pump (IABP). This heart assist device is used in counterpulsation to improve myocardial function by increasing coronary perfusion, and decreasing aortic end-diastolic pressure (i.e. the resistance to blood ejection from the heart). However, this device can only be used acutely, and patients are bedridden. The subject of this research is a novel heart assist treatment called the Chronic Intermittent Mechanical Support (CIMS) which was conceived to offer advantages of the IABP device chronically, whilst overcoming its disadvantages. The CIMS device comprises an implantable balloon pump, a percutaneous drive line, and a wearable driver console. The research here aims to determine the haemodynamic effect of balloon pump activation under *in vitro* conditions.

A human mock circulatory loop (MCL) with systemic and coronary perfusion was constructed, capable of simulating various degrees of heart failure. Two prototypes of the CIMS balloon pump were made with varying stiffness. Several experimental factors (balloon inflation/deflation timing, Helium gas volume, arterial compliance, balloon pump stiffness and heart valve type) form the factorial design experiments. A simple modification to the MCL allowed flow visualisation experiments using video recording. Suitable statistical tests were used to analyse the data obtained from all experiments.

Balloon inflation and deflation in the ascending aorta of the MCL yielded favourable results. The sudden balloon deflation caused the heart valve to open earlier, thus causing longer valve opening duration in a cardiac cycle. It was also found that pressure augmentation in diastole was significantly correlated with increased cardiac output and coronary flowrate. With an optimum combination (low arterial compliance and low balloon pump stiffness), systemic and coronary perfusions were increased by 18% and 21% respectively, while the aortic end-diastolic pressure (forward flow resistance) decreased by 17%. Consequently, the ratio of oxygen supply and demand to myocardium (endocardial viability ratio, EVR) increased between 33% and 75%. The increase was mostly attributed to diastolic augmentation rather than systolic unloading.

Dedication

"Read! In the name of your Lord, Who has created (all that exists)" (Holy Quran, 96.1)

I dedicate this thesis and the journey to arrive to this point to the Allah Almighty, and also to my parents for their continuous love, support and prayer.

Acknowledgement

I would like to thank my main supervisor, Prof. Geoff Tansley, for his guidance, advice and support throughout this journey. I have gained quite a considerable knowledge, and hopefully I will be able to surpass his expertise and wisdom in coming years. I would also like to convey my gratitude to DR. David Richens of Nottingham City Hospital, for always clearing my doubts with regards to cardiovascular physiology. Also to all the support staff at Aston University especially those in the Model Design Lab, and the Mechanical Engineering Workshop.

My thanks are also extended to my colleagues and friends at MB171 especially Ashwatha Rajamani, Omkar Joshi, Joel Shubash, Joe Davies, Syed Shah Rukh, Tom Drew, Clara Xu, Laura Leslie, and others for the memorable learning experience that I gained in the UK.

My gratitude is reserved to Government of Malaysia, Ministry of Higher Education of Malaysia, and my employer, Universiti Teknologi Malaysia, without whom, this once in a lifetime opportunity would not have materialised.

To all my friends here at Birmingham, especially those in the Malaysian Community in Birmingham group, I genuinely appreciate the bond between us. May Allah's mercy and blessing is bestowed upon all of us. Also, my friends from Malaysia studying here in the UK : Sahana Harun, Eti F Zain, Nabil Ahmad Salimi, Fina Roslan, Kina Rinski, Hana Shamsuddin, Izwan Masngut, Salman Hassan, Syafiq Shah, and Syed Umar; I thank all of you for the friendship.

To my siblings, nieces and nephews, who has been the constant source of support and motivation for me to finish this endeavour, please receive this unreserved thank you.

I would also like to extend my heartiest gratitude and love to my dearest wife, Noradilah Maarof, who has always stayed by my side, and be the port to where I sail back after every storm in the sea. This thesis is one small tribute that I can give.

Table of Contents

List of Figures

A.Z.M. Khudzari

List of Tables

Notation

$\bar{x}$	Mean of the first variable	
$\bar{y}$	Mean of the second variable	
ΔP	Pressure difference	mmHg
$\Delta Proot$	Pressure difference at aortic root	mmHg
ΔV	Volume difference	mL
BSA	Body surface area	m^2
C	Compliance	mmHg/mL
CO	Cardiac output	L/min
cov_{xy}	Covariance of x and y	
EF	Ejection fraction	
h	height	cm
H	height	m^2
HR	Heart rate	beats/min
L	Length of vessel	m
$LVVed$	Left Ventricular Volume at end of diastole	mL
MAP	Mean arterial pressure	mmHg
P_{dia}	Aortic end-diastolic pressure	mmHg
PP	Pulse pressure	mmHg
P_{sys}	Aortic systolic pressure	mmHg
Q	Blood flowrate	L/min
$QcorMean$	Left coronary artery mean flowrate	mL/min
r	Radius	μm
R	Resistance	mmHg/mL/min or dynes.s/cm^5
r	Coefficient of correlation	
R^2	Coefficient of determination	
r_s	Spearman's coefficient of correlation	
S	Myocardium wall stress	dyne/cm^2
SV	Stroke volume	mL
s_x	Standard deviation of the first variable	
s_y	Standard deviation of the second variable	
W	Weight	kg
η	Fluid viscosity	cP
TTI	Tension Time Index	mmHg.s
$DPTI$	Diastolic Pressure Time Index	mmgh.s

Acronyms

ACC/AHA	American College of Cardiology and American Heart Association
AoEDP	Aortic End Diastolic Pressure
AoP	Aortic Pressure
AoPmax	Aortic Systolic Pressure
BSA	Body Surface Area
BTR	Bridge-to-Recovery
BTT	Bridge-to-Transplantation
CABG	Coronary Artery Bypass Graft
CAD	Coronary Artery Disease
CB	Compliant Body
CHF	Congestive Heart Failure
CI	Cardiac Index
CIMS	Chronic Intermittent Mechanical Support
CO	Cardiac Output
DOE	Design of Experiment
dP	Pressure difference (PADA – AoPmax)
DPTI	Diastolic Pressure Time Index
DT	Destination Theraphy
EABP	Extra Aortic Balloon Pump
EC	European Commission
ECG	Electrocardiography
EDPVR	End-Diastolic Pressure-Volume Relationship
EF	Ejection Fraction
EU	European Union
EVR	Endocardial Variability Ratio
EVR	Endocardial Viability Ratio
GLP	Good Laboratory Practice
HF	Heart Failure

HR	Heart Rate
IABP	Intra Aortic Balloon Pump
ID	Inner Diameter
IDCM	Idiopathic Dilated Cardiomyopathy
IPBP	Internal Pressure Balloon Pump
LA	Left Atrium
LAP	Left Atrial Pressure
LCA	Left Coronary Artery
LV	Left Ventricle
LVAD	Left Ventricular Assist Device
LVEDD	Left Ventricular End-Diastolic Diameter
LVEDV	Left Ventricular End Diastolic Volume
LVEF	Left Ventricular Ejection Fraction
LVESV	Left Ventricular End Systolic Volume
LVP	Left Ventricular Pressure
MCL	Mock Circulatory Loop
MI	Myocardial infarction
NGO	Non-governmental Organisation
NHLBI	National Heart, Lung, and Blood Institute
NYHA	New York Heart Association
OC	Outer Case
OD	Outer Diameter
PACD	Peri Aortic Counterpulsation Device
PADA	Peak Aortic Diastolic Augmentation
PP	Pulse Pressure
QcorMean	Left Coronary Artery Mean Flowrate
RBP	Rotary blood pump
SB	Straight Body
SV	Stroke Volume
SVR	Systemic Vascular Resistance
TTI	Tension Time Index

UK	United Kingdom
USA	United States of America
VAD	Ventricular Assist Device
WIA	Wave Intensity Analysis

Chapter 1 Introduction

This chapter introduces briefly the concept of the Chronic Intermittent Mechanical Support (CIMS) system. The CIMS system is intended as a device to treat heart failure, primarily for a specific patient cohort suffering from heart failure secondary to idiopathic dilated cardiomyopathy (IDCM), or ischaemic heart failure. The CIMS device may also be used for those with other causes of heart failure as a chronic support device for the patient to recover or as supporting device whilst awaiting heart donation.

This thesis discusses the development and testing of an *in vitro* model of the CIMS balloon pump. In the CIMS system, the balloon pump is implanted at the ascending aorta while connected to the driver console. Experimental work on a human mock circulatory loop (MCL) was carried out to discern the effect of various experimental factors on CIMS balloon pump efficacy whilst implanted in the ascending aortic of the MCL.

1.1   Heart Assist Device for Heart Failure Treatment

The heart is a vital organ; the transport of oxygen and nutrients to every cell in human body is carried out by way of blood circulation network consisting of systemic (from the heart to body and back to the heart) and pulmonary (from the heart to the lungs and back to the heart) circulation as illustrated in Figure 1-1. As a result of a number of physiological complications the heart may degrade to a state where its main function cannot be delivered satisfactorily. Without corrective measures being taken, the heart will deteriorate to congestive heart failure condition, and may lead to certain mortality within a short time frame.

The treatment of congestive heart failure, more simply known as heart failure (HF), depends on the severity of the disease. Patients suffering from heart failure exhibit symptoms such as shortness of breath, fatigue, and fluid retention either in the lungs or at extremities (i.e. hands/ankles). Early stage HF, once diagnosed, may be treated with medical intervention including drugs, overall lifestyle adjustment focusing on better stress management, food intake adjustment and physical exercise. Though some people may recover or at least remain stable, for some, the disease progresses further, restricting everyday activity and requiring more comprehensive treatment. Treatment usually begins with pharmacological drug treatment, where

the drug dosage depends on the patient condition; with increasing severity, drug dosage may be increased, or necessitate stronger pharmacological products. In some cases, corrective surgery is performed. For a patient refractory to drug treatment, heart transplant is the definitive therapy ('the gold standard' treatment). However, access to transplantation is limited, and some patients are contraindicated for heart transplantation; an alternative is mechanical assistance for their failing heart.
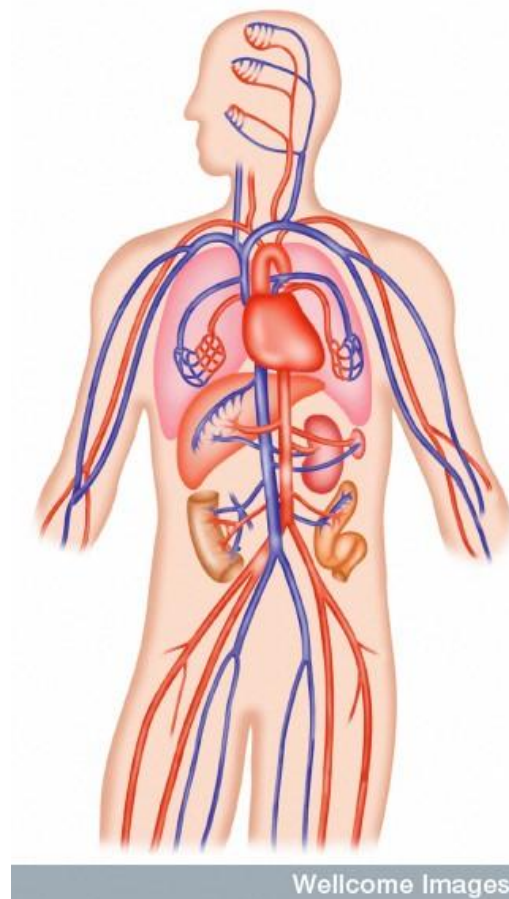
Figure 1-1: Blood circulation in the human body, the red vessel is the arteries, while the blue blood vessels are the veins. (With kind permission from Wellcome Library, London)

Heart failure can be treated with mechanical heart assist devices. A review of existing mechanical heart assist device and their classification is presented in Chapter 2.

Mechanical heart assist device can be categorised by 1) how the device is positioned in the blood circulation (either series or parallel), 2) the blood pump type (rotary/displacement) and 3) duration used (short/acute, medium, or long term). The parallel type includes pusher plate type (synchronous activation) and rotary blood pumps (typically constant speed). An example of a parallel and long term pusher plate type heart assist device is illustrated in Figure 1-2; the pusher

type balloon pump is attached to the heart's apex, and the outflow conduit anastomosed to the ascending aorta.
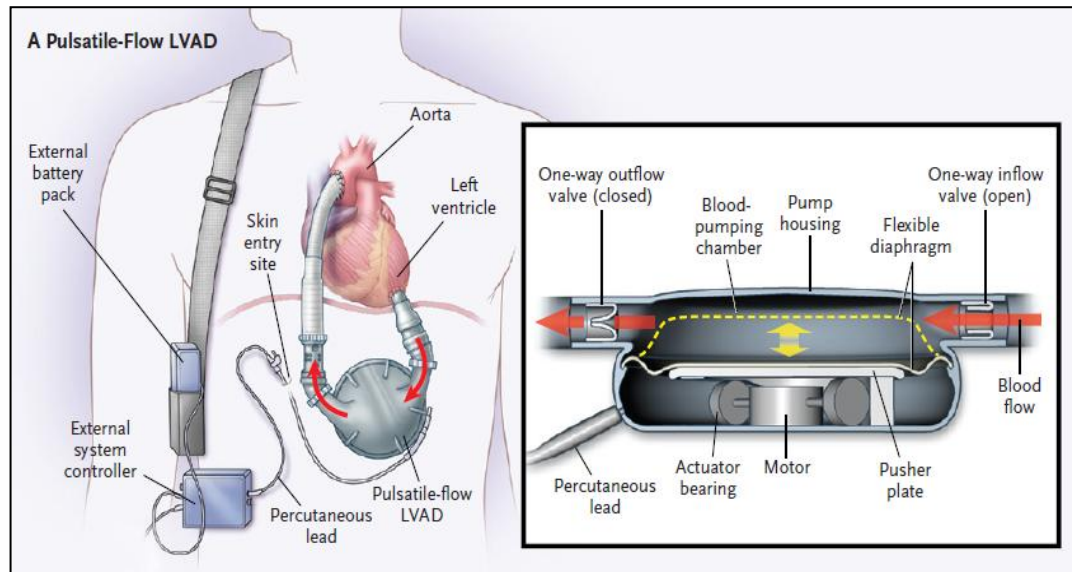
Figure 1-2: An example of a series type balloon pump. The blood is sucked into the blood pump chamber from the apex of the left ventricle and pushed out into the ascending aorta via an outflow conduit anastomosed to the ascending aorta. Reproduced with permission from (Slaughter et al., 2009) Copyright Massachusetts Medical Society

The series type devices are always counterpulsation (explained further below), and mounted in the aorta. A well known example is the intra-aortic balloon pump (IABP), illustrated in Figure 1-3, which is widely used and understood by medical practitioners; however, the IABP is an acute assist device. Another example is the chronic support extra-aortic balloon pump (EABP), a cuff-type balloon pump that tries to capitalize on counterpulsation, however, the EABP type still faces some problems in counterpulsation.

Counterpulsation technique, employed by the IABP, works by inflating the balloon at the descending aorta in diastole (heart relaxation period), thus pushing blood in both upstream (towards the heart) and downstream towards other organs thus increasing flow rate in both directions. Just prior to systole (heart contraction period), wherein blood is ejected from the left ventricle, the device deflates reducing the pressure in the root of the aorta and removing obstruction to blood flow into the aorta. The reduced pressure leads to less work performed by the left ventricle, and this relieves the heart thus increasing myocardial function.
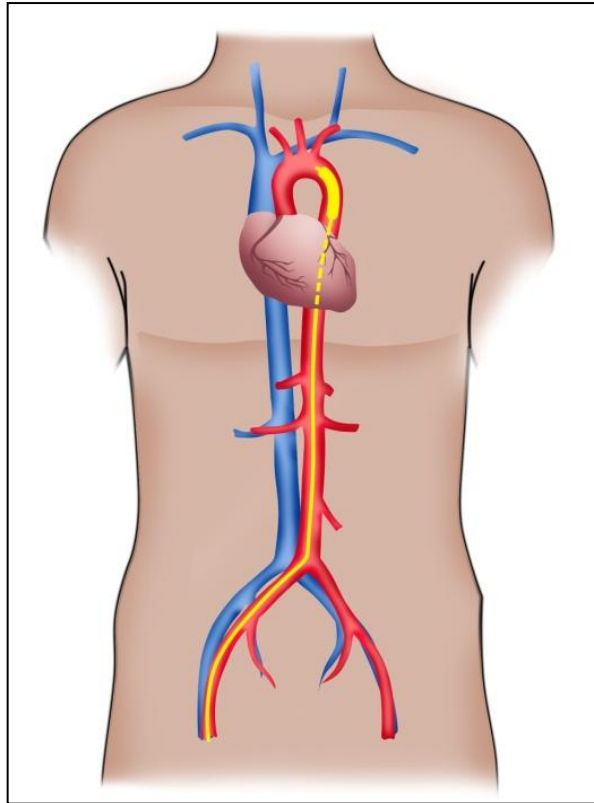
Figure 1-3: Intra aortic balloon pump (IABP) inserted from femoral artery up to 10-20 mm from left subclavian artery

The IABP device is used routinely on a failing heart from a few hours to a few weeks and effective for myocardial function improvement with small volume displacement ranging from 30 mL to 50 mL; device implantation is usually through the femoral artery and it is placed about 10 to 20 mm distal to the left subclavian artery (Quall, 1993a, Vohra and Rosin, 2004). The benefits from IABP counterpulsation are increased myocardial oxygen supply, decreased myocardial oxygen demand by decreasing resistance to blood ejection (Krishna and Zacharowski, 2009), and increased perfusion to the coronary arteries (Trost and Hillis, 2006). One measure of the balance between oxygen supply and demand is the endocardial viability ratio (EVR) which is discussed in relationship to IABP in chapter 2.

1.2   Chronic Intermittent Mechanical Support (CIMS)

The success of counterpulsation devices such as the IABP in relieving heart failure symptoms acutely is a great motivation in this study to develop a chronic counterpulsation device. It would be beneficial to have a device that employs a counterpulsation method which can be implanted at the ascending aorta, as it is has been shown that greater haemodynamic augmentation can be yielded by a device located closer to the aortic valve than one located more distally (Nosé et al., 1963, Furman et al., 1970). More proximal location brings the added advantage of reducing resistance faced by the heart when ejecting blood; this is discussed more in subchapter 2.5.

The Chronic Intermittent Mechanical Support (CIMS) – is proposed as a new device which is the subject of this study (Tansley and Richens, 2010). The CIMS device is designed with several objectives in mind:

1. to provide chronic heart treatment by relieving heart failure symptoms for specific cohorts of patients,
2. to augment systemic and coronary circulation by implanting the balloon pump at the ascending aorta. Increased coronary perfusion means increased myocardial oxygen supply,
3. to decrease the afterload (the resistance to blood egress from the ventricle) faced by the heart, thus decreasing myocardial oxygen demand.

The CIMS device comprises of a double layered balloon pump made from biomedical grade flexible membrane enclosed by a vascular graft illustrated in Figure 1-4.
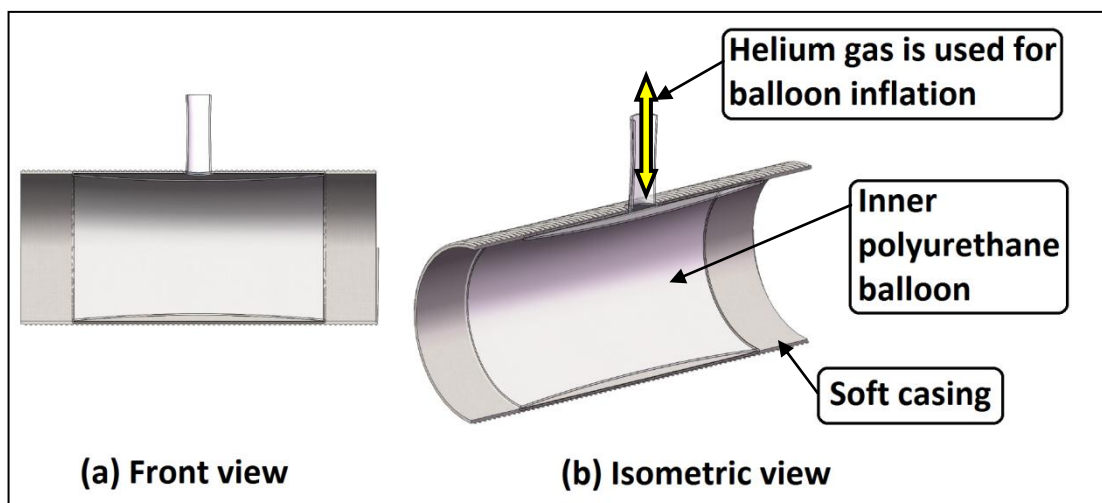
Figure 1-4: Proposed *in vivo* CIMS balloon pump with a front view and isometric cross sectional view

This is to be implanted in-series at the ascending aorta (after resecting a portion of aorta) between the aortic valve and the brachiocephalic artery. This device also includes a percutaneous driveline, consisting of Helium gas driveline and an electrical signal line, connecting the balloon pump and an external ambulatory driver which will cause the balloon to inflate and deflate. Figure 1-5 illustrates the position of implantation of the balloon of the CIMS within the ascending aorta.
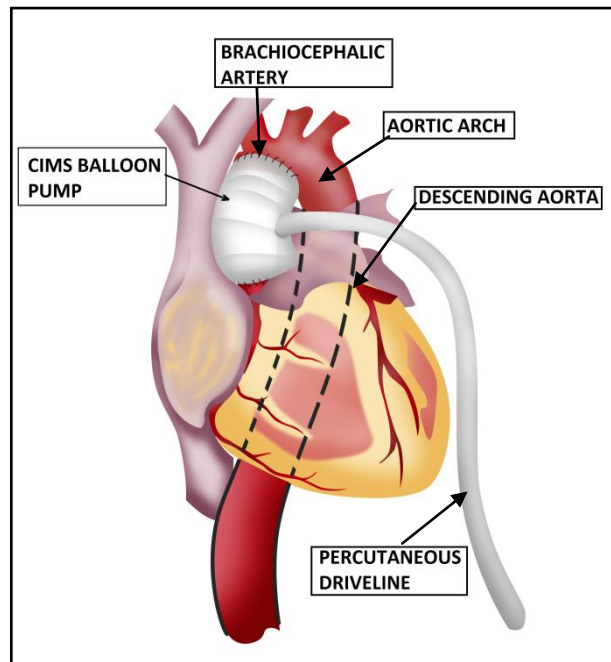
Figure 1-5: The implantation site for a CIMS balloon in the ascending aorta distal to the aortic valve and proximal to the brachiocephalic artery. A portion of the ascending aorta is resected and the balloon pump graft is sewn inter-positionally.

Figure 1-6 shows the assembly of implanted CIMS device in a patient. A human skin interface that serves as the connector between the percutaneous line and the wearable device outside of the patient's body is placed at the waist. CIMS usage would differ from IABP usage, as the IABP patient is immobilised by the bulky IABP driver console (refer to Figure 3-59) and fragility of the femoral cannula. The human skin interface acts as a gateway into the human body, allowing disconnection; the driver console can be plugged in when required and disconnected when mechanical support is not needed. The electrocardiogram (ECG) signal from the heart is collected and analysed by the wearable driver and used as the activation reference for the balloon pump. Normally for an IABP patient, the timing for balloon inflation and deflation can be adjusted using either ECG waveform or by using the aortic pressure waveform. The CIMS device proposed here will also use either the ECG signal or the aortic pressure waveform as the trigger for balloon activation. The wearable external control driver also houses the Helium gas canister and a

dedicated pump for the implanted balloon activation. A battery to power the driver and pumping action of the CIMS balloon pump is placed alongside the driver.
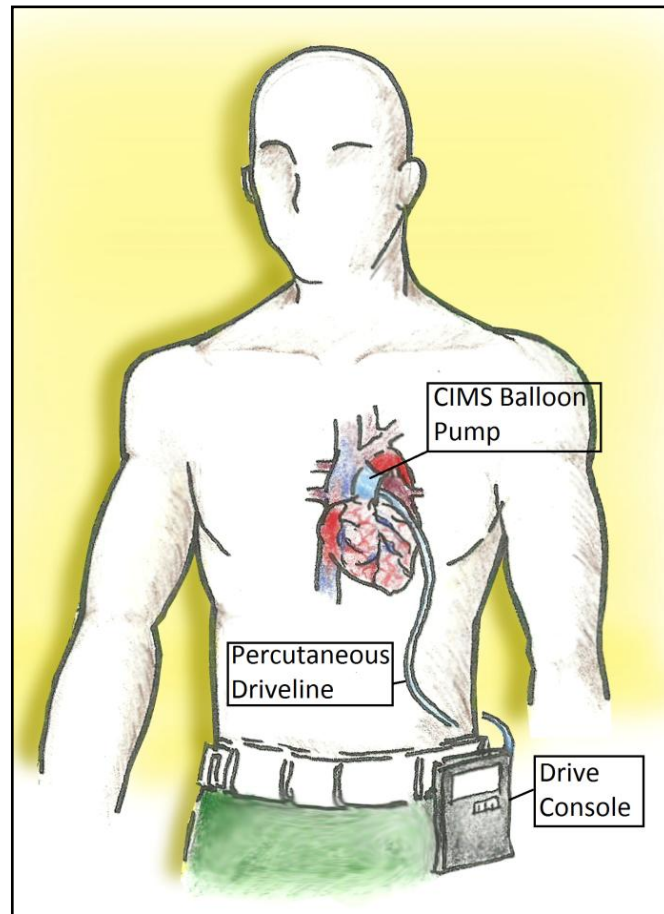
Figure 1-6: CIMS device showing: the externally-worn controller and battery on the patient's waist, a percutaneous driveline breaking through the skin and which carries pulses of Helium gas to the implanted balloon, and implanted balloon housed within the walls of the aorta which ejects blood from the aorta on balloon inflation.

Any biomedical device designed for human implantation will have to go through several development and testing steps before it can be implanted in humans. The logical and ethical way is to conduct early-stage experiments outside of the body i.e. *in vitro*. This is also a prerequisite for any medical device to be approved by the FDA (in the USA) under Good Laboratory Practice (GLP), as well as in Europe where approved medical devices are awarded the CE mark (Klepinski, 2006). Any results yielded from *in vitro* tests while they may not be fully representative of haemodynamics and neurohormonal response of a human body, will pave the way for further redesigns to ensure better reliability and increase the device's efficacy. This thesis focuses on *in vitro* study to understand the CIMS balloon pump characteristics.

Further elaboration on CIMS is given later (2.6 Chronic Intermittent Mechanical Support (CIMS)), especially suggestions for the indications and contraindications for its implantation.

1.3 Research Aims

The research aims are to develop an *in vitro* CIMS balloon pump prototype and determine the level of augmentation to systemic and left coronary artery circulation, and the reduction of aortic end diastolic pressure i.e. resistance to blood ejection arising from its use, as well as the augmentation of myocardial oxygen supply/demand ratio.

1.4 Research Objectives

To achieve the above aims the following objectives were planned:

1. to assemble a physiologically correct human mock circulatory loop simulating systemic and left coronary artery circulation to serve as an *in vitro* test platform,

2. to construct a balloon pump prototype that was able to deliver adequate displacement volume for the counterpulsation technique,

3. to investigate the flow augmentation by the CIMS balloon pump prototype within the human mock circulatory loop,

4. to show that the aortic end diastolic pressure (AoEDP) is reduced due to counterpulsation,

5. to investigate the flow dynamics effects due to balloon pumping using appropriate flow visualisation techniques,

6. to establish that the CIMS device is appropriate for supporting a specific cohort of patients.

1.5   Thesis structure

This thesis consists of six chapters.

The second chapter gives background information and recent literature necessary to enable the reader to understand where CIMS device will fit into the heart treatment arsenal. A brief explanation on how the heart works, as well as a comprehensive review on heart failure and its treatment - especially involving mechanical heart assist devices is given. The intra aortic balloon pump (IABP) is the precursor to the CIMS device; a brief but concise subchapter is dedicated to reviewing IABP and similar volume-displacement mechanical heart assist devices using the counterpulsation technique, and then a comprehensive sub-chapter is dedicated to discuss CIMS treatment including possible patient selection criteria. The first step in the device development was to make an *in vitro* prototype. Thus, an in vitro human mock circulatory loop (MCL) was needed, and a subchapter is dedicated to giving a brief introduction to MCL. Different kinds of MCLs have been assembled in research centres around the world, with varying degrees of complexity and purpose, and as such the ability to mimic physiological conditions also differs amongst these MCLs. A summary of important aspects of a mock circulatory loop is presented.

Chapter 3 is dedicated to Methodology. The rationale for *in vitro* modelling of the CIMS balloon pump is explained and the construction of *in vitro* prototypes is presented. The human mock circulatory loop (MCL) is essential to the experimental exercise and its assembly is explained in detail. Haemodynamics data is acquired using specialised hardware which drives a data acquisition system; this custom program using Labview™ software was used to monitor and change the working parameters, and to record haemodynamics data concurrently. Different heart conditions were simulated by manipulating the experimental rig. The experimental procedure for the CIMS balloon pump is presented A factorial design method was used to design experimental procedures to minimise error and confounding variables effect, as well as to reduce the duration of the experimental period, due to several interconnected experimental factors that might affect the interpretation of experimental results. Appropriate statistical analysis was chosen and the justification is given. Prior to systole, due to sudden balloon deflation, the pressure decrease was seen to cause premature aortic valve opening. Video recording was employed to record these events and to help explain the mechanics of premature valve opening.

Results from the experiments described in Chapter 3 are presented in two subsequent chapters.

In Chapter 4, the results from factorial design experiments are presented. The experiments were conducted to determine the effect of experimental factors such as arterial compliance to response outputs such as cardiac output, left coronary artery flowrate and aortic pressure changes. Statistical test such as two-way ANOVA or the non-parametric equivalent of ANOVA, the Scheirer-Ray-Hare test, were employed as the statistical tools to analyze all the data from two or more experimental factors. The correlations between diastolic pressure augmentation with cardiac output or left coronary artery flowrate are also presented. A subchapter is dedicated to presenting and discussing the ratio between oxygen supply versus demand (i.e. EVR), and the implication to heart failure treatment from CIMS balloon pump implantation.

In Chapter 5, the effects of sudden balloon deflation just before left ventricle contraction are discussed. Due to the decreased pressure in the ascending aorta from balloon deflation, the aortic valve opened prematurely, and the mechanical heart valve was observed to verify this. The variable factors that was chosen to investigate premature valve opening were balloon pump deflation time and arterial compliance. Video recording was employed to get a qualitative result. Aortic pressure difference across the aortic heart valve was analysed to get better insight of earlier heart valve opening. At the end of chapter 5, a discussion is presented as to whether premature valve leaflet opening is likely to be detrimental to myocardial function.

Finally, conclusions drawn from all the experiments are presented in Chapter 6. Since the CIMS balloon pump tested for this work is an *in vitro* model, obviously an *in vivo* version for clinical trial needs to be manufactured. The results and conclusions from this study are used to suggest future direction for CIMS device development and development of a treatment modality which would use CIMS.

Chapter 2 Background Review

This chapter will serve as a platform to familiarize the reader with necessary background information concerning heart failure treatment especially using mechanical-based heart assist devices. The CIMS device is elaborated further.

2.1   Introduction

This chapter starts with the heart's anatomical and physiological characteristics and its cardiac cycle. Subsequently the chapter discusses congestive heart failure (CHF) (also simply known as heart failure (HF)), followed by the many treatment options for heart failure. One treatment for heart failure is mechanical assistance, which is of particular relevance to this work. A thorough explanation of the history and the development of ventricular assist devices (VAD) are presented. The Chronic Intermittent Mechanical Support (CIMS) system is similar in activation technique i.e. counterpulsation with the Intra Aortic Balloon Pump (IABP), so a subchapter is dedicated to the IABP and similar counterpulsation based VADs implanted in and around the aorta. A more detailed explanation of CIMS is presented. Human mock circulatory loop review is also given as a prelude to the one used in this study. A summary is given at the end of this chapter.

2.2   The Human Heart

Discussion on the human heart: the history, anatomy and cardiovascular functions are presented.

2.2.1   A Brief History of the Heart

Starting with the Greek scholars (e.g. Galen) thousands of years ago, to Muslim physicians (e.g. Ibn Nafs and Avicenna) continuing to Italian Renaissance artists, most notably Leonardo da Vinci, the heart has been a fascinating topic for scholars, although their understanding was quite different from modern scientifically derived fact. Scientific understanding of the heart and body circulation started when William Harvey published his seminal text "*Exercitatio Anatomica de*

Motu Cordis et Sanguinis in Animalibus" (Exercise on the Anatomical Motion of the Heart and Blood in Animals) in 1628 (Harvey 1628). The authoritative book for several centuries dispelled the myths surrounding blood circulations and heart movement through scientific observation.

The heart is a vital organ to humans and one of the components in the cardiovascular system, the other one being the blood vessels. The heart is situated between two lungs, with two thirds situated to the left of the breastbone, illustrated in Figure 2-7. It beats at rest around 60 - 80 times per minute (variations exist for individuals) pumping out blood from the left ventricle, amounting to 5 - 7 litres per minute (L/min).
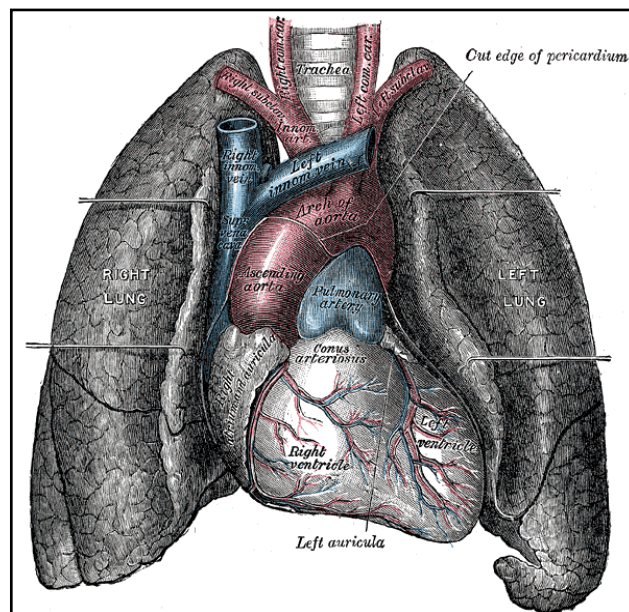
Figure 2-7: Heart position in the human body between lungs (H. Gray 1918)

The human heart is divided into four chambers. The upper chambers are the atria, while the lower chambers are the ventricles. Normally the chambers are identified by its position, i.e. left ventricle or right atrium. The myocardium cells i.e. myocytes of the heart makes up the muscle of each chamber; another specialised cells form the conduction fibers as the excitatory systems responsible for heart rhythm.
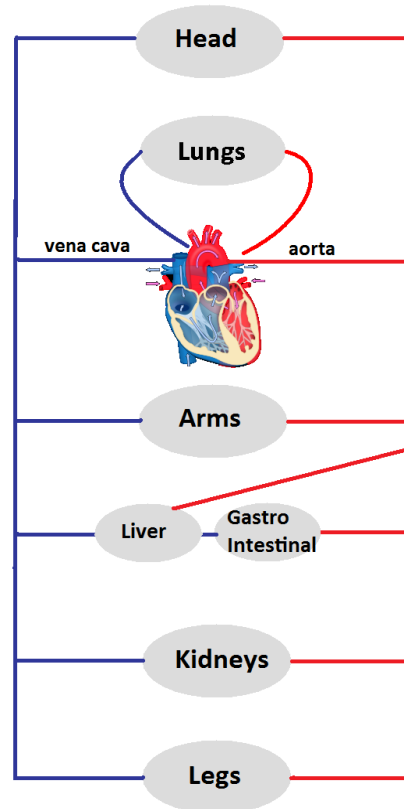
Figure 2-8: In-series and in-parallel configuration for vascular networks

Another aspect worth noting is how the atria and ventricles are configured in an *in-series* configuration. Blood moves from one heart chamber to the next one in unidirectional flow, and any changes in any heart chamber will affect the others and alter the whole body perfusion, and further explained in subchapter 2.2.5   Frank-Starling Mechanism.) Circulation for the kidneys and other organs, illustrated in Figure 2-8, is *in-parallel* circulation, which means that the blood flows into several organs from a main blood vessel.

Blood circulation in the human body can be divided into two: systemic and pulmonary circulation, illustrated in Figure 2-9. Pulmonary circulation is the flow circuit of deoxygenated blood for gaseous exchange from the heart through the lungs, and oxygenated blood from the lungs back to the heart. Systemic circulation is the blood circulation from the heart to blood vessels and other organs and back to the heart. The heart pumps oxygenated blood packed also with fluid, biochemical hormones, nutrients to peripheral organs by way of the arteries. An artery's main function is to transport blood at high pressure (mean arterial pressure at 90 to 100 mmHg). From the largest blood vessel i.e. the aorta, blood is transported until it reaches capillaries which are smallest in diameter (approximately 1 µm). The thin walled capillaries facilitate efficient nutrient,

O_2 and CO_2 exchange by diffusion. Heat exchange between cells and the outside environment is also facilitated by the heart through tiny capillaries near the skin. After the exchange process, deoxygenated blood packed with metabolic process by-products (e.g. waste, CO_2) flows into the venule, converging into veins before flowing into the venae cavae, the last stop before the right atrium.
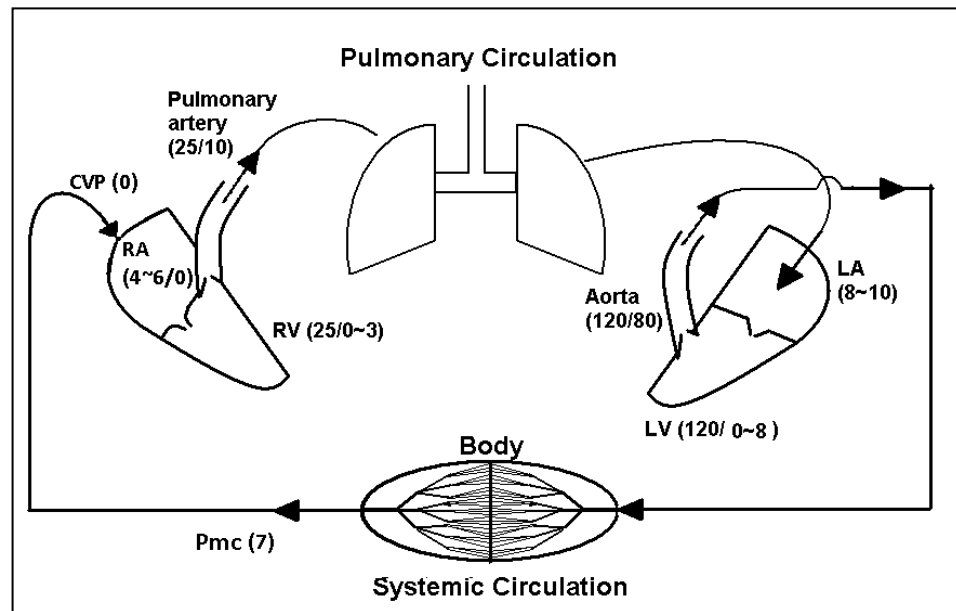
Figure 2-9: Pulmonary and systemic circulation of the human body. The numbers in brackets show the normal range of pressure fluctuation in respective chambers. The heart chambers is an in-series configuration pumps. RA: Right atrium, RV: Right ventricle, LA: Left atrium, LV: Left Ventricle, CVP: Central Venous Pressure, Pmc: Mean Circulatory Pressure (mmHg).

2.2.2 Cardiac Cycle

The heart pumps blood into lungs and the rest of the body intermittently causing pulsatile flow that resembles superposition of sinusoidal waves. The contraction and relaxation of heart chambers are controlled by opposing autonomic nerves; composed of the sympathetic and parasympathetic nerves innervating the myocardium. At the sinoatrial (SA) node which is the intrinsic pacemaker, action potential is generated thus causing atria contraction. The action potential propagates through the atrioventricular (AV) node before being conducted through a specialised pathway consisting of the HIS bundle branches and the Purkinje's fibres initiating ventricular contraction.

The relaxation and contraction phases of the heart muscles in a cardiac cycle are called diastole and systole. The cardiac cycle can be further categorised into four distinct phases. Each phase is

separated by the opening and closing actions of the heart valves. One cardiac cycle normally lasts for 0.8 - 1.0 second (60 - 80 beat per minute; beats/min), although the heart rate (HR) will change in accordance to physiological needs controlled by the autonomic nerves.
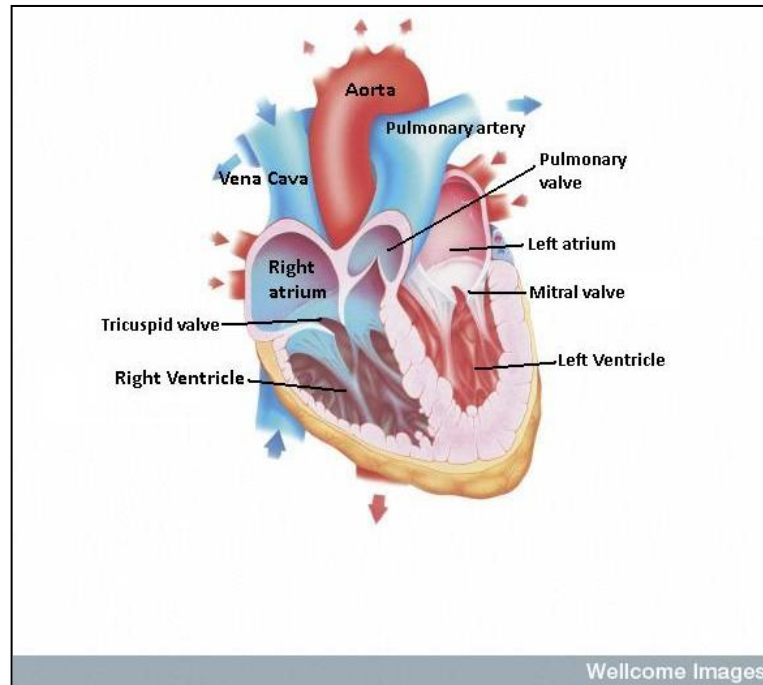
Figure 2-10: Blood circulation in the heart from the venae cavae to the right atrium, filling the right ventricle before being pumped into the pulmonary arteries. Oxygenated blood then flows into the left atrium before filling the left ventricle during diastole before ejected into the aorta. (With kind permission from Wellcome Library, London)

Figure 2-10 illustrates the complete flow loop to and from the heart. Blood flows from the body via the superior and the inferior venae cavae into the right atrium due to the pressure gradient between the mean circulatory pressure (Pmc) observed at the veins and the central venous pressure at the right atrium. The Pmc at the veins is maintained at approximately 7 mmHg (Klabunde, 2005, Levick, 2003, Guyton and Hall, 2006), while the central venous pressure (CVP) is typically 0 mmHg.

In early diastole, blood enters the right ventricle passively, but once the SA node triggers the electrical signal, the right atrium contracts thereby forcing more blood into the right ventricle. Once ventricular systole starts, right ventricular contraction increases the intraventricular pressure before pumping the blood into the pulmonary circulatory loop. The contraction imparts the blood with a pressure of about 25 mmHg. Gaseous exchange occurs in the lung, exchanging carbon dioxide (CO_2) with oxygen by diffusion processes. Once the exchange processes are completed, blood is directed to the left atrium by way of the pulmonary arteries. The blood pressure past the lungs is around 10 mmHg, and since the left atrium internal pressure oscillates

from 8 - 10 mmHg throughout the cardiac cycle, blood fills the left atrium passively due to the pressure gradient between ventricle and atrium (Guyton and Hall, 2006, Timms et al., 2005a).
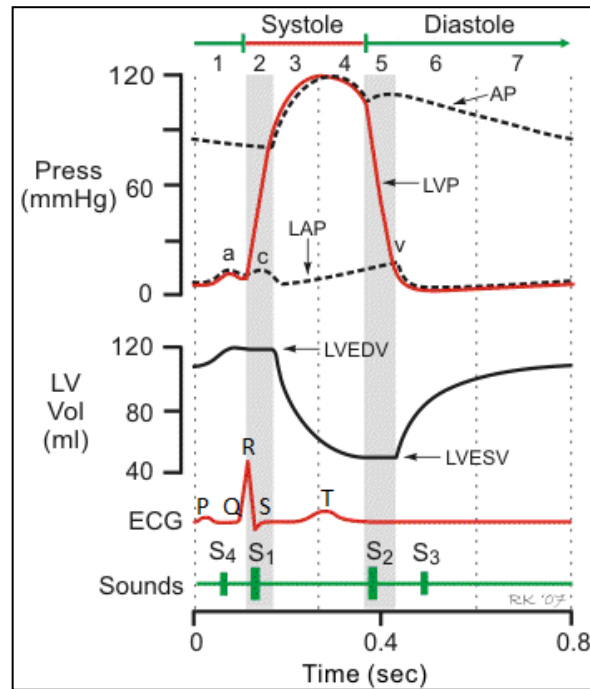
Figure 2-11: Cardiac cycle of the LV, LA, and aorta from systole to diastole. Electrocardiogram (ECG) signal is represented by P,Q,R,S and T wave, while S1 to S4 represent the heart sound due to valve opening/closing, heart chamber vibration or tensing of chordae tendineae[1] and atrioventricular ring in the heart chamber.(With kind permission from Klabunde (Klabunde, 1998))

Figure 2-11 illustrates the pressure waveform in a cardiac cycle in synchrony with the ECG signal and the resulting heart sounds. The cardiac cycle, focussing on the left ventricle, is described below (Levick, 2003, Klabunde, 2005).

Electrokardiogram (ECG) Signal

As mentioned previously and illustrated in Figure 2-11, the electrical signal triggers ventricular contraction originated at the SA node before propagating throughout the heart. The P, Q, R, S and T signage are explained in Table 2-1.

---

[1] Chordae tendineae: The heart strings, made of tendons, that connects heart valves (mitral and triscuspid) to papillary muscles.

Table 2-1: The P, Q, R , S and T wave of ECG signal and their meaning(Klabunde, 2005)

Nomenclature	Detail
P wave	When SA node is triggered, electrical current is propagated to AV node, and this causes atrial contraction.
QRS complex	The electrical current travels to the HIS bundle branch and Purkinje fibers, causing ventricular contraction i.e. a rapid depolarization occurs at the right and left ventricle. This is recorded by the longer duration and higher amplitude of QRS complex (particularly R wave)
T wave	Once electrical impulse has finished depolarizing ventricular muscle, then ventricular polarization takes place, during which the ventricle relaxes; this is represented by the T wave.

Phase 1: Filling (Diastole)

The filling phase of the LV starts when the intraventricular pressure decreases to a point where the pressure in the atrium is greater than the ventricular pressure. The pressure gradient opens up the mitral valve (inlet valve) allowing blood to flow passively into the ventricle from the pulmonary veins. This phase lasts roughly two-thirds (0.5 to 0.6 s) of the cardiac cycle. Atrial systole initiated by the P waves of the ECG contributes additional filling of the ventricle by 10% to 15% as compared to without the atrial contraction (sometimes known as atrial kick). During exercise, ventricular diastolic period is shortened while the contribution from atrial contraction is increases up to 40%. Intraventricular pressure at the end of diastole is called End-Diastolic Pressure (EDP), and is around 8 mmHg, while the ventricular volume, End-Diastolic Volume (EDV) is around 120mL. The aortic valve (outflow valve) is closed since intraventricular pressure is lower than the ascending aorta's pressure.

Phase 2: Isovolumetric Contraction (Systole)

Systole or ventricular contraction is initiated by the QRS complex of the ECG. The left ventricle contracts, and intraventricular pressure rises rapidly exceeding left atrial pressure but still below the pressure in the ascending aorta; both the inlet and outlet valve are closed thus making the left ventricle a closed space. The rapid rise of pressure reaches a point where the intraventricular pressure exceeds the ascending aortic pressure. This phase would be affected by CIMS balloon deflation; it is hypothesised to decrease end-diastolic aortic pressure, thus intraventricular pressure as well. Once the aortic valve opens, this phase is over.

Phase 3: Ejection (Systole)

Due to the higher pressure generated during the previous phase, the aortic valve is opened and the blood is ejected very rapidly into the ascending aorta. Within this period of about 0.3 second, almost two-thirds of the blood volume (70 to 80 mL) in the left ventricle is ejected, with the majority during early systole. The compliant ascending aorta expands to accommodate the incoming blood volume, since within that short amount of time blood cannot be ushered to peripheral arteries easily. Intra-aortic pressure will also increase accordingly.

As contraction of the ventricle weakens, so does the velocity of the blood ejected and intraventricular pressure. Eventually, the ventricular pressure will drop slightly below aortic pressure (by about 2 – 3 mmHg), although due to the outflow momentum of the blood, the aortic valve will not close immediately. Once the aortic valve closes, due to the closing of the aortic valve, a pressure surge, known as the dicrotic notch, occurs within the ascending aorta.

Phase 4: Isovolumetric Relaxation (Diastole)

Continuing from the previous phase, the aortic valve is closed, this makes the ventricle a closed chamber again since the mitral valve is also still closed. In this phase, the remaining blood volume, about 50 mL, is called the End-Systolic Volume (ESV). The heart relaxes and pressure within the chambers falls which leads to the opening of the mitral valve due to the pressure gradient between the pulmonary artery and the left ventricle. The next cardiac cycle commences again from phase 1.

2.2.3   Pressure-Volume Loop

Blood pressure and volume fluctuation in the left ventricle in one cardiac cycle can be plotted against each other, illustrated in Figure 2-12 making a close loop, termed as the pressure-volume (PV) loop.
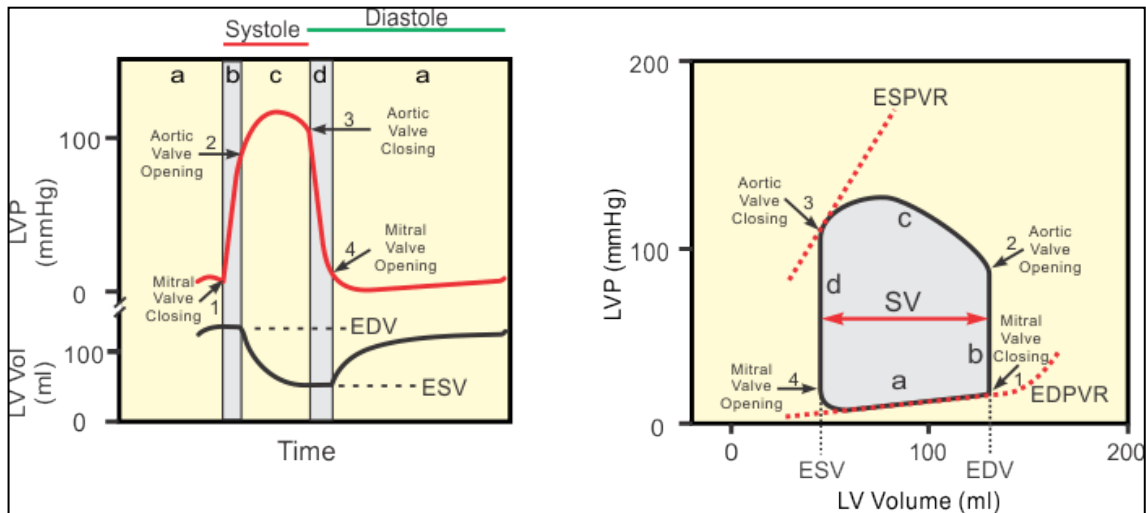
Figure 2-12: Left ventricular pressure and blood volume changes within a cardiac cycle (left) and the corresponding pressure-volume (PV) loop (right). EDV: End diastolic volume, ESV: End systolic volume, SV: Stroke volume, ESPVR: End-systolic pressure-volume relationship, EDPVR: End-diastolic pressure volume relationship (With permission from Klabunde (Klabunde, 1998))

The PV loop is plotted using mitral valve closure as the starting point (1). Once systole has started, the left ventricular pressure builds up, but the blood volume remains constant (Isovolumetric contraction), marking the vertical (b) line. Eventually the left ventricular pressure exceeds the aortic pressure at point 2, opening the aortic valve and ejecting blood into the ascending aorta. The pressure increase and decreasing blood volume yield line (c), which peaks before settling to point 3. The aortic valve closes indicating the start of diastole period. Since both the aortic valve and mitral valve are closed at this point, pressure decreases due to LV relaxation i.e. isovolumetric relaxation, which is reflected in vertical line (d). After a while, the mitral valve opens (at point 4), and the filling phase is started. The volume of blood remaining inside the left ventricle before chamber filling starts is known as the end-systolic volume (ESV). A slight pressure increase accompanies a big change in blood volume and that is marked by line (a), the end point of which represents the maximal left ventricular end-diastolic pressure (EDP) and end-diastolic volume (EDV).

The difference between EDV and ESV is the stroke volume (SV) i.e. the amount of blood ejected in a cardiac cycle. The filling curve (line a) is also known as the end-diastolic pressure volume relationship (EDPVR) and this curve signifies ventricle compliance. For a stiffened hypertrophied heart, the EDPVR slope is increased. The effect of a dilated heart to the PV loop is explained later (refer to Figure 2-20). Normal to the EDPVR line is the ventricular elastance or 'stiffness' since compliance is reciprocal of stiffness.

The end-systolic pressure volume relationship (ESPVR) line represents the limit of left ventricle contractility. Depending on the sympathetic nerve signal or any positive inotropic drug boosting heart contractility, the ESPVR line changes accordingly; the maximum pressure the left ventricle can generate at any given amount of end-diastolic blood volume is limited by the ESPVR line (Klabunde 2005). The heart condition whether it is normal or not, can be determined by PV loop tracing and discussed more in later subchapter (2.3.5   Cardiomyopathy).

2.2.4   Blood Circulation

The amount of blood ejected from a healthy heart at rest is usually around 5 - 7 L/min, termed as cardiac output (CO), and is computed by multiplying stroke volume, SV, with the number of heart beats in a minute (HR) as Eq. 2.1:

$$CO = SV \times HR.$$
<div align="right">2.1</div>

Thus, SV is easily computed, for example, with a CO = 5 L/min and HR = 60 beats/min, the SV is roughly 83 mL. During exercise, cardiac output may rise to $20 - 35$ L/min from $5 - 7$ L/min at rest. Indeed, from a normal resting rate of 50 - 100 beats/min, heart rate can shoot up to 180 - 200 beats/min during heavy exercise (Levick, 2003). During heightened bodily activity, the sympathetic nerves increase the rate of electrical impulses at the SA node, thus increasing the CO. Initially the increased HR means that the filling time is decreased (systole time is mostly fixed), and this could mean decreased SV. However, SV is increased by combinations of increased mean arterial pressure, pulse pressure, and central venous pressure (CVP) that leads to increased contractility from the Frank-Starling mechanism (refer to 2.2.5). The sympathetic nerve also increases SV by increasing contractility, increasing the rate of muscle heart relaxation to facilitate easier ventricular filling, and facilitating systemic vascular resistance reduction, thus increasing blood perfusion to periphery.

Cardiac output can also be described using Eq. 2.2. This method allows for a direct comparison between patients with regards to body structure.

$$CI = \frac{CO}{BSA}$$

2.2

where CI is the cardiac index, while BSA is the body surface area. There are several formulae to compute BSA [m^2], of which two are presented:

a) The Du Bois and Du Bois formula (Du Bois and Du Bois, 1916)

$$BSA = 0.20247 \times H^{0.725} \times W^{0.425}$$

2.3

where H is the height [m^2] , and W is the patient's weight.

b) The Mosteller formula (Mosteller, 1987)

$$BSA = \sqrt{\left(\frac{h \times W}{3600}\right)}$$

2.4

where h is the height in cm.

Using a representative sample of h = 1.8 m and W = 70 kg, the BSA calculated is 1.81 (Du Bois & Du Bois) and 1.87 (Mosteller), and with normal range of CO at 5 L/min, the CI is 2.76 L/min/m^2 (Du Bois), and 2.67 (Mosteller) L/min/m^2. The normal range of cardiac index is 2.6 - 4.2 L/min/m^2 (Klabunde, 2005).

The SV is influenced by two factors:

1) Myocardial contraction energy

Myocardial contraction can be heightened in two ways: (1a) the intrinsic mechanism of the heart muscle (2.2.5 Frank-Starling Mechanism) responding to preload, which is the myocardium wall stress, and (1b) from the sympathetic nerves intervention and the circulating hormone adrenaline. Increased contraction in turn ejects a greater amount of blood from the heart, thus increasing SV.

2) Afterload

The afterload is defined as the amount of myocardium wall stress, S, that is needed to eject blood. The wall stress is generated by the myocardium in a chamber with w thickness, r radius and P intraventricular pressure, described by Laplace's equation in Eq. 2.5.

$$S = \frac{Pr}{2w}.$$ 2.5

High arterial pressure means that the myocardium has to work harder since intraventricular pressure P must be greater than ascending aortic pressure for ejection to start. Normally, the aortic pressure is taken as afterload although that is not entirely accurate.

The calculation for mean arterial pressure (MAP) is not the arithmetic average of systolic and diastolic pressure as the time spent in diastole is normally 2/3 of the whole cardiac cycle and computed as Eq. 2.6:

$$MAP = P_{dias} + \frac{\left(P_{sys} - P_{dias}\right)}{3}.$$ 2.6
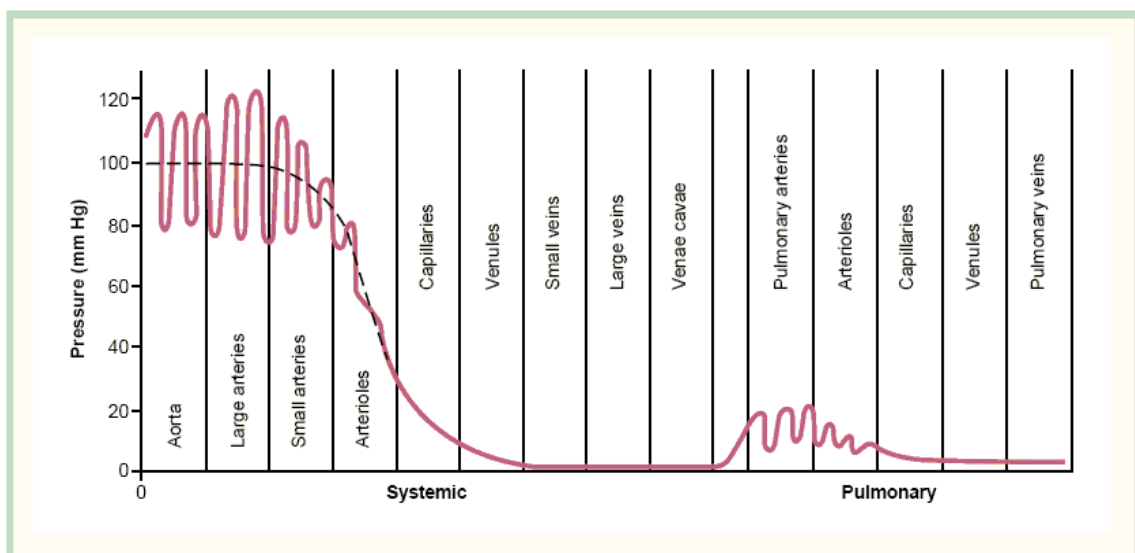
Figure 2-13: Blood pressure distribution across the systemic and pulmonary circulation. The dotted line is the MAP. It is highest at the aorta before gradually decreasing at capillaries (With kind permission from Elsevier) (Guyton and Hall, 2006)

Figure 2-13 illustrates the blood pressure distribution throughout the blood vessels in one full circulation. The MAP at the aorta is around 95 to 100 mmHg. The pulse pressure (PP: the difference between aortic systolic and diastolic pressures) increases as the blood flows into larger arteries such as the abdominal aorta but the MAP remains constant or decreases a little bit. The increasing PP (refer to Figure 2-15) at large arteries farther from the heart is caused by several factors: wave reflection, aorta becoming tapered downstream, blood vessel stiffness and wave reflection speed (Levick, 2003). The pulsatility of the blood pressure resumes at the pulmonary artery and lungs with MAP of about 16 mmHg (Guyton and Hall, 2006).

The aorta and other big arteries (> 1 mm) provide no real resistance. Starting in the smaller arteries region, MAP starts to decrease quite rapidly due to increasing collective resistance that offers the biggest resistance to blood flow. However, MAP maintains a constant pressure of about 17 mmHg at the vascular bed, enough for fluid exchange at the capillaries. The vascular resistance from arteries is sometimes called systemic vascular resistance (SVR) or total peripheral resistance (TPR). The relationship between MAP, CO and SVR (and CVP) can be summarised as:

$$MAP = (CO \times SVR) + CVP$$
<div align="right">2.7</div>

or when rearranged,

$$CO = \frac{(MAP - CVP)}{SVR}$$
<div align="right">2.8</div>

but since CVP is normally zero, then the equation is simplified:

$$CO = \frac{MAP}{SVR}.$$
<div align="right">2.9</div>
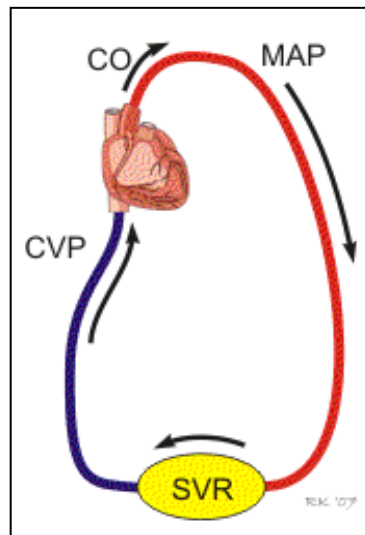
Figure 2-14: The relationship between MAP, CO, SVR and CVP. The MAP is generated with incoming CO from the heart and the SVR from the periphery. The CVP near the right atrium is normally 0 mmHg. (With permission from Klabunde (Klabunde, 1998))

Figure 2-14 illustrates the interconnectedness between CO, MAP and SVR; the CVP is normally at 0 (zero) mmHg, and influences the CO level by way of Frank-Starling mechanism, while SVR is independent of CO and MAP.

Blood flow, Q, in an artery is determined by two factors: 1) ΔP, the pressure gradient and 2) R, resistance impeding blood flow, between two points in the blood vessel. The relationship is expressed in Eq. 2.10, known as Darcy's law of flow (can also be applied to any geometric channel), which resembles Ohm's Law of current and voltage.

$$Q = \frac{\Delta P}{R}.$$
2.10

The biggest resistance to blood flow originates from small arterioles which contribute almost 2/3 of total systemic resistance (Guyton and Hall, 2006). Resistance can be expressed using Poiseulle Law which states that resistance is proportional to the tube radius' raised to the fourth power, r^4, expressed by Eq. 2.11.

$$R = \frac{8\eta L}{\pi r^4}.$$
2.11

Where L = length of the vessel, η = viscosity of the fluid (blood viscosity is 3 - 4 mPa.s at 37°C (Burton, 1972)[2]), r = radius of the blood vessel (in case of small arterioles, it is around $10 - 20$ μm). One of the assumptions of Poiseuille's law is the flow in the tube is laminar. Although blood exhibits non-Newtonian characteristics in nature, especially in small vessels (higher apparent viscosity), in high shear rates vicinity e.g. at the aorta, blood can be thought of as a Newtonian fluid (Shah, 2011). When Eq. 2.11 is substituted into Eq. 2.10:

$$Q = \frac{\Delta P}{R} = \frac{\Delta P \pi r^4}{8\eta L}.$$
2.12

The Poiseuille Law shows that resistance is extremely sensitive to radius changes. Local blood flow can be regulated by changing blood vessel radius resulting in a rapidly changing resistance due to the radius factor in Poiseuille's formula. Vessel arrangement contributes differently to total resistance value, *in series* arrangement yields a straightforward addition of all vessel resistance ($R_T = \sum R_n$), while *in parallel* arrangement resistance is as:

$$\frac{1}{R_T} = \frac{1}{R_1} + \frac{1}{R_2} + \frac{1}{R_3} + \cdots = \sum \frac{1}{R_n}.$$
2.13

---

[2] Water's viscosity is 1 mPa.s at 20.2°C. 1 mPa.s =1 cP (CGS unit)

Big blood vessels, and capillaries that form the vascular bed are arranged *in parallel*, and results in a low resistance environment compared to *in series* arranged small arterioles that offer much more resistance to blood flow. The SI metric unit for SVR is mmHg/mL/min; the old CGS metric system stated this as dynes.s/cm^5. The conversion factor between both units is: 1 dynes.s/cm^5 = 1333 mmHg/mL/s.

2.2.5   Frank-Starling Mechanism

Frank-Starling mechanism is one of the ways to increase the contraction energy of the heart, the other one is by hormonal secretion of adrenalin and sympathetic stimulation. The Franks-Starling mechanism dictates that whenever there is an increase in venous return due to increased CVP to the heart, heart chambers will expand (initial sarcomere length in myocytes is increased) thus generating correspondingly extra force to eject blood. The increased blood and pressure increases the preload, which is the diastolic wall stress that leads to increased contractility.

The Frank-Starling mechanism is important to maintain blood volume equilibrium between both sides of the heart, without which there would be a catastrophic imbalance between input and output from both sides of the heart, since input and output values are fixed. For example, if the right ventricle is ejecting 10% more than usual, while the left ventricle output remains the same, then the increasing blood volume output from the right heart would congest the lung and pulmonary circulation leading to pulmonary oedema (Burton, 1972, Guyton and Hall, 2006).

The main factor influencing the Frank-Starling mechanism is the venous return i.e. blood volume returning to the right atrium, although there are some that argue that CVP is a much better determinant for the stroke volume (Levick, 2003). CVP in turn is affected by mean circulatory pressure, Pmc.

2.2.6   Vasculature Compliance and Pulse Pressure

The blood ejected from the left ventricle during systole collects momentarily in the expanding ascending aorta since blood from the previous cardiac cycle has not completely drained into the distal arteries. Once the heart valve is closed, the aorta wall recoils and pushes the remaining

blood to the peripheral circulation. The intra aortic pressure decreases gradually, but end-diastolic pressure never reduces to zero due to blood vessel compliance. The pulse pressure (PP) for a normal young person is 40 to 45 mmHg. The distensibility of the aorta and arterial tree helps to maintain mean arterial pressure (MAP), thus providing constant blood flow to peripheral circulation. Without blood vessel compliance, the aortic pressure fluctuation would follow the left ventricle pressure waveform, and require more work from the heart to pump the same amount of stroke volume (Berne et al., 2004, Klabunde, 2005, Nichols and O'Rourke, 2005).

Compliance, C, is computed by dividing volumetric increase or stroke volume with pressure difference or PP:

$$C = \frac{\Delta V}{\Delta P} = \frac{SV}{PP}. \qquad\qquad 2.14$$

The unit for compliance is mL/mmHg. The arterial compliance however is not a linear relationship, with higher pressure and blood volume, compliance declines i.e. the blood vessel stiffens, and this increases the pulse pressure.

Arterial compliance also declines with advancing age due to atherosclerosis i.e. stiffening of arteries (Mitchell et al., 2004). For older people, the stiff vasculature causes higher PP with higher systolic pressure and lower diastolic pressure for a given stroke volume (Safar and Laurent, 2003), as illustrated in Figure 2-15.
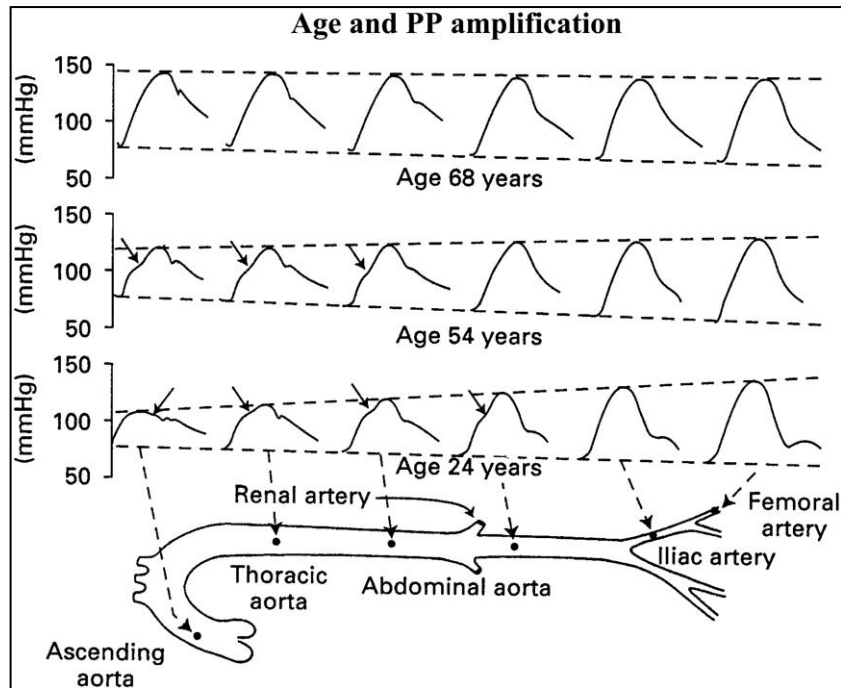
Figure 2-15: Pulse pressure wave progression along the blood vessel from ascending aorta until femoral artery. The pulse pressure increased as the measurement point getting farther from aorta i.e. PP increasing along the blood vessel. The PP also increasing with age (Nichols et al., 1998, Safar and Laurent, 2003).

The increase in systolic pressure, poses the heart with a mounting workload to overcome. Another adverse effect of arterial stiffening is faster wave reflection velocity. Ejection of blood distends the aortic wall and causes pressure waves to propagate into the periphery. Once it reaches the bifurcated branches, the pressure wave is reflected back. The reflected pulse wave then coincides with pulse pressure from the next cardiac cycle. In young normal adults, the reflected wave arrives to the aorta in late systole; while for older people, due to increased wave speed, it arrives earlier causing higher systolic pressure (Westerhof et al., 2010, Nichols and O'Rourke, 2005). Increased pulse pressure due to aging is also the best predictor index of mortality(Glynn et al., 2000). For heart failure patients, this poses another set of problems since the reflected pulse wave affects blood flow and has an adverse affects on systole augmentation (Cockcroft et al., 1997). Other diseases affecting arterial compliance are arterial hypertension (Dzau and Safar, 1988) and diabetes (Salomaa et al., 1995).

2.2.7   Coronary Circulation

Coronary circulation is vital for the heart to operate in normal fashion. In Figure 2-16, the left and right coronary arteries originate from the aortic root at the coronary ostia, just distal to the aortic valve. Each left and right branch covers respective parts of the heart although some overlap may exist.
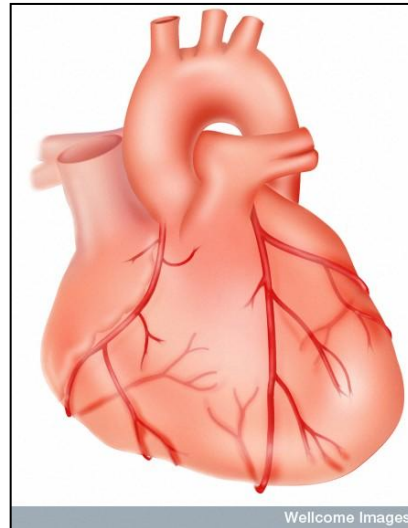
Figure 2-16: Coronary arteries originating from the root of ascending aorta and branched out to cover both left and right part of the heart. (With kind permission from Wellcome Library, London)

There are variations between individuals as to which artery is the dominant coronary blood vessel; 50% of individuals have the right coronary artery as the dominant artery, 30% receive equal amounts of blood from both arteries, while the remaining 20% have the left coronary artery as dominant (Berne et al., 2004). The major coronary arteries are on the surface of the myocardium i.e. the epicardial region. Farther away from the ostia, the arteries branch out and become smaller diving into the myocardium, i.e. subepicardial region, to form extensive microvascular resistance vessel that distributes blood to all myocytes. These microvascular vessels are essential in coronary flow distribution, especially on the left coronary arteries.

The mean coronary flow is around 225 mL/min (Guyton and Hall, 2006), although it is normally expressed in term of myocardial mass. In a normal resting condition, mean coronary flow is around 70 - 80 mL/min/100 g, during heightened physical activity coronary flowrate may increase up to 300 - 400 mL/min/100 g (Levick, 2003, Klabunde, 2005)[3].

---

[3] The weight for a 70 kg man's heart is around 350 g (Levick, 2003)

The left coronary artery has a unique flow characteristic. The microvascular capillaries in the subepicardial region are very sensitive to external pressure making it the main source of left coronary resistance. In early systole, myocardium compression rapidly increases resistance in the coronary arteries stopping or at least reducing the flow rate to almost zero. The coronary flow resumes during diastole as illustrated in Figure 2-17. The right coronary artery is also affected by the myocardial compression; however, the effect is not as severe as in the left coronary artery (Berne et al., 2004).
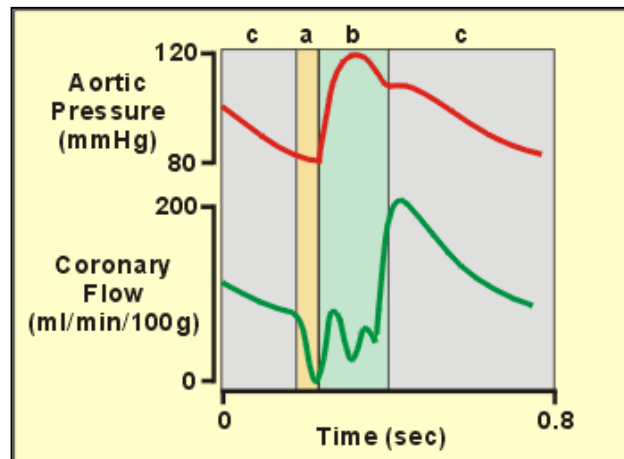
Figure 2-17: Pulsatile nature of the left coronary artery blood flow. During early systole, due to myocardial compression, the flow decreases to almost zero and picks up again during diastole. a: isovolumetric contraction in early systole, b: ejection in systole, c: diastole (With kind permission from Klabunde (Klabunde, 1998)).

2.3   Heart Failure

The heart failure disease is explained in detail in this subchapter.

2.3.1   Definition of Heart Failure

Cardiovascular disease (CVD) continues to be one of the top causes of mortality in the world and comprises range of diseases including coronary heart disease (CAD), valvular heart disease, hypertension, myocardial infarction and ultimately congestive heart failure (CHF), normally known as heart failure (HF). The World Heart Organization (WHO) reported that in 2004, CVD contributed to almost 30% of death of estimated worldwide death figures (58 million), with almost 32% of deaths being women, followed by men with almost 27%. The overall death reported worldwide due to cardiovascular disease was a little over 17 million and is projected to increase almost 30% to 23.4 million by 2030 (Mathers, 2004). In the United States of America, in 2006, there were

about 34% of deaths (actual figure of deaths = 2 426 264) attributed to CVD, with 287 754 deaths (11.9%) mentioning HF in the death certificate (Lloyd-Jones et al., 2010).

The textbook definition of heart failure (HF) is "*failure of the heart to pump enough blood to satisfy the needs of the body*" (Guyton and Hall, 2006). However, there are other definitions given by scholars such as by Denolin and his co-workers which states that:

> "*Heart failure is the state of any heart disease in which, despite adequate ventricular filling, the heart's output is decreased or in which the heart is unable to pump blood at a rate adequate for satisfying the requirements of the tissues with function parameters remaining within normal limits*" (Denolin et al., 1983).

Another definition of heart failure is at the point which the heart cannot maintain cardiac function without increasing the filling pressure i.e. atrial pressure.

These are not the only definitions proposed by scholars. However, there are many disagreements on HF definition due to conflict between physiological symptoms, which focus on circulatory organ dysfunction, and clinical symptoms such as dyspnoea (breathlessness) and lethargy (Adams and Zannad, 1998). To incorporate both physiological and clinical symptomatic markers, the Task Force of the European Society of Cardiology proposed the definition in 1995. The first and second criteria must be fulfilled in all cases (Cardiology, 1995, Remme and Swedberg, 2001):

1. symptoms of HF (at rest or during exercise),
2. objective evidence of cardiac dysfunction (at rest),
3. response to treatment directed towards HF (in cases where the diagnosis is in doubt).

The apparent similarity between definitions which point out the heart inability to supply blood according to the body's demand is evident. Due to the differences in defining what HF is, researchers use different guidelines for their studies and consequently published different conclusions. Brief HF prevalence, incidence, aetiology and some of the common symptoms of HF and physiological cardiac dysfunction are explained in later subchapter.

2.3.2 Heart Failure Risk Factor, Aetiology, Prevalence & Incidence

The risk factors of heart failure are not unique and are attributes of other diseases as well. The risk factors for the USA populations are (Jiang et al., 2001):

- gender (male)
- less education
- low physical activity
- cigarette smoking
- overweight
- hypertension
- diabetes
- valvular heart disease
- coronary heart disease (CAD).

For example, obese people are likely to suffer hypertension before progressing further to heart failure. From Jiang et al. (2001) study, coronary heart disease is the biggest risk factor with a relative risk of 8.11 (95% CI = 6.95 − 9.46)(Jiang et al., 2001). A 17-year longitudinal study in Sweden showed that hypertension and smoking were the biggest heart failure risk, while other independent risk factors were body weight, heart volume, ECG abnormality (at T-wave), variability of heart rate, breath flowrate index, stress and possibly a genetic marker (Fy-antigen)(Eriksson et al., 1989).

Various aetiology studies have discovered that coronary artery disease (CAD), hypertension, valve dysfunction, cardiomyopathy (e.g. dilated, hypertrophic and alcoholic), cardiac arrhythmias/conduction disturbance, pericardial disease, or viral infection (rheumatic fever or pregnancy) are causing heart failure in general population (McKee et al., 1971, McDonagh et al., 1997, Cowie, 2000, McMurray and Stewart, 2000, Klabunde, 2005).

Prevalence is the term to describe the amount of HF patients per population within the time frame of the study. A review study reported that the overall prevalence rate is from 3/1000 to 21/1000 (McMurray and Stewart, 2000).

Incidence is new occurrences that take place within the time frame of study, however the incidence rate is lesser known than prevalence of HF (McMurray and Stewart, 2000). Framingham Heart Study reported a 2/1000 cases per year (Ho et al., 1993b) while another study reported 1/1000 to 12/1000 cases per year (> 85 years) (Cowie, 2000). Some other studies gave 8/1000

(Remes et al., 1992), or 16/1000 (Rodeheffer et al., 1993). The apparent differences between these studies can be attributed to methodology used.

2.3.3   HF Survival and Mortality Rate

The prognosis for HF is not good. Once diagnosed, the one-year survival rate is 57% for men and 64% for women; the rate further decreased to 25% and 38% at 5-year respectively for men and women as tabulated in Table 2-2 (Ho et al., 1993a). It has even been reported that the clinical course and prognosis of CHF are "*surprisingly grim and not much better than those for cancer in general*" (McKee et al., 1971). A recent finding has suggested that HF is as deadly as most types of cancer when taking five-year survival rate for cancer into account, with only lung cancer rated as having a worse prognosis (Stewart et al., 2001).

Table 2-2: Estimation using Kaplan-Meier curve for overall survival rate after diagnosed with congestive HF (CHF) from Framingham Heart Study (Ho et al., 1993a)

	Median (years)	90 days	1 year	2 years	5 years	10 years
Men	1.66	0.73±0.02	0.57±0.03	0.46±0.03	0.25±0.02	0.11±0.02
Women	3.17	0.72±0.03	0.64±0.03	0.56±0.03	0.38±0.03	0.21±0.03

It is difficult to actually determine the mortality rates in the UK and other countries, due to the explicit guideline, by the World Health Organization (WHO), for doctors not to put HF as the underlying cause of death but rather as the mode of dying.((WHO), 1977) . In spite of that, there are studies that compiled the death certificate in the UK, and computed the mortality rate from HF; for example a group reported an annual rate of -2.9% (men) and -2.6% (women)(Goldacre et al., 2005).

2.3.4   Heart Failure Symptoms

The simplest definition of heart failure (HF) attributes the inability of heart to supply adequate perfusion to the whole body. Due to decreased perfusion, whenever there is an increased physical activity, fatigue and dyspnoea (breathlessness) occur. This is one of the main symptoms of HF.

Another symptom is oedema or fluid retention that normally shows at the ankle or inferior extremities (peripheral oedema), or fluid retention at lungs (pulmonary oedema) depending on which side of the heart is failing.

In case of the left side failure, the inability of heart to pump adequate blood increases hydrostatic pressure differences between the heart and the lung, which hinders blood entry into the left heart. This causes fluid retention in the lungs, causing the patient to experience breathlessness. In a patient's x-ray, pulmonary oedema will manifest itself as an anomaly in the lung, as illustrated in Figure 2-18. For the right side failure, the systemic circulation faces an increasing pressure gradient from the right atrium due to increased right atrial pressure. Instead of CVP roughly at 0 mmHg, the CVP increases up to +5 mmHg, which is typical in damaged heart (Guyton and Hall, 2006), and causes peripheral oedema at lower extremities such as at the ankle.
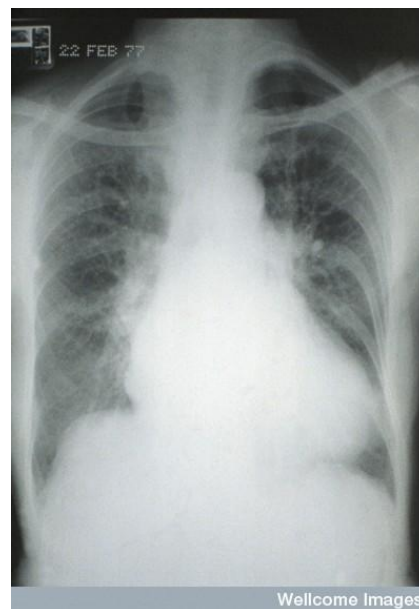
Figure 2-18: X-ray of a HF patient showing a dilated heart and excessive fluid at the lungs. (Picture courtesy of Wellcome Library, London)

Another way of categorising HF depends whether dysfunction occurs in systole or diastole. For the systolic dysfunction, it is characterized by reduction in the ejection fraction (EF) due to pumping failure, caused by enlarged end-diastolic chamber volume due to myocardium enlargement. It is rare to find systolic dysfunction without accompanying diastolic impairment; in clinical practice, the occurrences of HF with cardiomegaly are normally associated with systolic dysfunction characteristics. Diastolic dysfunction, on the other hand, although is not so easily diagnosed is defined as filling volume impairment due to increased filling resistant (Federmann

and Hess, 1994). The increased filling pressure due to hypertrophied heart leads to increased pressure within the lungs, and this brings about pulmonary oedema.

2.3.5 Cardiomyopathy

The cardiomyopathy (a form of heart failure) is a disease where the heart experiences structural changes resulting in enlargement (dilation) and/or hypertrophy (stiffening) of ventricular chamber. The incidence of dilated cardiomyopathy is 36.5/100,000 as opposed to hypertrophied cardiomyopathy at 17.9/100,000 population (Codd et al., 1989). There are various kinds of cardiomyopathy as tabulated in Table 2-3:

Table 2-3: Types of cardiomyopathy and its dysfunction category

Systolic Dysfunction	Diastolic dysfunction
• Dilated cardiomyopathy (DCM) • Ischaemic cardiomyopathy • Arrhythmogenic right ventricular cardiomyopathy (ARVC) • Non-compaction cardiomyopathy	• Hypertrophied cardiomyopathy • Restrictive cardiomyopathy

Depending on types of cardiomyopathy the resulting HF is either an inability to pump blood efficiently due to loss of inotropic ability (systolic) or it could be a normal ejection fraction but with increased filling pressure (diastolic), and if left untreated would progress to congestive HF.

In this report, the dilated cardiomyopathy (DCM) is discussed in general and the idiopathic dilated cardiomyopathy (IDCM) will be further explained. Compared to other types of cardiomyopathy, the dilated cardiomyopathy is much more common (Mohan et al., 2002, Lloyd-Jones et al., 2010), although some of the patients may be without any symptoms, while the rest would progress to congestive heart failure (CHF) stage. Figure 2-19 is an image of a heart with a dilated cardiomyopathy. There are various kinds of causes leading to DCM such as electrolyte, nutritional or endocrine abnormalities, chronic hypertension, infection, infiltrative or rheumatologic or valvular heart or neuromuscular disease, myocardial ischaemia, tachyarrhythmia and toxins (Mohan et al., 2002).
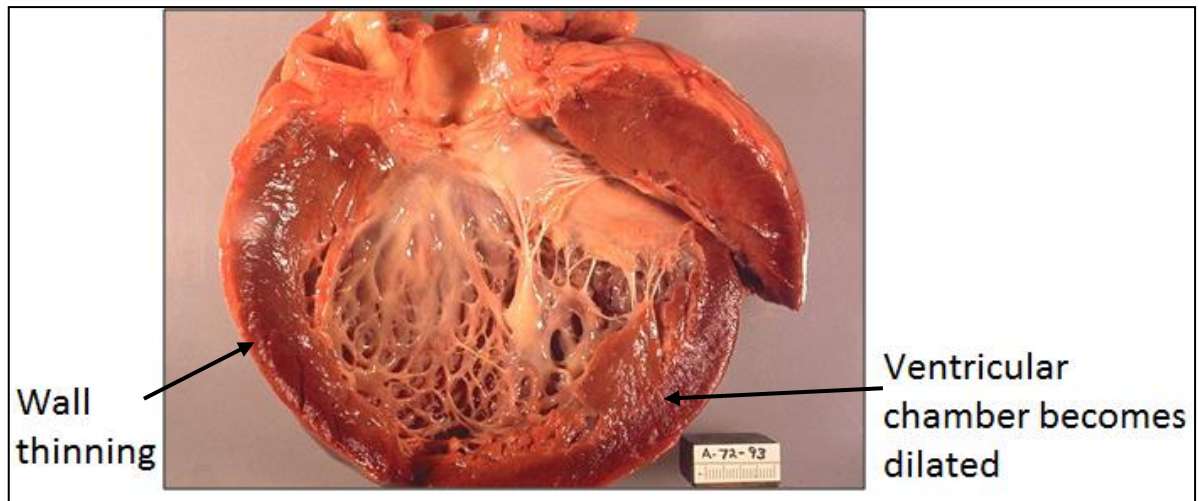
Figure 2-19: Cross section of a HF secondary to idiopathic dilated cardiomyopathy. Note the enlarged size and spherical shape of the LV wall. (Image courtesy of Public Health Image Library (PHIL). http://phil.cdc.gov)

Since the cardiomyopathy is one of the causes leading to HF, the clinical features are quite similar to HF, with symptoms relating to left ventricular or biventricular systolic dysfunction. Vague symptoms without any specific cause such as fatigue, weight loss, appetite loss first emerge before further progressing to peripheral oedema, dyspnoea, orthopnoea[4] and paroxysmal nocturnal dyspnoea[5]. There were also cases of sudden death secondary to IDCM although uncommon (Mohan et al., 2002).

The systolic dysfunction effect is loss of inotropy i.e. weakening myocardial contractile power to push blood into the next chamber. The effect of IDCM to the PV loop is illustrated in Figure 2-20, where the systolic dysfunction is illustrated by the decreased ESPVR slope. There is a reduction in the volume of blood ejected from the left ventricle in systole due to the loss of ventricular contractility. The increasing end-systolic blood volume means with incoming blood during diastole, the end-diastolic volume increases, and in effect shifts the end point (point 1 of Figure 2-12) to the right on the compliance curve i.e. EDPVR line which also means an increase in preload. However, the combined end-diastolic blood volume is smaller than end-systolic volume, hence decrease in SV ejected (Kato et al., 1996, Klabunde, 2005).

---

[4] A type of breathing difficulty occurs when lying down. The symptom is relieved when taking upright position.
[5] Paroxysmal nocturnal dyspnoea: a type of dyspnoea (shortness of breath) that occurs when the patient sleeps, often after one or two hours. It is relieved by sleeping in upright position
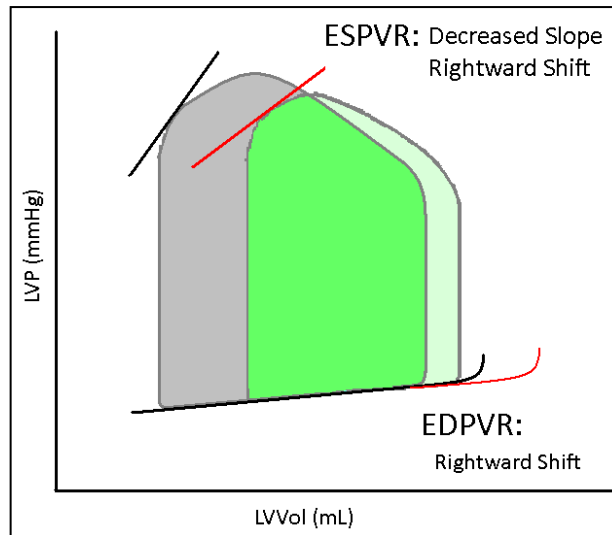
Figure 2-20: The effect of IDCM to PV loop. The ESPVR slope reduction means reduced contractility, as well as EDPVR curve shift to the right hence increasing both end-systolic and end-diastolic blood volume; this leads to overall less stroke volume and reduced left ventricular peak systolic pressure

Normal ejection fraction (EF) is around 65% - 70%, but in cases of systolic dysfunction HFthis may fall below 20%. One of the inclusion criteria for IDCM is an ejection fraction of below 45% as shown in Table 2-4.

Table 2-4: Diagnostic criterion for IDCM (Mohan et al. 2002)

Inclusion	- LVEF < 45% and/or fractional shortening < 25% (>2 SD below mean) - LV end-diastolic diameter > 117% of the predicted value
Exclusion	- Systemic hypertension (>160/100 mmHg) - Coronary artery disease (>50% in one or more major branches) - Chronic excess alcohol (>40g/day :women, >80g/day : men) - Systemic disease known to cause dilated cardiomyopathy - Pericardial diseases - Congenital heart disease - Cor pulmonale - Rapid, sustained supraventricular tachycardia

The diagnosis of IDCM is done by exclusion of other aspects of cardiomyopathy rather than diagnosing IDCM directly (Manolio et al., 1992, Mohan et al., 2002).

There has been lots of evidence that IDC patients respond well to treatment by Left Ventricular Assist Device (LVAD), Hetzer et al. (1999) reported that all 19 patients suffering HF secondary to DCM enrolled in their trial evaluating mechanical heart assistance had improved cardiac functions (Hetzer et al., 1999). Other notable studies reported 75% survival rates over 5 years after explantation of LVAD (Dandel et al., 2005), while another study reported over 85% survival rates after 4 years with aggressive drug treatment (Birks et al., 2006).

2.4   Method of Treatment

Heart failure (HF) is initiated from various pathophysiological causes (refer to 2.3.2   Heart Failure Risk Factor, Aetiology). There are several models to explain HF progression. Those models are: the haemodynamics model consisting of cardiorenal and cardiocirculatory models, and the neurohormonal model. Each model yields specific treatment strategy focusing on respective model prediction of HF mechanism (Mann and Bristow, 2005). For example, cardiocirculatory model was proposed as a result of observation that in HF patients, compromised blood perfusion from reduced cardiac output was the result of myocardial pump failure. That finding leads to administration of positive inotropes increasing the heart's contractility, and intravenous vasodilator decreasing peripheral resistance to boost cardiac output.

The goals of HF treatment are:

1) to reduce the clinical symptoms of HF i.e. alleviating pulmonary/peripheral oedema and dyspnoea,
2) to slow HF deteriorating process , if the above is difficult,
3) to improve myocardial function,
4) increasing survival rate.

There are two HF classification systems in use at present to diagnose the level of HF disease. The New York Heart Association (NYHA) classification, a functional classification, recognises the symptomatic condition of the disease. NYHA classification divides HF into four classes, from mild cases (Class I) to severe and chronic cases (Class IV) (Association, 1964). However, NYHA classification does not address any possibility of patients with underlying risk factor progressing to HF, thus hindering effective treatment management (Mosterd and Hoes, 2007).

The American College of Cardiology and American Heart Association (ACC/AHA) proposed a classification system that focuses on the evolution and progress of HF. The ACC/AHA classification has four categories, namely stage A to D (Hunt et al., 2001). Both classifications, NYHA and ACC/AHA, are usable and overlap with each other. One interesting fact about ACC/AHA classification is that a patient may progress from stage A to stage D, but the recovery path is not in reverse, contrary to NYHA functional classification where with some pharmacological treatment, patient with NYHA Class IV could be reversed to Class III (M. Jessup & Brozena 2003). Table 2-5 tabulates both NYHA and ACC/AHA classifications.

Table 2-5: HF classification coding and corresponding treatment

NYHA class	AAC stage	Treatment
-	**A** -At high risk developing HF in the future but no functional or structural disorder	• Lifestyle adjustment, education • Reduction of risk factors • Treatment for underlying disease such as diabetes and/or hypertension by prescribing ACE inhibitors or angiotensin-receptor blocker (ARB) in some patient
I -no daily limitation and no symptoms from ordinary activities	**B** -Those with structural disorder but no symptoms at any stage	• ACE inhibitors and β-blocker in all patients
II -slight or mild limitation of activity. Comfortable at rest but can tolerate mild exertion	**C** - has previous or current symptoms of HF in the context of an underlying structural heart problem, but	• Administration of diuretics and digoxin, and salt intake reduction • Cardiac resynchronization (in case of bundle-branch block) • Surgical intervention, heart valve

III -has considerable limitation on any activity, only comfortable at rest	managed with medical treatment	corrective surgery • Aldosterone antagonist
IV -any physical activity brings on discomfort and symptoms occurs even at rest	D - advanced stage requiring hospital based support, a heart transplant or palliative care	• Inotropes • Mechanical assistance • Heart transplantation • Hospice
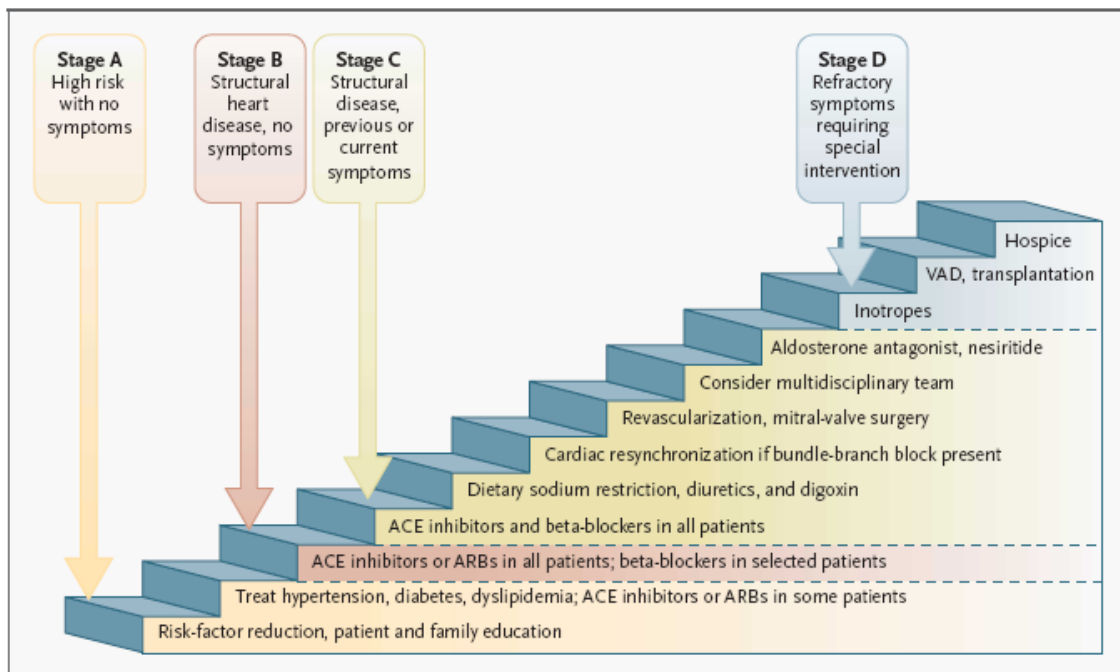
Figure 2-21: The HF treatment in accordant to classification by ACC/AHA. Reproduced with permission from (Birks et al., 2006) Copyright Massachusetts Medical Society

Figure 2-21 illustrates the treatment given to a patient, which can be divided into several distinct ways: pharmacological treatment, non-pharmacological treatment such as cardiac resynchronization therapy (CRT), surgical intervention or mechanical assistance i.e. left ventricular assist device (LVAD), total artificial heart (TAH), and lastly heart transplantation (Birks et al., 2006). An example of surgical intervention is corrective surgery on impaired coronary artery

which might involve revascularization (enlargement of the coronary artery) by angioplasty, stent introduction or surgical approach such as the coronary artery bypass graft (CABG) or the off-pump coronary artery bypass (OPCAB) surgery. It was reported that these approaches improved cardiac performance and reduced sudden death risk (Baumgartner 2001). Other examples of surgical intervention are valve restructuring or exchange of native valve to prosthetic valve, either mechanical heart valve (MHV) or bio-prosthetic valve.

The standard pharmacological drugs for congestive HF treatment are tabulated in Table 2-6 (Remme and Swedberg, 2001, Levick, 2003, Klabunde, 2005).

Table 2-6: Standard pharmacological drugs for HF patient

Drug	Effect/objective
ACE inhibitors	The main effect is decreasing vascular resistance thus increasing CO. The drug works by lowering the level of angiotensin II, consequently the level of aldosterone. This reduces the level of arterial vasoconstriction. ACE inhibitor dilates the arteries and veins, thus decreasing vascular resistance.
Loop diuretics	Its main objective is to reduce fluid retention thus reducing cardiac distension, dyspnoea and oedema (pulmonary, peripheral).
Beta blocker	Reducing heart rate thus increasing ejection fraction.
Positive Inotropes	Increasing failing heart's contractility thus increasing cardiac output.
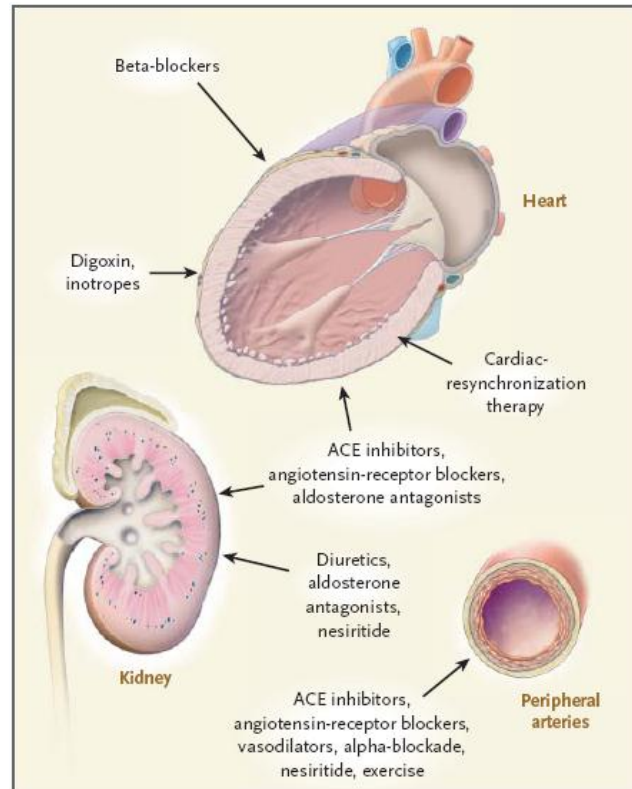
Figure 2-22: Medical treatment to the failing heart is almost always a multi fold approach. The prescribed medicines not only intended for the heart, but also affecting other organs such as the kidneys that controls angiotensin, and renin secretion. Reproduced with permission from (Birks et al., 2006) Copyright Massachusetts Medical Society

Figure 2-22 illustrates the target organs of pharmacological drugs. The objectives are to improve symptoms and to reverse the damage from cardiovascular disease. Some of the drugs are also used for other disease, e.g. ACE inhibitors for hypertension. For example, the ACE inhibitor affects peripheral arteries vasodilation, the kidneys secretion of renin and aldosterone, the heart's remodelling and hypertrophy and renal blood flow(Birks et al., 2006).

The last available option for HF treatment and also the gold standard is the heart transplantation. The first human transplantation was successfully carried out in 1967, although the patient died from complications (Barnard, 1967). Compared to early days of heart transplantation, where the actuarial survival rate for one, five and ten years was 68%, 41% and 24% respectively (Robbins et al., 1999); the prognosis of heart transplantation has progressed tremendously at around 87% for 1-year survival rate, 72% for 5-year survival rate and 50% for 10-year survival rate (UNOS, 2007). The cyclosporine introduction in 1985 increased survival rate from 70% at 1-year to more than 80% at 1-year (Hunt, 1998). Figure 2-23 illustrates the Kaplan-Meir survival trend for heart transplantation surgery.
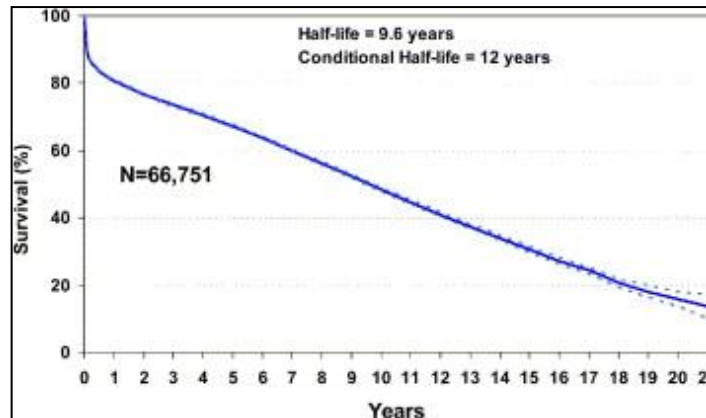
Figure 2-23: The Kaplan-Meier survival for heart transplantation between January 1982 and June 2003. (With kind permission from Elsevier) (Taylor et al., 2005)

In spite of the excellent heart transplantation track record, donor limitation has made it difficult for this treatment to be in widespread use. In the UK, donated heart figure for cardiac transplantation has not changed much since 1979, or even in the whole world, and most probably this trend continues in the future. Heart transplant operation in the UK for year 2007/2008 was just 135 cases, a clear decrease from 162 recorded for year 2006/2007 (Transplant, 2008). Worldwide, heart transplantation surgery record was around 3000 cases/year with the USA leading the pack; for example 2333 cases of heart transplantation were reported in 2010[6].

2.5   Mechanical Assistance for the Failing Heart

Another option to treat heart failure is by mechanical assistance, which is discussed hereafter.

2.5.1   Brief History of Heart Assist Device

One French physiologist in 1812, Le Gallois, put forward suggestion that by providing perfusion to an organ, it can be kept alive. The first documented description of artificial heart was penned and illustrated by Étienne-Jules Marey in 1881 (Ratner, 2004). Carrel and Lindbergh back in 1935 described the usage of mechanical circulatory assistance in animal testing in their seminal book '*The Culture of Organs*' (Carrel and Lindbergh, 1935). The first successful mechanical circulatory assist in clinical setting on human was demonstrated by Dr. Gibbon when he used the heart-lung machine to perform cardiopulmonary bypass surgery in 1953, successfully proving that human can be supported by machine (Gibbon, 1954). The roller pump, invented by a Dr DeBakey,

---

[6] http://optn.transplant.hrsa.gov/latestData/rptData.asp

originally intended for donor-to-patient blood transfusion, was incorporated in the heart lung machine and still remained in use (DeBakey, 2003).

An early example of a total artificial heart (TAH) was in 1957, where Dr. Kolff's group headed by Dr. Akutsu fabricated an artificial heart made of polyvinylchloride, and implanted the TAH in an anaesthetised dog. The dog was supported for 90 minutes thus proving that an artificial heart could support the circulation of an animal (Akutsu and Kolff, 1958). Another example was from Dr. DeBakey's group where a patient was successfully supported postcardiotomy by using a biventricular device until the patient heart was strong enough to be weaned off after 10 days of support (Liotta et al., 1963, DeBakey, 1971).

The desperate need to treat congestive HF spurred a new interest onto LVAD, especially in the wake of dismal result from early years of heart transplantation period. After support from the USA government through the National Heart, Lung, and Blood Institute (NHLBI) in the 70's and 80's, the result was evident in 1978, when the first usage of LVAD as a bridge to transplantation (BTT) for heart and kidney was successful (Norman et al., 1978). Early LVADs were pneumatically driven, however an electrically actuated LVAD[7] were successfully tested in 1984 (Portner et al., 1985). The mechanical heart assist devices available now range from a simple and relatively cheap balloon pump to a more expensive and complex TAH.

The mechanical assistance is recognized as a stop-gap option for the most severe patients while serves to assist blood circulation for the other less severe patients. Normal indicators for implantation of a heart assist device into a HF patient are: patient's condition (NYHA class III or IV), refractory to pharmacologic treatment, receiving maximal inotrope support and/or receiving an intra aortic balloon support. Those in the heart transplantation list who exhibit severe chronic HF criteria such as cardiac index less than 2 L/min.m^2 is considered for heart assist device implantation, with intention of Bridge-to-Transplantation (Mancini and Burkhoff, 2005). More exhaustive indications are tabulated in Table 2-7 (Kirklin and Naftel, 2008).

---

[7] Novacor LVAD, World Heart Corp, California, USA

Table 2-7: LVAD indications depending on the treatment intention (Kirklin and Naftel, 2008)

Treatment intention	Indication
Bridge to Transplantation (BTT) *(The device is implanted with intention of supporting the patient until heart donor is found)*	• End stage HF despite inotropic support • Supported with/without IABP • Acute renal dysfunction • Pulmonary hypertension (PA systolic pressure > 60 mmHg) • Refractory to inotropic support • Deemed to be suitable for mechanical assist therapy
Bridge to Recovery (BTR) *(Patient is expected to recover when implanted with an LVAD)*	• Acute myocardial infarction • Acute myocarditis with shock • Acute cardiac failure post cardiac surgery
Destination Therapy (DT) *(For end-stage HF patient, and also not included in the transplantation list, DT device is implanted permanently)*	• Class IV HF with chronic disabling condition • Refractory to optimal therapy • Low myocardial oxygen consumption < 12-14 mL/(kg-min) • Dependant to inotropic support intraveneously • Expected mortality rate within a year > 50%

A more thorough lists of LVAD indication/contraindication as a DT is given by Stevenson and Shekar (2005) in their review of LVAD as a long term mechanical support. The patient can only be included into the selection if he/she is at the end stage condition for more than 60 days out of the three months under observation (Stevenson and Shekar, 2005).

The LVAD implantation is also extended for those not included in the heart transplantation list. Depending on the respective HF treatment centre inclusion criteria, the patient could be implanted with the intention of Bridge-to-Transplantation (BTT), Bridge-to-Recovery (BTR) or Destination Therapy (DT)(Mancini and Burkhoff, 2005, Williams and Oz, 2001).

There are three ways of using mechanical means to augment blood perfusion (Jeevanandam et al., 2002):

1. direct augmentation to the heart using a deformable membrane wrapping the heart. This technique is known as dynamic cardiomyoplasty,
2. using a mechanical pump to direct blood from the left atrium/ventricle to the aorta,

3. energy is supplied to a portion of the vascular system during diastole to increase blood perfusion and to reduce afterload.

The third method is also known as counterpulsation. Figure 2-24 illustrates the classification of various heart assist devices according to the type of augmentation method.
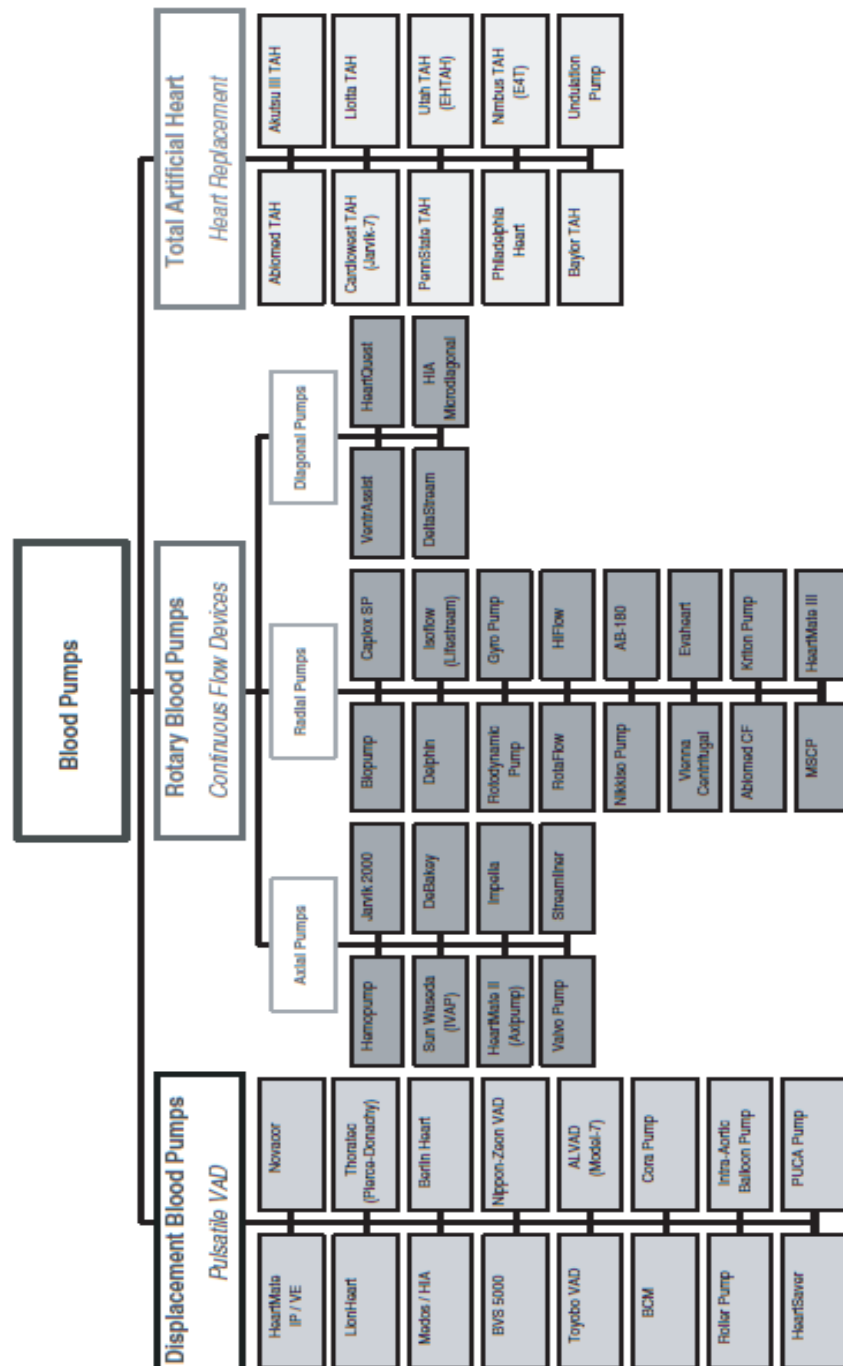
Figure 2-24: Classification of mechanical heart assist devices. The devices are classified according to activation method, either by pushing blood from the device chamber by deformable membrane, or by using impeller, or by replacing the native heart with an artificial heart. (With kind permission from Sage Publications) (Reul and Akdis, 2000)

Displacement blood pump are also known as pulsatile blood pump due to the usage of pusher plate or a deformable membrane. The activation of pulsatile blood pump might be independent of heart rhythm, or it could be anti-phasic such as IABP. The displacement pump is sensitive to preload but can withstand high afterload.

Contrary to the displacement blood pump, flow from the rotary blood pump is continuous flow. The rotary blood pump (RBP) is categorised into axial, radial, or diagonal type. Hydraulic efficiency (i.e. maximum flow output vs supplied power) is best in the radial design, but similar output can be achieved with a smaller axial type. The rotary blood pump has the characteristics of preload insensitivity and afterload sensitivity (Miller, 2006).

There are differences between a radial and an axial rotary blood pump, but the most prominent is the size. Axial flow blood pumps are smaller and only have one moving part (the central impeller), suspended by magnetic bearing, thus decreasing thrombus formation. The flow output of a radial blood pump is around 5 – 7 L/min with 100 mHg pressure increase; however, an axial blood pump has to rotate at a much higher velocity to achieve the same output thus the rotational speed of the diffuser is very high at 15,000 – 25,000 rpm compared to radial/diagonal design (1500 – 3000 rpm) (Miller, 2006).

The diagonal type combines both axial and radial characteristics, thus has mixed advantages and disadvantages. Due to the advantages of rotary blood pumps such as lower blood damage, smaller size, lower filling volume, better transportability and absence of spallation, rotary blood pumps have been introduced for medical applications where the majority of rotary type pump are of radial type(Reul and Akdis, 2000). Among rotary blood pumps available are Jarvik 2000 (axial type), DeBakey (axial type) (Figure 2-25), and Medos DeltaStream DP1 ® (diagonal).
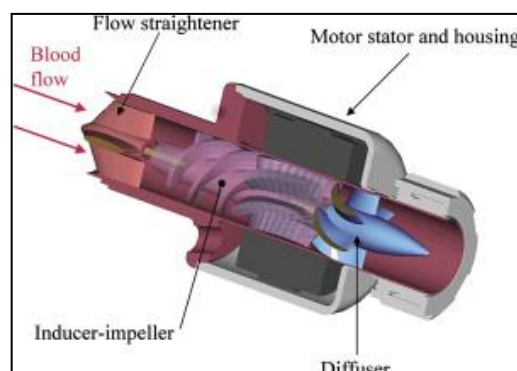
Figure 2-25: A cross section of the MicroMed DeBakey VAD. (With kind permission from Elsevier) (Frazier and Jacob, 2007)

An orthotropic Total Artificial Heart (TAH) is a blood pump that replaces the explanted natural heart in terms of anatomical replacement and function. Such a system, which would replace the human heart reliably and without complications for months or eventually years, does not yet exist. The TAH is used for terminally ill patients at end-stage of CHF and either waiting for heart transplantation, or not listed in heart transplantation list. The TAH device available in the market is intended for BTT. An example is the SynCardia temporary TAH illustrated in Figure 2-26, which is now a FDA, CE and Health Canada approved TAH[8].
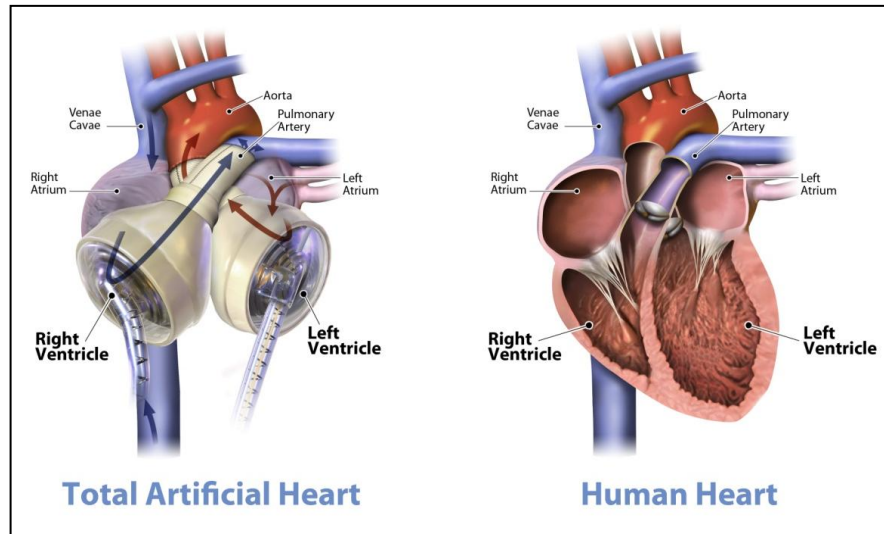
Figure 2-26: A SynCardia temporary total artificial heart implanted to replace failing native heart as a temporary measure awaiting heart for transplantation. (With kind permission from SynCardia System Inc.) (http://www.syncardia.com)

A 10-year pivotal study using SynCardia temporary TAH was conducted at five separate centres on 81 patients. The survival rate to transplantation between TAH implanted and non-implanted control group was statistically significant (79% vs. 46%, $p < 0.001$). The post-implantation rate of survival for transplanted patient with a TAH are 86% (one-year) and 64% (five-years) (Copeland et al., 2004).

There is another type of a blood pump classifications proposed by Olsen (2000) that classified the blood pump type into several generations. The first generation blood pumps are the pulsatile or positive displacement blood pumps, which are primarily used as a BTT device. The second generation is the blood contacting mechanical bearing rotary blood pump, which then progressed to the third generation blood pump with a magnetic levitation system that minimises contact with moving parts; in the third generation type, only the levitated impeller is the moving part. The

---

[8] http://www.syncardia.com/images/stories/files/FactSheet_Total-Artificial-Heart.pdf

fourth generation blood pump was theorised to move blood using magneto-hydrodynamics principle (Olsen, 2000).
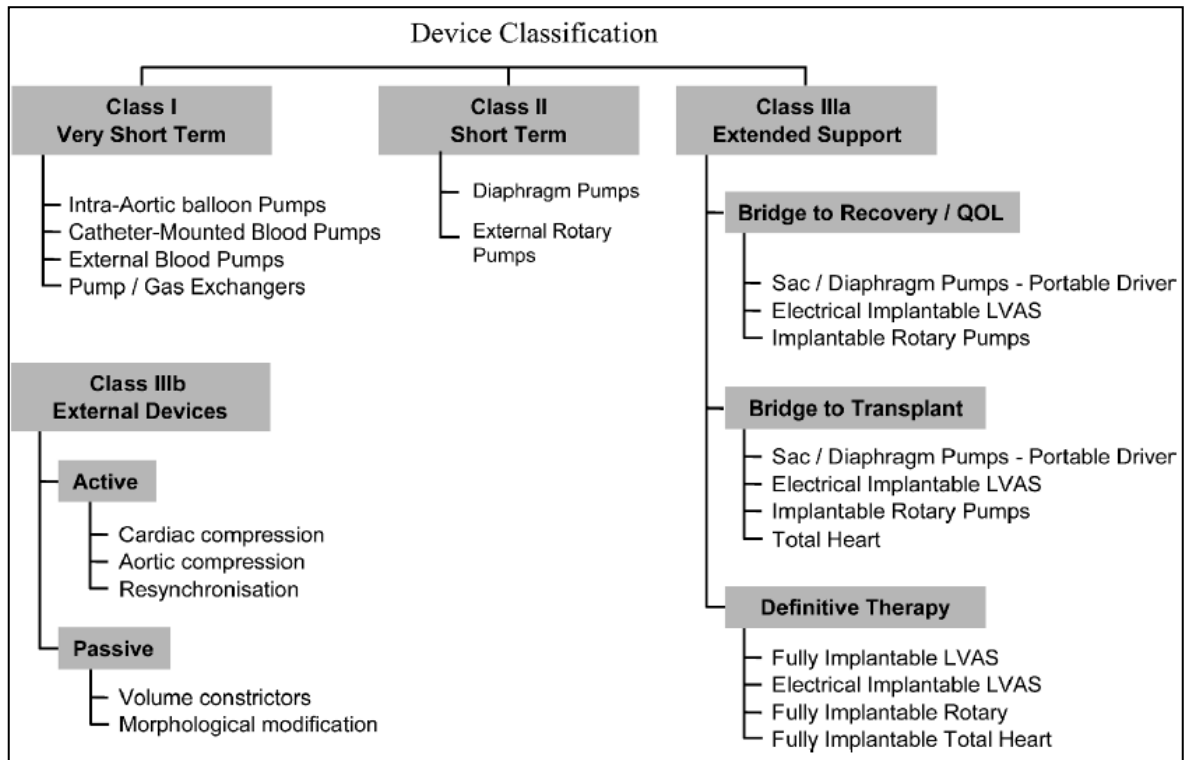
Figure 2-27: Heart assist device classification based on the intended us of device, from short term to long term support (with kind permission from Sage Publications) (Wheeldon, 2003)

Figure 2-27 illustrates another classification system that divides devices according to period of use; from a very short term of a couple of hours (Class I) to few weeks to months (Class II), or the Class III (extended support group) that was designed to become the alternative to the heart transplantation with some permanently implanted, hence the Destination Therapy (DT) subgroup (Wheeldon, 2003).

A multi centre randomised trial (REMATCH: Randomized Evaluation of Mechanical Assistance for the Treatment of Congestive Heart Failure) was conducted with the objective of studying the effectiveness of mechanical heart assist devices compared with optimal medical management. The LVAD used was a pulsatile displacement type[9]. The result tabulated in Table 2-8 shows that the usage of LVAD prolonged the survival of patients compared to those in the medical therapy group at one-year and two-year evaluation period (Rose et al., 2001). The finding from that

---

[9] HeartMate VE, Thoratec Corporation, CA, USA.

seminal paper won the approval from the FDA to classify the LVAD as a BTT device while being a candidate for a DT device.

Table 2-8: Survival rate for one year and two years reproduced from REMATCH study (Frazier et al., 2001)

Kaplan-Meier survival rate	LVAD treatment	Medical therapy
1-year	52%	25%
2-year	23%	8%

A non-randomised trial (INTrEPID: Investigation of Nontransplant-Eligible Patients Who Are Inotrope Dependant) aimed to determine the long term effectiveness of Novacor LVAD[10] on non transplant candidate patients. Both 6 months and 12 months results showed significant LVAD effect compared to optimum medical treatment (6 months: 46% vs. 22%,$p = 0.03$; 12 months: 27% vs. 11%, $p = 0.02$)(Rogers et al., 2007). This has reinforced the positive effect of LVAD augmentation on LV functional capacity, as well as prolonging the survival of the patient.

There has been quite a polemic on the differences between pulsatile and non-pulsatile blood pumps, especially the effect of pulsatility to human physiology (Undar and Fraser, 2002, Undar, 2004, Travis et al., 2007). A randomised trial was carried out by Slaughter et al. (2009) to compare the outcome between pulsatile[11] and non-pulsatile i.e. continuous axial blood flow[12]. The result is tabulated in Table 2-9, where the non-pulsatile i.e. continuous flow blood pump patients showed a higher survival rate, although both pulsatile and non-pulsatile type yielded a significant effect in increasing patient's quality of life and functional capacity (Slaughter et al., 2009).

Table 2-9: Survival rate between non-pulsatile and pulsatile blood pump at one-year and two-year period (Slaughter et al., 2009)

Kaplan-Meier survival rate	Non-pulsatile blood pump	Pulsatile blood pump
1-year	68%	55%
2-year	58%	24%

---

[10] World-Heart, Oakland, California, USA
[11] HeartMate, XVE, Thoratec Corp., CA, USA
[12] HeartMate II, Thoratec Corp., CA, USA

The main reason given for the low rate of pulsatile flow blood pump survival rate was durability of the heart assist device. In the pulsatile blood pump cohort, 36% (24 out of 66 patients) was excluded from the trial due to pump replacement or repair operation. For the non-pulsatile blood pump patient, the value was only 10% (Slaughter et al. 2009).

Two important findings from above are:

1) mechanical heart assist device is proven to prolong end-stage HF patient life far better than with optimal medical treatment only,
2) continuous flow blood pump has shown to increase survival rate compared to pulsatile blood pump due to its durability.

There is an ongoing registry for clinical trials conducted using blood pump at the USA since 2003. The INTERMACS registry was set up to collect relevant information regarding VADs implantation all over the USA. The data is then used to provide better guidance for researchers to improve patient selection criteria, upgrade existing heart failure treatment strategy. The same data is also used to improve existing and next generation devices development and relevant regulation. Furthermore, with the registry information, further heart failure treatment research can be carried out more effectively (Kirklin et al., 2008). At present, there are more than 6000 patients registered with the INTERMACS since 2006.

The patients enrolled in the INTERMACS were divided into seven profiles as depending on the conditions when VAD was implanted as tabulated below (Stevenson et al., 2009).

Table 2-10: INTERMACS profile description(Stevenson et al., 2009)

	INTERMACS profile	Description
1	Critical cardiogenic shock	Also known as "Crash and burn" patients. Patients are in critical condition refractive to increased inotropic support leading to life-threatening hypotension. The condition is further confirmed with increasingly dangerous acidosis and/or lactate levels.
2	Progressive decline	Despite intraveneous inotropic support, patients bodily function continue to decline with evidence from renal function, decreased nutritional absorption, and deteriorating volume balance. "Sliding on inotropes". Patients are also intolerant to inotropic theraphy

3	Stable but inotrope dependent	The patient bodily function is stable with the help of intravenous inotropic support, or temporary circulatory support device, or both. However, effort to wean patient has failed. "Dependent stability"
4	Resting symptoms	The patients show congestion symptom daily while in rest or during activities of daily living. Administration of diuretics is difficult due to frequent congestion level change. May change from/to profile 5.
5	Exertion intolerant	House bound patient who is comfortable at rest, and even during normal daily activity. Further intervention depend on nutritional status and organ function performance.
6	Exertion limited	No evidence of oedema, patient is able to perform daily activity, and comfortable at rest, although after a few minutes of meaningful activity, the patient tend to be overcome with fatigue."Walking wounded"
7	Advanced NYHA III	The patient is healthy enough to withstand meaningful activity (although limited up to mild physical exertion).

There has been tremendous change in the way heart failure treatment is managed with the advent of the INTERMACS registry. Data from the INTERMACS was disseminated quickly, compromise of thousands of valuable data unrestricted by limitation of randomized clinical trial scope. The clinical practice has evolved thanks to the data gained and managed by the INTERMACS registry (Miller et al., 2010).

2.5.2 Myocardium Reverse Remodelling

One favourable effect of HF treatment is myocardium reverse remodelling. There are several ways ventricular remodelling can be initiated. Those would be: 1) from myocardial infarction (MI), which occurs acutely and insults the myocardium causing myocyte necrosis, thus initiating infarct expansion acutely and chronically, 2) aortic valve stenosis, thus restricting the left ventricular outflow, causing increased intraventricular pressure i.e. pressure overload, 3) mitral valve regurgitation which causes volume overload to the left ventricle; also a factor inducing ventricular

remodelling (Opie et al., 2006) and 4) aortic regurgitation which causes increased preload and end-diastolic volume (Bonow et al., 2011).

In response to all those factors, heart remodelling is indicated by several physiological changes such as cardiomyocyte hypertrophy, changes in collagen amount, phenotype and collagen cross-linking. For HF patients especially secondary to the dilated cardiomyopathy, the severity of the disease is manifested by the leftwards shift of end-diastolic pressure volume relationship (EDPVR) (in PV loop), decreased ejection fraction, wall thinning, and geometrical change in the LV chamber from the normal elongated to a more spherical shape (Levin et al., 1995, Pieske, 2004).

Alongside with study focusing on pharmacological drug effect (further discussed below), there were several other studies that investigated the effect of LVAD on reverse remodelling of the dilated heart.

Studies of the LVAD's effect on HF patients have revealed many interesting facts. The mechanical unloading of the heart reduces the heart's workload, as well as increasing coronary perfusion and this further decreases the myocardium oxygen demand. The mechanical unloading of the LV led to increased LV function in term of EDPVR normalisation (Levin et al., 1995, Madigan et al., 2001), LV ejection fraction (Frazier et al., 1996, Müller et al., 1997, Hetzer et al., 1999, Frazier and Myers, 1999), cardiothoracic ratio (Frazier et al., 1996), and histological data showed that with LVAD myocyte recovery is feasible (Dipla et al., 1998).

Not only the LVAD implantation contributed to haemodynamic aspect, but was also found to encourage reverse remodelling in a dilated heart independently. One hypothesis is that LVAD induced favourable systemic condition (biochemical milieu) for normalising beta-adrenergic axis separately from haemodynamic support effect (Klotz et al., 2005). Another major contributor for myocardial reverse remodelling is by the regression of cellular hypertrophy (Zafeiridis et al., 1998).

A study was published reporting that it takes almost 40 days for the myocardium to reach maximum structural reverse remodelling (Madigan et al., 2001), and for molecular reverse remodelling, it is even quicker, at 20 days. The finding of a peak time for myocardium normalization by Madigan's group was also reported by various other researchers albeit at different time at around 30 days (Frazier et al., 1996, Birks et al., 2006, Maybaum et al., 2007).

There are studies questioning effect of prolonged LVAD support to myocardium recovery (McCarthy et al., 1995), and weaning concept after supported by LVAD for an extended time (Hetzer et al., 1999). That doubt was further exacerbated when patient explanted from the LVAD

had a recurrence of HF and died despite showing remarkable improvement during LVAD implantation; five patients from Hetzer et al. (1999) study died after HF recurrence post-explantation. Although some of the researchers expressed doubts regarding the effect of LVAD post-explantation, there have been studies that showed the possibility of LVAD explantation with increasing success.

Non-standard drug treatment affecting collagen cross-linking has been suggested as the proper way to go forward in HF management treatment (Brower et al., 2006). Another example is with an aggressive non-standard pharmacological regime, using clenbuterol coupled with an efficient LVAD (pulsatile blood pump) management, it was possible to achieve a high percentage of explantation rate at 73%, and freedom from HF recurrence after explantation, at 100% (one-year) and 89% (four-years) (Birks et al., 2006). Birks et al. result, however, is unique, since some research centres recorded around 24% to 30% wean rate (Müller et al., 1997, Dandel et al., 2005). Recently, using continuous flow blood pump, the same group has managed to replicate the result from the previous study for 60% of their patient, with an estimated survival rate of 88.3% at 1 and 3 years, without any HF recurrence (Birks et al., 2011). The initial concept of LVAD as BTT has shifted to BTR and even DT for congestive heart failure patient with contraindication to transplantation.

One study has shown that there are several factors that can serve as a cardiac stability predictor index after weaning from the LVAD. Those are pre-explantation LV ejection fraction (LVEF), left ventricular end-diastolic diameter (LVEDD) and relative wall thickness, as well as the stability of cardiac recovery from unloading, duration of LVAD support and HF duration before LVAD implantation, although the study was concentrated to patients suffering from idiopathic DCM (Dandel et al., 2008).

2.5.3   Intra Aortic Balloon Pump (IABP)

The intra aortic balloon pump (IABP) is a volume displacement type blood pump, used in various stages of invasive heart surgery from peri-operative, intra-operative to post-operative, to help maintain a stable cardiac function. The IABP is also used for patients undergoing percutaneous coronary angioplasty, or suffering unstable angina pectoris or cardiogenic shock. In the USA, it was estimated that IABP was used on 42,000 patients in 2002 (Kozak et al., 2005).

The feasibility of the counterpulsation technique that takes advantage of decreased coronary resistance during diastole was first demonstrated by the Kantrowitz brothers in their seminal paper "*Experimental Augmentation of Coronary Flow by Retardation of the Arterial Pressure Pulse*" (Kantrowitz, 1953). Although the study is not quite related to the aortic flow diastolic augmentation, it paved the way to the inception of the IABP. The first successful attempt on working IABP was by Mouloupolous group in a mock loop setting in 1962. The balloon pump was made by placing a distensible balloon condom over a catheter that later was inserted into an aorta. Carbon dioxide, CO_2, was used as the transport gas in the driveline, and the IABP was inflated during diastole and deflated during systole (Moulopoulos et al., 1962). The development of various counterpulsation devices was actively undertaken by many researchers, such as Clauss et al. (1961) whom tested an extracorporeal pump that remove blood from the femoral artery during systole and pump it back during diastole (Clauss et al., 1961). Counterpulsation technique using autologous muscle in a hemidiaphragm wrapped around the distal thoracic aorta, also known as aortomyoplasty, was also investigated (Kantrowitz, 1987).

In Kantrowitz's 1968 seminal paper introducing the IABP for the first time in a clinical setting, the IABP was inserted into two patients. Both of them showed a tremendous recovery. One of the patients, a 45 years old female with a myocardial infarction prior to hospitalization, was in cardiogenic shock, comatose, in an anuric condition and refractory to medical treatment. Just when the prognosis was deemed hopeless, the IABP was inserted. The patient showed "…*upward trends in systolic and diastolic pressure and a reduction in central venous pressure were observed during intervals of pumping. The urinary output increased from zero to an average of 40 cc/hour*"(Kantrowitz et al., 1968). After 7 hours of IABP support, one of the patients recovered and eventually discharged from hospital. The other patient also showed an improvement from cold and clammy body to warm and dry. However, during repositioning of balloon pump when the activation of the IABP was discontinued, the patient's condition deteriorated and he died. Autopsy revealed many underlying contraindications, which were eventually included into present guidelines criteria, particularly the anterior descending branch of the left carotid artery was occluded (Kantrowitz et al., 1968).

The indications for the IABP are (Trost and Hillis, 2006):

- cardiogenic shock
- intractable ventricular arrhythmias
- post-myocardial infarction (MI) angina or unstable angina refractory to medical therapy

- HF refractory to medical therapy (only used as a temporary supportive measure while awaiting cardiac transplantation)
- haemodynamic support and stabilisation for high-risk catheterisation, angioplasty and coronary artery bypass grafting (CABG).

The above list was supported by a worldwide registry study from over 243 hospitals in 18 countries comprising 17540 records of 16909 patients, although the number one indicator for the IABP deployment was to provide support and stabilisation (at 20.6%) (Ferguson et al., 2001). Subsequent report of the same registry database still showed similar indications (Cohen et al., 2003). In spite of numerous indications, those with an aortic regurgitation, a severe peripheral vascular disease and an uncontrolled septicaemia or a bleeding diathesis are contraindicated from using the IABP (Trost and Hillis, 2006).

Complication due to the IABP is low; only 2.6% of patients suffered severe effect due to major limb ischaemia, severe bleeding, balloon leak, failed insertion and death from the IABP failure(Ferguson et al., 2001). In another study, the highest complication is the limb ischaemia at 0.9% and the mortality directly caused by IABP was 0.05% (Cohen et al., 2003).

The balloon deflation is usually triggered by the peak R wave of the ECG waveform that corresponds to end of systole. Figure 2-28 illustrates the signals used to initiate balloon inflation. The inflation of the balloon commences in the middle of T wave. Sometimes, due to electrical interference or from electrocautery, the ECG signal is inadequate to guide balloon activation. Instead, arterial waveform can be used by matching balloon inflation at the time of dicrotic notch which marks aortic valve closure (Trost and Hillis, 2006, Stenz, 2006).

Figure 2-28: The timing for IABP's balloon activation can be selected using either aortic pressure's dicrotic notch or the ECG's T wave. AP: Aortic pressure, ECG: Electrocardiography

The effectiveness of flow augmentation is determined by the correct and precise timing of balloon inflation and deflation. As stated by Kantrowitz, "*The hemodynamic efficacy of balloon pumping is critically dependent on precise timing of both inflation and deflation in relation to the events of the cardiac cycle*" (Kantrowitz et al., 1992). The operator of the driver console monitors the augmentation of diastole pressure, and selectively controls the inflation and deflation of the balloon to achieve a proper and safe IABP timing (Quall, 1993c). Indeed, improper timing yielded reduction in cardiac output (Wieting et al., 1971). A computer simulation by Jaron et al (1985) yield results suggesting optimal inflation point at dicrotic notch, while deflation timing is a tradeoff between external (blood perfusion) and internal (cardiac energy consumption) variables (Jaron et al., 1985). An *in vitro* study revealed that inflation timing had little influence on stroke volume, while early deflation had some minor negative effect on stroke volume (Niederer and Schilt, 1988).
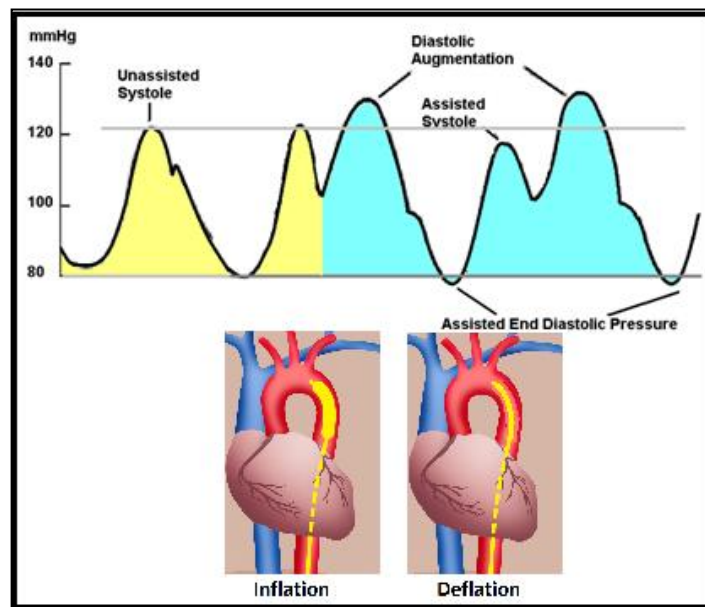
Figure 2-29: Balloon inflation and deflation causing diastolic augmentation and also reducing afterload

Figure 2-29 illustrates the effect of diastolic augmentation to aortic pressure waveform. The action of elevating arterial pressure during diastole is called the diastolic augmentation. The balloon inflation during diastole pushes blood proximally and distally and helps peripheral and coronary perfusion respectively. The deflation of balloon just before systole creates very low pressure region decreasing the aortic pressure; consequently the resistance to eject blood by the LV is reduced. The effect of aortic diastolic pressure reduction can be seen by lowering of peak systolic pressure compared with non-assisted systolic pressure. Less resistance by the left

ventricle decreases myocardial workload (Quall, 1993b, Trost and Hillis, 2006), although the reduction of aortic end-diastolic pressure effect is lost when the patient is in hypotensive condition (Akyurekli et al., 1980).

In terms of metabolic effect, the patient benefits by decreasing myocardial oxygen demand due to afterload reduction and this helps relieve the LV from excessive work to pump blood into the ascending aorta. Left ventricular function is increased by heightened myocardial perfusion due to the increased diastolic pressure in the ascending aorta thus increasing coronary flow (Akyurekli et al., 1980). As a result, global LV systolic function improved (Cheung et al., 1996) as well as diastolic function (Khir et al., 2003). Coronary artery perfusion is greatly dependant on normal arterial structure, since severe aortic stenosis will impede any diastolic augmentation effect from the IABP (Kern et al., 1993). Even the activation of IABP only yield small percentage of blood displaced toward coronary arteries with regards to balloon volume, although still considered a significant increase in coronary perfusion (Kolyva et al., 2010b). Decreased myocardial oxygen consumption was reported to be directly correlated with afterload reduction, and not increased coronary flow for ischaemic patients suffering from medically refractory angina(Williams et al., 1982). Other metabolic effects are favourable increase of urine output, lactate usage and venous oxygen saturation while lactic acidosis is decreased (Papaioannou and Stefanadis, 2005).

The main effect of diastolic augmentation from IABP use is increased myocardium oxygen supply versus myocardium oxygen demand. One way to quantify myocardium oxygen supply and demand is by using endocardial viability ratio (EVR). Myocardial oxygen demand for total left ventricular work has been correlated with the area under the LV systolic curve, termed as tension time index (TTI), thus serves as a reliable predictor (Sarnoff et al., 1957). While myocardial oxygen supply from coronary flow can be determined using diastolic pressure time index (DPTI). The DPTI is defined as the net area between aortic pressure and left ventricular pressure during diastole. Figure 2-30 illustrates an example of how DPTI and TTI is defined. The ratio of oxygen supply and demand can be estimated by dividing DPTI with TTI, termed as endocardial viability ratio (EVR) (Philips et al., 1975), expressed in Eq. 2.15.

$$EVR = \frac{DPTI}{TTI} \qquad\qquad 2.15$$
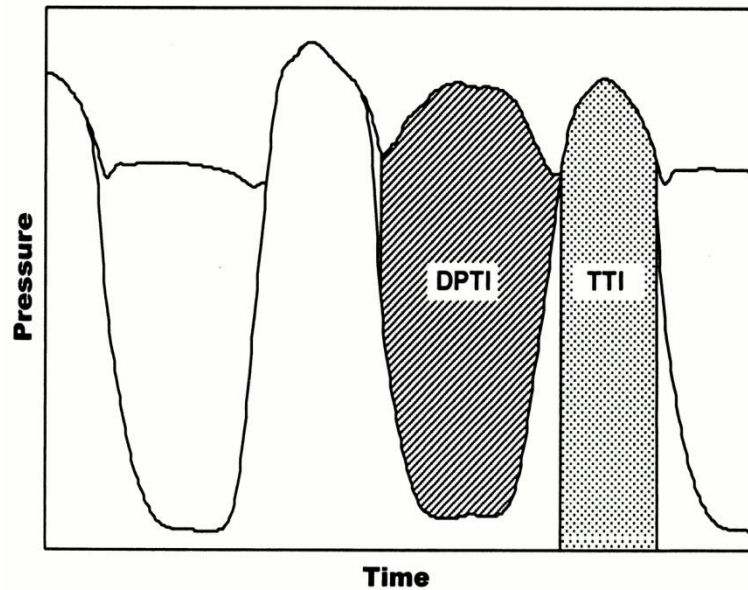
Figure 2-30: The diastolic pressure time index and tension time index is defined as per different shaded area. (With kind permission from Elsevier, (Cmolik et al., 2001))

The ratio of demand and supply varies from healthy heart to failing heart. In a healthy person, the EVR is 1.0, a perfect balance of supply against demand (Quall, 1993b). A failing heart suffering from diminished aortic pressure and increased myocardial oxygen demand naturally has a lower EVR value. Diastolic augmentation by counterpulsation (e.g. through the use of an IABP) has been shown to increase EVR. EVR is investigated in Chapter 4 in association with the CIMS balloon pump.

Technical and biological factors affecting the performance of IABP are (Papaioannou and Stefanadis, 2005):

1) aortic blood pressure, a systolic blood pressure less than 60 mmHg will render the IABP ineffective,

2) stroke volume ejected during systole should be almost the same value as the IABP balloon capacity to render optimal effect,

3) heart rate, the range of 80 to 110b pm is deemed the best range for IABP efficiency,

4) arterial stiffness; stiffer arterial has been shown to increase IABP efficiency especially on cardiac output,

5) balloon displacement volume. Bigger balloon means that higher volumetric displacement can be achieved. However, care must be taken not to occlude inside lumen of the aorta,

6) balloon inflation/deflation speed must be as fast as possible.

A low arterial compliance blood vessel induced low arterial pressure changes from the IABP augmentation (Papaioannou and Stefanadis, 2005). The effect of arterial compliance on the efficacy of the IABP seems to go beyond arterial blood pressure and heart rate as demonstrated in mock circulatory loop and clinical studies. In fact, arterial compliance can be thought as the independent factor determining the efficacy of IABP augmentation (Papaioannou et al., 2002, Papaioannou et al., 2004).

The indications for intra-operative and post-operative are well known, but indications and effectiveness for peri-operative are still an ongoing debate (Baskett et al., 2002, Baskett et al., 2005).

In short, intra aortic balloon pump (IABP) is an acute mechanical heart assist device that delivers relief to heart failure patients; by increasing myocardial perfusion, decreasing resistance faced by the heart from the aorta, decreasing myocardial work, and increasing the ratio of myocardial oxygen supply versus demand. However, aside from the short-term usage of IABP, this mode of treatment is non-ambulatory thus depriving the patient of mobility and normal quality of life.

2.5.4   Pulsatile VAD in, on and around the Aorta

Since the introduction of counterpulsation method by Moulopoulos in 1962, and subsequent successful clinical application by Kantrowitz brothers in 1968, IABP technology gradually matured to present level. There have been considerable spin-off projects trying to manipulate counterpulsation technique on the aorta using various balloon pump designs.

The research on the most optimum site for a balloon pump was conducted by Nosé et al. (1963) and, in separate research, by Furman et al. (1970). Findings from both works indicate the ascending aorta as being the optimal location for diastolic augmentation (Nosé et al., 1963, Furman et al., 1970). The greater the distance of the assist device from the aortic valve, the lower the effect of augmentation would be. Figure 2-31 shows the implantation sites of the assist device by Nosé's group.
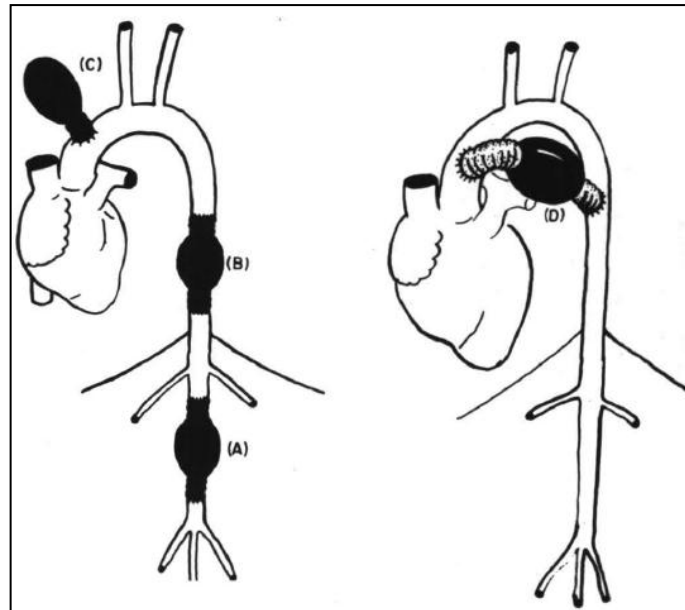
Figure 2-31 : Various experimentation site for diastolic augmentation effect ; A) abdominal aorta, B) thoracic aorta, C) end-to-side anastomosis at ascending aorta and D) bypass end-to-side bridging between ascending and descending aorta. *(With kind permission from Wolters Kluwer/Lippincott, Williams & Wilkins*) (Nosé et al., 1963)

Furman's group made a silicone rubber cuff reinforced with a Dacron graft and a 15 mL polyurethane balloon taped onto it. The cuff was then wrapped around the ascending aorta of a mongrel dog, activated using counterpulsation method. Their results, other than confirming the finding of Nosé's group, showed that a smaller displacement volume (10 mL) at the ascending aorta was better than an intra aortic balloon pump (30 mL) placed at descending aorta (Furman et al., 1970).

Another attempt to exploit the ascending aorta as implantation site was led by J.N. Nanas. The device was quite similar to configuration C of Nosé's trial in Figure 2-31. A chamber made out of polyurethane with a valveless orifice is implanted at the ascending aorta by way of a Dacron vascular graft illustrated in Figure 2-32. The efficacy of the paraaortic counterpulsation device (PACD) was demonstrated by trials on animals comparing PACD with IABP (Zelano et al., 1992, Charitos et al., 1998), and on patients with severe HF condition (Nanas et al., 1996). It was demonstrated that even for a small capacity of 30 mL stroke volume, the PACD was significantly better compared to a 40 mL IABP (Terrovitis et al., 2003). The valveless balloon structure might have increased blood volume stored at the aorta during systole, thus increasing local compliance. The stored blood volume is ejected during diastole thus increasing cardiac output.
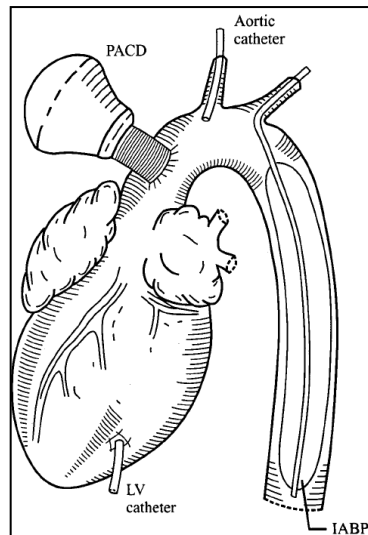
Figure 2-32 : Paraaortic Counterpulsation Device (PACD) implanted at the ascending aorta. *(With kind permission from Springer Science+Business Media)*(Terrovitis et al. 2003)

After IABP, Kantrowitz tried many other types of heart assist device employing counterpulsation technique. Using findings from Nosé's experiment of optimal augmentation site, a balloon pump was positioned along the aortic arch, and the tip of the balloon was a mere centimetre from the aortic valve. They however abandoned the project because "it *proved too cumbersome*" (Kantrowitz, 1987).

Figure 2-33 : The ascending aortic balloon pump has an oval shape to increase aortic diastolic pressure by occluding the ascending aorta during diastole. (With permission from Elsevier) (B. P. Meyns et al. 2000)

A group from Catholic University Leuven of Belgium tested an oval shaped balloon pump named ICS-Supracor[13] illustrated in Figure 2-33. Contrary to the IABP, the device is implanted at the ascending aorta just distal to the heart. The oval-shaped balloon occludes the entire ascending aorta when inflated thus increasing aortic root pressure. The animal trial showed a significant increase in the peak diastolic aortic pressure as well as myocardial blood flow (Meyns et al., 2000).

Another version of an implantable IABP, the Kantrowitz CardioVAD (KCV) was designed by Kantrowitz's group using knowledge and expertise gained from the IABP and previously discontinued devices, illustrated in Figure 2-34 (Kantrowitz, 1987).
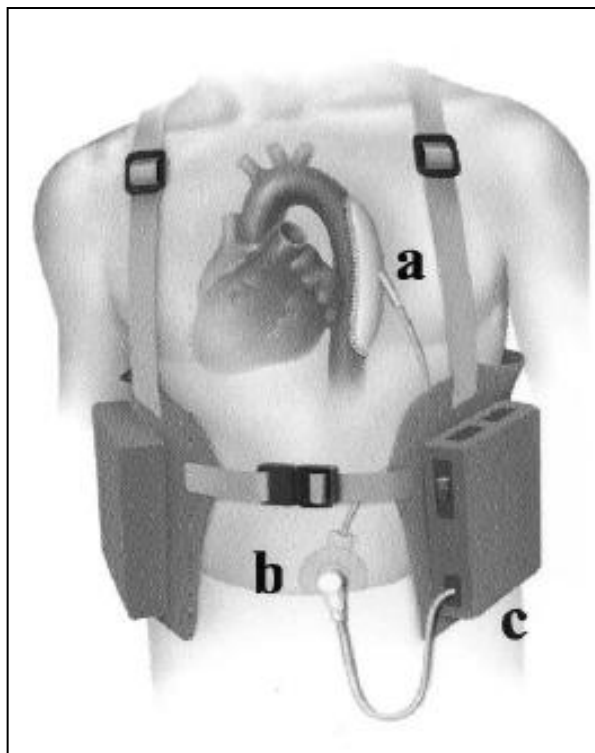
Figure 2-34 : Diagram of Kantrowitz CardioVAD (KCV) implanted in human body consisting of a) blood pump, b) percutaneous access site and c) ambulatory driver console. *(With kind permission from Wolters Kluwer/Lippincott, Williams & Wilkins)* (Valluvan Jeevanandam et al. 2002)

The KCV uses the counterpulsation method to displace blood. Contrary to the short term IABP, the KCV is implanted permanently by replacing an excised portion at the descending aorta. Inflation and deflation of KCV's balloon pump is similar to the IABP, but it is carried out through an external drive unit by way of a percutaneous line. The KCV displacement volume is 60 ml, far larger than adult version of the IABP. One important aspect of the KCV is the percutaneous access

---

[13] Abiomed, Denvers, MA, USA

device (PAD) that uses autologous fibroblast cultured from a skin sample of intended patient. Previous animal test had shown no adverse chronic effect (Freed et al., 1985).

KCV was designed not to take over heart's native function to pump blood but rather the design intent was to support the heart by decreasing afterload. With a non-valve construction, the probability of mechanical failure that has plagued positive displacement balloon pump as reported by Slaughter et. al. (2009) could decrease significantly (2.5.1 Brief History of Heart Assist Device). The KCV balloon pump blood contacting area is textured polyurethane, intended to foster the formation of a nonthrombogenic psesudointima over the intravascular surface of the pump, and as such no anti-coagulation is needed. The control algorithm used by the external device is quite simple; for patient with severe biventricular dysfunction, uncontrolled tachyarrhythmia or native valvular disease, KCV is contraindicated. Clinical trial showed good result, the cardiac output was increased by 40% depending on afterload condition of the patient. There were reductions in the pulmonary capillary wedge pressure (PCWP), and the right atrium pressure, with an increase in cardiac index after one month of implantation. The KCV is designed as a non-obligatory LVAD, where the patient can turn it on or off, and also an option to disconnect from the external unit, for example during personal cleansing (bathing or showering), amongst useful features that increase quality of life (Valluvan Jeevanandam et al. 2002; Valluvan Jeevanandam 2004).

Another attempt on commercialisation of balloon pump technology is the C-Pulse VAD or also known as extra-aortic balloon pump (EABP)[14]. The device is wrapped around the ascending aorta and secured in place using a Dacron tape thus making it a non-contacting blood pump. The EABP is pneumatically driven through a percutaneous line using an external drive and was designed for ambulatory setting. Displaced blood volume is 20 mL. During diastole, a portion of the cuff is inflated, causing a "thumb printing" effect onto the ascending aorta. Figure 2-35 illustrates how the EABP activates and pushes the blood in the ascending aorta proximally and distally.

---

[14] Sunshine Heart Inc, NSW, Australia.
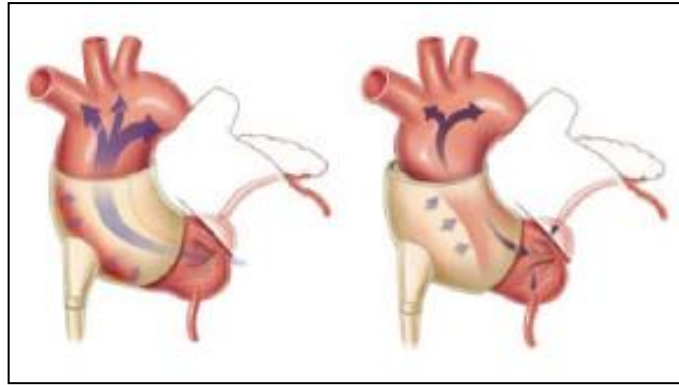
Figure 2-35: Extra-aortic balloon is wrapped around the ascending aorta. The left figure is during systole i.e. non-assisted period, while the right one is when the balloon is activated thus pushing the blood bidirectional in the aorta. *(With kind permission from Wolters Kluwer/Lippincott, Williams & Wilkins)*(Legget et al., 2005)

The non-blood contacting feature of the EABP diminished any contact with blood so no anti-coagulation drug is needed, thus the risk of emboli and haemorrhage is lowered. Although there might be complication from continuous contact between the cuff and the outer cells, acute trial showed no adverse effect on the ascending aorta (Legget et al., 2005). It was also reported that diastolic augmentation by the EABP is comparable to the IABP even though displacement volume is 20 mL, half of 40 mL IABP (Legget et al., 2005); this is most probably due to the implantation site of the EABP at the ascending aorta. In another study comparing the EABP and IABP on coronary flow index, the EABP was much more effective in augmenting diastolic coronary flow by more than two fold (Davies et al., 2005). A multi-centre human trial in the USA is in progress (Sales and McCarthy, 2010).

2.5.5 Counterpulsation LVAD summary

It is evident that counterpulsation technique is effective in providing mechanical unloading; more so when coupled with optimum implantation site at the ascending aorta that maximizes unloading factor with minimal volume displacement. Increased peripheral and coronary flow relieve organ demand and reduce lethargy, while decreased afterload allows myocardium to work less, and this may initiates reverse remodelling. Coronary flow augmentation helps overall LV diastolic function further (Khir et al., 2003).

The non-obligatory feature of two LVADs discussed previously allowed a better quality of life by offering the option to turn the LVAD on or off. The percutaneous line can also be unhooked if the

patients intend to have a shower or any other activities. The option of not using anti-coagulation drug is also a plus factor for the KCV and EABP devices. Polyurethane elastomer used in the KVC promotes the formation of endothelial cells, and this decreases any formation of thrombus due to immunological rejection. The EABP which is wrapped around the ascending aorta might pose chronic problem with aorta adventitia.

There has been suggestions that counterpulsation is the best way to help maximize recovery if the amount of unloading necessary for recovery can be quantified and translated for better HF treatment management (Simon et al., 2008). The CIMS device proposed in this study is a novel idea that implants a balloon pump at the ascending aorta, with all the advantages of non-obligatory support system for a specific cohort of HF patients.

2.6   Chronic Intermittent Mechanical Support (CIMS)

The CIMS device is further discussed here. This subchapter discusses the structure of the device, the control of the device and its indications.

2.6.1   CIMS Indication and Contraindication

The CIMS device is introduced in the first chapter, while this subchapter describes the rationale of HF treatment using CIMS device, and presents the indications and contraindications of the CIMS device.

The objective of the CIMS device is to improve myocardial oxygen balance, and chronic support of the failing heart. These are achieved by augmenting perfusion to the coronary artery and peripheral circulations and through afterload reduction. Mechanical unloading provided from afterload reduction is also hypothesised to facilitate myocardium reverse remodelling (a reduction in the severity of myocardial dysfunction) in specific patient populations. The level of support given by the balloon pump will be commensurate with the patient's condition. A patient in end-stage heart failure condition who is severely affected by heart disease will have to keep the device functioning continuously, but for those with less pronounced cardiomyopathy, the device may be turned off for extended periods. However, since the balloon pump is implanted permanently by replacing the native ascending aorta, it will not be explanted; in case of a relapse

reactivation of device will be swift. The CIMS devices may be thought of as a portable IABP, but which should deliver similar (or better) therapeutic value with less displacement volume.

The patient cohort that will most likely to benefits from this modality treatment has to meet several criteria:

- diagnosed with heart failure in NYHA Class III or IV
- refractory to tolerable standard medical treatment (beta-blocker, ACE inhibitor, diuretics, positive inotrope)
- cause of heart failure is dilated cardiomyopathy (idiotic, ischaemic, or other irreversible cause)
- cardiac index < 2.0 L/min.m^2
- patients excluded for transplantation.

These indications are taking into account criteria off IABP and similar counterpulsation device (Trost and Hillis, 2006, Jeevanandam et al., 2002, Hayward et al., 2010). The inclusion of IDCM as one of the criteria for the CIMS device implantation, comes from the feasibility of recovery due to mechanical unloading being applied on the heart (Mueller and Wallukat, 2007). Other factors that might be favourable for the CIMS balloon pump effectiveness are:

1) 'stiff' vasculature or low arterial compliance vasculature.

There are evidences that in a low compliance vasculature i.e. stiff vasculature, balloon pump augments better compared to high compliance vasculature are presented (refer to 2.2.6 Vasculature Compliance and Pulse Pressure). The CIMS balloon pump manipulates this fact. Also, since the CIMS balloon pump implantation site is at the ascending aorta, which contributes greatly to total arterial compliance (Westerhof et al., 2009), vascular and device compliance factor is deemed important.

2) Pulsatile flow balloon pump.

There is also a suggestion that pulsatile flow blood pump is more suited for myocardial recovery compared to non-pulsatile i.e. continuous flow blood pump (Krabatsch et al., 2011). Pulsatile blood pumps generate physiological nature of flow while unloading the heart, and this is apparently an important factor for reverse remodelling. Studies by Birks et al. (2006) supported this suggestion. Since the CIMS is a pulsatile flow device providing mechanical unloading, the right combination for myocardial recovery is available.

Combining these factors support the CIMS device claim to be an ideal candidate for HF treatment as a BTR or DT for specific cohort of HF patients. Heart failure due to ischaemic heart disease or other systolic dysfunction HF may be applicable as well if the intention is BTT or DT. The exclusion criteria or the contraindications for chronic support by the CIMS device are:

- aortic dissection,
- arrhythmia.

However, arrhythmia might not be a contraindication if a preventive measure such as pacemaker is implanted.

2.6.2 Pressure Detection Mechanism

For the IABP device, balloon activation is timed to coincide with diastole by either synchronizing with the dicrotic notch (using a pressure sensor) or with the T wave of the ECG signal (Figure 2-27). Balloon activation is managed automatically in the driver console using either signal. There is a dedicated tiny hole for blood pressure measurement at the tip of the IABP connected to a pressure transducer. The implanted CIMS device cannot use the same feature for possible infection and thrombus formation. The CIMS device has to rely on a separate detection signal method to IABP. Similar to the IABP, there are two ways balloon activation timing can be synchronised using physiological signals:

1) ECG signal

   Electrodes implanted directly on the heart's epicardial region relay the ECG signal through percutaneous driveline to the wearable driver outside on the patient's waist. An example of a VAD using this method is the C-Pulse VAD (an EABP) (Mitnovetski et al., 2008).

2) Aortic pressure waveform.

   The pressure fluctuation in the ascending aorta is detected by placing a pressure transducer at the proximal part of the balloon pump, allowing precise pressure measurement, and a faster reaction time from the controller. A suitable pressure transducer may be a piezoresistive-based strain gauge device, as drift in these devices is unimportant since only a relative value of pressure is needed to detect the dicrotic notch and not an absolute value (as is needed by rotary VADs).

An appropriate algorithm to automatically determine the proper inflation and deflation timing is used in the controller. A fail-safe measure is embedded in the controller algorithm to prevent accidental override fatal to the patient. A physician will configure the optimum setting for the patient before educating the patient how to use the controller for day-to-day usage.

2.6.3   Novel Alternative to Mechanical Heart Assist Device

The chronic intermittent mechanical support (CIMS) system proposed to treat heart failure symptoms and alleviate patient's suffering is novel in these ways:

- ❖ balloon pump activation can be turned on or off
- ❖ ambulatory setting enabling higher quality of life; while offering continuous/intermittent myocardial function augmentation
- ❖ the device can be disengaged for better lifestyle management
- ❖ has no interaction with aortic wall thus decreasing inflammatory reaction
- ❖ valveless construction, thus decreasing thromboembolic phenomenon
- ❖ may induce reverse remodelling

In term of INTERMACS profile, patients suitable for the CIMS device are most likely to be in profile 4, 5, and 6.

The similarities and differences between the CIMS and EABP (C-Pulse) device is summarised in Table 2-11.

Table 2-11: Differences between the CIMS and EABP (C-Pulse) device

	CIMS	EABP (C-Pulse)
Type	Volume displacement	Volume displacement
Activation method	Counterpulsation	Counterpulsation
Implantation site	Ascending aorta	Ascending aorta
Implantation method	Inserted in-series with the aorta after a portion of the ascending aorta is cut	Cuff type balloon wrapped around the ascending aorta
Valve	Valveless	Valveless

Risk of inflammation at the ascending aorta	No	Possible
Risk of debris formation	No	Possible (the external palpation of the ascending aorta may introduce debris which might enter any three of the arteries at the aortic arch causing microemboil at the brain)
Anti-coagulation	Maybe	No
Reverse remodelling	Possible	Possible
Driver control	Can be turn on and off, and can be disconnected for a short time.	Can be turn on and off, and can be disconnected for a short time.

The C-Pulse device has undergone acute animal (Davies et al., 2005) and clinical trials (Legget et al., 2005, Hayward et al., 2010), while prolonged human trial is still underway (Mitnovetski et al., 2008).

2.7   Human Mock Circulatory Loop (MCL)

The human mock circulatory loop used by other researchers is discussed here.

2.7.1   Human Mock Circulatory Loop Review

The human mock circulatory (MCL) is an essential experimental rig with the main purpose to test the mechanical response of the VAD to simulated physiological conditions and its effect oncirculation; the data gained can be used to refine the design of the device. The result from the experimentation can then be submitted to the Food and Drugs Administration (FDA) before clinical animal and *in vivo* human trial permission be granted in the USA (Klepinski, 2006).

There are various MCL designs: the most basic of which provides steady flow for heart valve test, while a MCL for pulsatile flow can be made up of only two-element Windkessel model catering

only to systemic circulation, progressing to the advanced ones that simulate systemic and pulmonary circulation, with the ability to responds to haemodynamic changes accurately. Some researchers insist on using a MCL that can simulate not only the haemodynamic aspect of human circulation (flowrate, resistance, pressure waveform), but the input impedance characteristic of human circulation as well.

In general the MCL needs to be able to (Pantalos et al., 2004, Timms et al., 2005a):

1. simulate varying physiological condition of the heart from normal resting to severe HF,
2. adherence to Frank-Starling mechanism i.e. heart output corresponding to blood input from venous return,
3. flexibility to accommodate different kinds of VADs by providing appropriate cannulation site.

Some other factors are also important (Rosenberg et al., 1981):

4. analytical model can be developed according to the design of the mock loop as a way to establish mock loop's reliability,
5. easy operability and handling.

The early types of MCL, in 1950s, were called pulse duplicator since their main objective was to simulate appropriate haemodynamic activity for heart valve prostheses testing. McMillan et al. (1952) made a pulse duplicator, later perfected in 1955, to investigate flow past a heart valve. (McMillan et al., 1952, McMillan, 1955). Their design inspired another group to come up with a mechanical pulse duplicator which used an explanted human heart for heart valve's flow visualisation experiment illustrated in Figure 2-36; they used a linkage system of cam and piston enabling various simulation of ventricular pressure waveforms (refer to Figure 2-40) (Davila et al., 1956).
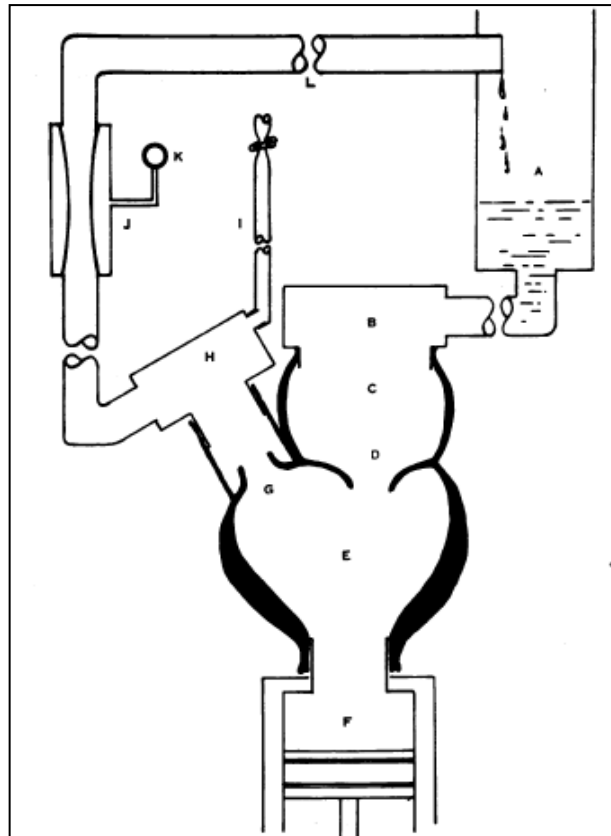
Figure 2-36: Schematic diagram of pulse duplicator with explanted heart for heart valve flow visualisation. A) reservoir cum left atrium B) atrial viewing chamber, C) left atrium, D) mitral valve, E) ventricle, F) piston pump, G) aortic valve, H) aortic valve viewing chamber, I) aortic tube, J) peripheral resistance simulating chamber, K) peripheral resistance manometer, L) site for rotameter (With kind permission from Wolters Kluwer/Lippincott, Williams & Wilkins) (Davila et al., 1956)

Heart valve testing was carried out using pulse duplicators/MCLs with varying degrees of complexity, from a steady flow circuit to more elaborate and accurate ones (Raftery et al., 1968, Duran et al., 1964, Cornhill, 1977, Morsi, 2000, Hildebrand et al., 2004). Cornhill et al. (1977) constructed a pulse duplicator system for heart valve testing experiments comprised of three-elements Windkessel model (proximal resistance, arterial compliance and peripheral resistance), and while that is fairly standard, input impaedance analysis was chosen to examine the effectiveness of the Oxford aortic-pulmonary heart valve prostheses and the pulse duplicator system. The resulting flow and pressure waveforms were physiological except for pressure spike 'ringing' at dicrotic notch which is a known characteristic of mechanical heart valves. The Fourier components and input impedance of the resulting waveforms agree to *in vivo* data to a high degree (Cornhill, 1977). One example of recent compact pulse duplicator for heart valve testing designed to be in a closed incubator is illustrated in Figure 2-37.
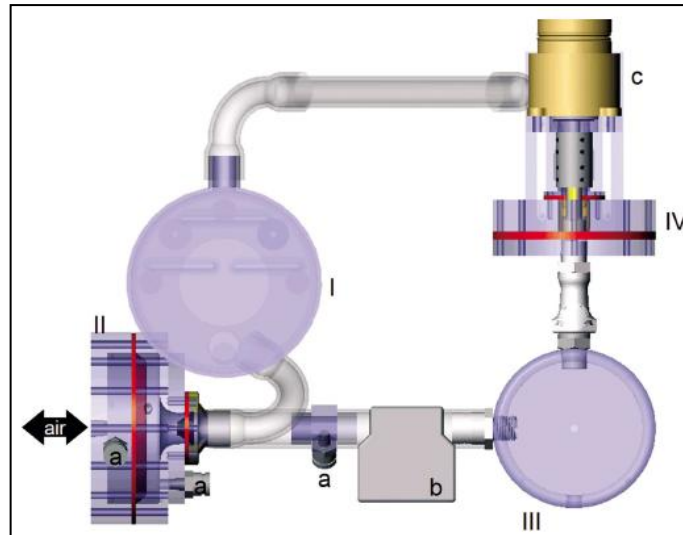
Figure 2-37: Schematic diagram for MCL used to test biologically active mechanical heart valve under varying MAP and flowrate. I) left atrium, II) left ventricle, III) compliance chamber, IV) variable resistor, a) pressure sensor, b) flowmeter c) stepper motor. (With kind permission from Springer) (Hildebrand et al. 2004)

A rather crude MCL simulating both systemic and pulmonary circulation was constructed to test early model of TAH, the MCL had two separate water columns distal to respective left and right ventricle to simulate afterload (60 mmHg for aorta and 20 mmHg for pulmonary artery). There was no compliance chamber to simulate aortic pressure waveform, nor dedicated peripheral resistance element, although the author mentioned that the resistance increased with flow (Kolff, 1959).

A notable early TAH specific MCL was by Donovan (1975). The MCL consisted of a systemic and pulmonary circulation along with a bellows based lever system as a passive flow resistance response in the pulmonary arteries and systemic arteries. The TAH used was the Kwan-Gett artificial heart, and the result from the MCL was shown to be comparable to *in vivo* result from a calf (Donovan, 1975). Donovan's MCL design was popular and has been adopted by many other researchers for *in vitro* TAH experiment.

Rosenberg's group constructed a MCL for TAH and biventricular assist device (BiVAD) testing since 1971, and reported the improved version 10 years later. Their MCL consisted of a systemic and pulmonary circulation made of a capacitance, resistive and inertance element alongside with a reservoir for chamber preload. The initial design process employed analogue computer simulation of the MCL system, before subsequent fine tuning was carried out for the MCL setting (Rosenberg et al., 1981). A similar looking MCL was constructed by Orime's group to test Baylor TAH system

before proceeding to *in vivo* test. The results were indicative of a stable TAH system and showed good biocompatibility (Orime et al., 1994).

Flow visualisation inside an anatomically correct LV was carried out using ultrasonic Doppler velocimeter capable of bidirectional velocity measurement by Cassot et al. (1985). Another aim was to provide a physiologically correct simulator for testing heart valve prostheses. The main results were presented in term of Fourier and impaedance analysis, and were shown to be in excellent agreement with *in vivo* data obtained from a canine (Cassot et al., 1985). Other instance was using a deformable silicone modelled after a dilated heart on a MCL for better understanding of flow dynamics within the left ventricular during cardiac cycle. The study was a preparation for LVAD inflow cannula placement experiment in the dilated LV (Gregory et al., 2009)
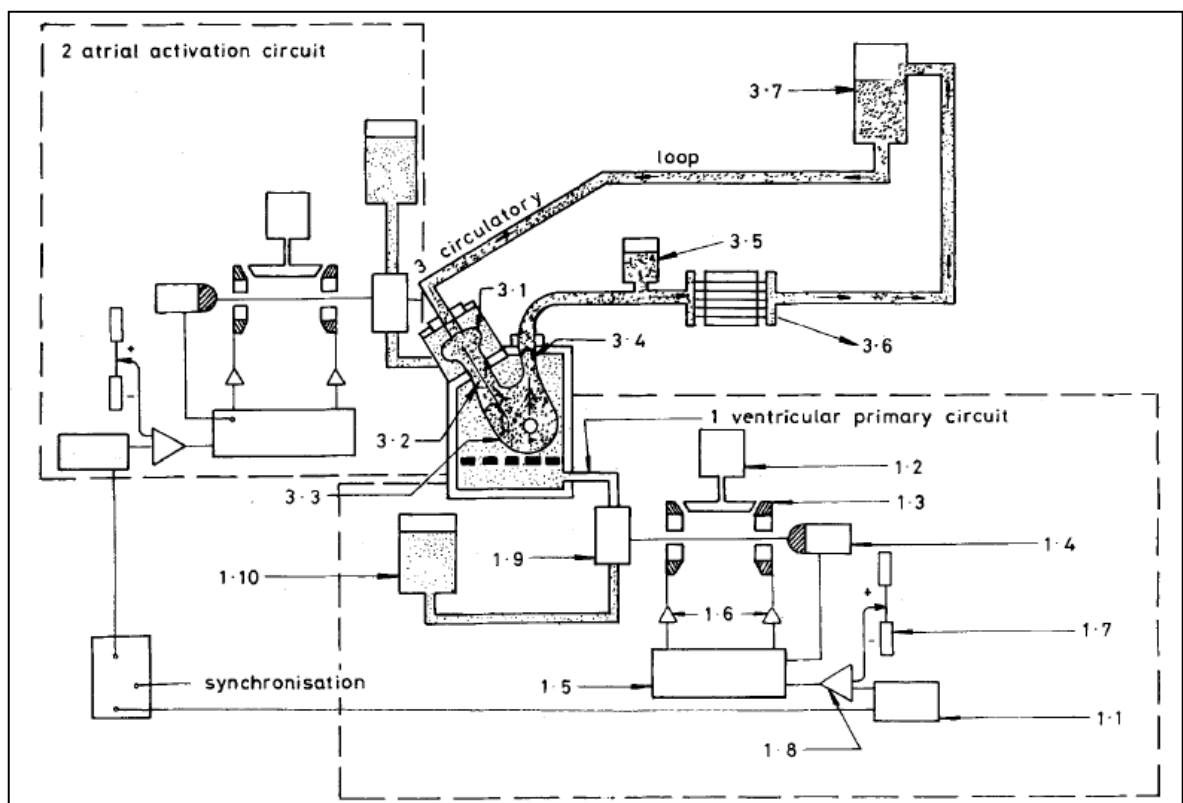
Figure 2-38: Schematic diagram of MCL by Cassot et al. 1.1) synthesizing generator, 1.2) motor, 1.3) clutch, 1.4) tachymeter, 1.5) comparator, 1.6 & 1.8) amplifier, 1.7) mean flow regulator, 1.9) pump, 1.10) reservoir, 3.1) atrium, 3.2) mitral valve, 3.3) ventricle 3.4) aortic valve, 3.5) compliance, 3.6) resistance, 3.7) reservoir (With kind permission from Springer) (Cassot et al., 1985)

Other than testing VADs or TAHs, a MCL can also be used as a teaching tool as illustrated in Figure 2-39. The MCL was constructed using a syringe as the LV chamber, a custom made mitral and aortic valve, a glass cylinder as the atrium and a silicone rubber tube as the aorta. Frank-Starling mechanism adherence was achieved by placing an external chamber made of surgical glove finger

around the syringe. However, impedance mismatch was reported possibly from silicone aorta length (Zannoli et al., 2009).
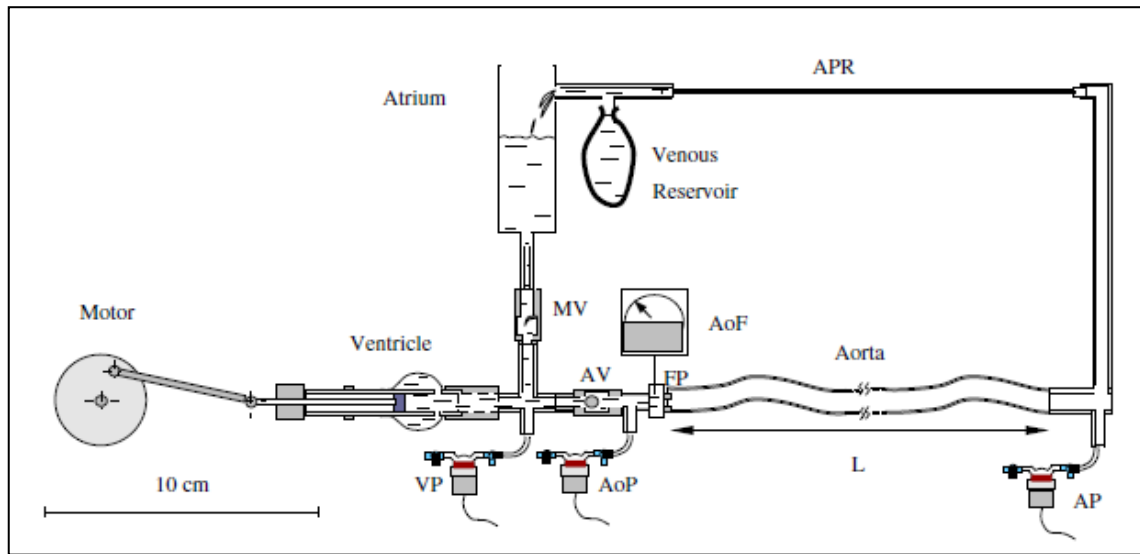
Figure 2-39: Mock circulatory loop with horizontal and vertical arrangement (With permission from Elsevier) (Zannoli et al., 2009)

Liu et al. (2006) constructed a complete systemic and pulmonary circulation MCL for the purpose of testing an axial rotary blood pump (RBP). The MCL consist of an arterial compliance, a venous compliance and a peripheral resistance element which is a three-element Windkessel model. The resulting aortic pressure waveform was in good agreement with physiological pressure waveform. (Liu et al., 2006). The MCL was also used by Wu's group to determine the effectiveness of LVAD physiological control system (Wu et al., 2007).

Seeking to take advantage of both physical hydraulic simulation and numerical simulation, a hybrid model of a numerical-physical model was constructed by Ferrari's group (Ferrari et al., 1994, Ferrari et al., 2001, Ferrari et al., 2002, Ferrari et al., 2005b, Kozarski et al., 2008). Numerical simulation advantages were low cost, flexible and accurate but cannot test physical devices such as an IABP or a LVAD, thus the hybrid approach.

A compact mock circulatory system (600mm × 600mm × 600mm) consisting of both pulmonary and systemic circulation suitable for VAD and BiVAD experimentation, with additional structure to simulate congenital heart disease as well as other structural failure was constructed in 2005 (Timms et al., 2005a) and upgraded until its final version in 2011 (Timms et al., 2011). The final version was able to simulate various kinds of cardiovascular conditions from normal (resting) to both left and right HF, myocardial infarction (MI), structural failure such as atrial/ventricular

septal defect and aortic/mitral heart valve regurgitation. The MCL was constructed based on a five-element Windkessel i.e. characteristic resistance, arterial compliance, peripheral resistance, inertial component and venous compliance element. Frank-Starling mechanism adherence was also incorporated in the design of the MCL. Vasculature compliance was simulated using multi-chamber Windkessel controlled by a solenoid valve across connecting pipes. Up to date, this MCL is one of the most advanced versions.

Clearly there are many requirements that need to be fulfilled in order to construct a physiologically correct MCL in term of pressure waveform, flowrate, characteristic/peripheral resistance, impaedance matching, structural similarity and response to changing cardiovascular condition i.e. Frank-Starling mechanism, baroreceptor response and many others. Factors such as cost, construction time, physiological accuracy and response, should be taken into consideration before designing and assembling the MCL.

2.7.2   Physiological Parameters for MCL

There are suggestions of what variables are needed to be simulated in experimental study, e.g. systemic and pulmonary vascular resistance, arterial compliance, venous compliance, each heart's chamber pressure fluctuations, aortic pressure and flow rates (Pantalos et al., 1998). This subchapter discusses variables and parametric values used in MCL cardiovascular simulation.

i) Cardiac output (CO)

The cardiac output of patients suffering end-stage HF secondary to dilated cardiomyopathy is below than that of normal baseline. Most MCLs set CO for HF condition at around 3.0 L/min, with Recovering HF condition at about 4.0 L/min. The CO parameter is the most important index to be simulated since CO reduction is characteristic of HF. Cardiac output value in MCLs is achieved by changing the contractility level of LV chamber (in case the MCL lacks Starling-mechanism), and/or by adjusting peripheral resistance element.

Another way to control the amount of stroke volume (SV), thus CO, is by using a cam-controlled piston. Different stroke length ejects different amount of SV and the rotational velocity determines the HR value. Figure 2-40 illustrates an example of a piston coupled with a drive

linkage system that gave physiological pressure waveform with different stroke volume (Davila et al., 1956).
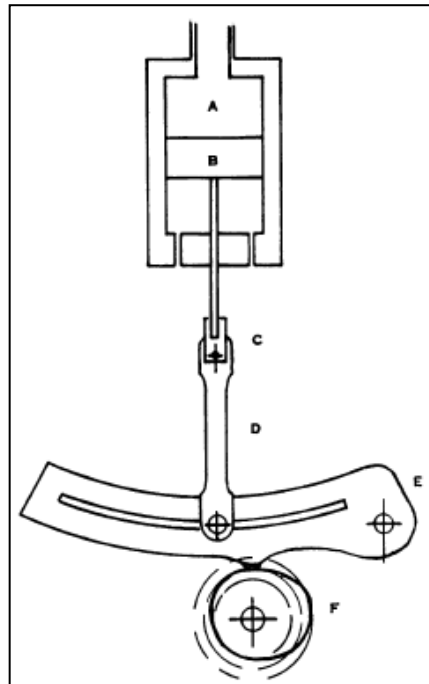
Figure 2-40: The piston pump with cam driven linkage system to push fluid. Different configurations result in different SV. A) Pump cylinder, B) piston, C) universal joint, D) piston drive shaft, E) rocker-arm, F) cam. (With kind permission from Wolters Kluwer/Lippincott, Williams & Wilkins) (Davila et al., 1956).

ii) Heart Rate

In MCLs, the HR is controlled according to the mode of pressure activation. For example, a piston pump rotational speed can simply be increased or decreased. The ratio between systole and diastole is normally chosen to be 40/60, although there are researchers opting for slightly different value. Normal physiological value range is around 34/66 to 39/61 (Levick, 2003). Some examples of HR value are tabulated in Table 2-12:

Table 2-12: Values for HR and corresponding ratio of systole and diastole in a cardiac cycle

Heart Rate	Systole/diastole ratio	Researcher
60 (all conditions)	40/60	(Daniel Timms, Mark Hayne, et al. 2005)
60 (HF)	32/68	(Kolyva, Biglino, et al. 2010)
72 (all conditions)	NA	(S C Koenig, G M Pantalos, et al. 2004; Kenneth N Litwak et al. 2005)

iii) Stroke Volume (SV)

The stroke volume (SV) is defined as the amount of blood volume ejected from the left ventricular chamber during systole. Rearranging the Eq. 2.1 for SV:

$$SV = \frac{CO}{HR}.$$

2.16

Ejection fraction (EF) is the ratio between ejected blood volume, SV, and end-diastolic blood volume:

$$EF = \frac{SV}{LVVed}.$$

2.17

LVVed is the Left Ventricular Volume at end-diastolic period. With normal SV at 80 mL and LVVed at 120 mL, the EF is rated at 67%. The normal physiological value of EF is 65% - 70%. Patients suffering from HF have a low EF value, sometimes going less than 25%, which is one of the indications for LVAD implantation or heart transplantation (refer to Table 2-4).

iv) Pressure

The normal range of each heart chamber's pressure is illustrated in Figure 2-9. The left ventricular (LV) pressure is achieved by adjusting contractility of the LV chamber. For a MCL that uses a pneumatic system, by adjusting the amplitude for air compressor, LV pressure is easily controlled. Other mechanisms include piston pump with fixed stroke volume displacement, or a programmable linear actuator capable of generating pre-programmed LV sinusoidal waveform.

Simulated aortic pressure range in MCL is achieved by appropriate air volume in the compliance air chamber[15] (for Windkessel type), or by careful spring constant parameter and adjusting proper value/point for peripheral resistance.

For a MCL consists of only systemic circulation, fluid enters the left atrium directly. The left atrial pressure is achieved and maintained by the height of the water column as the potential energy according to $P = \rho h g$ formula[16]. Some MCLs may simulate atrial kick in diastole by an additional pneumatic pump at atrium chambers (Timms et al., 2005a).

Preload is often defined as the amount of volume or pressure at the end of diastole. That is not entirely correct, although most MCL use left atrial (LA) pressure as an indicator. Normal LV end-diastolic pressure is around 8 mmHg, but for a failing heart, factors such as dilated heart and

---

[15] Air chamber is also referred to as Windkessel chamber. Windkessel = air chamber in Germany.
[16] ρ = fluid density, h = water column height, and g = standard gravity constant (9.81 m/s^2)

decreased contractility often see the pressure increased to more than 15 mmHg. Timms' group sets the LA pressure at 8 - 10 mmHg (normal) and 18 – 22 mmHg (HF) (Timms et al., 2005a).

In MCLs, Normal mean arterial pressure (MAP) is set at 95 – 100 mmHg, while for HF, MCL is set around 55 – 60 mmHg, and the Recovering HF condition is set at about 80 mmHg.

v) Resistance

The systemic vascular resistance (SVR) can be calculated using Eq. 2.8 (CO = MAP/ SVR). Taking into account the normal healthy male with MAP = 94 mmHg[17] and CO = 5 L/min, the computed SVR is about 18.8 mmHg.min/L or 1.13 mmHg.s/mL. Textbook values ranges from 1.0 to 1.2 mmHg.s/mL (Levick, 2003, Guyton and Hall, 2006). For pulmonary vascular resistance value, it is around 0.18 mmHg.s/mL (Levick, 2003).

For a lumped parameter model, resistance can be simulated at just one point/part in the system. A simple screw clamp operated manually can be used to control the degree of peripheral resistance, for example the one used by (Duran et al., 1964), although some researchers used a more complicated mechanism; e.g. the adjustable tube clamp/tourniquet (Legendre et al., 2008), the gate-type valve (Sharp and Dharmalingham, 1999), open cell foam (Pantalos et al., 2004), sintered aluminium oxide (Cornhill, 1977), automatic bellows and valve (Donovan, 1975) , computer controlled proportional control pinch (Timms et al., 2005a, Timms et al., 2005b) amongst others. Table 2-13 tabulates SVR values from other studies.

Table 2-13 : Resistance value reported by various researchers

Heart condition	Resistance value (SVR) [mmHg.s/mL] (dyne.s/cm^5)	Researcher
Normal	1.08 (1439)	(Timms et al., 2005a)
HF	0.95 (1266)	
Normal	1.00 (1335)	(Pantalos et al., 2004)
HF	1.43 (1902)	
HF	1.22 (1624)	(Kolyva et al., 2010a)
Recovering HF	0.98 (1300)	(Ferrari et al., 2002)
Normal	1.86 (2485)	(Cornhill, 1977)

---

[17] This value is calculated from aortic pressure of 120/80 mmHg.

vi) Compliance

The normal physiological value of the systemic arterial compliance is 2 mL/mmHg (Levick, 2003). While the systemic venous compliance is much higher at 24 times more than systemic artery, since venous distensibility is eight times greater than the artery, and the amount of blood stored in the venous blood vessel is around 64% of blood volume compared to arterial blood volume at 20% i.e. three times more (Guyton and Hall, 2006).

With an aortic pressure of 120/80 mmHg (PP = 40 mmHg), and SV = 80 mL, the arterial compliance, *C*, is:

$$C = \frac{dV}{dP} = \frac{SV}{PP} = \frac{80}{(120-80)} = \frac{80}{40} = 2 \left[\frac{mL}{mmHg}\right].$$

However, if the runaway blood volume is taken into consideration[18]:

$$C = \frac{dV}{dP} = \frac{67.2}{40} = 1.68 \left[\frac{mL}{mmHg}\right].$$

Obviously for different range of pulse pressure and stroke volume the total arterial compliance value would be different. Some compliance values from other studies are tabulated in Table 2-14.

In most MCLs, arterial compliance is simulated by compressing air in the Windkessel chamber during systole, while in diastole, the compressed air expands and the pressure waveform follows natural decay similar to physiological ones (Donovan, 1975, Timms et al., 2005a, Liu et al., 2006).

Other researchers stimulate arterial compliance using rolling diaphragm with spring-loaded piston chamber (Rosenberg et al., 1981, Pantalos et al., 1998). The compliance for rolling diaphragm chamber is determined by the spring's constant; in systole the spring is pushed, while in diastole, the spring recoils in the same manner as native aorta. Some used both Windkessel chamber and spring-loaded compliance chamber (Ferrari et al., 2002). An air chamber comprised with three air compartments was used to simulate different levels of compliance (Timms et al., 2010, Timms et al., 2011). Table 2-14 tabulates compliance values in MCLs.

---

[18] Roughly around 16% of blood drains into peripheral arteries during cardiac cycle, since aorta is not a close chamber (Berne et. al., 2004)

Table 2-14: Compliance values used for mock circulatory loops by other researchers

Heart condition	Compliance value [mL/mmHg]	Researcher
HF	0.94	(Kolyva et al., 2010a)
Normal	1.3	(Pantalos et al., 2004)
HF		
Recovering HF	1.8 (total arterial)	(Ferrari et al., 2002)
	80 (systemic venous)	
Normal	1.33	(Knierbein et al., 1992)
Normal	1.0 (systemic arterial)	(Donovan, 1975)
	10 (systemic venous)	
	1 (pulmonary arterial)	
	5 (pulmonary venous)	
Normal	1.55 (systemic)	(Rosenberg et al., 1981)
	4.84 (pulmonary)	
Normal	2 (aortic)	(Timms et al., 2005a)
	22.5 (Systemic venous))	
	2.95 (Pulmonary artery)	
	7.1 (pulmonary venous)	
HF	1.2 (aortic)	
	11.5 (Systemic venous))	
	2.95 (Pulmonary artery)	
	7.1 (pulmonary venous)	
Normal	2.0 (Systemic arterial)	(Liu et al., 2006)
	50 (Systemic venous)	

The aorta in the human body is a long blood vessel which is soft and quite elastic, in fact, several magnitudes over rubber (Burton, 1954). Some researchers try to simulate that by fabricating a thin and soft extendable elastomeric material from rubber or silicone, in a long tube although only for one heart condition (Zannoli et al., 2009). To simulate larger arterial compliance range accurately, a silicone aorta was attached to the Windkessel chamber (Kolyva et al., 2010a, Cassot et al., 1985). Compliance simulation in MCL by employing Windkessel chamber offered the best compromise in term of ease of operability and adjustment to changing simulated cardiac

condition; the cost will be quite minimal, although normally venous compliance chamber will be quite big/tall (Liu et al., 2006).

2.7.2.1 Air Volume in Windkessel Chamber Calculation

The amount of air inside the chamber determines the arterial compliance and pulse pressure. Any MCL using the Windkessel chamber to simulate physiological compliance will have to store enough air volume correctly (Liu et al., 2005). An example is given for normal heart condition. By assuming that during cardiac cycle air expansion is adiabatic, Boyle's Law (Eq. 2.17) can be used:

$$PV = constant. \qquad\qquad 2.18$$

To determine the amount of air needed to achieve normal heart condition at aortic pressure (120/80 mmHg) and SV (83 mL):

$$P_1 V_1 = P_2 V_2 \qquad\qquad 2.19$$

Where, 1: diastolic state and 2: systolic state. As such, P_1 = 840 mmHg (80 mmHg + 760 mmHg), P_2 = 880 mmHg, $V_2 = V_1 - SV$, since the incoming water volume i.e. SV during systole is reducing or compressing the amount of air in the chamber. This calculation assumes no runaway fluid into peripheral circulation. Solving for V_1 (air volume at end diastole):

$$P_1 V_1 = P_2(V_1 - SV)$$

$$V_1 = \frac{P_2 \times SV}{P_2 - P_1} = \frac{P_2 \times SV}{PP}$$

$$V_1 = \frac{880 \times 83}{40}$$

$$V_1 = 1826 \, mL \cong 1.83 \, L.$$

As for the arterial compliance:

$$C = \frac{SV}{PP} = \frac{83}{40} \cong 2.08 \left[\frac{mL}{mmHg}\right].$$

It was reported that the air volume in the Windkessel chamber was regulated between 1034 mL to 2068 mL in order to achieve compliance level between 1.06 mL/mmHg to 2.13 mL/mmHg (Knierbein et al., 1992).

2.7.3 Left Coronary Artery Simulation in MCL

Left coronary artery (LCA) and its branches supply left side of the heart covering left atrium and left ventricle. MCL simulation of coronary perfusion is normally of the left coronary artery, since LCA has a far greater significance due LCA network on the left heart side.

Coronary artery flow is affected from myocardium contraction, as well as the pressure fluctuation in the ascending aorta; the magnitude of coronary flow rate depends on aortic pressure as the driving force for the coronary perfusion (Geven et al., 2004).

One of the main problems simulating LCA flowrate on MCL was the value of flow rate reflecting human physiology. Most of the data from the literature cannot be used directly since most of the *in vivo* studies use coronary flow reserve as an indicator[19] or expressing the coronary flow normalized with heart mass. Some of the comparable data in mL/min unit are tabulated in Table 2-15.

Table 2-15: Coronary flow value from various sources

Category (*in vivo/in vitro*)		Coronary artery flowrate	Researcher
Global coronary flow	(Human)	225 mL/min	(Guyton and Hall, 2006)
Mean LCA (HF)		67 mL/min	
Mean LCA (Recovering)	(MCL)	97 mL/min	(Koenig et al., 2004)
Mean LCA (Normal)		104 mL/min	
Mean coronary artery (Normal)	(MCL)	80 mL/min	(Geven et al., 2004)

The unique biphasic coronary waveform in Figure 2-17 can be simulated using a silicone or Latex collapsible tube, pressurised at the same time as the LV chamber. The pressure exerted onto the soft tube can either be from compressed air for the LV sac, or by using liquid directed from the LV chamber. The simultaneous compression of the collapsible tube at early systole mimicked compression of subepicardial part of the myocardium vascular bed as per the waterfall model proposed by Downey and Kirk (Downey and Kirk, 1975). Figure 2-41 illustrates one method to simulate early systole compression.

---

[19] Coronary flow reserve is the ratio between maximal coronary blood flowrate and resting blood flowrate.
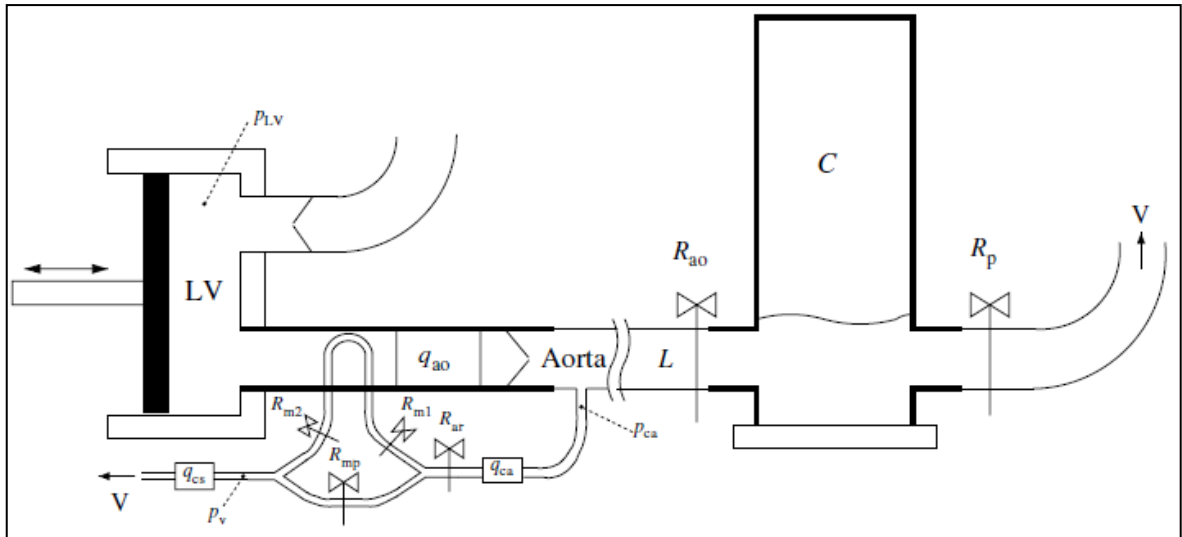
Figure 2-41: The schematic diagram of the MCL and coronary arteries simulation, coronary tube is compressed as the piston increases LV pressure. LV : Left ventricle, L: length, R: resistance, C: Compliance, V: water flow, q: flowrate, ao: aorta, ca: coronary artery, cs: coronary sinus, m: myocardium (With kind permission from IOPScience) (Geven et al., 2004)

2.8   Wave Intensity Analysis

Wave Intensity Analysis (WIA) was originally formulated to solve gas dynamic problem before being applied on arterial mechanics (Parker and Jones, 1990),. The WIA approach uses methods of characteristics to solve the nonlinear 1D Euler differential equation of an elastic tube; WIA differs from that spectral based impaedance analysis, i.e. impaedance analysis using Fourier transformation, as WIA is a time-domain analysis enabling a more accurate description and far easier interpretation of waves in arteries (Parker, 2009a, Parker, 2009b). Some of the advantages of WIA in contrast to impaedance analysis are the non-assumption of arterial wave linearity, less reliance on periodicity, the arterial waves transmitted are summations of smaller waves, and since the calculation is done in time domain, this enables quantitative and qualitative assessment of arterial waves (Khir and Parker, 2005). Many clinicians preferred WIA since the result can be computed on site, and can be understood intuitively (Sugawara et al., 2009).

Since its introduction, WIA has been used to study arterial waves in the ascending aorta (Khir and Parker, 2005), coronary arteries (Davies et al., 2006), changes due to failing heart (Curtis et al., 2007), and even to explain the mechanism and effect of LVAD to arterial flow and pressure (Kolyva et al., 2009). There are four characteristics waves in WIA as tabulated in Table 2-16.

Table 2-16: Four types of waves in wave intensity analysis. The ↑ sign refers to increasing pressure or flow acceleration, while ↓ sign refers to decreasing pressure or flow deceleration.

Type	Pressure	Flow
Forward Compression Wave (FCW)	↑	↑
Forward Expansion Wave (FEW)	↓	↓
Backward Compression Wave (BCW)	↑	↓
Backward Expansion Wave (BEW)	↓	↑

The actions of IABP counterpulsation can be determined using WIA; one study showed that the balloon inflation caused a BCW i.e. increase of the aortic root pressure and retrograde flow (towards the heart), while the balloon deflation decreased the ascending aortic pressure and increasing forward flow i.e. a BEW (Kolyva et al., 2009).

2.9   Summary

The second chapter aimed to provide the reader with background knowledge about cardiovascular physiology, pathological conditions leading to HF, as well as the treatment available at present. One of the options available, mechanical assistance for HF treatment was discussed at length. A specific subchapter was provided with mechanical heart assist device history and development from early years to present days. Special mention was given to volume displacement type left ventricular assist device (LVAD) placed in, on and around aorta. The history, usage, deployment, complication, performance index, and mode of activation of the IABP were also discussed. Continuing from the first chapter, CIMS indication and contraindication were presented. Justifications on the suitability of CIMS modality treatment to failing heart were elaborated. A review of MCL for in *vitro* balloon testing was given. Lastly, wave intensity analysis (WIA), an arterial wave mechanics analysis tool was presented briefly.

Chapter 3 Methodology

This chapter is dedicated to the methodology used to achieve the objectives stated in the first chapter. Several approaches were used to tackle and overcome the technical and analytical problems in the course of this study.

3.1 Introduction

Subchapter 3.2 describes the *in vitro* balloon pump designs. Two designs were drafted. For this study, silicone was chosen as the deformable inner lining. The justification of using silicone is elaborated later in this subchapter.

Since this study was based entirely on experimental work, an appropriate experimental rig was required. The construction and handling of a human mock circulatory loop (MCL) to simulate the systemic and coronary circulation is described in subchapter 3.3.

The aim of this study was to determine the efficacy of the CIMS balloon pump: 1) to decrease cardiac workload by afterload reduction prior to systole, and 2) to increase perfusion to the systemic and coronary circulations. Several experimental factors were chosen, and the reasons are explained. Factorial design method was used to design the experimental procedure and the results were then analysed using the appropriate statistical test. A subchapter dedicated to the explanation of these experimental and the analytical procedures is presented.

A flow visualisation technique was employed to verify the effect of balloon deflation on the aortic heart valve opening motion and is described in subchapter 3.5. Some changes to accommodate visual inspection in the MCL are explained. The video recording and the analysis technique of the premature opening of the aortic heart valve are described.

At the end of this chapter, a summary is given.

3.2 Balloon Pump Construction

The design and manufacture process of the *in vitro* CIMS balloon pump prototype is presented.

3.2.1 Prototype Conception

The effect of counterpulsation from a CIMS balloon pump was investigated by implanting an *in vitro* prototype in the MCL. Instead of a soft body balloon pump, a rigid body type was chosen; the soft body type balloon pump is not suitable for balloon innate compliance experiment as it may confound the result. Two different shapes of rigid body balloon pump prototype were made:

1) a straight body (SB) balloon pump and,
2) a compliant body (CB) balloon pump.

The compliant body (CB) balloon pump has an extra space to allow a deformable membrane to expand during ventricular systole, thus increasing balloon pump's compliance (refer to 3.2.3.2 Compliant Body).

3.2.2 Silicone Membrane

The Silastic T4[20] silicone elastomer was selected as the material for the deformable membrane of the balloon pump prototype due to its translucent property plus several mechanical properties suitable for this study. Once cured, the silicone has a tensile strength of 6.68 MPa and the hardness around 40 Shore A, which is categorized as medium level hardness. This means that it has the distinctive flexibility and acceptable durability needed for continuous action of inflation and deflation within the balloon pump body.

Further explanation of silicone curing process, mould pouring and Silastic T4 datasheet is presented in Appendix A.

---

[20] Dow Corning, Michigan, USA

3.2.3 Prototype Balloon Pump

The balloon pump prototypes were made using rapid prototype machines which gave the finished product accuracy within ±0.5mm of the desired dimensions of the 3-dimensional computer aided design (CAD) software SolidWorks ™[21]. The stl format file from the CAD model was used by the rapid prototyping machine, to build the product layer by layer. Two machines with different technology were used: 1) Fused Deposition Modelling (FDM) technology and 2) stereolitography technology. In general, the manufacturing cost was cheaper using the FDM technology; however, finishing the balloon pump to make it waterproof and gas impermeable product added to the final cost. The stereolitography (SLA) technology on the contrary was much more expensive based on the cost of one cm^3 of raw material, however, since the material allows for a translucent end product, it was much suited for visual inspection and was used to make the CB balloon pump. More details of the machines used in this study are given in Appendix D.

3.2.3.1 Straight Body

The design for a rigid body balloon pump was primarily based on nominal dimensions of the human ascending aorta; the inner diameter was set at 25 mm while the distance from the aortic valve to the brachiochepalic artery was 70 mm. Since the *in vivo* version will need to be sewn into the ascending aorta, the rigid section of the *in vitro* balloon pump was set at 50mm. When fully inflated, the volume displaced was 25 mL; although the volume displacement of a straight body CIMS balloon pump was less than an adult IABP designed (range: 30 to 50 mL), it was hypothesised to offer comparable or better haemodynamic augmentation.

A cylindrical silicone membrane was inserted into the balloon pump body, and both ends were turned back over cylindrical end. Since the silicone membranes OD was smaller than that of the balloon pump, the turned-back silicone membrane was held by itself. PTFE pipe thread tape was applied at both ends to prevent water or gas leakage, and to ensure a tight fit between the balloon pump body and pipe connector in the experimental rig (Refer to Figure 3-50).

The physical part of the SB type balloon pump is made according to model drafted as per Figure 3-42. Figure 3-43 shows the assembled straight body balloon pump with the cylindrical silicone

---

[21] Solidworks 2010, Dassault Systèmes SolidWorks Corp., Waltham, MA, USA

membrane. The balloon pump was rapid prototyped using a FDM (Fused Deposition Modelling) process (refer to Appendix D-1).
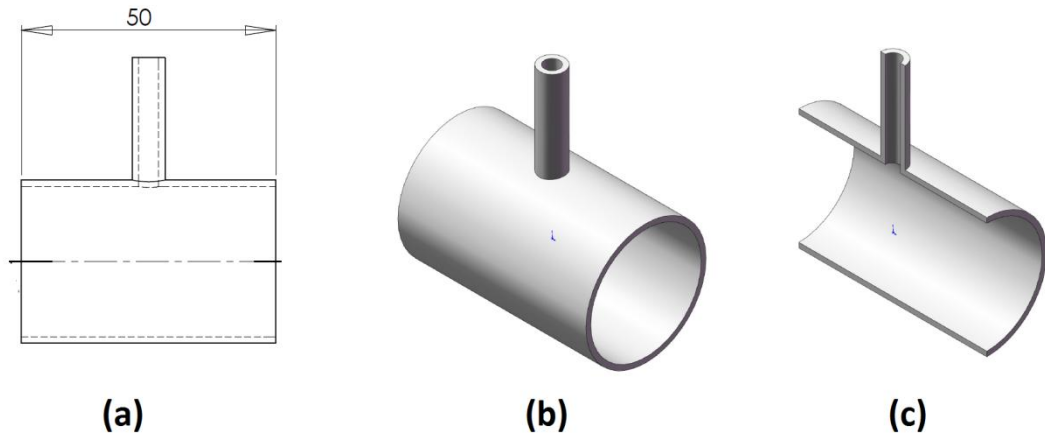
Figure 3-42: Sketch of SB balloon pump design. (a) Front view, (b) isometric view, (c) isometric section view
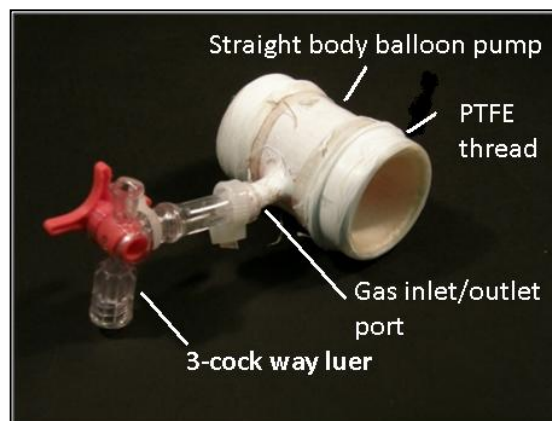
Figure 3-43: The SB balloon pump with silicone membrane enclosed. The balloon pump was manufactured using FDM process. PTFE pipe thread tape was used to provide a tighter fit between the balloon pump and pipe connector.

A single port was placed in the middle of the body for Helium gas to flow in and out to inflate and deflate the balloon. A 3-cock way luer connector allowed access for either a pressure transducer or Helium gas driveline. This design was replicated in the CB balloon pump.

3.2.3.2 Compliant Body

The effect of different balloon pump innate compliances on haemodynamics response was compared experimentally between a straight body (SB) balloon pump and a compliant body (CB) balloon pump. The CB balloon pump was designed with an extra cylindrical space between the silicone membrane and the rigid body. The additional volume was approximately 7 mL while the thickness of the silicone membrane was 0.5 mm; the combination of additional 7 mL and thin silicone membrane, gave an additional compliance effect.

The CB type balloon pump was made, according to the model drafted in CAD software as illustrated in Figure 3-44, by using a rapid prototyping machine of SLA technology. The final product, illustrated in Figure 3-45, was translucent thus facilitating visual inspection during balloon inflation and deflation. Compliance measurement was carried out according to procedures laid out in Appendix D; the balloon pump's static compliance value was 0.11 mL/mmHg.
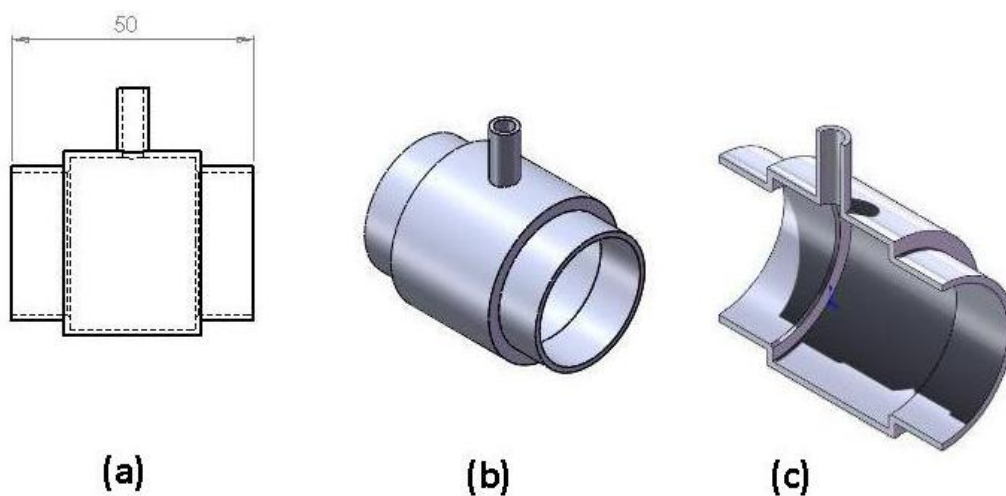
Figure 3-44: Sketch of CB balloon pump design. (a) Front view, (b) isometric view, (c) isometric section view.

Figure 3-45: Compliant body balloon pump made using a UV-curable photopolymer resin.

The technical drawings for both designs are illustrated in Appendix D-2.

3.2.3.3 Differences between SB and CB

The main difference between both types of balloon pump is obviously the balloon pump structure. The extra space of 7 mL allowed the silicone membrane to be pushed back during systole, allowing extra bit of water in the ascending aorta part of the MCL.

The silicone membrane used on the CB type balloon pump was 0.5 mm, thus it was easier for the silicone to be expanded during counterpulsation exercise.

A water column volume and pressure experiment (in Appendix D) confirmed that the CB type balloon pump expanded when the water pressure increased.

3.3   Human Mock Circulatory Loop (MCL)

The human mock circulatory loop (MCL) used in this study is explained here.

3.3.1   Introduction

The human mock circulatory loop (MCL) is an experimental rig where human cardiovascular physiology was simulated; its assembly is described here. The objectives for the constructed MCL were:

1) to simulate varying degrees of heart conditions from Normal to Heart Failure
2) to simulate different compliance levels in a heart condition
3) to provide an experimental rig to investigate the CIMS balloon pump
4) to provide an end-to-side anastomosis for a VAD through the left ventricle's apex.

The MCL used in this study was a continuation of a basic MCL at Nottingham University (Good, 2006). The basic design of the MCL was retained and upgraded to incorporate better hardware and a data acquisition system (DAQ). The original version of the MCL was assembled to simulate pulsatile flow out of the left ventricular sack in the left ventricular chamber (refer to Figure 3-48). A simple loop connected the outflow and the inflow part of the left ventricular sack. Furthermore, tube for the loop was 12 mm in internal diameter. The final version of the MCL used in this study is as shown in Figure 3-46.

The MCL is a two-element Windkessel model consisting of a compliance chamber (for the arterial compliance) and a total peripheral resistance element. While it may not be as advanced as MCLs discussed in previous chapter, through combinations of hardware and software configured for the MCL, pressure and flowrate waveforms were simulated with good accuracy to physiological waveforms.
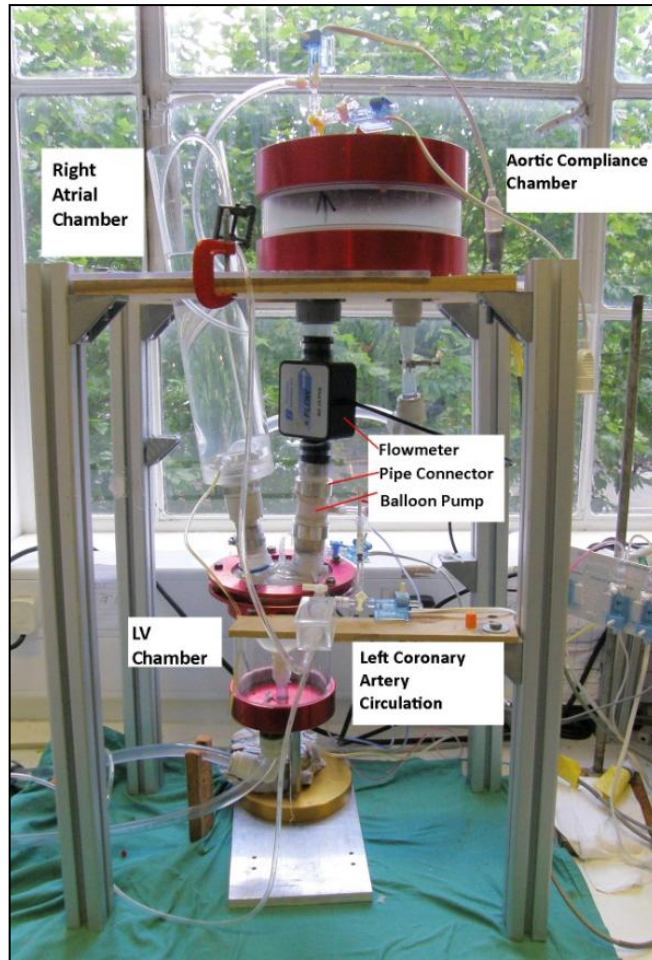
Figure 3-46: Aston University MCL used in this study

3.3.2   MCL Overview

The schematic drawing for the MCL connected to the DAQ system, flowmeter and IABP driver is illustrated in Figure 3-47.

A square wave signal was sent to the 3-way proportional pressure regulator[22] . The proportional pressure regulator valve was controlled using a piezoelectric element that accurately opens and closes the valve according to the signal received, and can reasonably simulate any wave shape sent from the DAQ. Any change in the amplitude of the square wave was translated into the amount of air pressure allowed into the LV chamber.

---

[22] MPPES-3-1/2-PU-PO-010, Festo Ltd, UK
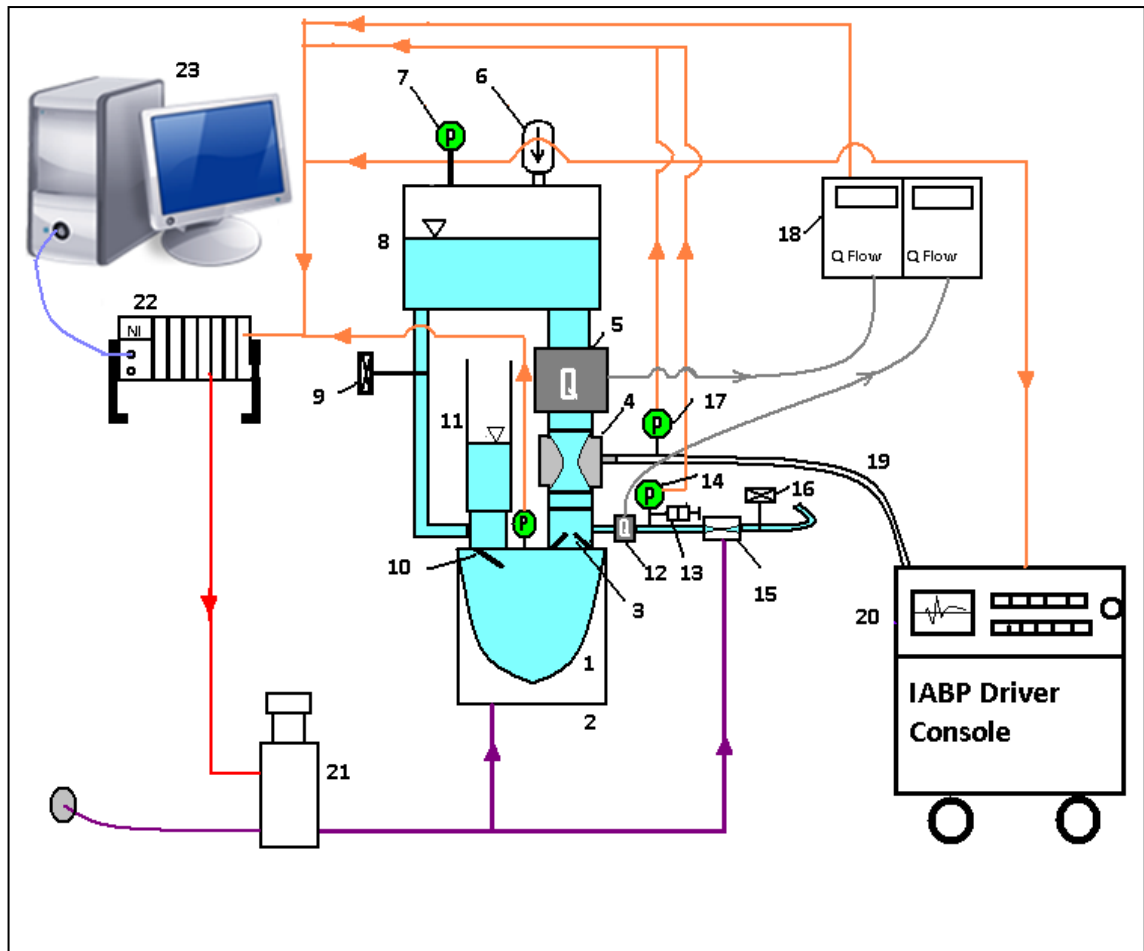
Figure 3-47: The schematic diagram of the human MCL used to investigate the effect of CIMS balloon pump. 1) LV silicone sack 2) LV chamber 3) Aortic valve 4) CIMS balloon pump 5) Flow sensor 6) Air bellow 7) Aortic pressure transducer 8) Arterial compliance chamber 9) Resistor 10) Mitral valve 11) Left atrial chamber 12) Flow sensor 13) Compliance syringe 14) Left coronary artery pressure transducer 15) Systolic resistor 16) Resistor 17) Balloon pump pressure transducer 18) Flow meter 19) Helium gas driveline 20) IABP console 21) Proportional pressure regulator 22) DAQ system 23) Personal Computer (PC)

The regulator allowed pressurised air to fill up the LV chamber during systole; and cut off the pressurised air inlet on completion of systole. A hole in the bottom of the LV chamber allowed a conduit to pass from the LV apex (for purposes of other studies – in to RBP LVAD) and because it was oversized it also allowed pressurised air to escape during diastole, and facilitated passive filling of the LV sack.

Figure 3-48: Left ventricular chamber with left ventricular silicone sack inside it. Notice the connection to PVC tube from the apex of the silicone sack.

Passive filling of the LV sack was further facilitated by the thick wall of the sack (around 2 mm) which would naturally re-assume its diastolic shape. The LV sac was designed to hold up 250 mL of water, equivalent to almost double the normal physiological value, to simulate the LV volume in dilated cardiomyopathy (DCM).

Figure 3-49 shows the top of the LV silicone sac; the inflow (left atrium) and outflow (aorta) conduits house heart valves, while a tube connected to a pressure transducer at mid-ventricle height allows for LV pressure measurement.

Figure 3-49: LV silicone sack top part that houses heart valves. Notice a tube is inserted at the middle of the top part to measure LV pressure.

LV contraction increases intraventricular pressure, and once the LV pressure exceeds the aortic pressure, the aortic valve opens up. The aortic valve was a 25 mm bileaflet mechanical heart valve (MHV)[23] . The transparent tube used as the ascending aorta was a PVC tube with ID = 25.4 mm.

---

[23] St. Jude Medical (SJM) Standard® Bileaflet Valve, St. Jude Medical, Minnesota, USA

Two smaller holes for Tygon ® tubes (ID 3.2 mm, OD 4.8mm)[24] were located 15 mm distal of the aortic valve; one for the left coronary artery (LCA) circulation, the other was connected to a pressure transducer to measure pressure just distal to the aortic valve. The tubes were fixed in place by employing a waterproof flexible silicone sealant[25].
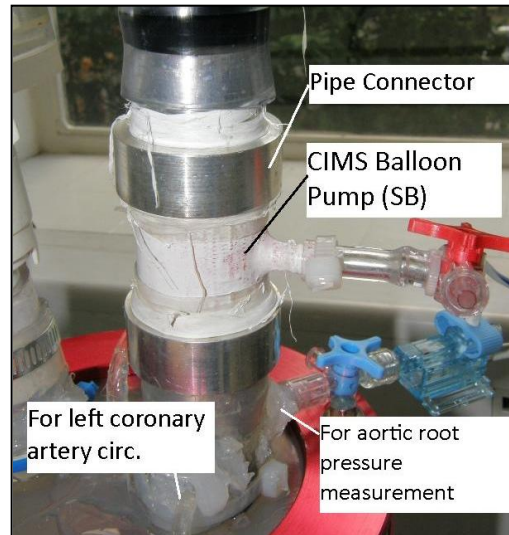
Figure 3-50: Two smaller tubes come off the ascending aorta for the left coronary artery and aortic root pressure measurement. The CIMS balloon pump was inserted in-line using two pipe connectors.

In Figure 3-50, the position of the Tygon tubes is shown and CIMS balloon pump was connected in-line with the ascending aorta section using two pipe connectors.

Distal to the CIMS balloon pump was the 25 mm ID aortic flow sensor[26] shown in Figure 3-51. The flowsensor measured the volumetric fluid movement by utilizing the ultrasonic transit time technology. The flowsensor is non-resistive and has a bidirectional flowrate measurement capability; which proved to be an important feature that allowed accurate measurement of forward and backward flow.

---

[24] R3603, Saint-Gobain Inc., France
[25] Loctite 595 Clear Silic RTV, Loctite Inc., USA
[26] ME 25PXN, Transonic System Inc., Ithaca, NY, USA

Figure 3-51: Flow sensor used to measure aortic flowrate at ascending aorta
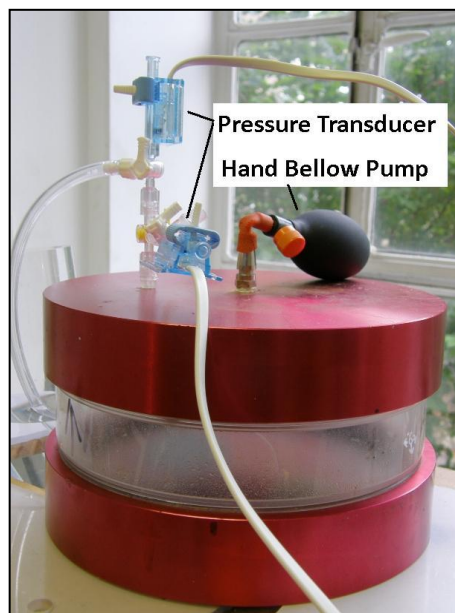
Figure 3-52: Aortic compliance chamber. On top of the chamber, are aortic pressure transducer for DAQ hardware and IABP console.

To simulate physiological arterial compliance, an air chamber also known as a Windkessel chamber was used as shown in Figure 3-52. The volumetric capacity was approximately 3.1 L, sufficient to simulate large ranges of aortic compliance values. A transparent acrylic cylindrical body (OD 200 mm x 3 mm) facilitated visual observation. On top of the air chamber, there was a port for a handheld bellow to pump additional air inside the air chamber as well as to bleed air to the surrounding environment, and a luer connector to which two 3-way stopcock connectors were attached. The 3-way stopcock was also used to release air into the surrounding environment. At each 3-way stopcock, a pressure transducer was connected. Both pressure transducers measured aortic pressure from the air trapped inside the aortic compliance chamber, one was dedicated to the DAQ hardware for data display and recording while the other was for the IABP console. Inflow water was through ID 25 mm PVC tube while the outflow tube was ID 12

mm. The rationale was that flow past the aorta was branching to the peripheral circulation and reducing in size.

A manual flow resistor was placed on the PVC tube between the aortic compliance chamber and the left atrial chamber to simulate total peripheral resistance (TPR). By manually changing the amount of contraction/stenosis on the PVC tube, the flowrate of the MCL can be adjusted.
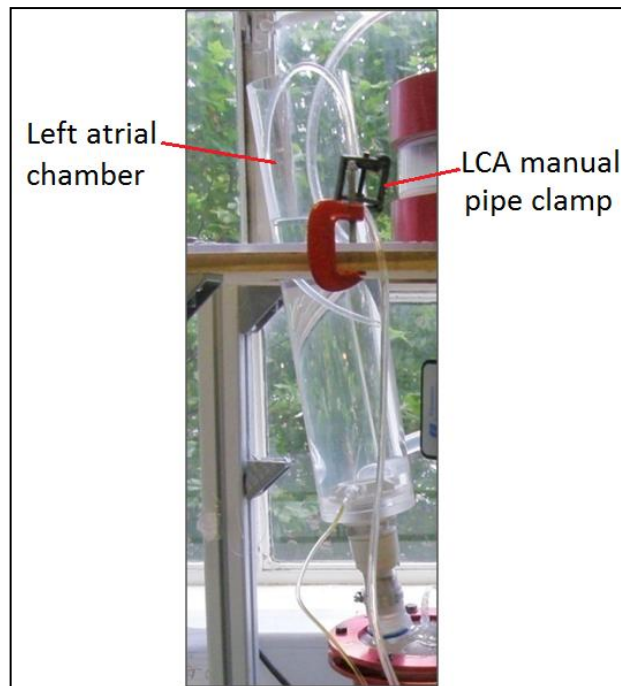
Figure 3-53: The left atrial chamber. Notice the pressure driveline for atrial pressure at the bottom side of the chamber. It is connected to a pressure transducer not shown in this picture. Manual clamp for LCA circulation is placed near to end of tube.

The smaller PVC tube was connected to the left atrial (LA) chamber as shown in Figure 3-53. It was made of clear acrylic tube (OD 76 mm x 3mm x 335 mm). The chamber can be filled with approximately 1.23 L of water, exerting potential pressure of around 23 mmHg. There was a hole for the pressure transducer at the side of the chamber. Left atrial pressure (LAP) is defined as the potential pressure on top of the mitral valve for this study; as such, pressure differences between the pressure point and mitral valve have to be taken into account when calibrating the LAP.

The mitral valve between the left atrial chamber and the LV silicone sack was a 25mm tilting disc valve type[27]. The valve was carefully orientated to allow for physiological flow into the LV sac.

---

[27] Bjork-Shiley Standard, USA

3.3.3 Left Coronary Artery Circulation

The left coronary artery (LCA) circulation was also made of a two-element Windkessel model (coronary compliance and total coronary artery resistance) similar to the systemic circulation and was fabricated in 3.2 mm ID Tygon® tube. Most of the elements in the LCA circulation are shown in Figure 3-54. The flowrate was measured by an ultrasound flow sensor[28]. The LCA compliance was simulated by a 1 mL syringe, and by trial and error, an air volume of around 0.5 to 0.6 mL was found to be appropriate in simulating physiologically accurate LCA flowrate.

The most important characteristic of LCA flow is the early systolic depression due to myocardium compression of the coronary arteries. To simulate early systolic compression, a watertight small acrylic box (45 mm x 30 mm x 30 mm) with a deformable thin silicone tube (wall thickness ≈ 0.3 mm) was inserted in-line of the LCA circulation. The deformable silicone tube inside the box was compressed at the same time with the LV silicone sack, thus simulating early systolic compression similar to the physiological waveform. This method was similar to those used by Geven and Gaillard (Geven et al., 2004, Gaillard et al., 2009)
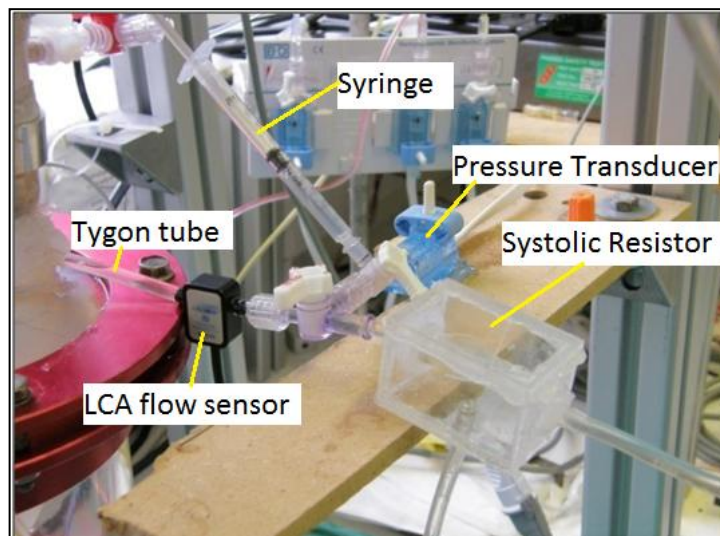
Figure 3-54: The LCA circulation part of the MCL. The circulation comprised of a two-element Windkessel model (compliance and resistance). Flowrate was measured using an ultrasound flowsensor. Early systolic compression was simulated by the systolic resistor (housed in the cuboid container) distal to the 3-way stopcock. Between the 3-way stopcock and the pressure transducer was the 1 mL syringe that acted as a compliance chamber.

Overall flow rate through the LCA circuit was controlled by a manual flow resistor (throttle) shown in Figure 3-53. Manual adjustment ensured close resemblance to the physiological waveform through setting the minimum flowrate in the waveform close to 0 mL/min.

---

[28] ME 4PXN, Transonic System Inc., Ithaca, NY, USA

The target value for LCA flowrate is tabulated in Table 3-17.

Table 3-17: The target value for LCA flowrate

	Heart Failure	Recovering heart	Normal heart
LCA flowrate (mL/min)	64 – 68	78 – 82	90 - 92

3.3.4 DAQ Hardware, Software and Related Measurement Devices

The data Acquisition System (DAQ) is an essential element for any experimental study. A chassis[29] shown in Figure 3-55, able to hold up to 8 different input and output (I/O) cartridges was connected to PC by a USB cable. For this study, one analog output cartridge (NI 9201), one analog input cartridge (NI 9263) and two strain based cartridges (NI 9237) were installed in the chassis.
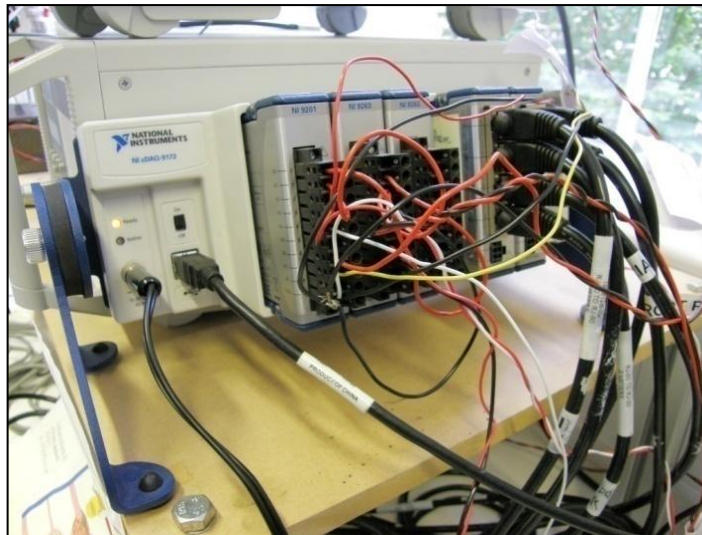
Figure 3-55: USB DAQ chassis used as the terminal to transmit and receive data in this study.

The fluid pressure was measured by using a disposable pressure transducer[30] which comprises a piezo-resistive element to convert pressure on a strain gauge membrane into electrical voltage. The data was transmitted to the DAQ hardware by way of an interface cable[31] which was then connected to a special cable[32] for the simultaneous bridge module cartridge for strain based data

---

[29] NI cDAQ-9172 ,NI, Austin, Texas, USA
[30] BD DTXPlus™ (682018), Becton, Dickinson and Company Inc., USA
[31] BD Transducer Interface Cable, Becton, Dickinson and Company Inc., USA
[32] RJ50 Connectivity 779521-01, NI, Austin, Texas, USA

(NI 9237) in the USB chassis described above. A cable checker was used for rough calibration of pressure measurement, and was further fine tuned before starting the MCL for experimentation.

Figure 3-56: TS410 Flowmeter for fluid volumetric measurement. The above flowmeter is for the LCA circulation while the one at the bottom is for the peripheral circulation. The LCD displayed mean flowrate value.

Instantaneous flowrates measured at the ascending aorta and left coronary artery were sent to the flowmeter[33] which converted the signal from the flowsensor into mean and instantaneous flowrates. The flowmeters shown in Figure 3-56 were connected to the analog input cartridge at the DAQ chassis for simultaneous mean and instantaneous flowrate display and data recording.

A software for DAQ processing and control was used to manage DAQ process. Labview™ [34] is a graphical programming language suited to process simultaneous input and output signal from and to the DAQ hardware. For example, a square wave signal was generated in the LabView Virtual Instrument (VI), and simultaneously sent to the DAQ hardware's output cartridge module and to the 3-way proportional pressure regulator. A snapshot of the front panel and corresponding virtual instrument display is shown in Figure 3-57.

Signals from the MCL were acquired at 2000 Hz sampling frequency, and were averaged and then scaled down to 200 Hz for easy data manipulation. All signals were then subjected to a low-pass filter of 7 – 10 Hz to get rid of the excessive noise, especially the Aortic Root Pressure signal; the

---

[33] TS410, Transonic System Inc., Ithaca, NY, USA
[34] National Instrument, Austin, Texas, USA

closing action of the mechanical leaflet produces excessive pressure spikes known as 'ringing' as can be seen in Figure 3-57 and Figure 3-58.
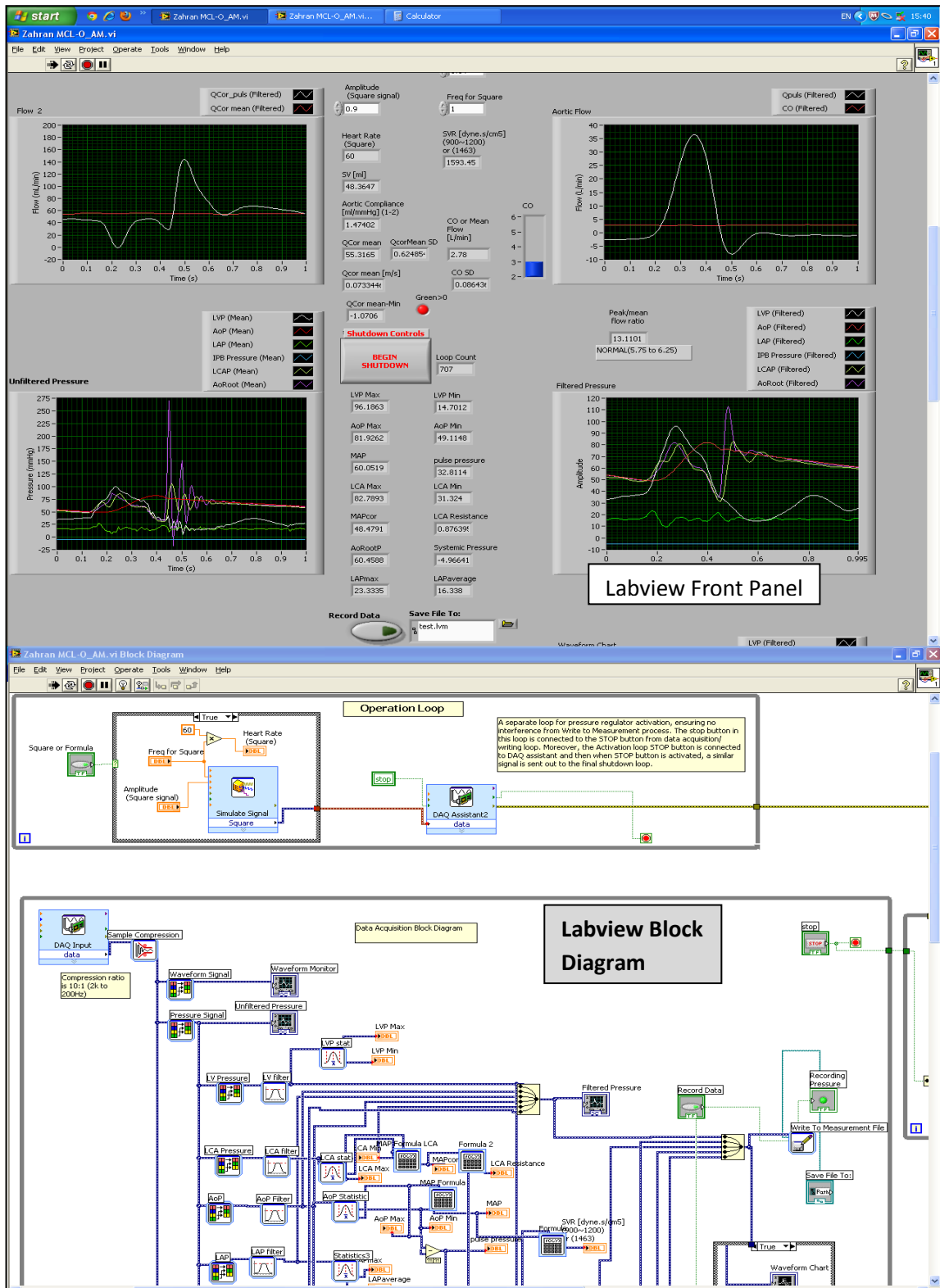
Figure 3-57: A snapshot of LabView VI used in this study. On to top is front panel which displays real time haemodynamic data (pressure and flow rate) and MCL control, while the bottom one is the block diagram panel where subroutine is written.

3.3.5 MCL Parameters

The value of mean arterial pressure (MAP), cardiac output (CO), heart rate (HR), stroke value (SV) and aortic compliance for Heart Failure (HF), recovering heart (Recovering) and normal heart condition are tabulated in Table 3-18. Those values were chosen by gathering relevant data from textbook and literature (Levick, 2003, Guyton and Hall, 2006, Klabunde, 2005, Burton, 1972, Timms et al., 2005a).

Table 3-18: The target haemodynamic parameters for the MCL for three different level of heart condition, and further subdivided to three different levels of arterial compliance (high, medium and low). MAP: Mean Arterial Pressure, CO: Cardiac output, HR: Heart Rate, SV: Stroke Volume, LAP: Left Atrial Pressure, LVP: Left Ventricular Pressure, AoPmax: aortic systolic pressure, AoEDP: aortic end-diastolic pressure. The Air Volume referred to air volume in the aortic compliance chamber. The arterial compliance level is further divided into three levels: High, Medium and Low.

Heart Condition	(Heart Failure)			(Recovering)			(Normal)		
MAP (mmHg)	57			80			95		
CO (L/min)	3			4			5		
HR (beats/min)	60			60			60		
SV (mL)	50			66.7			83.3		
LAP (mmHg)	16 – 18			12 – 14			8 – 10		
LVP	80/10	-	-	100/10	-	-	120/0	-	-
Arterial Compliance level	High	Medium	Low	High	Medium	Low	High	Medium	Low
Aortic Compliance (C) (mL/mmHg)	2.5	1.65	1.25	2.5	1.65	1.25	2.5	1.65	1.25
Pulse Pressure (PP) (mmHg)	20	30.3	40.0	26.7	40.4	53.3	33.3	50.5	66.7
AoPmax (mmHg)	70.3	77.2	83.7	97.8	106.9	115.6	117.2	128.7	139.4
AoEDP (mmHg)	50.3	46.9	43.7	71.1	66.5	62.2	83.9	78.2	72.8
Air Volume (L)	2.1	1.4	1.0	2.1	1.4	1.1	2.2	1.5	1.1

The value of LVP at each heart condition is predetermined for C = 2.5 mL/mmHg as a reference for other levels of compliance, and might be different depending on the level of AoP for each heart condition.

In subchapter 2.7.2   Physiological Parameters for MCL), the equations to calculate the exact amount of air volume in a hermetically sealed chamber, for a given aortic end-diastolic pressure (AoEDP), as well as pulse pressure (PP) are given. The corresponding aortic pressure, PP and air volume values in Table 3-18 were calculated using those formulae. In practice, it was much easier to achieve the desired aortic compliance level by targeting the aortic systolic and diastolic pressure. During operation, the air volume (or the water height) inside the aortic compliance chamber was controlled by way of the manual bellows pump and the 3-way stopcock, air volume influenced the aortic pressure waveform.

3.3.5.1 Aortic Pressure (AoPmax and AoEDP) Calculation Method

Determination of aortic pressure (systolic: AoPmax and diastolic: AoEDP) is given here.

For aortic compliance, C, defined as the ratio between volumetric changes, SV, and pulse pressure, PP, per Eq. 2.15, rewritten as:

$$C = \frac{SV}{PP}.$$

Since SV is defined as the result of CO divided by HR (refer Eq. 2.1), substitution of Eq. 2.1 in the above Eq. 2.15 yields a compliance value calculated by:

$$C = \frac{\frac{CO}{HR} \times 1000}{PP}. \tag{3.1}$$

The MAP (Eq. 2.6) is the sum of AoEDP and one third of PP (PP = AoPmax − AoEDP), rearranging Eq. 2.6 for AoEDP:

$$AoEDP = MAP - \frac{1}{3}\left(\frac{\frac{CO}{HR} \times 1000}{C}\right). \tag{3.2}$$

Since the value of CO, HR, MAP and C has been predetermined as above in Table 3-18, AoEDP was computed by substituting those values into the above Eq. 3.2, and by substituting the result into Eq. 2.5, the value of PP and subsequently the value AoPmax is computed:

$$PP = 3 \times (MAP - AoEDP). \qquad\qquad 3.3$$

Using value of PP, AoPmax is computed.

$$AoPmax = AoEDP + PP. \qquad\qquad 3.4$$

3.3.6 Procedure for Starting and Operating the MCL

The procedure for starting the MCL in order to simulate the desired heart condition and arterial compliance is explained in this subchapter. Before starting the procedure, all pressure gauges were zeroed. The pressure transducers (LV chamber, CIMS balloon pump and left atrial chamber) were adjusted to mid-ventricular height (mid LV silicone sac. The other three pressure transducers were placed at or near to the point of measurement e.g. the aortic pressure transducer was fixed on top of the aortic compliance chamber, the aortic root pressure transducer was fixed to the Tygon tube coming off the ascending aorta section, while the LCA pressure transducer was placed after the flow sensor in the LCA circuit.

The steps used to achieve a predetermined heart condition and compliance level were:

1. The aortic compliance chamber was opened to environment.
2. The left atrium was filled with distilled water to the mid left atrial chamber height.
3. The LabView virtual instrument (VI) file for MCL operation was opened and the pressure correction constant for the LCA pressure, aortic root pressure and aortic pressure was set to correspond to the water height in the LA chamber. However for LV chamber and CIMS balloon pump it was maintained without any adjustment. The LAP was measured only from the side of the LA chamber, appropriate adjustment was carried out.
4. Air pressure from the source was set at 2 bar, the square wave amplitude set at 0.8 (for HF condition), and the program was executed.
5. Once the MCL was started, the water level at the aortic compliance chamber increased rapidly, and it was adjusted with hand bellows and 3-way stopcock. The appropriate height was calculated from air volume in Table 3-18. LAP level was adjusted by adding more water if necessary.
6. The flowrate at the ascending aorta section was checked against value in Table 3-18, and the rate was fine tuned by using the flow resistor.

7. The range of LVP and AoP was checked. If the maximum targeted point was still not achieved, the square wave's amplitude was increased gradually to increase LV's contractility.

8. The pressure waveforms of all points were checked for physiological accuracy, especially the aortic pressure, aortic root pressure and LCA pressure.

9. If not, the MCL was stopped by pressing the BEGINNING SHUTDOWN button, and redo procedure steps 4 – 8.

10. If it was necessary to lower the LAP, some of the water in the LV sac was drained by opening the gate valve.

11. For LCA circulation, it was adjusted by tuning the flow resistor for LCA circulation to reproduce the accurate physiological waveform. This operation normally require minute adjustment, thus a complex operation to balance interacting factors.

Figure 3-58 shows the LabView VI written to control the MCL as well as displaying pressure waveforms, aortic flowrate, LCA flowrate and numerical values of haemodynamic parameters in real-time. Data can be easily recorded with a click of a button in the Labview VI front panel.

Square, sinusoidal and custom (Fourier series) waveforms were used to drive the volumetric contraction of the LV sac. As these waves gave very similar outflows from the LV silicone sac, a square wave was used throughout the study; the square wave was simpler to generate and consumed less processing time compared to the sinusoidal wave. The pressure regulator was not sufficiently quick to be able to produce a customized waveform at rates greater than 60 beats/min. The activation period of square wave was set to 40% for all heart simulated conditions.
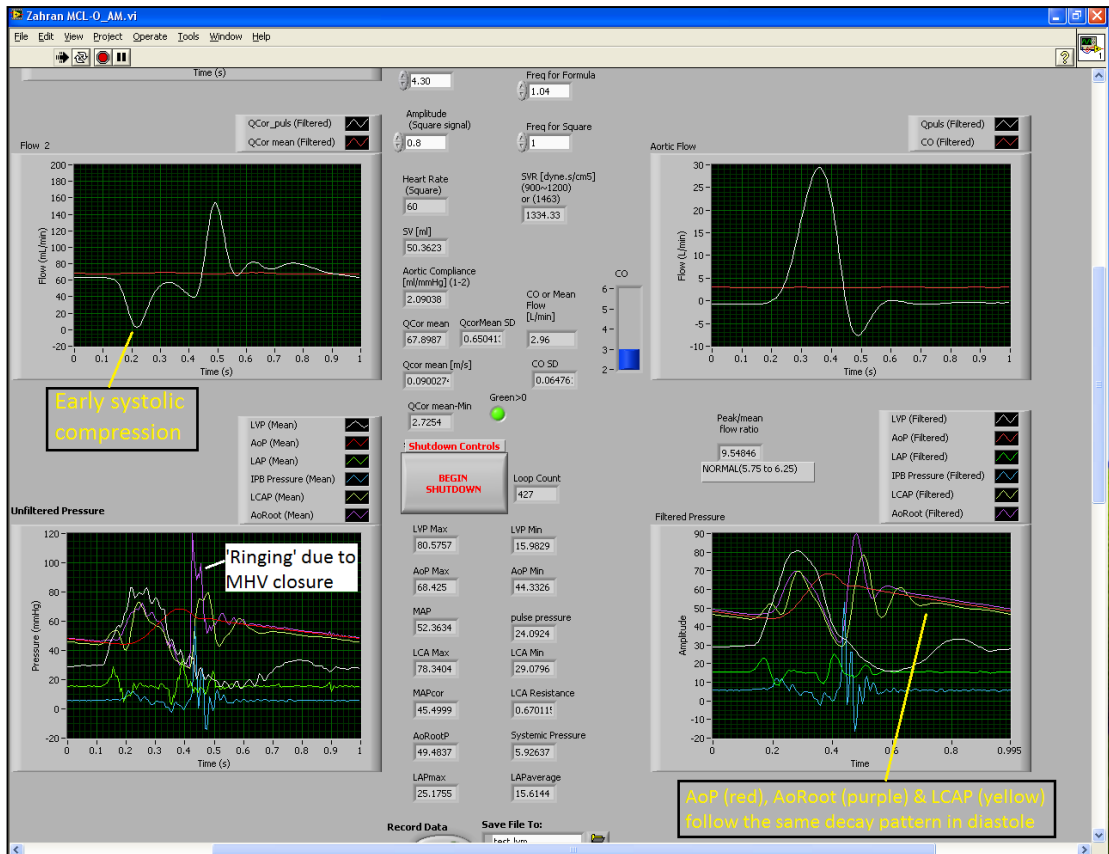
Figure 3-58: The VI front panel for MCL operation. The top left display is the LCA flowrate, notice the early systolic depression, the top right panel is the aortic flowrate waveform, bottom left panel is the unfiltered pressure waveform, while the bottom right is the filtered pressure signal. Notice that AoP, LCA pressure and aortic root pressure follow the same decay pattern in diastole.

3.3.7   IABP Console

In Figure 3-59, the IABP driver console[35] used for the CIMS balloon pump activation for this study is shown; the console is a lightweight compact device, designed to be portable in various terrains. Figure 3-60 shows the front panel of the IABP console when balloon pump was not activated.

---

[35] Bard H-8000 TransAct IABP (C. R. Bard Inc., New Jersey, USA). The company no longer manufactures any IABP-related equipment.
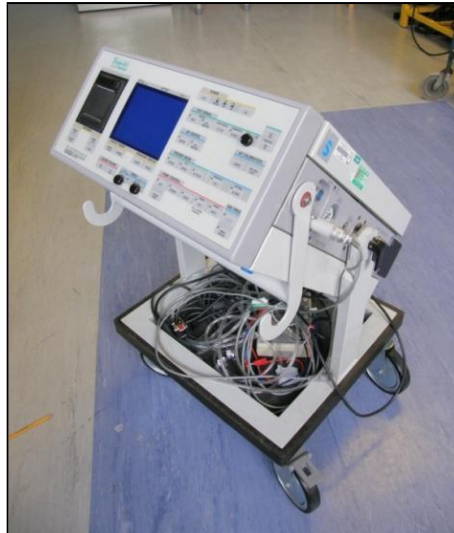
Figure 3-59: The H-8000 Bard IABP console used in this study.
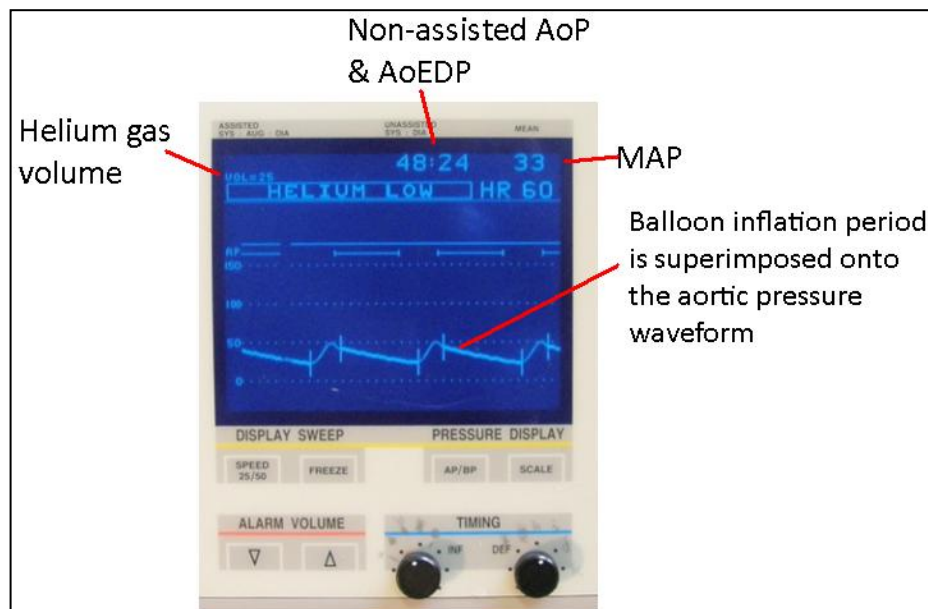
Figure 3-60: The front panel of the IABP console while not activated

The driver also has several panels for options relating to IABP operation e.g. there were two options for arterial pressure signal; either from a pressure transducer (XDUCER) or from an external pressure monitoring system (EXT MONITOR) acquired using a phono-phono cable 100 mmHg/V.

Once the ON button was pressed, Helium gas was transferred between the balloon pump and IABP console. The inflation and deflation period was implemented according to the range chosen beforehand, although the range can be adjusted manually using knobs at the TIMING panel. The value of the augmented aortic pressure was displayed alongside with systolic and diastolic aortic

pressure. However during data recording, no adjustment was allowed. Figure 3-61 is an example during the IABP console is activated.
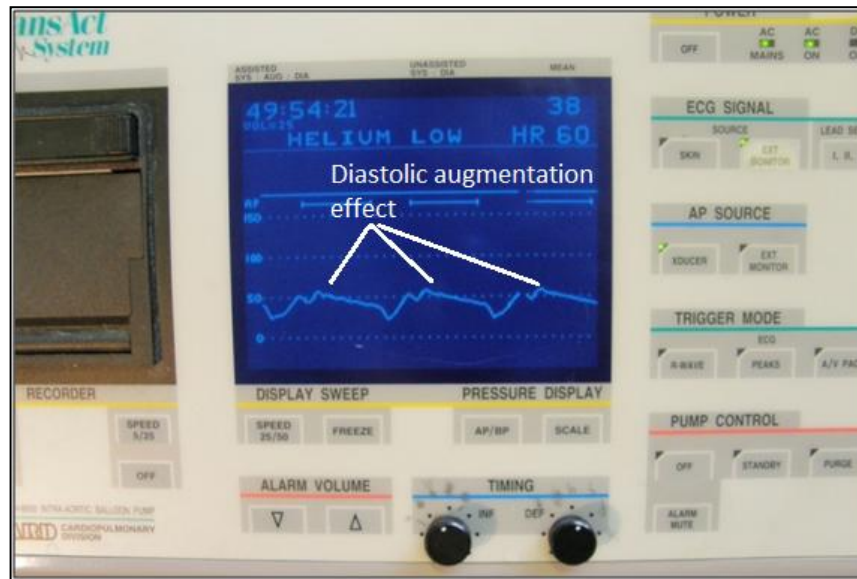
Figure 3-61: The IABP console in activation mode. Notice that diastolic pressure is augmented, while on top left LCD display, the augmented pressure is displayed in the middle.

3.4   Design of Experiment (DOE)

The experiments conducted were carried out using the factorial design method. That method and statistical tools used to analyze the data is presented here.

3.4.1   Data Measurement & Recording

This subchapter involves the data recording procedure, data extraction methods and data analysis. Important parameters are explained and justified. The procedure to record haemodynamic data before, during and after the augmentation was:

1. Flow was allowed to stabilise following initialization of the MCL.
2. Non-assisted circulation data was recorded for around 100 s prior to assist with the CIMS being activated.
3. Assisted circulation data was then recorded for 200 s following activation of the CIMS.
4. The data was recorded for a further 40 s after the augmentation was ceased.

The longer period for assisted circulation period was to allow the flow to stabilise. There were also instances where high fluctuations in flowrate and pressure meant that a larger dataset was needed to acquire a stable consecutive period of data. It was decided from statistical reasoning that 30 s sample period was required, refer to Appendix B.

The raw data (in .lvm format) was then converted into a Microsoft Excel[36] format before processing using Matlab's[37] script file to yield several parameters:

- Maximum and minimum left ventricular pressure (LVPmax & LVPmin)
- Maximum and minimum aortic pressure (AoPmax & AoPmin)
- Mean arterial pressure (MAP)
- Mean left atrial pressure (LAPaverage)
- Mean left coronary artery pressure (LCAPaverage)
- Peak Aortic Diastolic Pressure (PADA)
- Pressure difference between PADA and AoPmax (dP)
- Cardiac output (CO)
- Mean left coronary artery (QcorMean)
- Helium gas pressure (Internal pressure balloon pump-IPBP)

Peak Aortic Diastolic Pressure (PADA) was the highest aortic pressure recorded during assisted circulation in diastole, while dP was the differences between PADA and AoPmax. The graph in Figure 3-62 illustrates the pressure and flowrate waveforms for several parameters listed above both for non-assisted (non-activated) and assisted circulation (activated) respectively.

The effect of balloon augmentation to the LCA circulation is illustrated in Figure 3-63. Clearly, pressure and flowrate of LCA were augmented during diastole. The magnitude of the diastolic augmentation is demonstrated by LCA flowrate shape, where the peak instantaneous flowrate is in the region of 200 mL/min, compared to non-assisted circulation at less than 150 mL/min.

The numerical results are shown in Figure 3-64 and Figure 3-65. All columns were measured data except for several columns: MAP (from AoPmax and AoPmin), Rcor (LCA resistance: from QcorMean and LCAPMean) and dP (from PADA and AoPmax).

---

[36] Microsoft Excel 2007, Microsoft Inc., Redmond, Washington, USA
[37] Matlab R2009b, Mathworks Inc., Natick, MA, USA
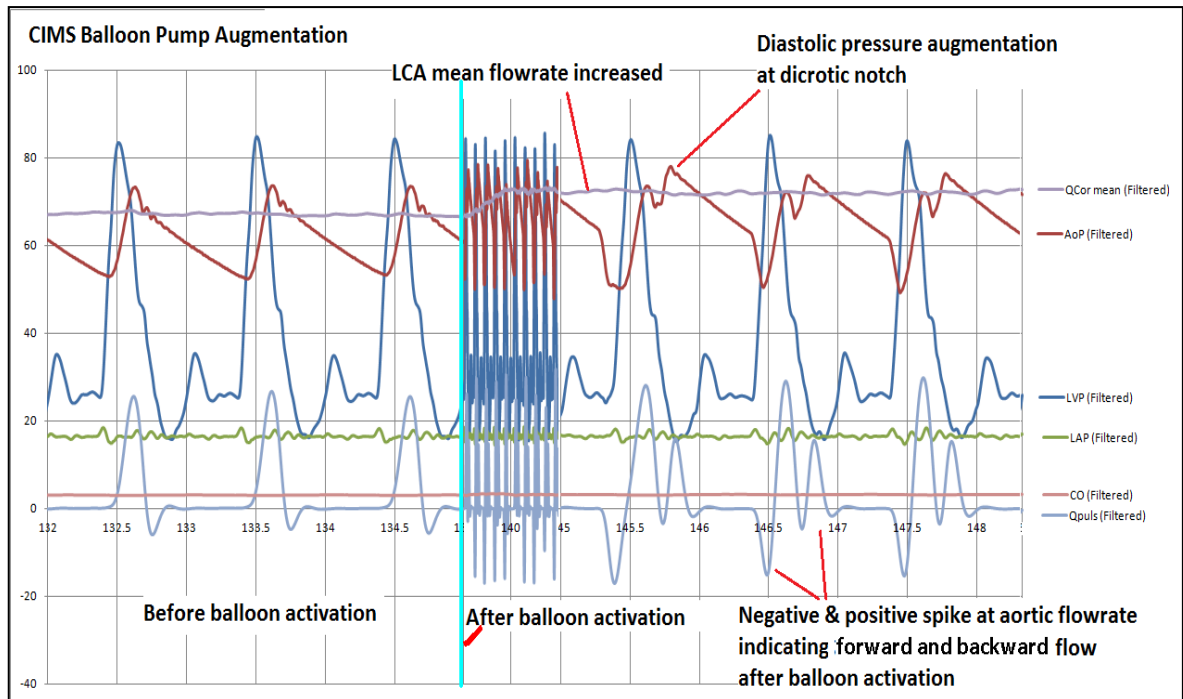
Figure 3-62: Haemodynamic parameters during assisted period. Diastolic augmentation is clearly evident in aortic pressure and aortic flowrate waveform.
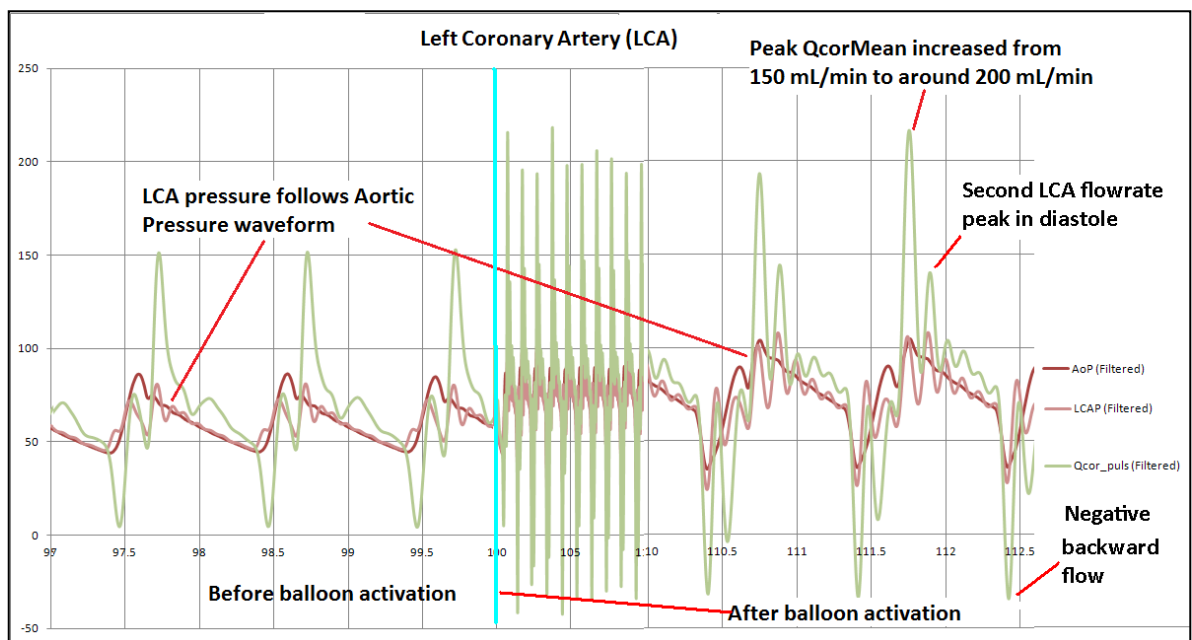
Figure 3-63: The left coronary artery during non-assisted period. LCA pulsatile flow and pressure were augmented during diastole.

	t	LVPmax	LVPmin	AOPmax	AOPmin	MAP	LAPave	CO	QCorMean	LCAPMean	Rcor	PADA	dP	IPB Pre(min)
NON-ASSISTED	1	76.756	12.336	88.362	44.661	59.228	16.112	3.081	64.218	59.373	0.925			-35.818
	3	76.231	12.788	86.353	44.387	58.376	16.111	3.081	64.506	58.623	0.909			-35.989
	5	76.489	12.953	86.155	44.363	58.294	16.096	3.089	64.544	58.523	0.907			-35.784
	7	76.998	12.407	87.613	44.395	58.801	16.106	3.095	64.500	58.695	0.910			-35.744
	9	75.778	12.326	86.308	43.314	57.645	16.127	3.066	64.434	57.133	0.887			-36.201
	11	76.562	12.693	86.050	44.695	58.480	16.103	3.084	64.150	58.433	0.911			-35.818
	13	77.023	12.713	88.135	44.067	58.756	16.125	3.077	64.362	58.867	0.915			-35.669
	15	76.027	12.419	86.484	44.477	58.479	16.111	3.116	64.845	58.357	0.900			-35.861
	17	75.809	12.611	85.036	44.264	57.854	16.125	3.100	64.921	57.457	0.885			-35.933
	19	76.837	12.478	86.780	44.325	58.477	16.107	3.081	64.169	58.390	0.910			-35.701
	21	76.049	12.542	88.127	43.095	58.106	16.137	3.043	63.747	58.421	0.916			-35.457
	23	76.292	12.152	88.585	43.351	58.429	16.131	3.054	64.053	58.196	0.909			-35.545
	25	76.035	12.994	85.586	44.994	58.524	16.111	3.094	64.397	58.965	0.916			-35.347
	27	76.795	12.621	86.717	44.610	58.646	16.109	3.118	64.823	58.612	0.904			-35.610
	29	77.112	12.407	88.017	43.665	58.449	16.119	3.089	64.835	58.259	0.899			-35.586
	31	75.927	12.074	86.144	44.383	58.304	16.115	3.078	64.962	57.788	0.890			-35.789
	33	76.279	12.738	86.079	44.724	58.509	16.111	3.088	64.538	58.695	0.909			-35.371
	35	76.522	12.695	87.631	43.504	58.213	16.095	3.100	64.580	58.290	0.903			-35.480
	37	76.589	12.727	86.873	44.707	58.762	16.097	3.105	64.590	59.165	0.916			-35.362
	39	76.048	12.421	86.342	44.252	58.282	16.109	3.103	65.085	58.028	0.892			-35.679
	41	76.636	12.539	85.846	44.898	58.547	16.095	3.097	64.779	58.358	0.901			-35.614
	43	76.345	12.718	87.419	43.411	58.081	16.118	3.069	64.488	58.207	0.903			-35.291
	45	76.517	12.229	88.096	43.897	58.630	16.097	3.091	64.452	58.298	0.905			-35.578
	47	75.697	12.055	87.942	43.869	58.560	16.120	3.073	64.206	58.367	0.909			-35.545
	49	75.652	12.733	87.009	43.608	58.075	16.104	3.078	64.342	58.602	0.911			-35.310
	51	75.892	12.543	86.200	44.078	58.119	16.125	3.105	64.632	57.789	0.894			-35.569
	53	76.038	12.680	85.791	44.086	57.988	16.107	3.072	64.280	57.761	0.899			-35.319
	55	76.316	12.343	85.931	44.327	58.195	16.100	3.053	63.886	57.681	0.903			-35.456
	57	76.111	12.582	86.243	44.298	58.279	16.103	3.064	64.124	58.148	0.907			-35.504
	59	76.629	12.616	86.376	44.667	58.570	16.093	3.077	64.334	58.395	0.908			-35.312
count	30													
AVERAGE		76.33	12.54	86.81	44.18	58.39	16.11	3.08	64.46	58.33	0.90			-35.61
SD		0.41	0.23	0.95	0.51	0.31	0.01	0.02	0.32	0.48	0.01			0.23
SE		0.07	0.04	0.17	0.09	0.06	0.00	0.00	0.06	0.09	0.00			0.04

Figure 3-64: The numerical data of haemodynamics parameters during non-assisted period

	t	LVPmax	LVPmin	AOPmax	AOPmin	MAP	LAPave	CO	QCorMean	LCAPMean	Rcor	PADA	dP	IPB Pre(min)
ASSISTED	110	73.808	11.831	88.225	38.266	54.919	16.125	3.487	76.695	67.247	0.877	93.441	5.216	-55.609
	112	74.910	12.145	89.545	38.274	55.364	16.095	3.437	76.060	68.722	0.904	96.284	6.740	-54.636
	114	74.748	12.125	90.151	38.097	55.448	16.099	3.480	75.772	69.235	0.914	95.813	5.663	-53.948
	116	73.653	12.390	87.554	38.058	54.557	16.120	3.492	76.003	67.657	0.890	94.181	6.626	-57.214
	118	74.414	11.948	88.558	38.580	55.240	16.108	3.513	75.948	68.673	0.904	94.603	6.045	-55.848
	120	74.083	11.803	88.703	39.148	55.666	16.103	3.554	75.737	67.823	0.896	94.546	5.844	-54.349
	122	72.194	12.927	88.657	36.147	53.651	16.121	3.524	75.575	68.422	0.905	95.251	6.594	-53.689
	124	74.210	11.822	87.756	39.210	55.392	16.083	3.522	75.730	68.223	0.901	93.786	6.030	-53.644
	126	74.123	12.158	87.510	39.162	55.278	16.092	3.521	76.208	68.012	0.892	93.142	5.632	-53.484
	128	75.030	12.308	89.763	39.307	56.125	16.078	3.517	76.468	69.833	0.913	98.098	8.335	-55.079
	130	75.670	11.980	91.116	37.560	55.412	16.092	3.499	76.863	69.350	0.902	97.594	6.478	-52.976
	132	74.645	12.125	89.098	37.770	54.879	16.121	3.469	76.686	68.416	0.892	96.355	7.258	-54.198
	134	75.038	11.902	90.815	38.501	55.939	16.086	3.477	76.580	69.710	0.910	97.846	7.031	-50.744
	136	74.293	12.089	89.883	38.368	55.540	16.077	3.492	76.597	69.983	0.914	96.329	6.446	-57.046
	138	75.124	11.919	90.701	37.935	55.523	16.096	3.476	76.483	68.740	0.899	96.719	6.018	-55.092
	140	74.646	12.161	89.475	37.379	54.744	16.094	3.460	76.009	68.818	0.905	95.798	6.323	-50.981
	160	73.922	11.904	89.360	37.448	54.752	16.091	3.545	75.825	67.377	0.889	94.845	5.485	-51.473
	162	74.946	12.325	89.775	38.014	55.268	16.084	3.544	75.246	69.624	0.925	97.345	7.570	-54.209
	164	74.861	12.346	90.869	37.963	55.598	16.072	3.591	75.738	69.388	0.916	97.079	6.210	-53.728
	166	74.190	11.983	88.789	37.371	54.511	16.081	3.588	75.989	67.838	0.893	94.892	6.102	-56.096
	168	74.183	12.058	87.635	38.677	54.997	16.080	3.508	75.193	67.379	0.896	92.627	4.992	-54.562
	170	75.234	11.791	90.984	39.248	56.493	16.067	3.505	75.224	70.207	0.933	97.315	6.331	-51.009
	172	73.316	12.230	88.941	37.663	54.756	16.065	3.508	75.412	68.610	0.910	93.895	4.954	-56.672
	174	74.330	12.260	87.869	39.303	55.492	16.053	3.502	76.168	69.179	0.908	95.651	7.782	-54.088
	176	74.846	11.960	88.727	39.649	56.008	16.047	3.551	76.376	69.493	0.910	95.807	7.081	-55.153
	178	74.839	11.582	90.927	38.442	55.937	16.068	3.528	75.904	68.993	0.909	97.243	6.316	-55.303
	180	74.612	12.253	88.819	38.153	55.041	16.070	3.517	75.438	69.013	0.915	95.707	6.888	-54.827
	182	74.976	12.156	89.215	37.893	55.001	16.064	3.522	75.590	68.866	0.911	96.109	6.894	-52.861
	184	75.569	12.325	91.218	37.610	55.479	16.068	3.536	75.568	70.131	0.928	98.322	7.104	-55.238
	185	74.512	12.142	87.623	40.025	55.891	16.062	3.578	76.170	69.061	0.907	94.291	6.668	-55.244
count	30													
AVERAGE		74.50	12.10	89.28	38.31	55.30	16.09	3.51	75.98	68.80	0.91		6.42	-54.30
SD		0.70	0.25	1.18	0.82	0.58	0.02	0.04	0.47	0.84	0.01		0.79	1.69
SE		0.13	0.05	0.22	0.15	0.11	0.00	0.01	0.09	0.15	0.00		0.14	0.31

Figure 3-65: The numerical data of haemodynamic parameters during assisted period

At the bottom part of Figure 3-64 and Figure 3-65, are the rows showing statistical data for each of the columns i.e. the average (the arithmetic mean of the group), the standard deviation (SD) and the standard error (SE).

3.4.2 Statistical Method

The main objective of this study was to determine whether the balloon pump activation has any effect on the haemodynamics of the systemic and LCA circulation. To achieve that objective, the differences between non-assisted and assisted circulation need to be assessed whether the differences were significantly different and not due to random occurrences.

Statistical analysis offers a reliable and scientific way of quantifying and clearly detects any differences between two or more groups. The conclusion drawn using statistical analysis was far more reliable as differences between parameters are tested thoroughly.

Statistics tries to answer a well-put research question in the form of a hypothesis; an example of such a well-put question might "does the activation of the balloon pump increased the perfusion to the systemic and left coronary circulation?" The research question was then formulated into two contradicting hypothesis:

Null hypothesis (H_0):

> There is <u>NO</u> statistically significant difference between the mean of two groups i.e. the results indicate that the condition before and after balloon activation is the same.

Alternative hypothesis (H_1):

> There is a statistically significant difference between those two groups i.e. the result indicate that the activation of the balloon pump has an effect to the circulation.

The null hypothesis must always state there was no difference between two groups. Having formulated the null and alternative hypothesis for each experimental factor, the next course of action was to determine whether the null hypothesis was true or otherwise false by performing statistical test. If the null hypothesis is false, the alternative hypothesis is adopted; in the above case, the mean difference between two groups was statistically significant.

3.4.2.1 The Parametric Data

A type of statistical analysis used in this study is the analysis of variance (ANOVA), a parametric test for data that was normally distributed i.e. the data follows a bell curved distribution plot. There are several ways to determine whether data collected is normally distributed; the easiest one is to plot a histogram of all the data and if the plotted histogram resembles a bell-shaped curve, then the data can be said to follow normal distribution. Another visual method is known as the Normal Q-Q plot; if the data points plotted fall away from the straight line, then it is not from a normally distributed population. A much more objective and quantitative way to determine the data normality are by using either Kolmogorov-Smirnov or Shapiro-Wilk test, or both. Those tests compare the data against normally distributed data; if the tests showed p-value less than 0.05, the data is not normal. Shapiro-Wilk test is normally used for small sample size data ($N \leq 10$).

Parametric data is the term used for data following normal distribution pattern, and can be computed to give distribution parameters such as the average mean, the variance or the standard deviation. Data that violate the normality requirement is called a nonparametric data, and such data was transformed to rank (i.e. the original data was arranged in a numerical order, from the smallest to the highest one); instead of mean average, median (an indicator between two halves for a skewed distribution) was calculated.

3.4.2.2 Sample Size Calculation and Power Analysis

The power of a test signifies the sensitivity of the test to detect an effect if present, consequently rejecting the null hypothesis. The power of a test is defined to be $(1 - \beta)$, where β is the probability of committing a type II error i.e. rejecting the null hypothesis when it is true. The greater the power of the test, the easier it is to detect the effect and to reject the null hypothesis. Normally β is set to 0.2 or 0.1 meaning the power of the test is at 80% or 90%[38]. The magnitude of the power of the test is affected by the sample size. The higher the power of the test needs to be, the more samples need to be obtained. In this study, β is set to 0.1 i.e. 90 % power.

A decision has been taken to set the sample size to 30 for both flow conditions; this is due to the low variability of CO as exhibited in Figure 3-64 and Figure 3-65, where both SDs were around 0.02 to 0.04 L/min. Other response outputs variability is assumed to be low as well thus the 90%

---

[38] The power of a test is defined as percentage of $(1 - \beta)$

power of the test is enough to sense any differences. Equal sample size is an important factor for some of the post-hoc tests employed in this work (Tukey HSD or Nemenyi). Further explanation of sample size calculation is provided in Appendix B.

Factorial design method was employed in this study, and there must be at least two repetitions to fulfill analytical requirement. However, to what extent it has to be replicated depends on the standard deviation for each experimental factor, as well as the D value i.e. mean difference significant to the experiment, as well as the value of α and β. This study adopted normal engineering convention where three (3) replications were carried out.

3.4.2.3 Randomisation

One of the important requirements when using factorial design method is the randomisation of the order of the experiment and/or the data extracted from the experiment. The order of the experiment was randomized using a subroutine in Microsoft Visual Basic to generate random number. For example, as tabulated in Table 3-19, the list on the left is the combination between inflation (A to C) and deflation timing (G to J) (refer to Figure 3-68). Using random number generated for 12 numbers, the order was rearranged as in the right side table:

Table 3-19: The randomization of list order of the experimental combination

Before randomisation		After randomisation	
i	A-G	1	B-I
ii	A-H	2	B-J
iii	A-I	3	C-G
iv	A-J	4	C-J
v	B-G	5	A-J
vi	B-H	6	A-H
vii	B-I	7	A-G
vii	B-J	8	C-I
ix	C-G	9	C-H
x	C-H	10	B-G
xi	C-I	11	B-H
xii	C-J	12	A-I

Recall that ANOVA also requires that the data to be randomly chosen. Pressure and flowrate waveform data were recorded consecutively on a temporal axis; however, sample data for analysis was not taken consecutively but every other time point. This is illustrated in Figure 3-64 and Figure 3-65, where in column t (for time point), data was for t = 1, 3, 5…59 (non-assisted circulation) and t = 110, 112, 114…185 (assisted circulation). In certain cases, where the next data was not suitable, consecutive data was taken.

3.4.2.4 Student's t-test

The simplest form of statistical analysis is the Student t-test or Two-sample t-test. Basically the mean between two groups is compared to determine whether or not both came from the same population and whether any difference is not due to chance. The decision whether to accept the null hypothesis, H_0, or the alternative hypothesis, H_1, depends on the level of statistical significance, α, i.e. critical value defined beforehand. Common convention defines α =0.05[39] or 5% level of significance. If the corresponding normal distribution value of the test statistic is less than the critical value, then the null hypothesis, H_0, can be rejected at α level of significance.

Another way is by calculating the P-value which is the probability value able to demonstrate that the null hypothesis can be rejected with confidence. If the P-value computed is less than the critical value α predetermined, then the null hypothesis can be rejected at α level of significance, and accept the alternative hypothesis. $P < 0.05$ means that there is 95% or above chance that the mean between two groups is statistically significantly different.

The t-test requirement is that sample data are collected or measured from a normally distributed population, most cases show equal variance (although the t-test equations can be modified to accommodate unequal variance between groups), and the data is randomly taken.

 If the normal distribution criterion is severely compromised, nonparametric tests such as Mann-Whitney U-test or Wilcoxon signed-rank test can be used instead; however, these tests have a much lower power compared to parametric test.

---

[39] The critical value of α=0.05 is arbitrarily determined. It could be 0.10 (90% chance) or 0.01 (99% chance). In engineering practice and other scientific field, 0.05 is the usual value chosen. However, this also means that there is 1 in every 20 chances that there will be a mistake identifying real significance (a false positive)

3.4.2.5 Analysis of Variance (ANOVA)

The Student t-test is suitable for cases of one response output (i.e. one dependent variable) with one experimental factor (i.e. one independent variable) between two groups. However, the t-test is ill-suited to analyse more than two groups. It is not preferable to use Student's t-test across all groups since that will increase Type I errors i.e. rejecting the null hypothesis when it is true. As demonstrated by the formula $(1 - 0.95^n)$, as the group number (n) increases, the probability of incorrectly rejecting the null hypothesis, H_o, also increases. This is called the familywise error. For example, to compare the mean between three groups, the error associated will be higher at (1-0.95^3 =) 0.14 i.e. 14% instead of 5% if only two groups are involved, not to mention the complexity since the number of experiments also increase.

Analysis of Variance (ANOVA) circumvents the error rate inflation problem. ANOVA is a tool where the differences between experimental factors and the effect on dependant variable(s) are made clear while keeping the Type I error from inflating. ANOVA can also detect whether there is any interaction between experimental factors. It is not only a tool able to detect inter-group differences; it can also detect intra-groups difference. For each experimental factor, there were two or more levels; e.g. the heart condition: normal, recovering or heart failure. The experimental factor's effect is called the main effect while the effect between the experimental factors is called the interaction. There should be at least two replications for each set of combinations. The ANOVA hypotheses for two experimental factors A and B and the interaction are:

Experimental factor A:

   H_{0A}: The main effect of experimental factor A is NOT statistically significant.

   H_{1A}: The main effect of experimental factor A is statistically significant.

Experimental factor B:

   H_{0B}: The main effect of experimental factor B is NOT statistically significant.

   H_{1B}: The main effect of experimental factor B is statistically significant.

Interaction between A and B:

   H_{0C}: There is NO significant interaction between experimental factors A and B.

   H_{1C}: Experimental factors A and B have significant interaction between them.

There are several kinds of ANOVA test. The one-way ANOVA is used to detect significant mean difference between three groups or more involving only one experimental factor. The one-way ANOVA result will be similar to the Student t-test if there are only two groups in the experimental setting. An example of one-way ANOVA is the effect of a drug on three or more patient cohorts.

A two-way factorial ANOVA examines the effect of two experimental factors (factor A and B) on response output; an example is the effect of drug XYZ and physical therapy on treatment of a disease. The 2 × 2 factorial ANOVA, which is the easiest ANOVA test to perform, states that factor A and factor B have two levels; there are also 2 × 3 (factor A: 2 levels, factor B: 3 levels) or 3 × 3 (factor A: 3 levels, factor B: 3 levels). A three-way factorial design experiment, (A × B × C) or even higher factor ANOVAs, are available; however the result becomes increasingly difficult to interpret.

If the effect of an experimental factor was determined to be significant, and the experimental factors had more than two levels (e.g. A1, A2, A3), further testing must be done to ascertain the significance of mean difference between each level. Post-hoc tests are a modified t-test able to maintain the critical value of Type I error at 5% (or 1%). One example of a parametric type post-hoc test is the Tukey HSD test, which has a tight control over Type I error rate, although the variances of the groups and the sample sizes of both groups must be equal.

There are several requirements ANOVA has to met, 1) normally distributed data, 2) random sampling and 3) equality of variance[40]. Out of those three requirements, the equality of variance must be strictly adhered. In SPPS[41], the equality of variance is tested using Levene's test, and if the test showed $p < 0.05$, homogeneity of variance has been violated. In that case, nonparametric test must be used. The comparable nonparametric tests for ANOVA's are tabulated in Table 3-20.

Table 3-20: Parametric ANOVA and its corresponding equivalent nonparametric test

One-way ANOVA	≈	Kruskal-Wallis test
Two-way ANOVA without replication	≈	Friedmann's test
Two-way ANOVA with replication	≈	Scheirer-Ray-Hare (SRH) test

The nonparametric Scheirer-Ray-Hare (SRH) test is an extension of Kruskal-Wallis test for one-way ANOVA analogue (Zar, 2010, McDonald, 2009). In brief, the original data is rank-transformed,

---

[40] Variance is the mean sum of squares (SS) which represents the dispersion of individual data from the sample mean.
[41] PASW Statistics 18, IBM SPSS, IBM Corp., USA

changing original data into nonparametric data by assigning each sample value a numerical order. After which standard two-way ANOVA is performed on the rank-transformed data. The ANOVA result from the rank-transformed data are used to compute a new test-statistic, *H*, to which p-value is calculated for each main effect and interaction between main effects. The exact method of executing the test is detailed in Appendix B (B-1). Figure 3-66 illustrated the algorithm to choose appropriate statistical test in this study. Only if the normality of data and equal variance assumptions met, can the standard ANOVA analysis be employed; otherwise SRH test is required.

The nonparametric SRH test is of lower power compared to two-way ANOVA (i.e. it has a greater chance of type II error). However, the assumption of equal variance is of no importance, hence the flexibility to analyse nonparametric data.

Similar to Tukey HSD test, for nonparametric data, the Nemenyi test can be carried out to test significance difference amongst levels i.e. within group. The procedure is explained in Appendix B (B-2).
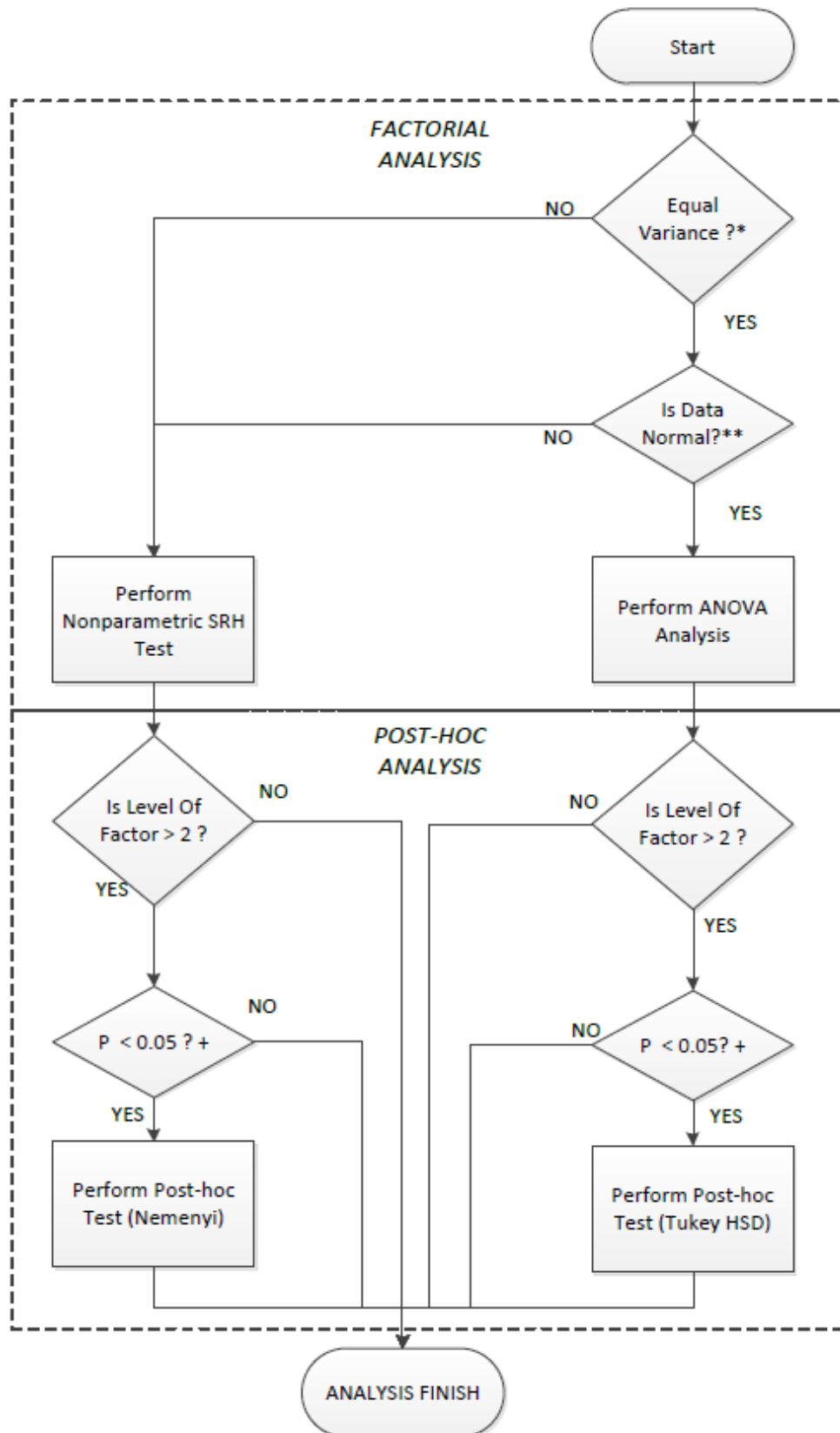
Figure 3-66: Flow chart representing the algorithm to choose the appropriate statistical analysis for the experimental data. (*:Performed using Levene's test of heomogeneity, **:Performed using Kolmogorov-Smirnov and/or Shapiro-Wilk test, +: p < 0.05 for experimental factor with level > 2)

3.4.2.6 Correlation between dependent variables

In the IABP console, during the balloon activation period, other than aortic systolic and diastolic pressure, the peak aortic diastolic pressure (PADA) is also displayed (refer to Figure 3-61). In a clinical setting, the augmentation effect of IABP is normally inferred from the magnitude of PADA. A CIMS balloon pump implanted in the body is designed to be as simple and unobtrusive as possible; although there is a pressure sensor, it has no flowrate sensor, thus no information on perfusion levels. The question is whether PADA is the suitable indicator for increased systemic and coronary circulation.

The answer to that question lies in the association between variables. To determine whether the association were statistically significant or not, the Pearson's correlation coefficient, *r*, was calculated, also the coefficient of determination, R^2, which described the strength of the association. The correlation, r, was calculated by normalizing covariance with standard deviation of the variables as Eq. 3.5 (Field, 2009):

$$ r = \frac{cov_{xy}}{s_x s_y} = \frac{\sum(x_i - \bar{x})(y_i - \bar{y})}{(N-1)s_x s_y}. \qquad 3.5 $$

In the case of normality violation, the Spearman test, r_s, a non-parametric test was used. Since the only interest was whether any correlation relationship existed between variables, two-tailed hypothesis was chosen. Statistical software, SPSS, was used to carry out the correlation test.

3.4.2.7 Experimental Factors and Response Outputs

The experimental factors investigated in this study are:

    i)   Balloon inflation timing (Inflation)

    ii)   Balloon deflation timing (Deflation)

    iii)   Helium gas volume (GasVol)

    iv)   Balloon pump design (Device Design)

    v)   State of arterial compliance (Arterial Compliance)

    vi)   Types of aortic heart valve (Aortic HV)

The MCL was set at failing heart (HF) condition, which was the fixed experimental factor for all experiments. Obviously, experiments where all experimental factors were combined and carried out more than once would be difficult, as would the complexity of analysis and interpretation of result, since there would be 2^6 = 64 combination of factors for one replication. If the above experimental factors were to be carried out concurrently, with two levels for each factor, two replications would mean 128 rounds of experiments. Clearly, a more efficient manner of experimentation was needed; factorial design experiment method fulfilled the requirement.

A factorial design experiment makes the experimental procedure a much easier and more effective exercise. A 2 x 2 factorial experiment with two replications only requires $2^2 \times 2$ = 8 rounds of experiments, while three replications requires $2^2 \times 3$ = 12 rounds. There were five experiments conducted and the explanation for each experiment is presented below.

In this study, the response outputs that were of importance are:

1) cardiac output (CO)
2) left coronary artery flowrate (QcorMean)
3) aortic systolic pressure (AoPmax)
4) aortic end diastolic pressure (AoEDP)
5) Pressure difference, dP

The ANOVA/SRH analysis was carried out for the first four response outputs. Pressure difference, dP, is defined as per Eq. 3.6, and was used for correlation analysis; Figure 3-67 illustrates the relationship:

$$dP_i = \frac{PADA_i - AoPmax_i}{AoPmax}.$$

3.6

The numerator was divided by the average of non-assisted circulation AoPmax to normalize pressure differences between AoPmax and PADA with regards to non-assisted AoPmax; this was done to eliminate between-group and within-group variability.
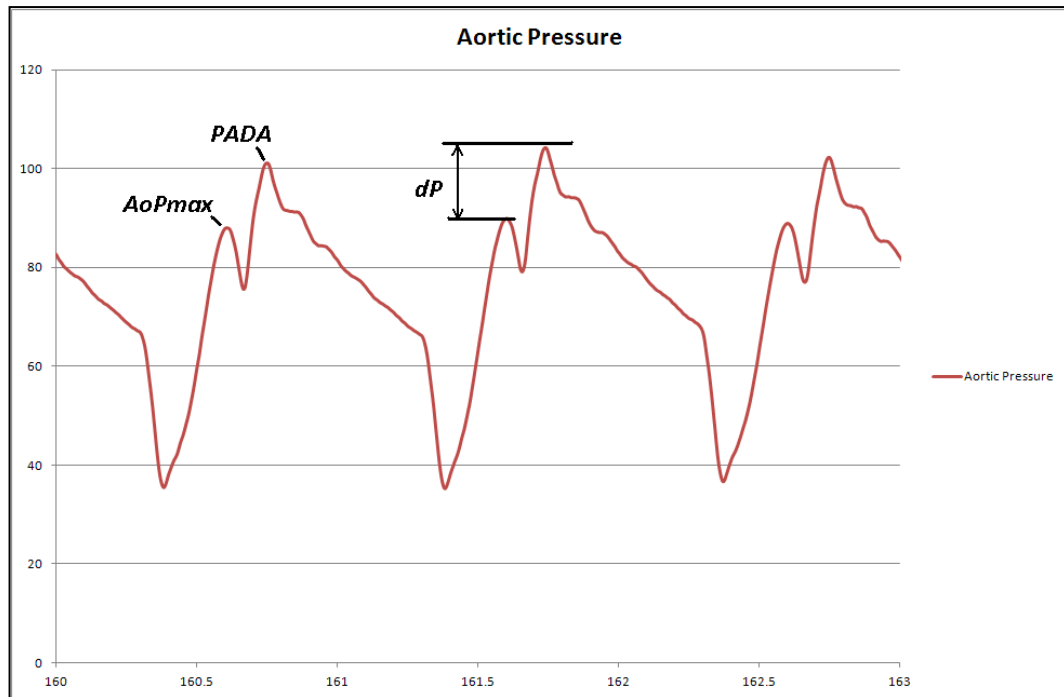
Figure 3-67: dP is the difference between PADA and AoPmax, normalized with AoPmax.

All four major experiments shared these research questions:

1) *Which combination of experimental factors optimised the response output?*

2) *What effects do the experimental factors have on the response output trend?*

A) **TIMING**

This experiment was to determine the effect of different inflation and deflation timings. Once the optimal setting was figured out, it was used as the fixed experimental factor throughout the later experiments.

Figure 3-68 illustrates the inflation and deflation timing point selections on aortic pressure waveform. There are three points for inflation timing (A, B, C), while four points for deflation point (G, H, I, J). Those points also synchronise to the aortic flowrate cycle which indicates aortic valve opening/closing position as tabulated in Table 3-21.
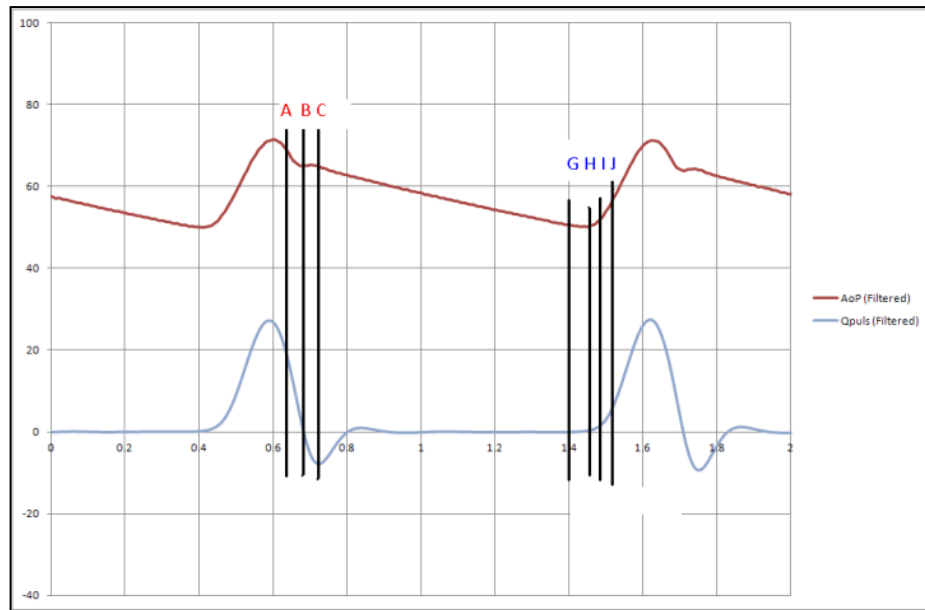
Figure 3-68: The targeted inflation and deflation timing point on aortic pressure waveform

Table 3-21: Inflation/Deflation points at aortic pressure waveform and its corresponding place in the cardiac cyle

Timing	Point	Note
Inflation	A	Early inflation, aortic valve still opened but aortic flowrate decreasing
	B	Dicrotic notch. Aortic valve closed
	C	Late inflation. Aortic valve closed
Deflation	G	Early deflation.
	H	Optimum point 1. Aortic valve begins to open
	I	Optimum point 2. Early systole where fluid is ejected into the aorta
	J	Late deflation. Aortic valve opened, fluid ejected at full force.

The reason deflation point had one more point selected was due to preliminary testing indicating deflation timing had considerable effect on the circulation; as such, more emphasis was given to deflation timing.

Prior to any experiments, the timing knobs were adjusted so that balloon inflation was set at the dicrotic notch, as displayed on the IABP console (refer to Figure 3-60) following Figure 3-68, the corresponding point on the timing knob was marked as the 'B' point. A similar exercise was carried out for 'H' deflation point and other points (A, B, G, I, J). There are 12 combinations for the 3 x 4 factorial ANOVA experiment as tabulated in Table 3-22.

Table 3-22: The combination of for each of timing's experimental factors and levels

TIMING		Deflation			
		G	H	I	J
Inflation	A	A-G	A-H	A-I	A-J
	B	B-G	B-H	B-I	B-J
	C	C-G	C-H	C-I	C-J

B) **Helium Gas Volume (GasVOL)**

The IABP console used in this experiment operated using Helium gas. The effect of different volumes of Helium gas in conjunction with different balloon innate compliances was explored in this experiment.

Table 3-23 tabulates the combinations between balloon pump type and Helium gas volume. Two levels of balloon innate compliance versus three levels of Helium gas volume were set. The balloon innate compliance levels, termed as Device Design, were represented by two kinds of balloon pump; the straight body (SB) and the compliant body (CB). The three levels of Helium gas volume (20, 25 and 30 mL) were set so that the Helium gas level could be categorised to low, optimum and high.

Table 3-23: The combination of balloon compliance and Helium gas volume

Helium Gas Volume	GasVol		
Device Design	20 mL	25 mL	30 mL
Straight body (SB)	SB & 20 mL	SB & 25 mL	SB & 30 mL
Compliant body (CB)	CB & 20 mL	CB & 25 mL	CB & 30 mL

C) **COMPLIANCE**

In this 2 × 2 factorial design experiment, the effect between Device Design factor with two levels (SB, CB), and Arterial Compliance factor, also with two levels of arterial compliance was explored. The arterial compliance levels were set at high compliance (C = 2.5 mL/mmHg) and low compliance (C = 1.25 mL/mmHg).

The balloon innate compliance was different between the SB (0 mL/mmHg) and CB (0.11 mL/mmHg), which made balloon pump compliance a dependent variable; however in this study both SB and CB were defined as independent factors.

A table tabulating the interacting experimental factors is shown in Table 3-24:

Table 3-24: A 2 x 2 factorial design between device design and arterial compliance

Device Design vs. Arterial Compliance	Device Design	
Arterial Compliance	Straight body (SB)	Compliant body (CB)
High (C2.5)	SB - C2.5	CB - C2.5
Low (C1.25)	SB - C1.25	CB - C1.25

D) **Type of Heart Valve vs. Arterial Compliance vs. Deflation Timing**

The last experiment scheduled for this flow/pressure study was made of three different experimental factors:

1) The types of heart valve (MHV or Bio-Prosthetic),

2) Arterial Compliance (high or low) and

3) Deflation timing (early, optimum and late).

It is in this batch of experiments that the effect of heart valve can be examined critically. The combination of those three experimental factors is illustrated in Figure 3-69. The 2 × 3 × 2 cube explores all possible combinations of these three experimental factors; there are 12 combinations for one replication.
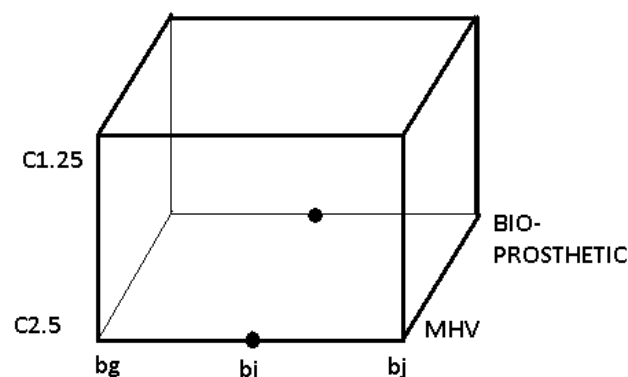
Figure 3-69: The combination of three experimental factors is illustrated by this cube

With increased factors, the randomised order combination posed a specific difficulty. The changing of parameters in the MCL were still within the same heart valve; however, the action of changing two different heart valves in a randomized order might have introduced unnecessary systematic bias and high experimental errors into the experiment; so the decision to separate between the types of valve (MHV & Bio-Prosthetic heart valve) was taken, and in effect conducting two different 2 × 3 factorial experiments.

Table 3-25 tabulates the combination of Deflation and Arterial Compliance factors for one level of heart valve type.

Table 3-25: 2 x 3 table combination of deflation timing and arterial compliance

Deflation vs. Arterial Compliance	Deflation		
Arterial compliance	Early (B-G)	Optimum (B-I)	Late (B-J)
High (C2.5)	C2.5 & B-G	C2.5 & B-I	C2.5 & B-J
Low (C1.25)	C1.25 & B-G	C1.25 & B-I	C1.25 & B-J

To maintain a tight control on systematic bias and experimental error, the MCL was turned off and started again after several combination tests. In statistical terms, this method is called '*blocking*'. The data were analysed separately; however the conclusion was drawn from both experiments.

All four types of experiments are tabulated in Table 3-26.

Table 3-26: Experimental factors and associated levels in respective factorial design experiment

Type of experiment		Experimental factor	Level
TIMING		Inflation	A,B,C
		Deflation	G,H,I,J
Helium Gas Volume (GasVOL)		GasVol	V20, V25, V30
		Device design	SB, CB
COMPLIANCE		Arterial Compliance	C2.5, C1.25
		Device design	SB, CB
HEART VALVE	Heart Valve Type: (MHV, BioPHV)	Deflation	G, I, J
		Arterial Compliance	C2.5, C1.25

3.4.2.8 Data Operation

All data obtained from the experiments was processed using Microsoft Excel 2007 and Matlab ® software before being fed into SPSS statistical software for further analysis.

Depending on the nature of the data (parametric or non-parametric), appropriate statistical tests were conducted as illustrated in Figure 3-66. If the data were non-parametric in nature, some of the calculations were done using Microsoft Excel 2007 software (Microsoft Inc., Redmond, Washington, USA).

The data fed into the SPSS statistical analysis software was for determining the effect on response outputs from multiple experimental factors, and not the difference between before and after balloon activation. If the latter was to be evaluated, the Student t-test or one-way ANOVA would be sufficient, and from initial experiments, it was found that balloon activation augmented haemodynamics characteristics (systemic and coronary perfusion, reduction of AoEDP etc.) significantly most of the time. Student t-test results are compiled in APPENDIX F – Student T-test Results. Factorial experiment allows for a more thorough understanding on effect from multiple factors compared to a single factor analysis.

The data used for the statistical analysis consisted of the ratio between each sample of the assisted flow and the mean of non-assisted flow. This was done to preserve the variability of the sample. If the ratio were calculated between mean assisted flow over mean non-assisted flow, yielding one value per combination, then only three values per combination (due to three repetitions) would be analysed; the result might not reflect the actual effect from the experiment. Instead, if each sample in assisted flow is divided by one mean value of non-assisted flow, then 180 values (90 per combination for 3 repetitions) are yielded. To facilitate easier understanding, results are presented in percentage (%) rather than ratio. The ratio and percentage were considered continuous data, a prerequisite for parametric tests.

3.4.2.9 Endocardial Viability Ratio

The endocardial viability ratio (EVR) is a suitable performance index for counterpulsation devices; diastolic pressure augmentation leads to increased aortic pressure area, and this is included in the EVR calculation. Figure 2-30 is an example of DPTI and TTI definition from an in vivo study. Figure 3-70 illustrates how DPTI and TTI is defined from left ventricular pressure and aortic pressure

measured in the MCL. The tension time index (TTI) is the integral of area under the left ventricular pressure (LVP) waveform during systole, defined starting from sudden LVP increase until the dicrotic notch (the light grey shaded part). The diastolic pressure time index (DPTI), is the integral of area between the aortic pressure and the left ventricular pressure, which is the dark grey area in Figure 3-70. The EVR value, according to Eq. 1.1, may be calculated for non-assisted and assisted circulation.
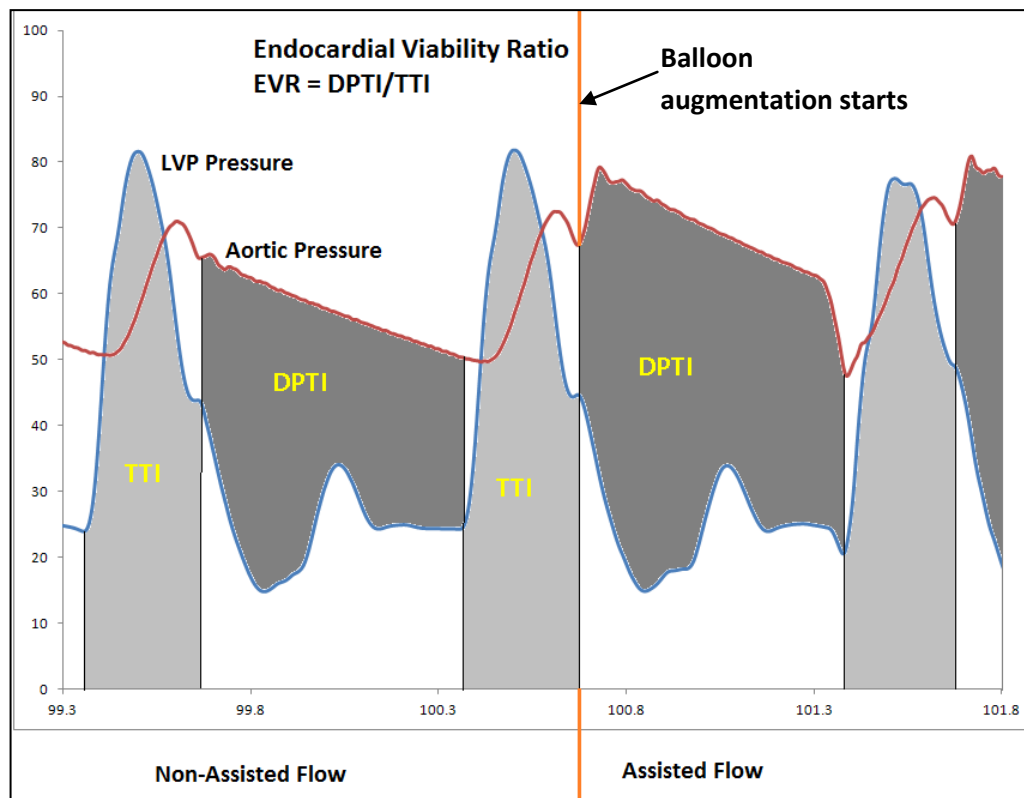
Figure 3-70: Diastolic augmentation due to balloon activation increases aortic pressure increasing myocardial oxygen supply, indicated by diastolic pressure time index (DPTI) shaded in dark grey; while myocardial oxygen demand is defined by tension time index (TTI) which is the light grey shaded area under systolic curve of the left ventricular pressure. The ratio of myocardial oxygen supply and demand is endocardial viability ratio (EVR).

Only 20 samples from each segment were randomly extracted, since the variances of samples are very small. Statistical tests were carried out to determine whether or not the EVR value before and after balloon activation was significantly different. A factorial analysis was carried out to discern the effect of different balloon pump designs and arterial compliances on EVR. Depending on equality of variance and normality of data distribution, parametric or non-parametric tests were used.

3.5   Flow Visualisation

The flow visualisation experimental method is elaborated here.

3.5.1   Introduction

Flow visualisation is an essential tool in understanding fluid flow phenomena as well as a suitable tool to validate a hypothesis. Figure 3-71 illustrates the relationship between pressure and flowrate during balloon activation. The Helium gas pressure inflates and deflates in diastole. At end-diastole, pressure inside the balloon decreased suddenly to about -40 mmHg in the balloon pump. Consequently, the deflation of the balloon pump near the heart valve caused a sudden pressure reduction, and this decreased the resistance against which the left ventricle had to pump against; it was hypothesised that this caused the aortic valve to open prematurely. During preliminary testing, it was observed that valve would appear to opened slightly longer when the balloon pump was activated.

To ascertain that balloon pump activation prolonged aortic valve leaflet opening time, it was necessary to record the valve leaflet motion during cardiac cycles.
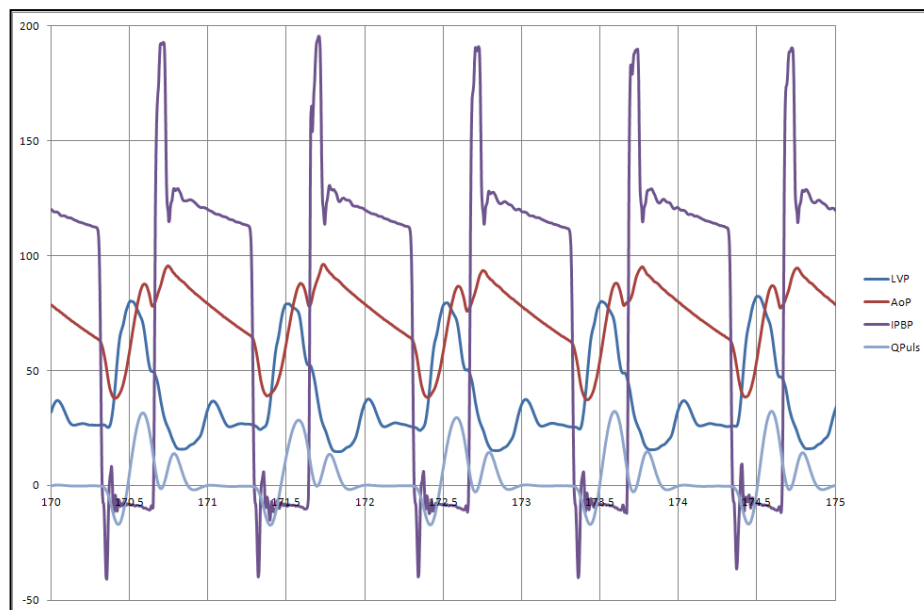
Figure 3-71: Pressure and flowrate waveform. The sudden decrease of Helium gas pressure is illustrated by IPBP line and coincides with negative flowrate of the aortic section.

3.5.2 Flow Visualisation Setup

To observe the valve leaflet motion, a few modifications were made to the MCL. The top part of the LV silicone sac, was modified by replacing the original silicone tube with a transparent acrylic tube (ID 26 mm) and the aortic MHV was fixed in place using a Loctite silicone sealant, shown in Figure 3-72. The mitral valve was still fixed at the original silicone tube housing.
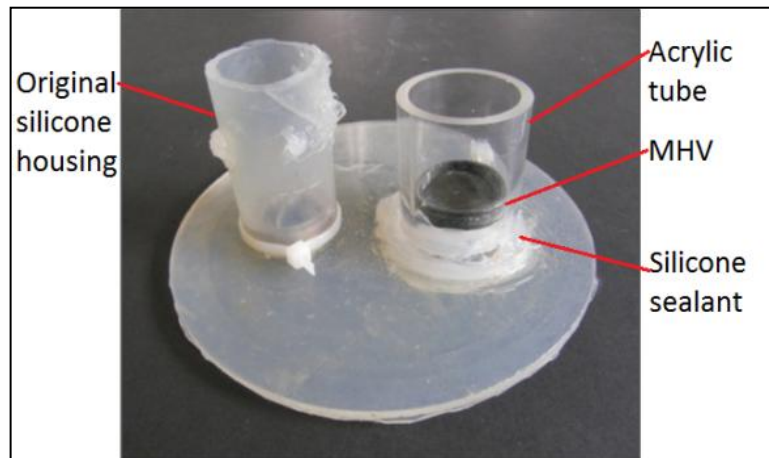
Figure 3-72: The top part of the LV silicone sac with a clear acrylic pipe fixed inside it with a bileaflet aortic MHV.

A different kind of balloon pump housing made of glass was used for flow visualisation experiment shown in Figure 3-73. The internal diameter of the glass balloon pump was the same as the rapid prototyped balloon pump.
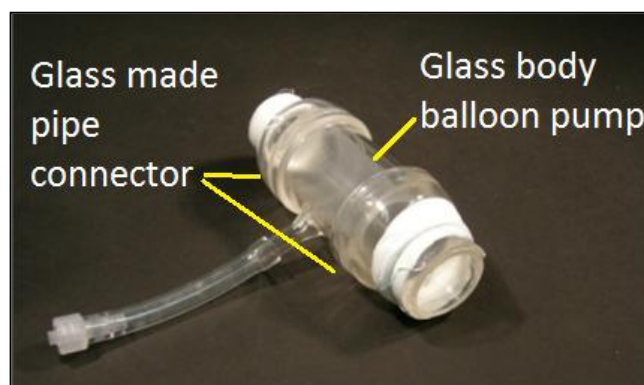
Figure 3-73: Balloon pump housing made of glass

Figure 3-74 and Figure 3-75 show the setup of the camera and red LED at the MCL to record the aortic bileaflet valve motion. The digital camera (SP-560UZ, Olympus Inc., Japan) is capable of

capturing high quality video (650 x 480 pixels at 30 frames/s). The camera's automatic white balancing was used during the video recording.
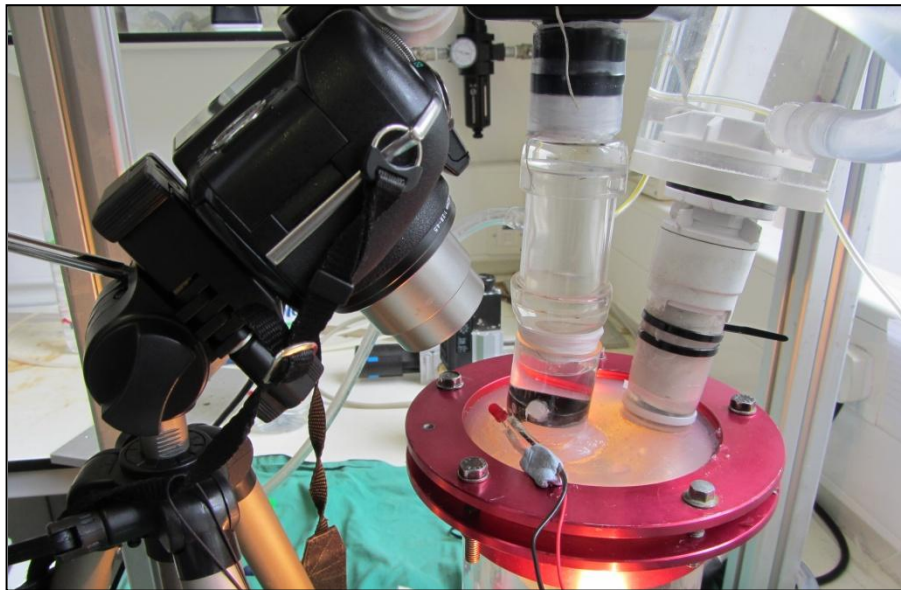
Figure 3-74: The setup for flow visualisation of the valve motion. A red LED was placed in front of the acrylic pipe

Figure 3-75 shows the zoomed in picture of the camera lens. It was set up very near to the acrylic pipe and placed at a suitable angle to record the leaflet motion as closely as possible. A red LED was placed in front of the acrylic pipe as a marker for video recording sequence. Macro focus mode was used.
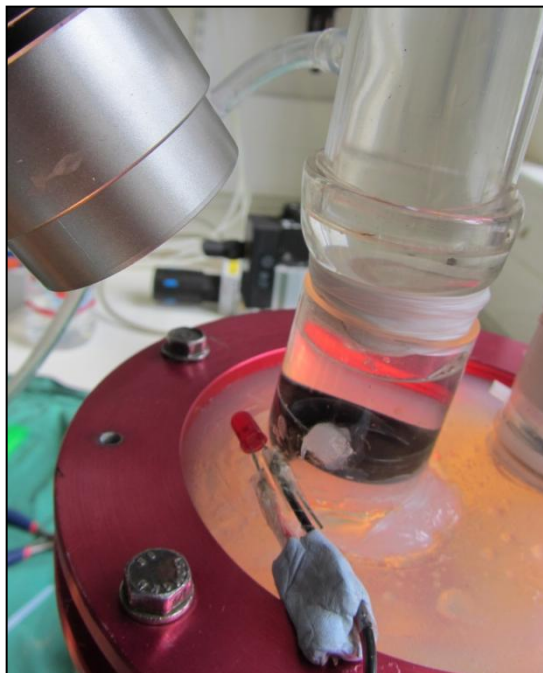
Figure 3-75: Zoomed in picture of the camera and the MCL rig

The video was taken and transferred to the PC for post-analysis process using a free multi-type video editor[42] shown in Figure 3-76. It was used to slice the original video recording into consecutive still pictures. Since the original video was taken at 30 frames/s, the resulting still pictures were 30 pictures for each second of video record. The interval between pictures was calculated to be 1/30 seconds i.e. 0.033 seconds. A sample of the resulting pictures is lined up as demonstrated at Figure 3-77.
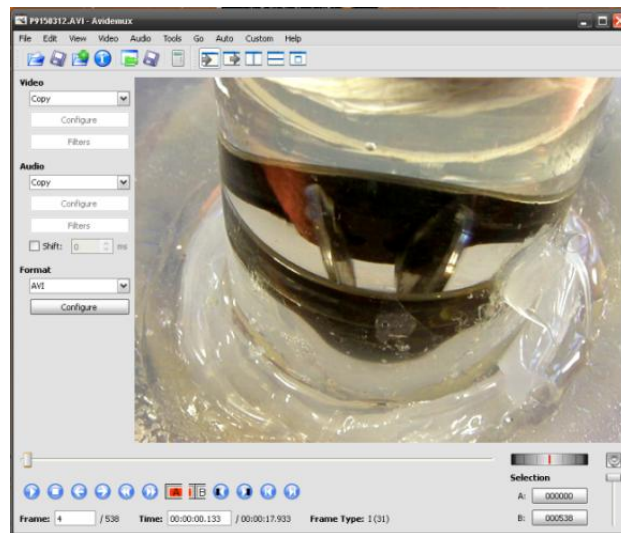
Figure 3-76: A snapshot of the Avidemux software used to slice still pictures from a video recording

The aim of this experiment was to validate the hypothesis that the aortic valve opened longer in assisted circulation. Two different videos were taken; a non-assisted circulation and assisted circulation, each for 15 seconds. MCL setting was set to heart failure (HF) condition with soft arterial compliance at C = 2.5 mL/mmHg. There were two settings for heart rate, 54 and 60 beats/min.
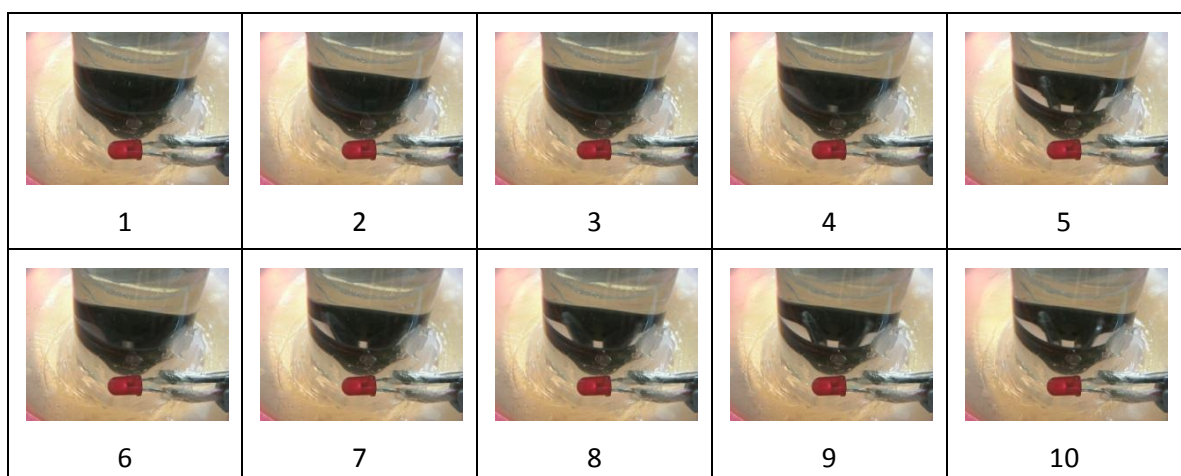
Figure 3-77: A sample of the consecutive still picture from a video of bileaflet valve motion during assisted circulation

---

[42] Avidemux ,Version 2.5.4 (r7200), Mean, http://www.avidemux.org

To determine the amount of time the valve opens up, visual inspection of each strip of 30 images for 10 seconds was done (in the case of 60 beats/min). The number of still images where the valve was open was summed. For example, in the above Figure 3-77, the still image from frame number four (4) is the first image to be counted. An average from each second of 30 images was computed. After confirming the normality of the data distribution, appropriate statistical test was performed.

3.6 Summary

This chapter presents the methods used in this study. For the *in vitro* experiments, the balloon pump housing comprised of a rigid body, the manufacturing method has been explained. Silicone elastomer was used as the deformable material.

An experimental rig appropriate to test the *in vitro* CIMS balloon pump was needed. The human mock circulatory loop (MCL) was designed and assembled to simulate correct physiological waveforms. Procedures to operate the MCL, IABP console, and data record was presented.

Raw haemodynamic data recorded needed to be sorted out and analysed. A method to accomplish that, and a brief introduction to statistical tests was also presented. The Student's t-test and Analysis of Variance (ANOVA), depending on the suitability, were used to determine whether the effect of experimental factors to the variables was statistically significant or not. Where the data violated the ANOVA test's fundamental requirement of parametricity, a nonparametric test was employed. Description of the nonparametric test was given. The experimental factors chosen to determine the CIMS balloon pump haemodynamic characteristics was laid out, as well as the response outputs. The order of the experiments was randomised. The justification, and method to randomise has been presented. Data from experiments were analysed using specialised statistical analysis software, SPSS.

The effect of balloon activation on flow was investigated using a flow visualization technique in the last subchapter. A different MCL setup was required to facilitate video recording. Avidemux (Version 2.5.4 (r7200), Mean, http://www.avidemux.org) was used to divide the video footage into digital still images. Visual inspection of images was carried out to count the number of frames in which the valve leaflet was open. The mean difference of opened valve period between non-assisted and assisted circulation was analysed using the Student t-test.

Chapter 4 *In vitro* **Balloon Pump Characteristics**

This chapter presents and discusses the experimental results of the *in vitro* CIMS balloon pump tests. Characteristics that were thought to be important to the efficacy of CIMS balloon pump were the inflation and deflation timing, the volume of Helium gas, the innate compliance of the balloon pump, the arterial compliance and the type of heart valve used in conjunction with the CIMS balloon pump. Response outputs from each experiment are the cardiac ouput (CO), left coronary artery flowrate (QcorMean), aortic systolic pressure (AoPmax), aortic diastolic pressure or end-diastolic pressure (AoEDP) and the pressure difference, dP, between peak aortic diastolic pressure (PADA) and peak aortic pressure (AoPmax). The correlations between dP with CO and QcorMean are presented.

4.1   Introduction

In each subchapter, results of the above response outputs and correlation tests are presented. Appropriate statistical analyses were performed according to the algorithm explained in chapter 3. Depending on the equality of variance of the data between groups and within groups, and the normality of data distribution, a parametric two-way ANOVA with replication test or the equivalent non-parametric ANOVA (the Scheirer-Ray-Hare (SRH)) test were employed. Suitable post-hoc analysis was performed if one of the experimental factors had more than two levels and the result was significant from the ANOVA or SRH test.

One counterpulsation device performance index widely used is the endocardial viability ratio (EVR). The EVR value signifies balance between myocardium oxygen supply and demand. A subchapter is dedicated for EVR value analysis using COMPLIANCE experiment data.

At the end of each subchapter, the overall result of experimentation is discussed, including the implications to heart failure (HF) treatment, and also how the results affected the future design of *in vivo* CIMS balloon pump. In 4.6 Overall Discussion, the results from all five experiments are corroborated and discussed more thoroughly and compared with available HF treatment, especially the types utilising positive displacement method (e.g. IABP). The conclusions were then drawn from all the results.

4.2 Balloon Timing

The effect of different balloon inflation and deflation timing was investigated. There were three different levels (A, B, C) for Inflation factor, four levels (G, H, I, J) for Deflation factor making up a 3 × 4 factorial design experiment. Experimental factors held constant were 1) heart condition in heart failure, 2) device design through the use of a straight body balloon pump (SB), 3) arterial compliance set at high ,C = 2.5 mL/mmHg (C2.5), 4) Helium gas volume set at 25 mL (V25), and 5) the aortic heart valve used was a mechanical heart valve (MHV)[43].

It was intended that the outcome from this experiment should identify the optimum point for balloon activation and suggest a trend in support yielded as a function of activation timing when the CIMS balloon pump was placed in the ascending aorta.

4.2.1 Result

As tabulated in Table 3-6, there are 12 combinations of Inflation and Deflation factors, making up one run of experiment, which were randomised and repeated three times each. Experimental data were analysed for cardiac output (CO), left coronary artery mean flowrate (QcorMean), aortic systolic pressure (AoPmax), aortic end-diastolic pressure (AoEDP). Lastly correlations between pressure difference in diastole, dP against CO and QcorMean are presented.

All values are the percentage ratio between assisted and non-assisted flow (refer to 3.4.2.8 Data Operation).

4.2.1.1 Cardiac Output (CO)

The aortic flowrate waveforms are illustrated in Figure 4-78 and Figure 4-79; all waveforms are normalised against the cardiac output of the non-assisted case. The former illustrates waveform when inflation point is fixed at point B, while deflation points are varied. There are distinct differences between early and late deflation, waveform (B-G) and (B-J), but not so much

---

[43] St. Jude Medical (SJM) Standard® Bileaflet Valve, St. Jude Medical, Minnesota, USA

difference between waveform (B-H) and (B-I). For non-assisted aortic flowrate waveform shape, please refer to Figure 3-59.
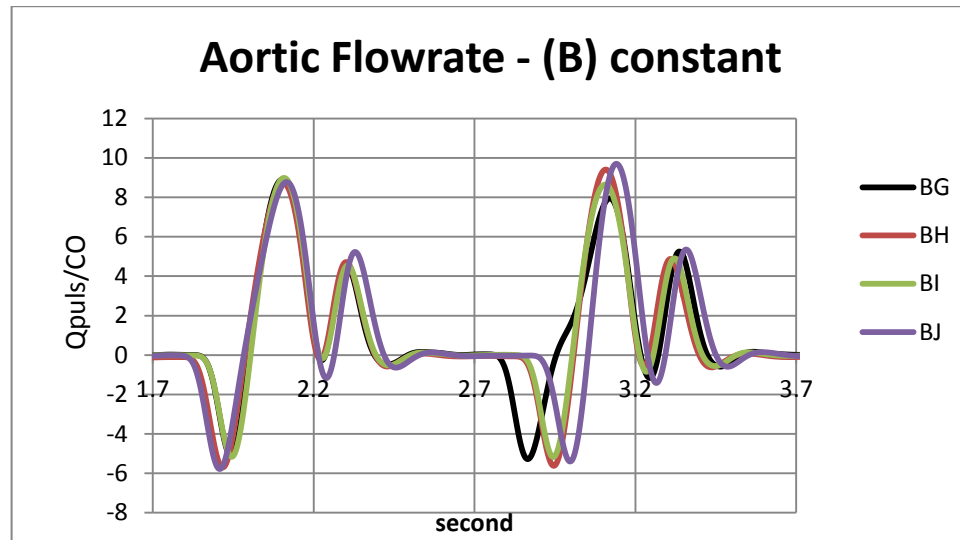
Figure 4-78: The pulsatile flowrate with varying deflation points with point B as constant point, normalised against non-assisted cardiac output (the ordinate is instantaneous flow/non-assisted C.O.)
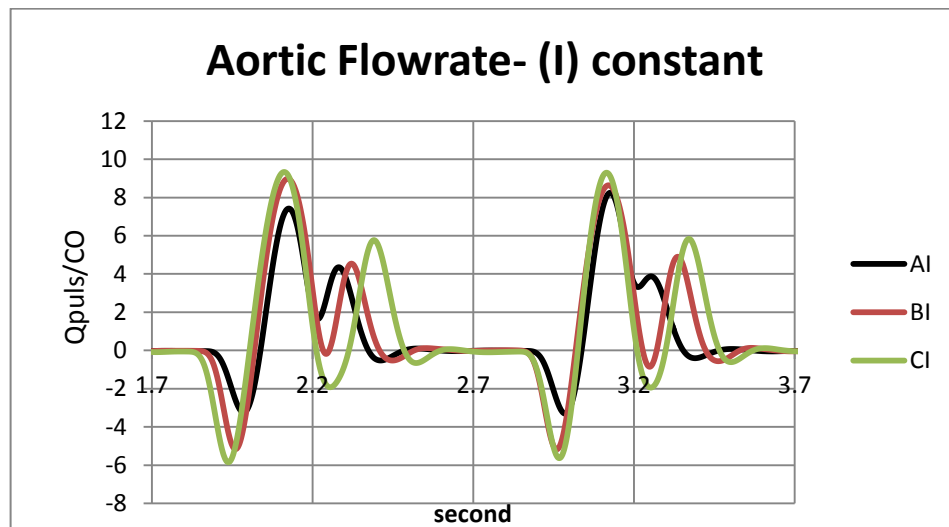
Figure 4-79: The pulsatile flowrate with varying inflation point with constant deflation point, I, normalised normalised against non-assisted cardiac output (the ordinate is instantaneous flow/non-assisted C.O.)

Figure 4-79 illustrates the effect on pulsatile flowrate when balloon pump inflation points were varied while deflation point remained constant at point (I). The height of the peak in assisted flow increases with later inflation (C-I is greater and later than A-I).

To quantify the significance of different balloon pump inflation and deflation timing, the cardiac output i.e. the mean flowrate is compared between non-assisted and assisted circulation.

Subsequent results are all presented in percentage difference between assisted and non-assisted circulation.

The means and standard deviations (SD) of Cardiac Output (CO) for each combination of Inflation and Deflation factor is tabulated in the Table 4-27.

Table 4-27: Means and standard deviation (in brackets) for CO of Timing experiments

CO		Deflation				Row Mean
		G	H	I	J	
Inflation	A	6.58 (2.28)	6.39 (2.13)	5.75 (2.64)	5.24 (2.79)	*5.99*
	B	6.77 (1.50)	6.17 (2.05)	7.03 (2.27)	4.26 (2.23)	*6.06*
	C	3.90 (1.72)	5.33 (2.06)	5.53 (1.61)	3.27 (2.13)	*4.51*
Column Mean		*5.75*	*5.97*	*6.10*	*4.26*	*5.52*

The overall effect of balloon timing variations on the mean value of CO was a minimal 5.52% inflow augmentation compared to non-assisted flow (range: 3.27% to 7.03%). The mean value for both row and column had little difference, with the exception of deflation point J at 4.26%. Further statistical analysis was performed to determine whether any of the differences were statistically significant.

According to statistical test flow chart (refer to Figure 3-66), equality of variance must be checked first, using Levene's test, and Table 4-28 shows that the data in this experiment had an unequal variance ($p < 0.001$).

Table 4-28 : Levene's test for equality of variance

Levene's Test of Equality of Error Variances Dependent Variable: CO			
F	df1	df2	Sig.
6.215	11	1068	.000

Since the homogeneity of variance requirement was not met, the non-parametric SRH test, (equivalent to two-way ANOVA with replication) was used. In Table 4-29, the SRH test result is tabulated.

Table 4-29: Non-parametric SRH test result for Timing experiment

Source	p-value
Inflation	2.89×10^{-21}
Deflation	2×10^{-21}
Inflation × Deflation	1.36×10^{-8}

Table 4-29 shows the result of SRH test, tabulating experimental factors at Source column, and the p-value. The full SRH test result is tabulated in Appendix C (C-1-1).

Further post-hoc test was carried out to determine which combination actually yielded a significant mean difference.

Post-Hoc (Inflation)

The algorithm for non-parametric post-hoc test, the Nemenyi test, is presented in Appendix B (B-2). A Kruskal Wallis test was carried out for Deflation factor which comprised of three levels for CO response output. The Mean Rank result from the Kruskal Wallis test was then used to calculate Sum Rank (Mean Rank × N), the level rank order was determined according to highest to lowest Sum Rank order as tabulated in Table 4-30.

Table 4-30: Mean Rank result from the Kruskal Wallis test with additional calculations of Sum Rank and ranking order of each level. k: number of levels

Response Output	Inflation	N	Mean Rank	Sum Rank	rank
CO	A	360	597.09	214952.4	2
	B	360	614.13	221086.8	1
	C	360	410.28	147700.8	3
	Total	1080		k =	3
				SE=	5918.142

The level rank order was then used in Nemenyi test; the results are tabulated in Table 4-31. The difference of rank sum between levels was calculated by subtracting the highest rank with the lowest (represented by Rb-Ra), and then with the next lowest rank. The test statistics, q, was computed by dividing the difference between rank sum with the SE, and compared with a

threshold value: q(α, *v* ,k), where α = 0.05, *v* = ∞, and k = 3 (Zar, 2010). If q > q(0.05,∞,3) then there is enough evidence to reject H_0.

The hypothesis for the test are "H_0: there is no statistical significance in mean difference between two groups; and H_A: there is statistical significance in mean difference between two groups ".

Table 4-31: The Nemenyi test result for Inflation factor

vs.		(Rb-Ra)	SE	q	q(0.05,∞,3)	Result	significant
B	C	73386	5918.142	12.4	3.314	Reject H_0	YES
B	A	6134.4	5918.142	1.04	3.314	Accept H_0	
A	C	67251.6	5918.142	11.36	3.314	Reject H_0	YES

Table 4-31 reports Nemenyi test results; the mean differences in (B vs. C) and (A vs. C) were significant but not (A vs. B). This means that for CO augmentation, there were no significant differences between point A and B i.e. early inflation and inflation timed at the dicrotic notch yielded similar amounts of CO augmentation.

Post-Hoc (Deflation)

Similar to the Inflation factor section, the Mean Rank result computed using a Kruskal Wallis test was used to compute Sum Rank for each level, thereafter rank-order was determined, and tabulated in Table 4-32. The null hypothesis is the same as with the Inflation section i.e. H_0: there is no statistical significance in mean difference between two groups.

Table 4-32: Kruskal Wallis test result and the computed Sum Rank. Rank is assigned accordingly. k: number of levels

Response Output	Deflation	N	Mean Rank	Sum Rank	rank
CO	G	270	574.28	155055.6	3
	H	270	600.54	162145.8	2
	I	270	605.46	163474.2	1
	J	270	381.72	103064.4	4
	Total	1080		k =	4
				SE =	5125.261

Pairwise comparison was carried out for Deflation factor comprised of four levels (G, H, I & J) by subtracting sum rank of the highest rank with the lowest one, and then the second lowest and so on. Since α = 0.05, *v* = ∞, and k = 4, then q(0.05,∞,4) = 3.633. Null hypothesis (that there is no

significance difference of CO augmentation with deflation timing) was rejected if the q value for each comparison was greater than threshold value of 3.633 (for q(0.05,∞,4), according to (Zar, 2010). The results are presented in Table 4-33.

Table 4-33: The Nemenyi test result for Deflation factor

vs		(Rb-Ra)	SE	q	q(0.05,∞,4)	Result	significant
I	H	1328.4	5125.261	0.259187	3.633	Accept H_0	
I	G	8418.6	5125.261	1.64257	3.633	Accept H_0	
I	J	60409.8	5125.261	11.78668	3.633	Reject H_0	YES
H	G	7090.2	5125.261	1.383383	3.633	Accept H_0	
H	J	59081.4	5125.261	11.52749	3.633	Reject H_0	YES
G	J	51991.2	5125.261	10.14411	3.633	Reject H_0	YES

Table 4-33 tabulates the result of Nemenyi post-hoc test for Deflation factor. Only comparison with point (J) yielded a statistically significant mean difference, i.e. (I vs. J), (H vs. J) and (G vs. J). In contrast, the percentage of CO yielded amongst point G, H and I, which correspond to deflation earlier than point J (refer to Table 3-18), were statistically similar.

Discussion

Augmentation of CO when subjected to different inflation and deflation points was quite minimal as demonstrated in Table 4-27, where the grand mean of CO was a 5.52% increase compared to non-assisted flow. Both experimental factors, Inflation and Deflation, showed significant main effect, although for Inflation factor only the mean difference with point C was significant, while results from early inflation (point A) and optimum inflation (point B) were deemed to be similar.

Figure 4-80 illustrates the means of CO percentage difference due to balloon pump activation from all combinations of Inflation and Deflation factors. Every combination with inflation point A (early) and B (optimum) yielded higher CO augmentation percentage compared to point C (later), while the highest output was yielded from combination B-I. Early and optimum (at dicrotic notch) inflation were better for CO augmentation than late inflation.
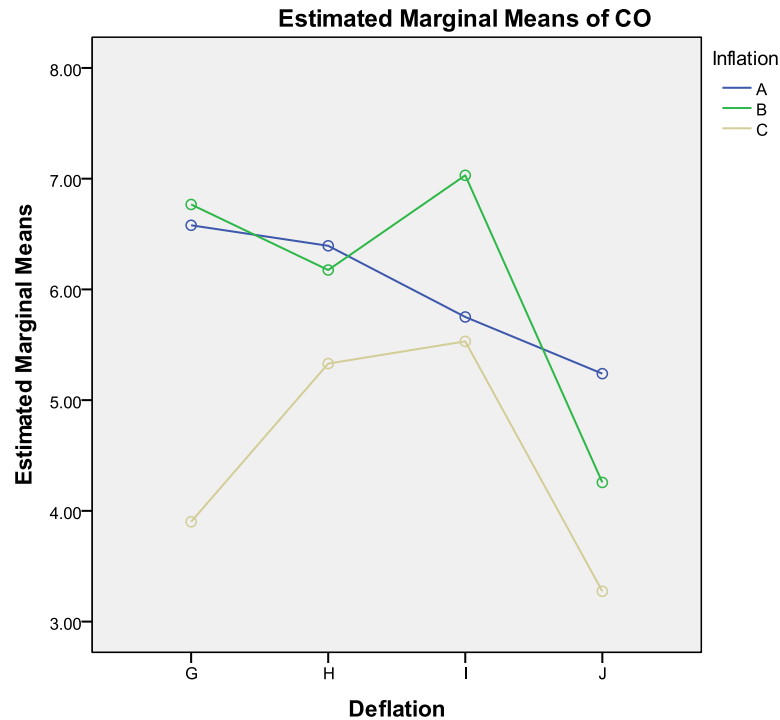
Figure 4-80: Means of for all combinations of experimental factors for CO output

While for Deflation point, mean differences amongst points G, H and I (.e. from early deflation to optimum point 2), were found to be similar, this was not so for point J. Since any combination at point J yielded lower mean value; later deflation past aortic valve opening is not advisable.

The best combination of inflation and deflation timing for CO augmentation is B-I. The inflation point B corresponding to the dicrotic notch is the same suggested inflation point for IABP. The deflation point I, corresponding to just after aortic valve opening, is different. This is discussed further in subchapter 4.2.2.

4.2.1.2 Left Coronary Artery Mean Flowrate (QcorMean)

Only important statistical test results are presented hereafter for the sake of clarity and brevity, while the supporting results and analysis are presented in Appendix C (C-1). Figure 4-81 and Figure 4-82 illustrate the left coronary artery (LCA) flow waveform; the former is with fixed inflation timing (point B: dicrotic notch), while the later has a fixed deflation timing (point I). Grey shaded areas indicate diastole. When deflation points are varied, the negative peaks vary accordingly. There is clear difference between B-G and B-J, but similar waveform from B-H and B-I.
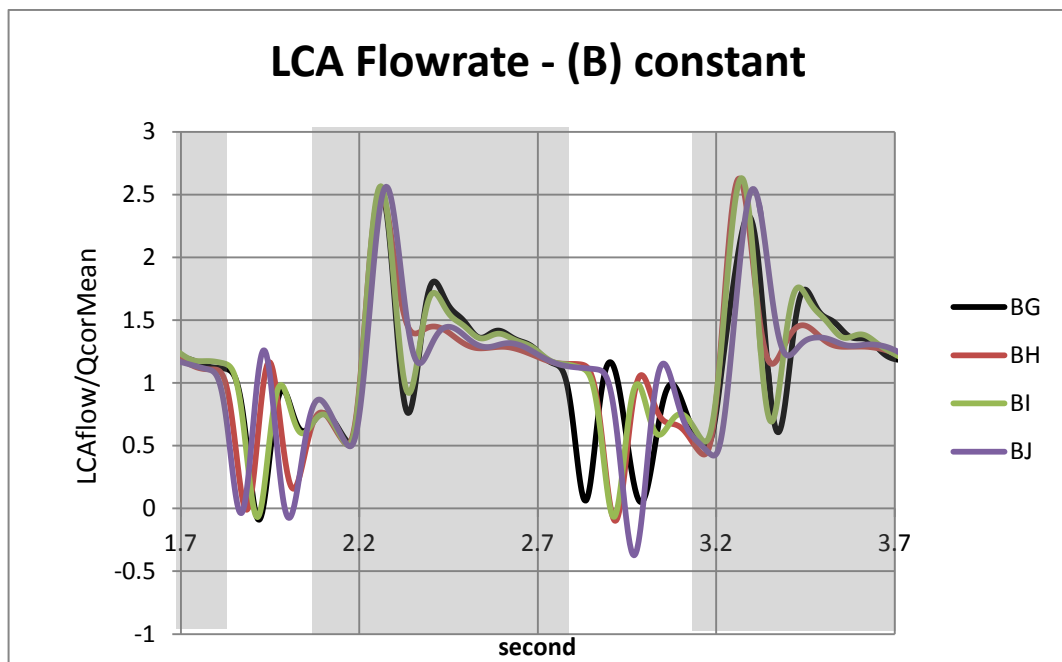
Figure 4-81: The pulsatile waveform of left coronary artery (LCA) flowrate when inflation point at dicrotic notch is fixed while deflation point is varied. Grey areas indicate diastole period (the ordinate is LCA flowrate/non-assisted mean LCA flowrate)
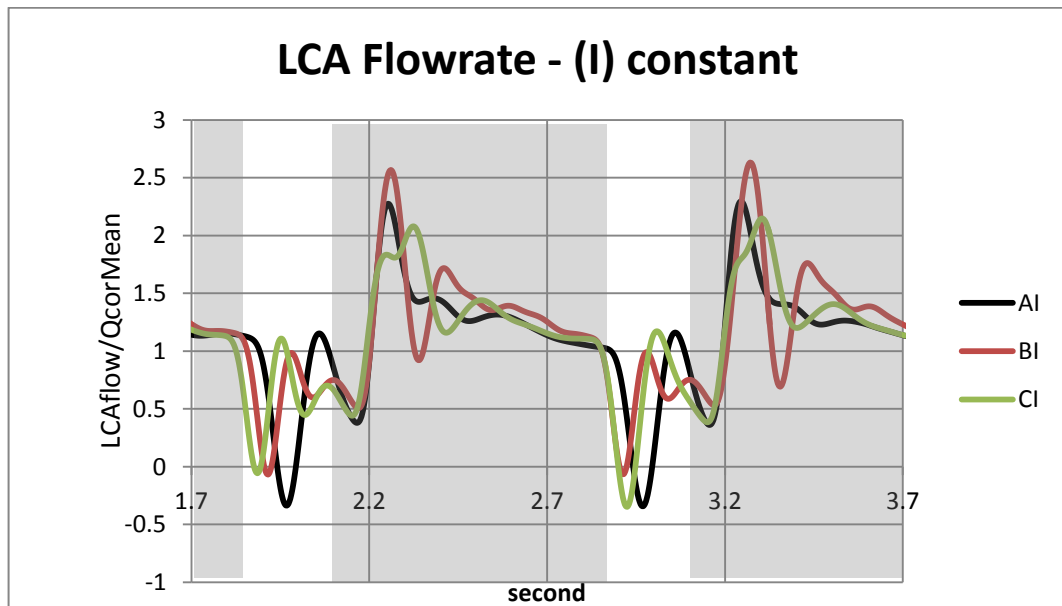
Figure 4-82: The pulsatile waveform of left coronary artery (LCA) flowrate when inflation point at dicrotic notch is varied while deflation point is fixed. Grey areas indicate diastole period (the ordinate is LCA flowrate/non-assisted mean LCA flowrate)

Figure 4-82 shows that varying balloon pump inflation timing affects secondary peak in diastole. Only balloon inflation at dicrotic notch (B-I) produces secondary peak, while the other two did

not. The difference between the mean LCA flowrate of non-assisted and assisted circulation is quantified as percentage and used for analysis.

Table 4-34 reports the means and standard deviations (SD) of flow augmentation on the left coronary artery (LCA) for each combination of Inflation and Deflation factors.

Table 4-34: Means and SDs (in brackets) for QcorMean of Timing experiment

QcorMean		Deflation				Row Mean
		G	H	I	J	
Inflation	A	8.78 (2.05)	8.67 (3.14)	9.89 (1.67)	8.54 (1.75)	*8.97*
	B	7.98 (1.63)	10.25 (2.26)	12.07 (1.97)	8.38 (1.78)	*9.67*
	C	9.21 (0.80)	9.07 (2.08)	9.34 (2.87)	7.48 (1.44)	*8.78*
Column Mean		*8.66*	*9.33*	*10.43*	*8.13*	*9.14*

The grand mean of flow augmentation for QcorMean was 9.14% (range: 7.48% to 12.07%). There was little difference in inflation (row) and deflation (column) means except for column I. Further statistical analysis was carried out to determine the statistical significance of mean differences amongst these combinations.

Table 4-35: The SRH test result for QcorMean of TIMING experiment

Source	p-value
Inflation	8.57×10^{-5}
Deflation	9.48×10^{-36}
Inflation×Deflation	3.49×10^{-16}

Non-parametric SRH test, equivalent to two-way parametric ANOVA, was used to analyse the 3 × 4 factorial experiment. The result is tabulated in Table 4-35. Inflation, deflation, and interaction all show significant effects (p < 0.001), so the Nemenyi post-hoc test was carried out to discern if any levels were significantly different from the others. The results are tabulated in Table 4-34 and Table 4-35.

Post-Hoc (Inflation)

Table 4-36: The post-hoc test result from Nemenyi test for Inflation point

	vs.	(Rb-Ra)	SE	q	q(0.05,∞,3)	Result	significant
B	C	34308	5918.142	5.79709	3.314	Reject H_0	YES
B	A	27230.4	5918.142	4.601174	3.314	Reject H_0	YES
A	C	7077.6	5918.142	1.195916	3.314	Accept H_0	

The hypothesis of the post-hoc test is similar as presented in 4.2.1.1 subchapter. Only the mean difference in two combinations were significant, (A vs. B) and (B vs. C), but not (A vs. C). This suggests that early and late inflation rendered the same amount of QcorMean augmentation. Point B (dicrotic notch) yielded a significant mean difference compared to other inflation points.

Post-Hoc (Deflation)

Table 4-37: The Nemenyi test result for Deflation point

	vs	(Rb-Ra)	SE	q	q(0.05,alpha,4)	Result	significant
I	J	88338.6	5125.261	17.23592	3.633	Reject H_0	YES
I	G	66654.9	5125.261	13.00517	3.633	Reject H_0	YES
I	H	38909.7	5125.261	7.59175	3.633	Reject H_0	YES
H	J	49428.9	5125.261	9.644172	3.633	Reject H_0	YES
H	G	27745.2	5125.261	5.413422	3.633	Reject H_0	YES
G	J	21683.7	5125.261	4.23075	3.633	Reject H_0	YES

It was found that all mean differences amongst the six combinations were significant, i.e. each deflation point had unique contribution to QcorMean augmentation with the highest yield by point (I) i.e. just after aortic valve opening

Estimated Marginal Means of QcorMean
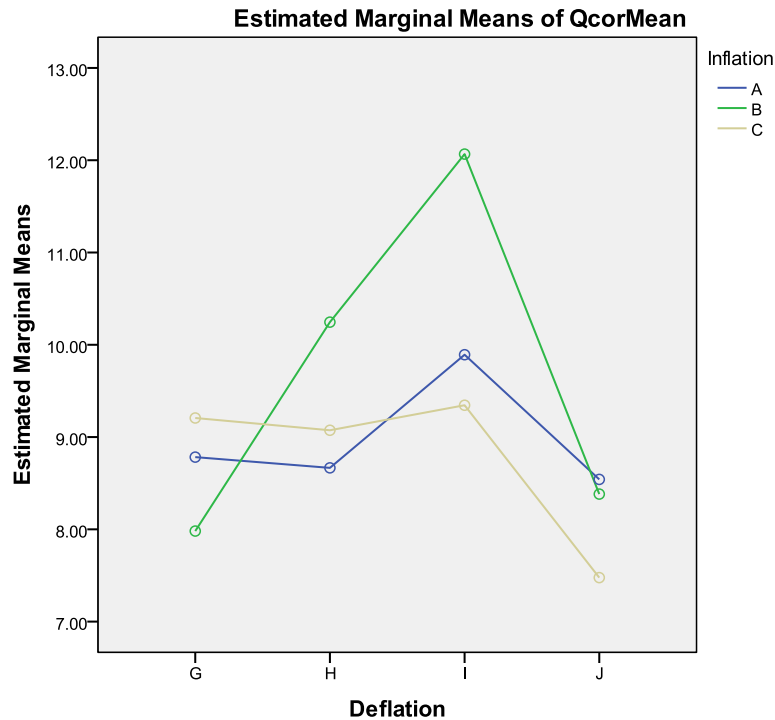
Figure 4-83: Mean value for all combinations of Timing experiment

Both experimental factors and the interaction effect were significant. Since the interaction effect was reported to be significant, future prediction of optimum inflation point cannot be made without consideration of deflation point and vice-versa. However, there is a clear indicator for highest yield of QcorMean augmentation (at combination B-I); this result is similar to the previous result wherein this combination also yielded the maximum output response for CO.

4.2.1.3 Aortic Systolic Pressure (AoPmax)

The effect of varying inflation and deflation balloon pump is illustrated in Figure 4-84 and Figure 4-85. Similar to previous subchapter, each figure shows how aortic pressure waveform changes when one factor is varied while the other is fixed. Pressures are normalized against the non-assisted mean arterial pressure (so the ordinal in these graphs is a ratio of the aortic pressure/non-assisted MAP).
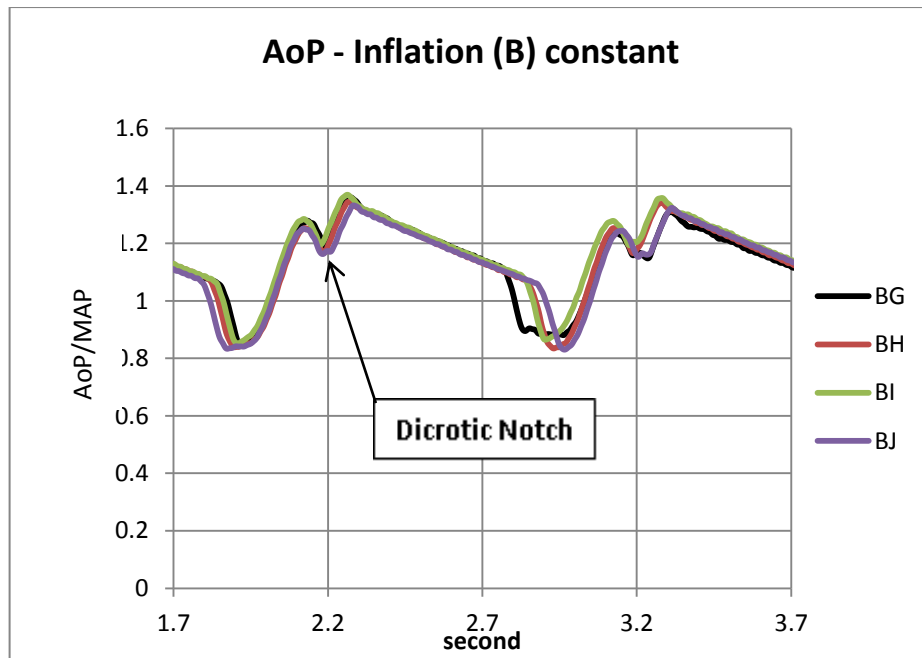
Figure 4-84: Aortic pressure waveform (ratio) when balloon inflation fixed at the dicrotic notch (B) while deflation timing is varied. (The ordinate is aortic pressure/non-assisted MAP)

The effect of early and late deflation is visible in Figure 4-84, but not much difference is evident between waveform B-H and B-I.
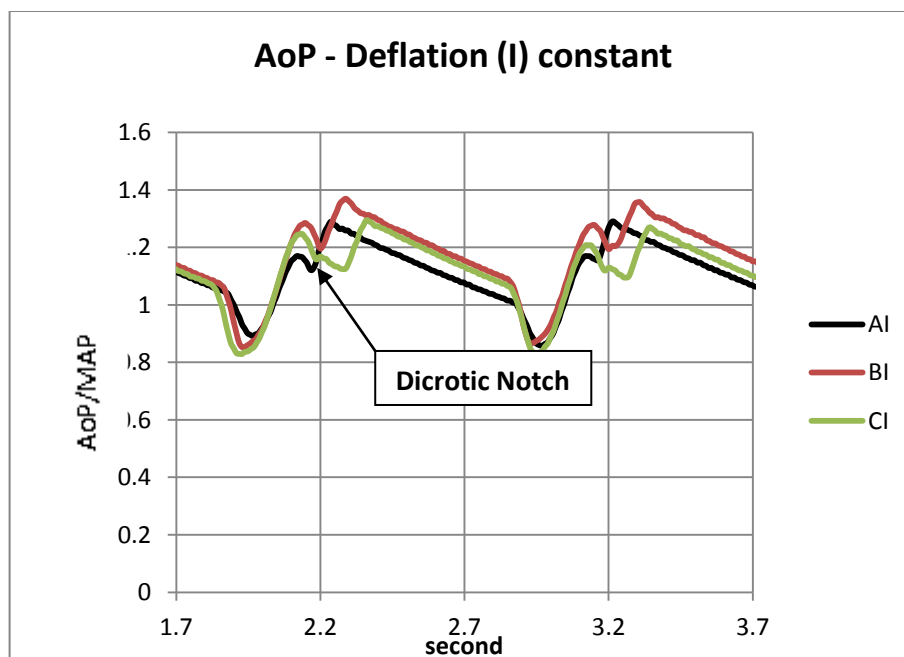
Figure 4-85: Aortic pressure waveform (ratio) with varying inflation points and fixed deflation point at (I) (The ordinate is aortic pressure/non-assisted MAP)

Inflation timing differences affect aortic pressure waveform shapes as illustrated in Figure 4-85; later inflation comes is seen in a later peak value in AoP; the value of which rises from A to B and

falls again from B to C. No appreciable difference in aortic end-diastolic pressure is evident. From these data, the aortic systolic and end-diastolic pressure is measured and used for analysis.

The means and standard deviations (SD) of aortic systolic pressure (AoPmax) augmentation in percentage for each combination of Timing experiment is tabulated in Table 4-38.

Table 4-38: Means and SDs (in brackets) for AoPmax for each combinations of Timing experiment

AoPmax		Deflation				Row Mean
		G	H	I	J	
Inflation	A	0.18	0.58	-1.28	-1.40	*-0.48*
		(2.34)	(2.98)	(3.11)	(3.04)	
	B	1.71	0.58	0.91	-2.55	*0.16*
		(1.40)	(1.92)	(2.13)	(2.97)	
	C	0.59	0.44	0.60	-2.78	*-0.29*
		(0.81)	(2.03)	(1.75)	(3.05)	
Column Mean		*0.83*	*0.53*	*0.08*	*-2.24*	*-0.20*

The grand effect of experimental factors Inflation and Deflation on aortic systolic pressure was reported to be a minimal -0.2 % decrease. The effect of Inflation factor did not show prominent differences as tabulated in the row means (range: -0.48% to +0.16%); the range was marginally bigger for Deflation factor (range: -2.24% to +0.83%).

Table 4-39: The SRH test result for AoPmax for Timing experiment

Source	P-value
Inflation	2.00×10^{-6}
Deflation	1.29×10^{-36}
Inflation × Deflation	1.21×10^{-11}

Table 4-39 reports the non-parametric SRH test. The Inflation, Deflation and interaction factors all showed significant main effects ($p < 0.001$).

The significance of interaction result from the SRH test prompted further post-hoc testing, using the Nemenyi test of Inflation and Deflation factors to determine which level was significantly different from others. The results are tabulated in Table 4-40 and Table 4-41.

Post-Hoc (Inflation)

Table 4-40: The Nemenyi test result for Inflation factor

	vs	(Rb-Ra)	SE	q	q(0.05,∞,3)	Result	significant
B	A	40237.2	5918.142	6.79896	3.314	Reject H_0	YES
B	C	32932.8	5918.142	5.56472	3.314	Reject H_0	YES
C	A	7304.4	5918.142	1.23424	3.314	Accept H_0	

Only two combinations showed a significant mean difference (A vs. B) and (B vs. C), but not (C vs. A). This result suggests that early inflation (point A) and late inflation (point C) yield similar response output.

Post-Hoc (Deflation)

Table 4-41 : Nemenyi test result for Deflation factor

	vs.	(Rb-Ra)	SE	q	q(0.05,∞,4)	Result	significant
G	J	85041.9	5125.261	16.5927	3.633	Reject H_0	YES
G	I	16426.8	5125.261	3.20507	3.633	Accept H_0	
G	H	10864.8	5125.261	2.11985	3.633	Accept H_0	
H	J	74177.1	5125.261	14.4728	3.633	Reject H_0	YES
H	I	5562	5125.261	1.08521	3.633	Accept H_0	
I	J	68615.1	5125.261	13.3876	3.633	Reject H_0	YES

Only three out of six mean difference combinations were significant ($p < 0.05$). Further inspection showed all significance combinations involved pairing with point (J) i.e. (G vs. J), (H vs. J) and (I vs. J). This suggests that other than for really late deflation (point J), other deflation timings yielded similar mean values.
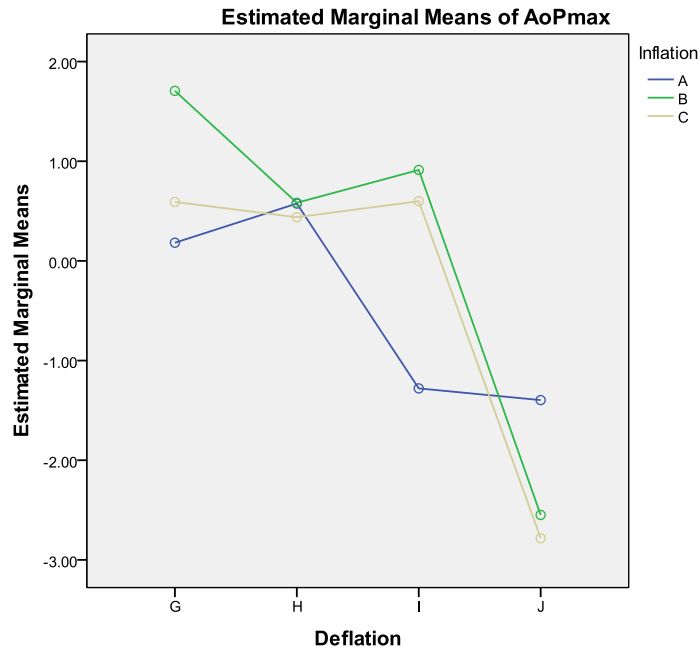
Figure 4-86: Plot of mean value for all combinations of experimental factor of Timing experiment

Figure 4-86 illustrates the mean value for each combination of Inflation and Deflation factor. The overall trend shows that as the deflation point was moved from early (G) to later (J), AoPmax mean value decreased.

The interaction factor was shown to be a significant effect on AoPmax mean value for points B and C (mid to late inflation) but not on early inflation (point A).

The effect of IABP on aortic pressure is reduction of both aortic systolic and diastolic pressure, which reduces the impedance to aortic flow; however, from CIMS balloon pump activation, the overall effect of timing variations to aortic systolic pressure was a minimal reduction. Greater reductions were recorded at very late deflation point (J) for all inflation points (A, B and C); but as previous results showed that point J yielded minimal CO and QcorMean, thus point J could be undesirable. Since optimum yield point (B-I) (CO and QcorMean subchapters) recorded only 0.9% increase; this might not pose adverse effect to myocardium wall stress.

4.2.1.4 Aortic End-Diastolic Pressure (AoEDP)

The means and standard deviations (SD) of augmentation (as a percentage) for each combination of different inflation and deflation timing on Aortic End-Diastolic Pressure is tabulated in Table 4-42.

Table 4-42: The means and SDs (in brackets) for each combination of AoEDP from Timing experiment

AoEDP		Deflation				Row Mean
		G	H	I	J	
Inflation	A	-3.58 (2.40)	-2.53 (3.73)	-2.71 (4.87)	-2.41 (6.46)	*-2.81*
	B	-2.76 (1.70)	-3.34 (2.35)	-3.11 (1.99)	-2.24 (5.62)	*-2.86*
	C	-2.69 (1.21)	-2.85 (2.29)	-3.11 (2.18)	-2.98 (5.44)	*-2.91*
Column Mean		*-3.01*	*-2.91*	*-2.98*	*-2.54*	*-2.86*

From Table 4-42, both Inflation and Deflation factor's mean value at Row Mean and Column Mean are shown to be quite similar. The variations of inflation and deflation timing on aortic end-diastolic pressure (AoEDP) yielded a grand mean value of -2.86% (range = -3.58% to -2.24%). Combination (A-G) gave the highest reduction at -3.58%. Statistical analysis was then carried out to determine significance of mean differences.

Table 4-43: The SRH test result for AoEDP response output

Source	P-value
Inflation	0.282
Deflation	0.095
Inflation × Deflation	0.044

In Table 4-43, both Inflation and Deflation factors show no significant main effect ($p < 0.05$), although there was significant interaction between factors, but just barely at $p = 0.044$.

Since the main factors (Inflation and Deflation) showed no significance main effect, no further post-hoc test was carried out. As reported in Table 4-43, only the interaction between the two factors has a statistical significance. The variations of different inflation and deflation timings have no significant effect; for example, early inflation reduces aortic end-diastolic pressure as effective as late inflation, and late deflation also is effective as early deflation. However, a significant interaction suggests that the response output is quite dependent on both experimental factors.

Figure 4-87 illustrates the mean value for all combinations of two experimental factors, Inflation and Deflation. The greatest AoEDP reduction is from combination A-G, while combination B-J is the least reduced. However, from the statistical analysis, any reduction is statistically similar to one another.
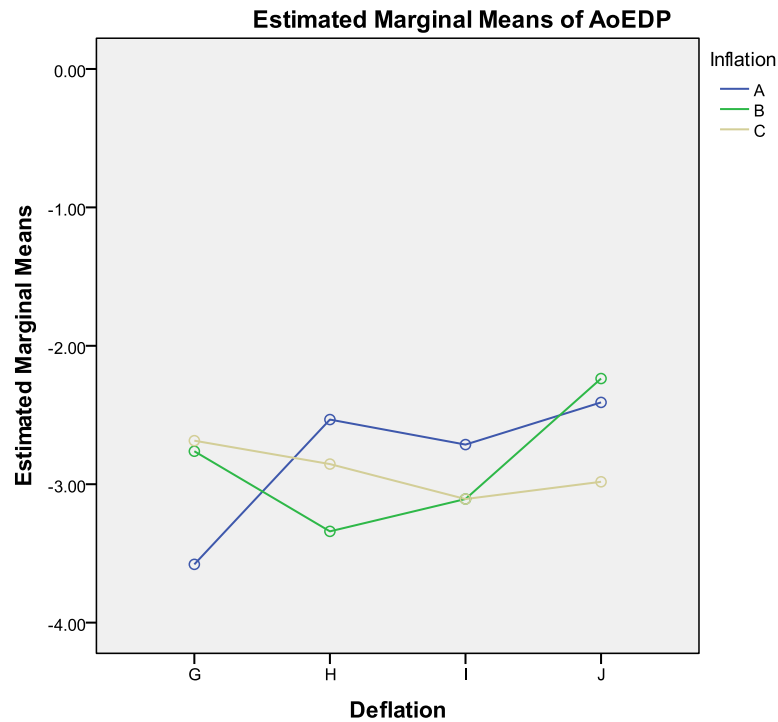
Figure 4-87: The mean value plot for all combination of experimental factors in TIMING experiment

The reduction of AoEDP is essential for myocardial workload reduction; however, from the results of TIMING experiment, it can be suggested that any combination of inflation and deflation point will be similar to each other, and will yield minimal afterload reduction.

4.2.1.5 Correlation

Correlation test of (dP vs. CO) and (dP vs. QcorMean) were carried out. As illustrated in Figure 3-67, pressure difference, dP, is defined as the percentage of difference between peak aortic diastolic augmentation (PADA) and AoPmax, and normalised with average of AoPmax (Eq. 3.5) rewritten below.

$$dP_i = \frac{PADA_i - AoPmax_i}{\overline{AoPmax}}$$

The main objective was to investigate whether the augmented diastolic pressure can be associated with increase of CO and QcorMean. Correlation test depends on data normality; for normally distributed data, Pearson's correlation test was used; otherwise, it was Spearman's correlation test.

dP vs. CO

Since the original data violated normality assumption, non-parametric correlation test was used. There was a significant correlation between the level of diastolic augmentation and CO mean value, r_S = .171, N = 1080, p < 0.01 (two-tailed). The coefficient of determination, R^2, revealed that only 2.9% of variation of CO can be attributed to dP (R^2 = 0.029).

dP vs. QcorMean

The Spearman correlation coefficient was r_S = .206, N = 1080, p < 0.01 (two-tailed), showing that there was a significant association between dP and QcorMean. However, the effect of that association was minimal at 4.2% as demonstrated by coefficient of determination, R^2 =0.042.

Discussion

The association of (CO vs. dP), and (QcorMean vs. dP) was found to be statistically significant; however, the variability attributed to either variables was very small, and thus it can be suggested that diastolic pressure augmentation has little effect on blood perfusion to periphery and coronary arteries under influence of varying inflation and deflation timing.

4.2.2 Discussion

The effect of different inflation and deflation timing when CIMS balloon pump activated was investigated in a 3 × 4 two-way factorial experiment, with one of the objectives was to identify combination yielding optimum response output. There were several response outputs analysed.

The best combination of inflation and deflation timing discovered for both cardiac output (CO) and left coronary mean flowrate (QcorMean) was (B-I: dicrotic notch inflation and early systole deflation); however, it was different with AoPmax where the best combination was (B − J (late

systolic deflation)). Afterload reduction by way of AoEDP reduction in this experiment was found to be statistically similar for whichever combination was chosen.

The B-I combination was chosen for the balloon inflation and deflation points for subsequent experiments. The point B which corresponds to dicrotic notch is the suggested inflation point for IABP, however, the recommended deflation point is somewhat vague only citing that deflation point should be set " *to deflate immediately before aortic valve opening*" (Trost and Hillis, 2006). For blood flow augmentation (peripheral and coronary), it was found that deflating the balloon pump during early systole (point I) was optimal for increasing cardiac output (CO).

Despite the optimum point chosen, the flow augmentation was not substantial. The overall grand mean for CO was a 5.52% with the maximum yield was 7% at combination B-I. LCA perfusion augmentation was slightly better; the grand mean was 9.1%, with the maximum yield at 12%, also at combination B-I. In term of LCA perfusion, whichever timing chosen, the myocardium blood supply would increase, and this in turn should increased the ratio of myocardial oxygen supply/demand ratio i.e. endocardial viability ratio (EVR).

Late balloon inflation suggested that the 'push' or momentum imparted to the fluid at the ascending aorta in diastole was less compared to when flow still ejected from the LV (point A), or aortic valve just closed (point B). One concern that might arise is the effect to LV wall stress from early balloon inflation due to impediment to outflow, although augmentation of aortic flow took place. The investigation on LV wall stress is reserved for future work.

It was found that the effect of different inflation/deflation timing to blood perfusion augmentation was not prominent, but still undeniably important. This was the same conclusion drawn by Niederer and Schilt examining the effect of early inflation and late deflation to stroke volume of an IABP (Niederer and Schilt, 1988).

The minimal reduction of AoPmax as demonstrated by the grand mean value of -0.20%, with maximum AoPmax reduction at -2.7%, suggested that inflation and deflation timing were not significant factors; there might be other independent factors playing a bigger role for AoPmax reduction.

The effect of different inflation and deflation timing combinations had a slightly bigger effect on AoEDP. The grand mean value of AoEDP was recorded to be -2.86%, with the maximum reduction at -3.56%. However, no combination was deemed to be significantly different from any other; any combination of inflation/deflation point is acceptable, hence optimum point (B − I) of CO and QcorMean is also acceptable.

In comparison with the clinical animal testing of Zelano et al. (1992)[44], the present CIMS *in vitro* results at combination B-I (augmentation percentage: CO = + 7.1 %, QcorMean = +12.1%, and AoEDP = -3.1 %), are better than the IABP results (augmentation percentage: CO = +2.9%, QcorMean = +12.9%, and AoEDP = +1.2%) ; however the prosthesis they used around the ascending aorta with 60 mL displacement volume, reported better results (augmentation percentage : CO = 29.6%, QcorMean = 24.4% and AoEDP = -11.5%). The effect of IABP late deflation was mentioned stating the probability of aortic impedance increase and consequently increasing myocardial oxygen consumption (Zelano et al., 1992), thus reinforcing the decision to chose combination B-I.

The correlation between the ratio of aortic diastolic augmentation, dP, with CO and QcorMean has been shown to be minimal. The resulting coefficient of determination, R^2, for (dP vs. CO) and (dP vs. QcorMean) was 2.9% and 3.2% respectively. The association of dP and blood perfusion with TIMING factors is weak, and the optimum point chosen will not be reflected with strong diastolic pressure augmentation.

4.3   Helium Gas Volume

In this experiment, the effect of varied Helium gas volume (20 mL, 25 mL and 30 mL) and different designs of CIMS balloon pump (SB and CB) was investigated in a 2 × 3 factorial experiment comprised of 6 combinations. Experimental factors made constant were 1) heart condition at heart failure (HF), 2) arterial compliance set at high (C2.5), 3) inflation/deflation timing set at B-I, and 4) aortic heart valve used was mechanical heart valve (MHV).

It was reasoned that the relationship between different Helium gas volume and balloon pump device design can be made clear; and also whether greater gas volume and/or device design affect haemodynamic response.

---

[44] The balloon pump used by Zelano et. al. (1992) was similar to configuration C of Figure 2-31.

4.3.1   Result

The results of the experiments are presented in the same order as previous subchapter; except for important statistical result, others are presented in Appendix C (C-2).

4.3.1.1 Cardiac Output (CO)

Figure 4-88 and Figure 4-89 illustrate the aortic flowrate when the amount of Helium gas is fixed and one of the balloon pump design is fixed respectively. All waveforms are normalised against mean flowrate of non-assisted flow. Compared to SB type, the CB type balloon pump yields higher maximum value in the first and second aortic flowrate waveform.
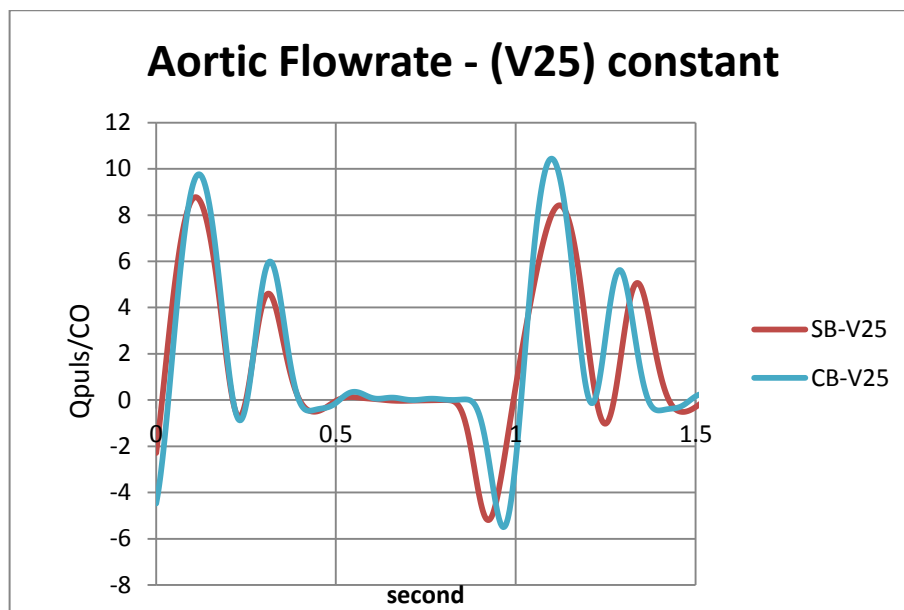
Figure 4-88: Aortic flowrate when Helium gas is fixed at 25 mL, while balloon pump design is varied. (the ordinate is instantaneous flow/non-assisted C.O.)
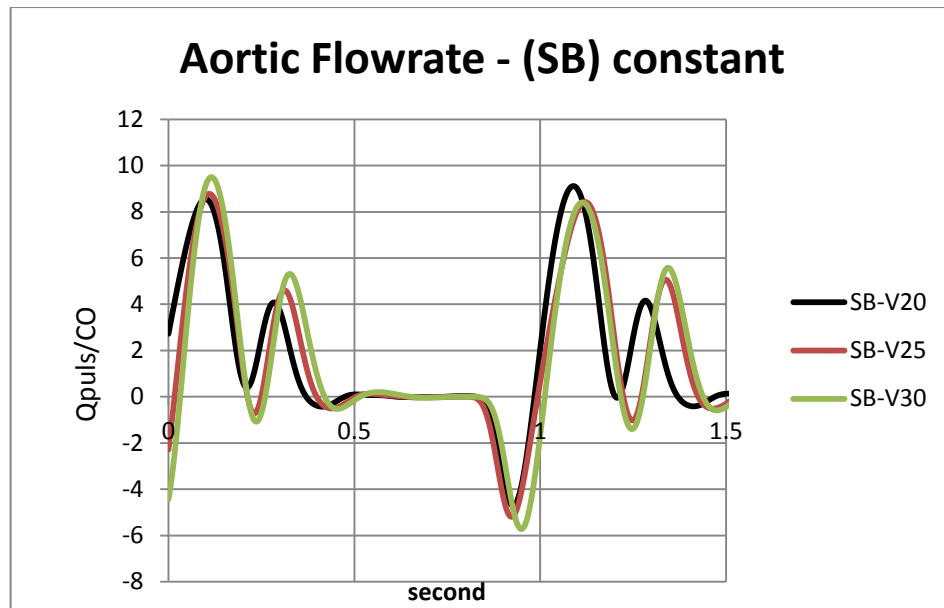
Figure 4-89: Aortic flowrate with SB type balloon pump and varying Helium gas volume (the ordinate is instantaneous flow/non-assisted C.O.)

In Figure 4-89, the effect of different amount of Helium gas volume is presented, where it can be seen that greater amount of Helium gas affects the height of secondary peak in diastole. The means of aortic flowrate i.e. cardiac output is used to compare between non-assisted and assisted circulation. The percentage difference was used for statistical analysis.

The means and standard deviations (SD) for each combination in the 2 x 3 factorial experiment between Helium gas volume (GasVol) and Device Design factors are tabulated in Table 4-44.

Table 4-44 : Means and SD (in brackets) for each combination for 2 x 3 factorial experiment

CO		GasVol			
		V20	V25	V30	Row Mean
Design	SB	5.27 (2.51)	6.70 (2.29)	5.12 (2.03)	*5.70*
	CB	8.98 (3.67)	11.52 (4.04)	11.16 (4.42)	*10.55*
Column Mean		*7.12*	*9.11*	*8.14*	*8.12*

The grand mean for the combined effect of Device Design and GasVOL experimental factor was 8.12% (range: 5.12% to 11.52%). The Device Design factor increases CO augmentation percentage for CB type almost twice compared to SB type balloon pump; while the GasVol factor yielded similar range with V25 as the highest output. The greatest CO augmentation was from combination (CB – V25) with 11.52% increase. Statistical analysis was carried out to determine significance of the results.

Table 4-45 : SRH test result for CO of Helium

Source	P-value
DeviceDesign	1.85×10^{-40}
GasVOL	3.203×10^{-5}
DeviceDesign × GasVOL	0.062

As tabulated in Table 4-45, both experimental factors reported significant main effect ($p < 0.001$), but not the interaction between factors ($p = 0.062$). Further post-hoc analysis was carried out for GasVol factor that has more than two levels.

Post-Hoc (GasVOL)

Table 4-46: Post-hoc Nemenyi test result for GasVOL factor

	vs	(Rb-Ra)	SE	q	q(0.05,∞,3)	Result	significant
V25	V20	13284	2093.3466	6.346	3.314	Reject H_0	YES
V25	V30	8553.6	2093.3466	4.086	3.314	Reject H_0	YES
V30	V20	4730.4	2093.3466	2.260	3.314	Accept H_0	

As tabulated in Table 4-46, there is a significant mean difference of (V20 vs. V25), and (V25 vs. V30). However, there is no significant mean difference of (V20 vs.V30). This suggests that V25 was the optimised Helium gas volume further illustrated in Figure 4-90, where V25 yielded higher augmentation in both levels of arterial compliance.
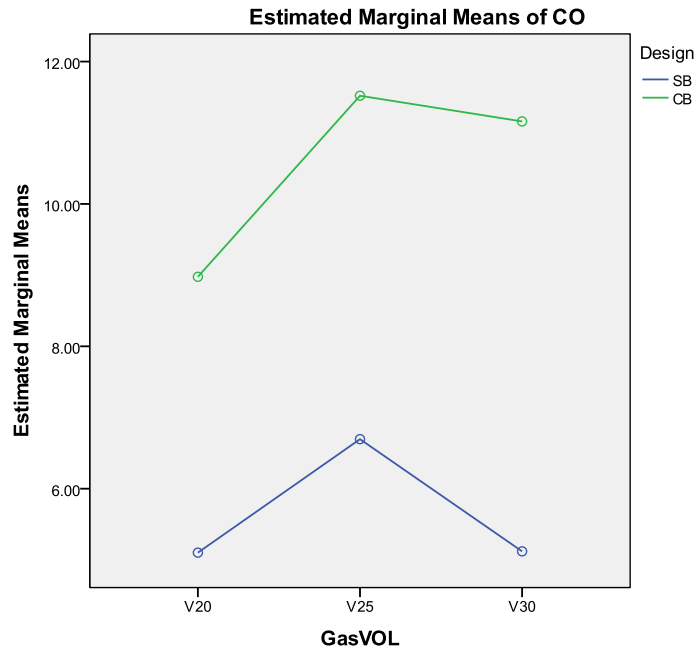
Figure 4-90 : The means for each combination of 2 x 2 factorial experiment for DeviceDesign and GasVol factors.

The type of the balloon pump was also a significant factor for CO augmentation; the CB type balloon pump was better across all levels of the GasVol factor, suggesting the effectiveness of extra space in CB design. From this experiment, combination (CB – V25) yielded the highest CO augmentation.

4.3.1.2 Left Coronary Artery Mean Flowrate (QcorMean)

The effect on LCA mean flowrate (QcorMean) from two experimental factors, Device Design and GasVol is illustrated in Figure 4-91 and Figure 4-92, when one factor is fixed while the other is varied. The former figure has a fixed SB type balloon pump with varied Helium gas amount, while the latter has a fixed Helium gas volume.
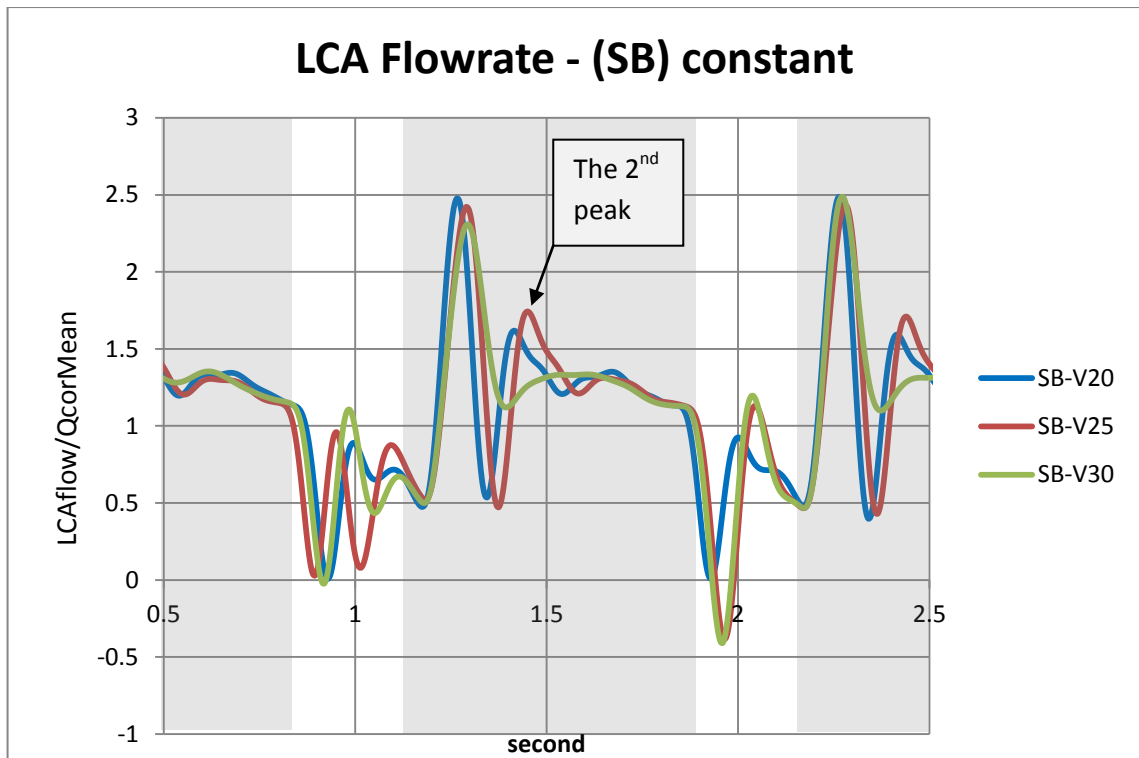
Figure 4-91: The effect of balloon pump activation when amount of Helium gas is varied with a fixed balloon pump type. Grey areas indicate diastole period (the ordinate is LCA flowrate/non-assisted mean LCA flowrate)

Except for SB-V30 that has no secondary peak after the first peak in diastole, there is no considerable difference amongst the shape of waveforms when different Helium gas volume was used to inflate and deflate the balloon pump. On the other hand, there is noticeable difference between SB and CB type of balloon pump as illustrated in Figure 4-92.

LCA Flowrate - (V25) constant
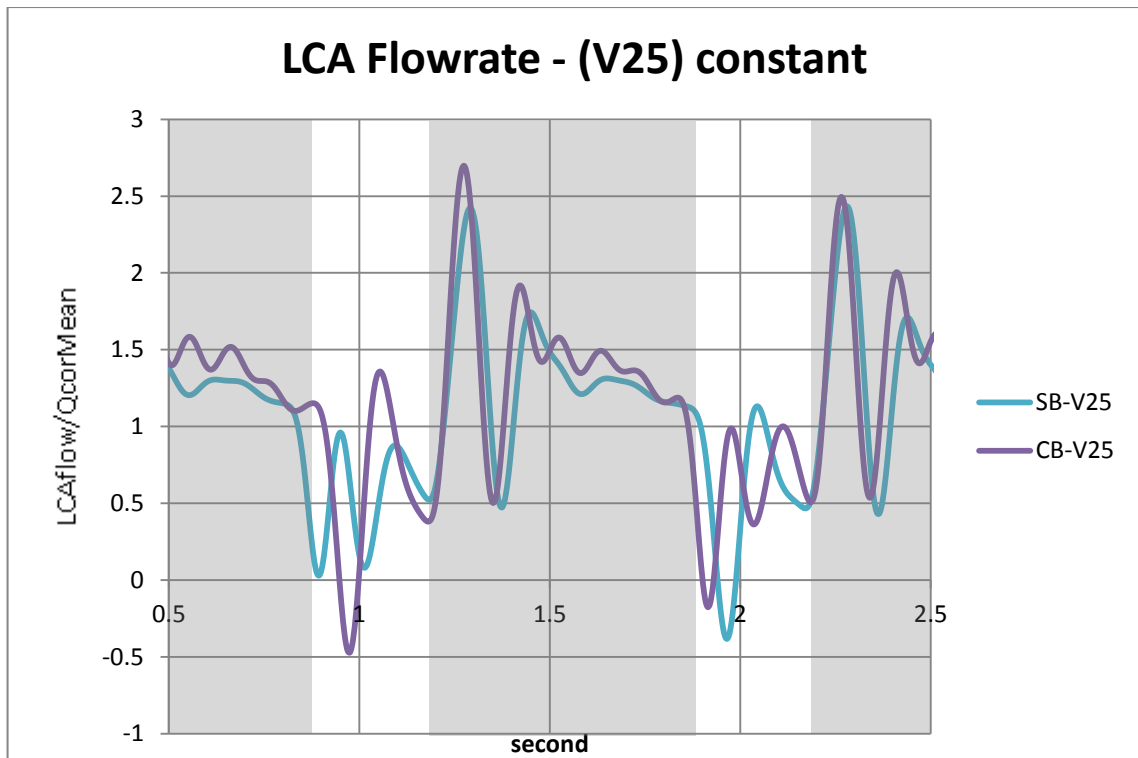
Figure 4-92: The effect of balloon inflation when Helium Gas is fixed while different types of balloon pump is used. Grey areas indicate diastole

The percentage ratio of mean flowrate value of non-assisted and assisted circulation is used for statistical analysis on effectiveness of GasVol and DeviceDesign factor in augmenting QcorMean. The means and standard deviations (SD) for each combination in the 2 x 3 factorial experiment are tabulated in Table 4-47.

Table 4-47 : Means and SDs (in brackets) for each combinations of 2 x 3 factorial experiment

Qcor Mean		GasVol			
		V20	V25	V30	Row Mean
Device Design	SB	5.34 (1.76)	8.59 (2.58)	9.85 (1.73)	*7.93*
	CB	8.02 (2.69)	11.56 (3.69)	15.60 (3.80)	*11.73*
Column Mean		*6.68*	*10.08*	*12.73*	*9.83*

The grand mean of augmentation from experimental factors was 9.83% (range: 5.34% to 15.6%). With increasing levels in both experimental factors, the QcorMean also increased. To find out

whether those differences amount to real difference and not due to chance, statistical analysis was performed.

Table 4-48: SRH test result for 2 x 2 factorial experiments between Device Design and GasVol factors

Source	P-value
DeviceDesign	1.196×10^{-23}
GasVOL	5.165×10^{-45}
DeviceDesign ×GasVOL	0.086

As shown in Table 4-48, both experimental factors main effect were significant (p < 0.001); however, the interaction between Device Design and GasVol was not significant (p = 0.086). Since GasVol factor showed significant difference, further post-hoc test on GasVol group was performed using the Nemenyi test.

Table 4-49 : Post-hoc Nemenyi test for GasVol factor

	vs	(Rb-Ra)	SE	q	q(0.05,∞,3)	Result	significant
V30	V20	41900.4	2093.3466	20.016	3.314	Reject H_0	YES
V30	V25	16084.8	2093.3466	7.684	3.314	Reject H_0	YES
V25	V20	25815.6	2093.3466	12.332	3.314	Reject H_0	YES

There was a significant difference amongst all combinations of the GasVol group, as shown in Table 4-54; each level was significantly different from each other.
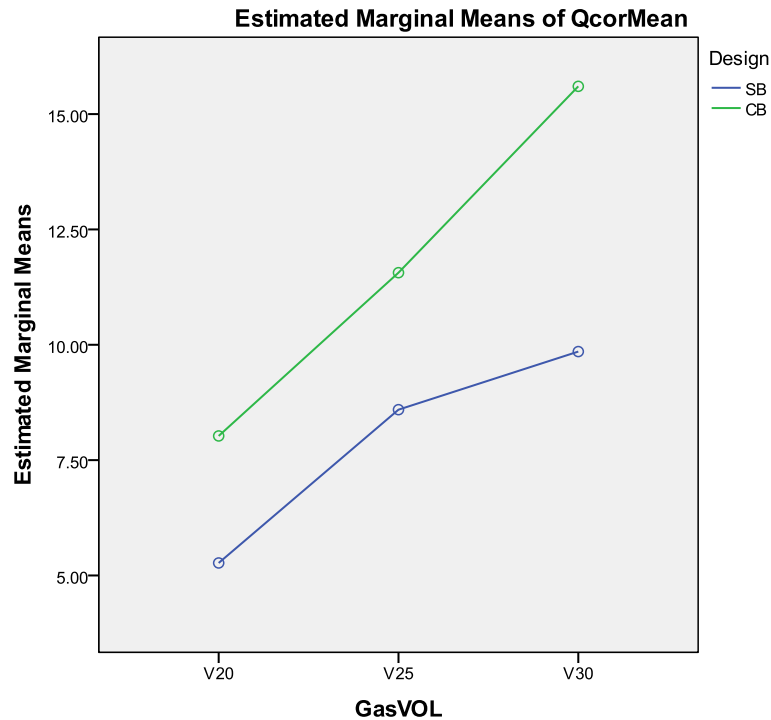
Figure 4-93 : The means for combinations in 2 x 3 factorial experiment of DeviceDesign and GasVol factors.

Figure 4-93 illustrates the mean of each combination in this experiment. Contrary to the previous CO result in GasVol experiment, LCA flowrate increased in conjunction with the amount of Helium gas. The greatest QcorMean augmentation was from combination (CB – V30), and at 15.6% the increased percentage was quite high.

For HF patients, increased blood perfusion to the LCA will increase oxygen supply against high demand. There was a probability that greater Helium gas used to inflate/deflate the balloon pump also increased the pressure to push additional flow into the left coronary artery circulation. The unique design of CB type balloon pump was also a considerable factor. Thus design of balloon pump at the ascending aorta in this *in vitro* study would increase blood perfusion to coronary arteries.

4.3.1.3 Aortic Systolic Pressure (AoPmax)

The effect of different type of balloon pump design and Helium gas volume on aortic pressure is illustrated in Figure 4-94, which has varied Helium gas volume and fixed balloon pump type. On

the contrary, Figure 4-95, illustrates aortic pressure waveform with different type of balloon pump and fixed Helium gas amount (25 mL).
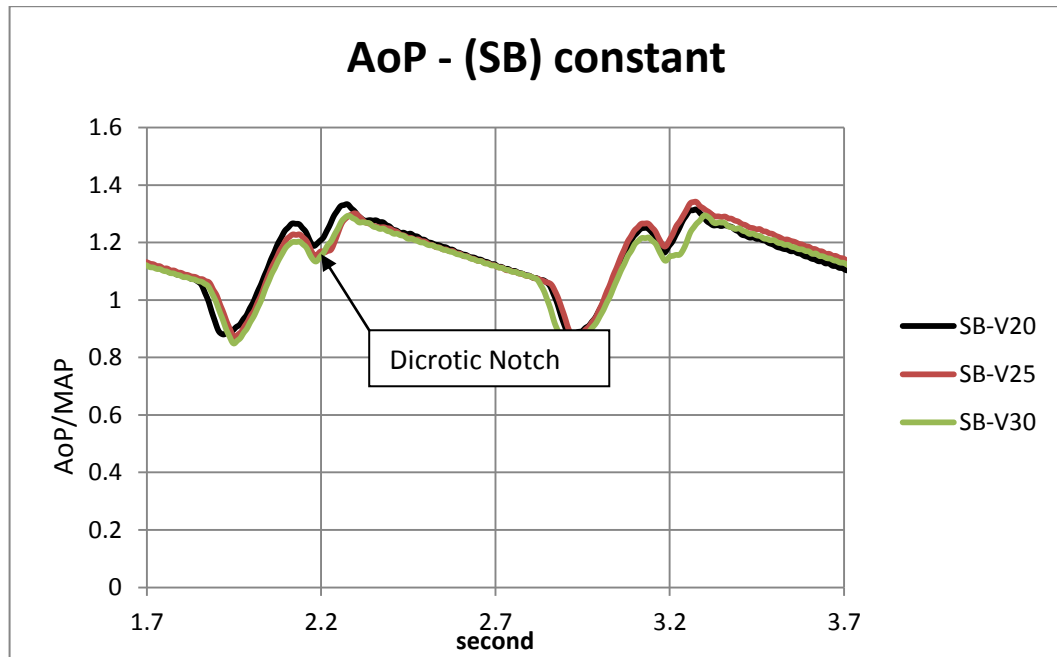
Figure 4-94: The aortic waveform with SB type balloon pump fixed and varied Helium gas amount. (The ordinate is aortic pressure/non-assisted MAP)

There was no noticeable difference on aortic pressure waveform with varying Helium gas volume. However, CB type balloon pump did influence aortic pressure waveform as illustrated in Figure 4-94 by
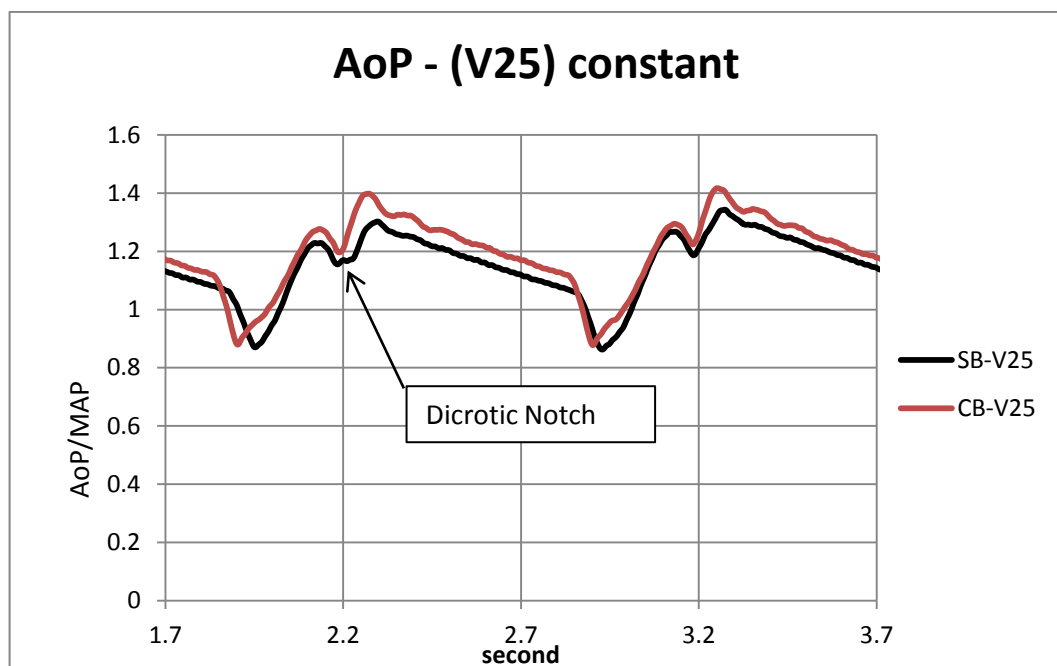
Figure 4-95: The aortic pressure waveform with fixed Helium gas volume and fixed SB type balloon pump. (The ordinate is aortic pressure/non-assisted MAP)

The aortic systolic pressure (AoPmax) and end-diastolic pressure (AoEDP) were measured. The percentage difference of non-assisted and assisted circulation was used for statistical analysis. The means and standard deviations (SD) of AoPmax when subjected to two experimental factors is tabulated in Table 4-50.

Table 4-50: The means and for 2 x 3 factorial experiment of DeviceDesign and GasVol factors

AoPmax		GasVol			
		V20	V25	V30	Row Mean
DeviceDesign	SB	0.53 (2.64)	0.86 (2.09)	-0.68 (2.02)	*0.23*
	CB	2.41 (3.45)	1.79 (3.78)	0.74 (4.34)	*1.65*
Column Mean		*1.47*	*1.32*	*0.03*	*0.94*

The overall effect of DeviceDesign and GasVol factors to the aortic systolic pressure (AoPmax) was minimal at 0.94% (range: -0.68% to 2.41%). The mean differences in row and column means also were minimal. To determine whether those mean differences were significant, and not due to chance, statistical analysis was carried out.

Table 4-51 : SRH test result for 2 x 3 factorial experiment for AoPmax

Source	P-value
DeviceDesign	1.037×10^{-11}
GasVOL	1.126×10^{-5}
DeviceDesign ×GasVOL	0.31

The SRH test result is tabulated in Table 4-51; there were significant main effect by both experimental factors (p < 0.001, but no interaction between them (p = 0.31).

Since the GasVOL factor showed significant main effect, further post-hoc test was carried out, and the result is shown in Table 4-52.

Table 4-52 : Nemenyi test result

	vs	(Rb-Ra)	SE	q	q(0.05, ∞,3)	Result	significant
V25	V30	12339	2093.3466	5.894	3.314	Reject H_0	YES
V25	V20	185.4	2093.3466	0.089	3.314	Accept H_0	
V20	V30	12153.6	2093.3466	5.806	3.314	Reject H_0	YES

The pairwise comparison between three levels of GasVol factor showed that only two combinations were significant, (V25 vs. V30) and (V20 vs. V30), but not between V20 and V25. The differences can be visualised easily when referring to Figure 4-96.
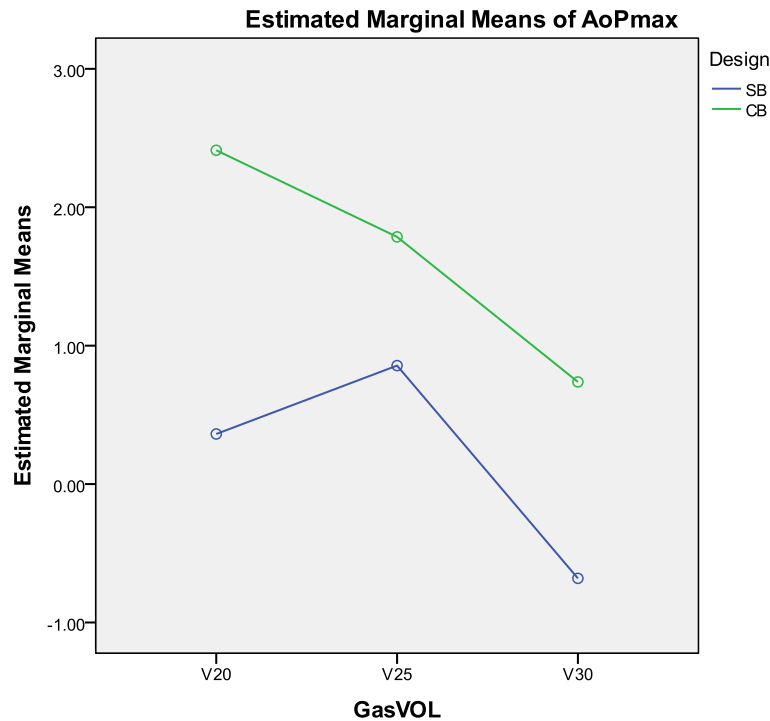
Figure 4-96 : Means for each combination of 2 x 2 factorial experiment

The overall effect of balloon pump activation to AoPmax was small as reported in Table 4-50; the statistical analysis proved that both DeviceDesign and GasVol experimental factors were significant. The greater the amount of Helium gas used would reduced AoPmax mean value. Also by using SB type balloon pump, the AoPmax mean value could be lower.

The counterpulsation of a balloon pump should decreased AoPmax value compared to non-assisted circulation, but there was no evidence to suggest a substantial AoPmax reduction can be achieved by DeviceDesign and GasVol factors. In this experiment, the AoPmax increase might not be detrimental since the augmentation percentage yielded was small and might not be significant clinically.

4.3.1.4 Aortic End-Diastolic Pressure (AoEDP)

The means and standard deviations (SD) for each combination of experimental factors, DeviceDesign and GasVol, is tabulated in Table 4-53.

Table 4-53 : Means and SDs (in brackets) of each combination for 2 x 3 factorial experiment between DeviceDesign and GasVol factors

AoEDP		GasVol			Row Mean
		V20	V25	V30	
Device Design	SB	-1.28 (2.92)	-1.86 (2.51)	-4.08 (2.49)	*-2.41*
	CB	-0.06 (3.35)	-1.95 (4.03)	-1.39 (6.25)	*-1.13*
Column Mean		*-0.67*	*-1.91*	*-2.74*	*-1.77*

The overall effect of DeviceDesign and GasVol factors was a minimal reduction of aortic end-diastolic pressure (AoEDP) at -1.77% (range: -4.08% to -0.06%). There was a small difference between levels of GasVol factor; with greater amount of Helium gas the greater the AoEDP reduction became. The DeviceDesign factor yielded AoEDP reduction with SB level reported greater reduction. To determine whether the mean differences were significant, statistical tests were performed; Table 4-54 tabulates the results.

Table 4-54: SRH test result for 2 x 3 factorial experiment

Source	P-value
DeviceDesign	2×10^{-4}
GasVOL	4.82×10^{-15}
DeviceDesign × GasVOL	0.001

There were significant main effects from both experimental factors ($p < 0.001$), and the interaction between the factors ($p = 0.001$). Further post-hoc test was carried out for the GasVol factor. As tabulated in Table 4-55, all three of the levels were significantly different from each other.

Table 4-55: Nemenyi test result for GasVol factor's levels

	vs	(Rb-Ra)	SE	q	q(0.05, ∞,3)	Result	significant
V20	V30	24028.2	2093.3466	11.478	3.314	Reject H_0	YES
V20	V25	11363.4	2093.3466	5.428	3.314	Reject H_0	YES
V25	V30	12664.8	2093.3466	6.050	3.314	Reject H_0	YES

From Device Design factor, it was found that the effect of SB was more prominent in reducing AoEDP especially the optimum reduction at combination SB – V30, as illustrated in Figure 4-97. As for the GasVol factor, there was a tendency for the AoEDP percentage value to decrease with increasing amount of Helium gas used during balloon activation.
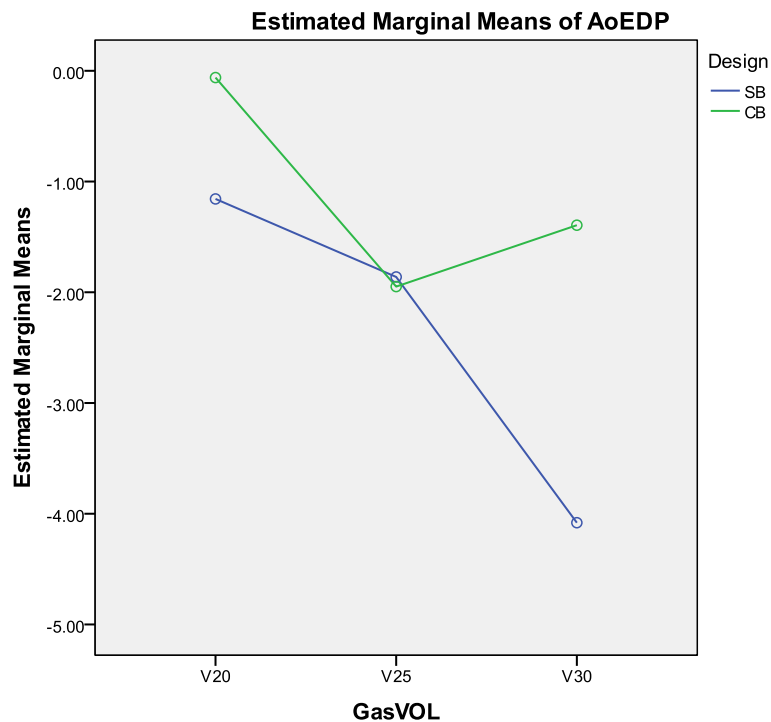
Figure 4-97 : Means for each combination for 2 x 3 factorial experiment of DeviceDesign and GasVol factors

The result from this experiment suggested that greater Helium gas volume would yield greater pressure reduction and thus afterload faced by the myocardium. Also, the effect of SB type balloon pump was also significant for greater afterload reduction. The minimal reduction of AoEDP when DeviceDesign and Helium gas volume factors investigated, hinted that there are other factors better suited for AoEDP reduction.

4.3.1.5 Correlation

dP vs. CO

The correlation between CO, QcorMean and the amount of peak aortic diastolic pressure which is represented by dP was investigated. The correlation test revealed that CO and dP were significantly related, r_S =.477, N = 540, p < 0.01, two tails. The coefficient of determination was R^2 = 0.228, meaning that 22.8% of variation in CO can be attributed to dP and vise versa.

dP vs. QcorMean

The association between dP and QcorMean was significant, r_S = .705, N = 540, p < 0.01, two-tails. The strength of the association was moderate, R^2 = 0.497, which meant 49.7% of QcorMean variations can be attributed to dP and vise versa; this can be considered as moderate strength association.

Discussion

It is clear from these results when Helium gas volume and DeviceDesign factor were combined, that the association of (dP vs. QcorMean) was greater compared to association of (dP vs. CO). Coronary perfusion was strongly associated with greater difference between PADA and AoPmax when more Helium gas was used to pump the balloon pump. This could meana greater force during balloon inflation.

4.3.2   Discussion

This round of experiment involved two experimental factors, 1) the DeviceDesign factor (2 levels: SB & CB), and 2) the GasVol factor (3 levels 20, 25 & 30 mL) making up a 2 x 3 two-way full factorial design experiment.

For the cardiac output, CO, the effect of both experimental factors yielded significant increase compared to non-assisted circulation, with combination CB − V25 yielded the highest mean percentage of CO augmentation. There was no interaction between experimental factors, thus,

the effect can be discussed separately; the optimum yield was always by V25 level (25 mL of Helium gas), and CB type balloon pump increased CO augmentation further.

The left coronary artery perfusion seemed to benefit from higher volume of Helium gas, where QcorMean percentage increased as greater amount of Helium gas volume was used, from 20 mL to 30 mL. The CB type balloon pump consistently yielded higher mean value. For patient needing higher LCA perfusion, e.g. heart failure secondary to myocardial infarction, a higher volume of Helium gas would lead to better coronary perfusion rate.

The effect of DeviceDesign type and GasVol on grand mean AoPmax was minimal at 0.94%. Since the overall effect was small, the clinical implication to heart's workload is hypothesised to be insignificant and could be ignored. The AoEDP reduction was shown to be statistically significant for both experimental factors, although the grand mean of AoEDP reduction was again minimal at -1.77%. Greater reduction of AoEDP could be achieved with bigger Helium gas capacity; however, the SB type balloon pump yielded greater AoEDP reduction compared to CB type. It seems that when DeviceDesign and GasVol factors involved, the reduction of aortic pressure leading to afterload reduction was very minimal and probably clinically insignificant.

The effects of compliant body (CB) type balloon pump was more pronounced to the augmentation of CO and QcorMean, while the straight body (SB) type, was better in reducing the mean value of AoPmax and AoEDP. The GasVol factor affected the response output quite differently. For CO, optimum yield was when Helium gas fixed at 25 mL. QcorMean response output increased with greater amount of Helium gas used. However, the reverse trend was demonstrated for AoPmax and AoEDP; with increasing amount of Helium gas, both variables reported reduction.

The *in vivo* CIMS balloon pump, when implanted would have some degree of innate compliance, and a finite volumetric capacity. This experiment suggests that with optimised balloon design, systemic and coronary perfusion would benefit with an equivalent optimum amount of Helium gas. The LCA perfusion was especially affected by greater amount of Helium gas thus would increase oxygen supply to myocardium i.e. increased EVR value. Aortic pressure reduction, normally associated with IABP activation, was small, and this suggests that other factors could be more prominent.

Lastly, the correlation coefficient of determination, R^2, of (dP vs. CO) and (dP vs. QcorMean) was 22.8% and 49.7% respectively. The effect of DeviceDesign and GasVol factors was moderate for association between dP and CO; however (dP vs. QcorMean) association was more substantial.

This experiment showed that diastolic pressure augmentation can be associated with increased perfusion to both periphery and coronary arteries.

4.4 Compliance

This experiment investigated the effect of 1) Device Design factor (SB & CB), and 2) Arterial Compliance factor with high and low arterial compliance level (C2.5 & C1.25) which resulted in a 2 × 2 full factorial experiment with four combinations (refer Table 3-21) on haemodynamic performance of CIMS balloon pump.

Experimental factors held constant were 1) heart condition at heart failure (HF), 2) balloon timing was set at (B-I), 3) Helium gas volume was set at 25 mL (V25), and 3) aortic heart valve used was mechanical heart valve (MHV).

It was hoped that the effect of optimum combination was found, and to detect which factors contributed more to flow and pressure augmentation.

4.4.1 Result

The results were presented in similar format as to previous subchapters. Only relevant statistical results are presented in main thesis body, the others are presented in Appendix C (C-3). The setup of the experimental design of 2 × 2 factorial experiment means that there was no post-hoc test carried out since there were only two levels in each factor.

4.4.1.1 Cardiac Output (CO)

The effect of two experimental factors, Device Design and Arterial Compliance on cardiac output performance is presented here. Figure 4-98 and Figure 4-99 illustrates the pulsatile aortic flowrate with one factor is fixed while the other is varied. In the former, the effect of different arterial compliance level is shown, while the latter shows the effect of different type of balloon pump.

There was no noticeable difference in the first positive peak in both figures, but in the second positive peak due to balloon inflation, the effect of varying levels of each factor can be seen e.g. combination CB – C1.25 caused higher maximum value compared to SB – C1.25 in Figure 4-99.
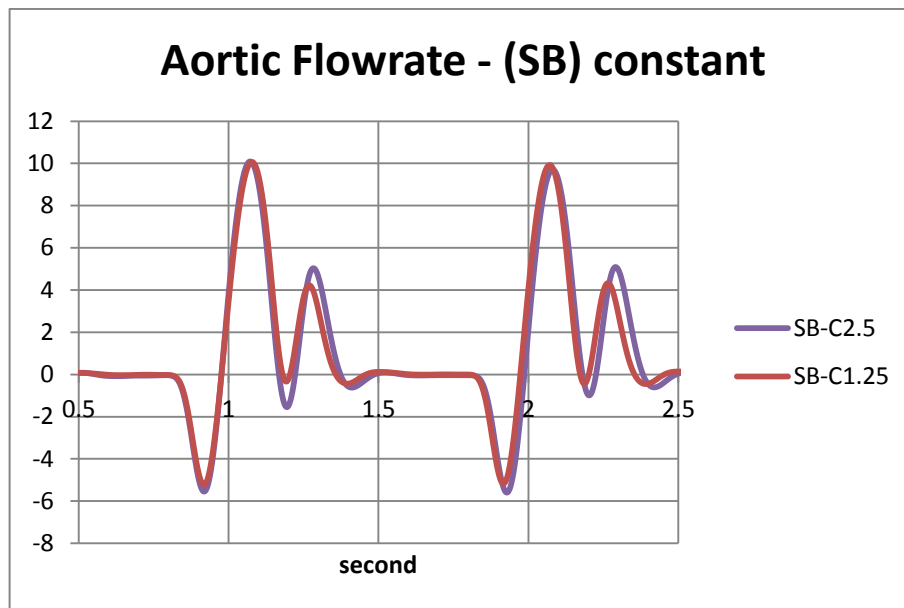
Figure 4-98: The aortic flowrate during balloon inflation with fixed SB type balloon pump with varying arterial compliance (the ordinate is instantaneous flow/non-assisted C.O.)
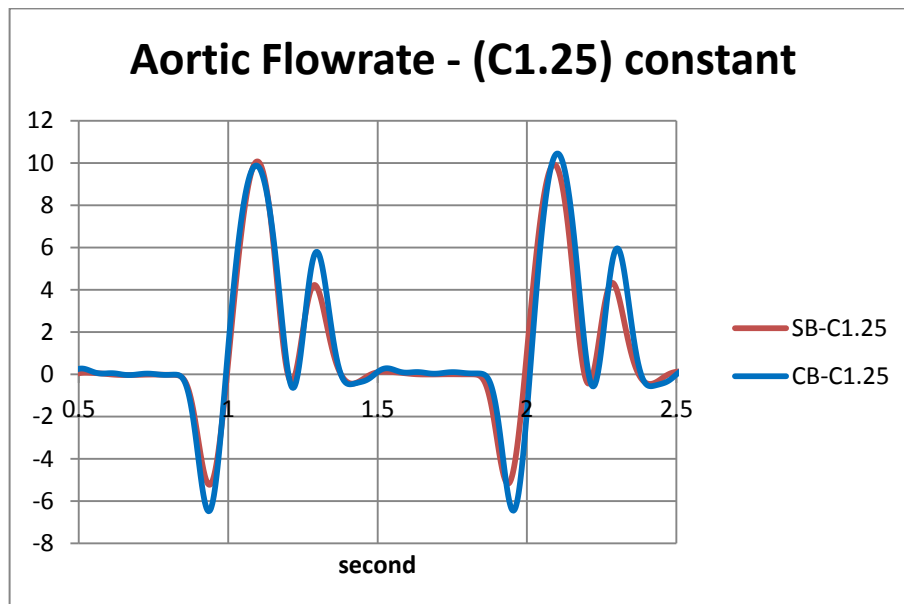
Figure 4-99: The aortic flowrate with fixed arterial compliance at C1.25 and varying type of balloon pumps (the ordinate is instantaneous flow/non-assisted C.O.)

The percentage difference of mean of aortic flowrate i.e. cardiac output between non-assisted and assisted circulation was used for statistical analysis.

The means and standard deviations (SD) of cardiac output (CO) for every combination of Device Design factor and Arterial Compliance factor are tabulated in Table 4-56.

Table 4-56: The means and SD (in brackets) of CO from combination of Arterial Compliance and DeviceDesign factor

CO		Device Design		Row Mean
		SB	CB	
Arterial Compliance	C2.5	7.56 (2.48)	13.40 (4.08)	*10.48*
	C1.25	12.67 (1.83)	18.03 (2.80)	*15.35*
Column Mean		*10.12*	*15.71*	*12.92*

The overall grand mean of CO augmentation compared to non-assisted flow, due to the Device Design and Arterial Compliance factor, was 12.92% (range: 7.56% to 18.03%). The mean difference between level at row and column mean was similar and the highest yield was from combination (CB – C1.25). To ascertain that the mean differences were not due to chance, further statistical analysis was carried out; Table 4-57 tabulates the outcome of the SRH test result.

Table 4-57: SRH test result for 2 x 2 factorial experiment with Device Design and Arterial Compliance factor

Source	P-value
DeviceDesign	8.91×10^{-31}
ArtCompliance	3.43×10^{-23}
DeviceDesign× ArtCompliance	0.458

The SRH test result showed both experimental factors had significant main effect on CO's augmentation ($p < 0.001$); however there was no interaction between them ($p = 0.458$).
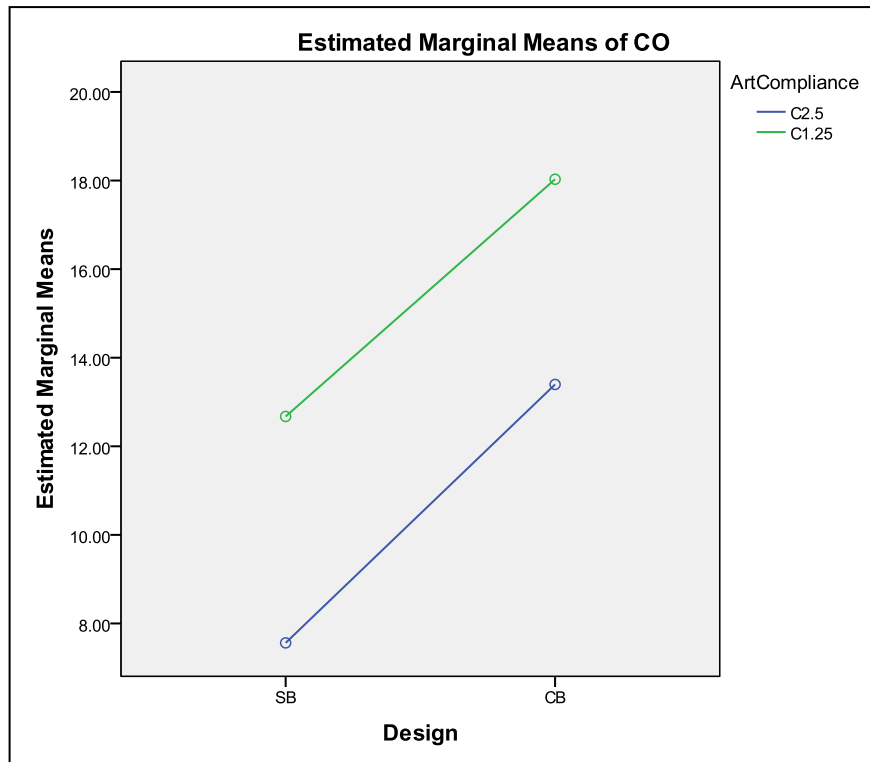
Figure 4-100: CO means for the COMPLIANCE experiment

There is a clear difference between mean for both experimental factors as illustrated in Figure 4-100. There was not enough evidence to suggest that the response output trend would react differently than what is illustrated, hence it can be safely suggested that low arterial compliance would always yielded higher output, likewise the CB type balloon pump generated greater augmentation. The best combination was by combination (CB – C1.25) at 18.03% i.e. low arterial combined with CB type balloon pump.

The implication of this finding to the augmentation of CO is obvious, especially for HF patient with stiffer aorta, although unfavourable in most clinical cases, when combined with optimised CIMS balloon pump having innate compliance, the systemic perfusion would be augmented favourably.

4.4.1.2 *Left Coronary Artery Mean Flowrate (QcorMean)*

The effect of fixed type of balloon pump (SB) and varied arterial compliance on pulsatile left coronary artery flowrate is shown in Figure 4-101. There are differences between both arterial compliance levels, especially at the second positive peak in diastole.
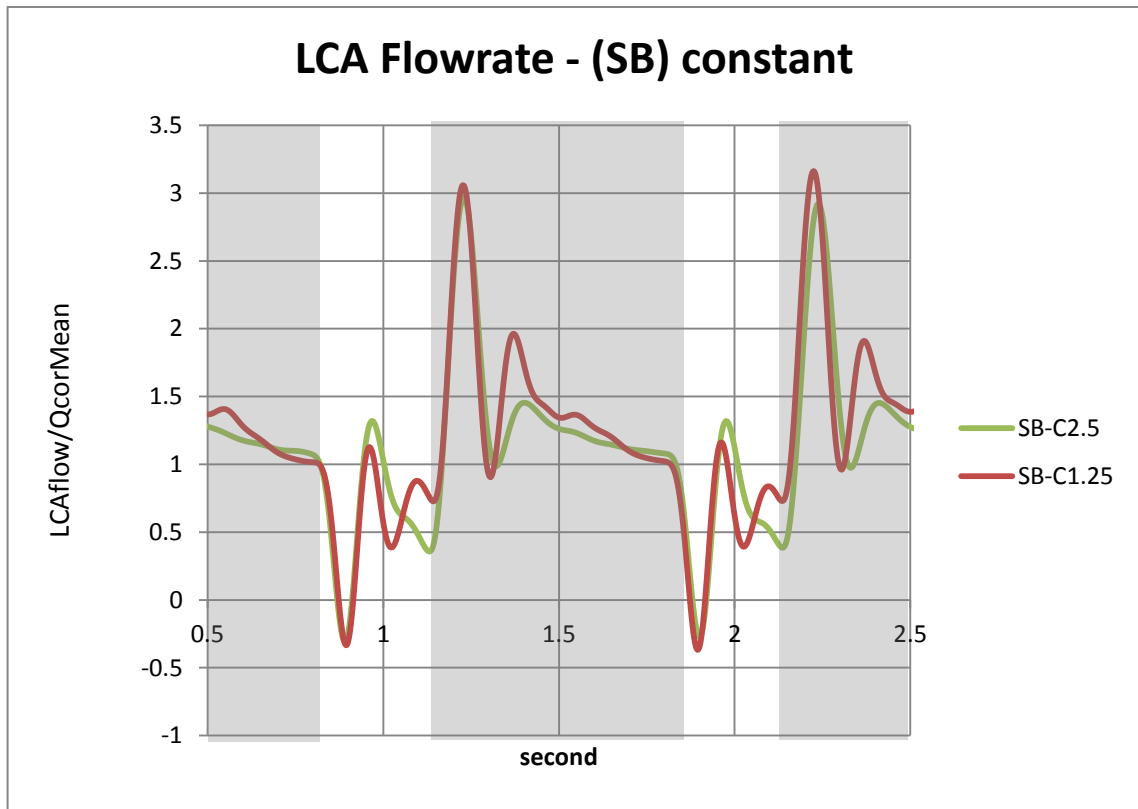
Figure 4-101: The pulsatile LCA flowrate with fixed SB balloon pump type and varied arterial compliance. . Grey areas indicate diastole period (the ordinate is LCA flowrate/non-assisted mean LCA flowrate)

Combination SB – C1.25 reported higher maximum value compared to SB – C2.5 for the second positive peak. Consequently, mean flowrate of SB – C1.25 was greater.
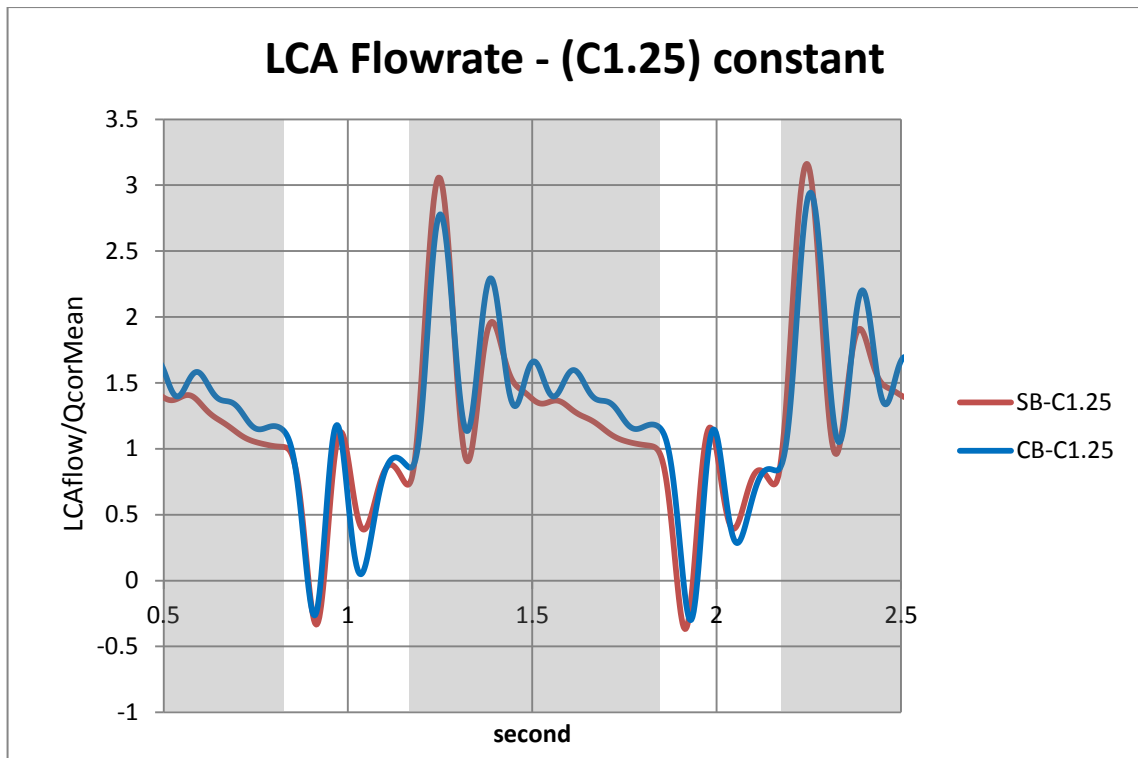
Figure 4-102: The pulsatile LCA flowrate with fixed arterial compliance and two different types of balloon pump

Figure 4-102 illustrates the effect of different balloon pump design on LCA pulsatile flowrate when arterial compliance is set to low (C1.25). Both waveforms show almost the same shape, although the values are different. The mean LCA pulsatile flowrate of non-assisted and assisted circulation is used to calculate the percentage difference, and used for statistical analysis.

The means and SDs for QcorMean response output are shown in Table 4-58.

Table 4-58 : The means and SDs (in brackets) from combination of Arterial Compliance and Device Design factor

QcorMean		Device Design		Row Mean
		SB	CB	
Arterial Compliance	C2.5	12.02 (2.35)	14.92 (2.82)	*13.47*
	C1.25	18.35 (1.31)	20.50 (3.70)	*19.43*
Column Mean		*15.18*	*17.71*	*16.45*

The grand mean of LCA augmentation compared to non-assisted flow, due to Device Design and Arterial Compliance factors, was 16.45% (range: 12.02% to 20.50%). The highest augmentation on LCA perfusion was of (CB – C1.25) combination at 20.5%. The difference at row mean was higher

than that of column mean. To determine that the mean differences were not due to chance, statistical analysis was carried out, and the result from the SRH technique is tabulated in Table 4-59.

Table 4-59: The SRH test result for QcorMean with 2 x 2 factorial experiment

Source	p-value
DeviceDesign	1.522×10^{-6}
ArtCompliance	1.237×10^{-44}
DeviceDesign × ArtCompliance	0.056

Both experimental factors were found to yield significant main effect ($p < 0.001$), however the interaction between the factors lacked enough evidence to reject the null hypothesis ($p = 0.056$).
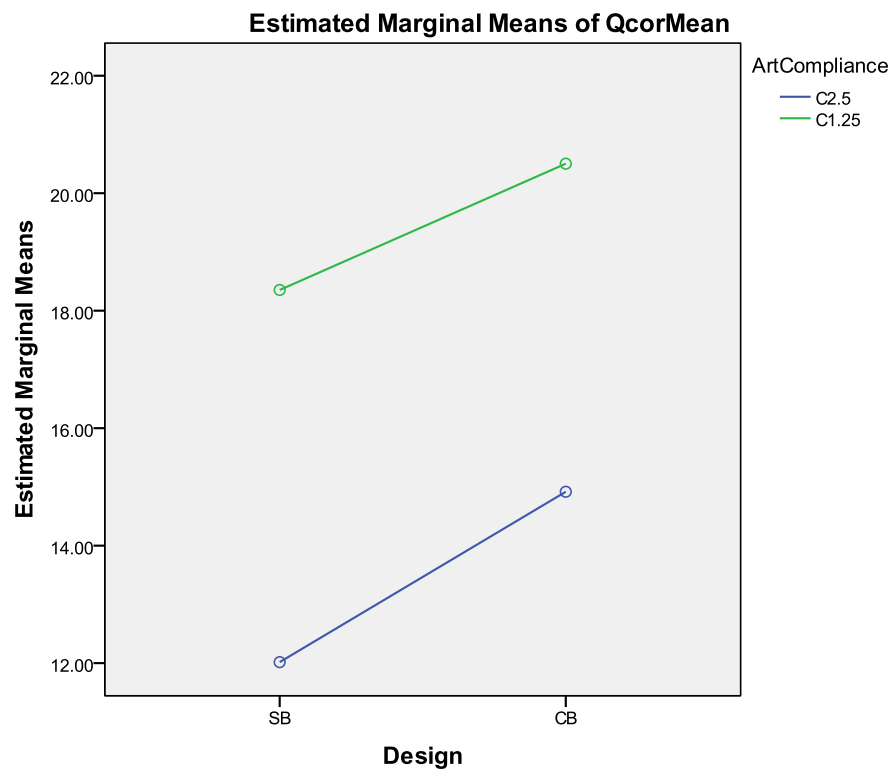
Figure 4-103: Left coronary artery flowrate (QcorMean) means for each combination of Device Design and Arterial Compliance factor

The mean of QcorMean augmentation due to the CIMS balloon pump activation is illustrated in Figure 4-103. The effect of Arterial Compliance factor was evident, as the output from low arterial compliance level (C1.25) for both types of balloon pump exceeded the output at higher arterial

compliance (C2.5) level. Furthermore, at every level of Arterial Compliance, CB type balloon pump exceeded SB type balloon pump outcome. Since there was no interaction between factors, each factor was independent; this means the result illustrated in Figure 4-103 are applicable whenever there is similar experiment.

From the results presented, the best combination would be of low arterial compliance (C1.25), and CB type balloon pump (CB − C1.25) yielding a 20.5% increase in LCA mean flowrate. This combination is similar to previous subchapter for CO (refer to subchapter 4.4.1.1), thus suggesting systemic and coronary perfusion is greatly influenced by balloon design, and arterial compliance level. This is further discussed in 4.4.2 Discussion section.

4.4.1.3 Aortic Systolic Pressure (AoPmax)

Similar to previous subchapters, Figure 4-104 and Figure 4-105 illustrates the effect of one experimental factor when the other is fixed.
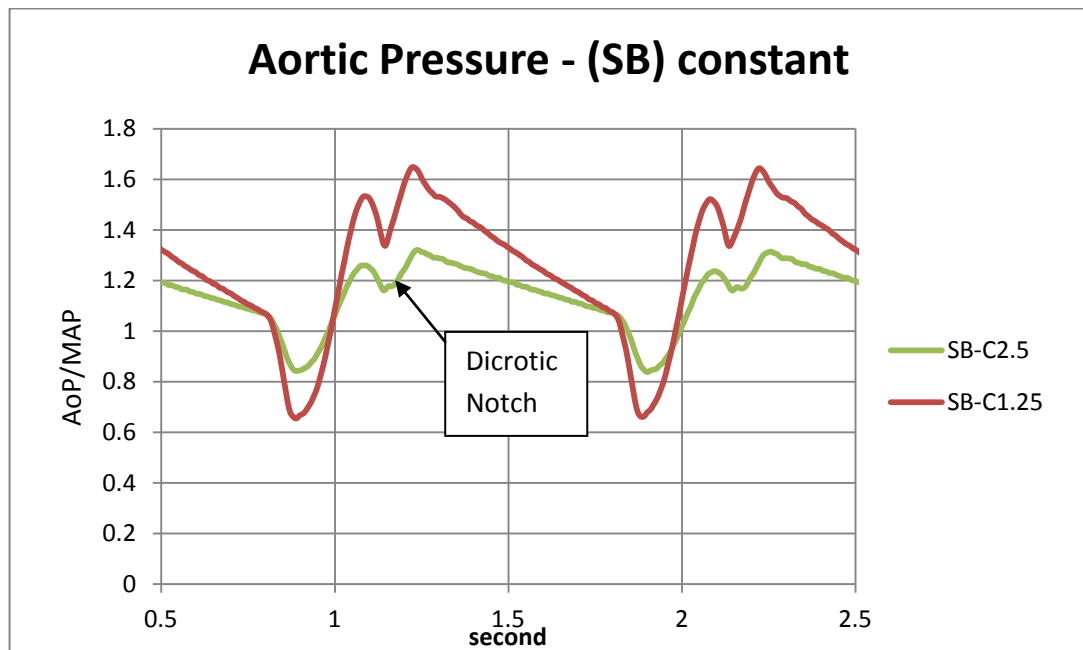
Figure 4-104: Aortic pressure waveform with fixed SB type balloon pump and varied arterial compliance (The ordinate is aortic pressure/non-assisted MAP)

The effect of different arterial compliance is shown clearly in Figure 4-104; aortic systolic and peak aortic diastolic pressure by SB − C1.25 is showing greater range compared to SB − C2.5. While the

effect of different type of balloon pump is illustrated in Figure 4-105, there appears to be little differencein the waveform shape, although some difference in magnitude may be seen.
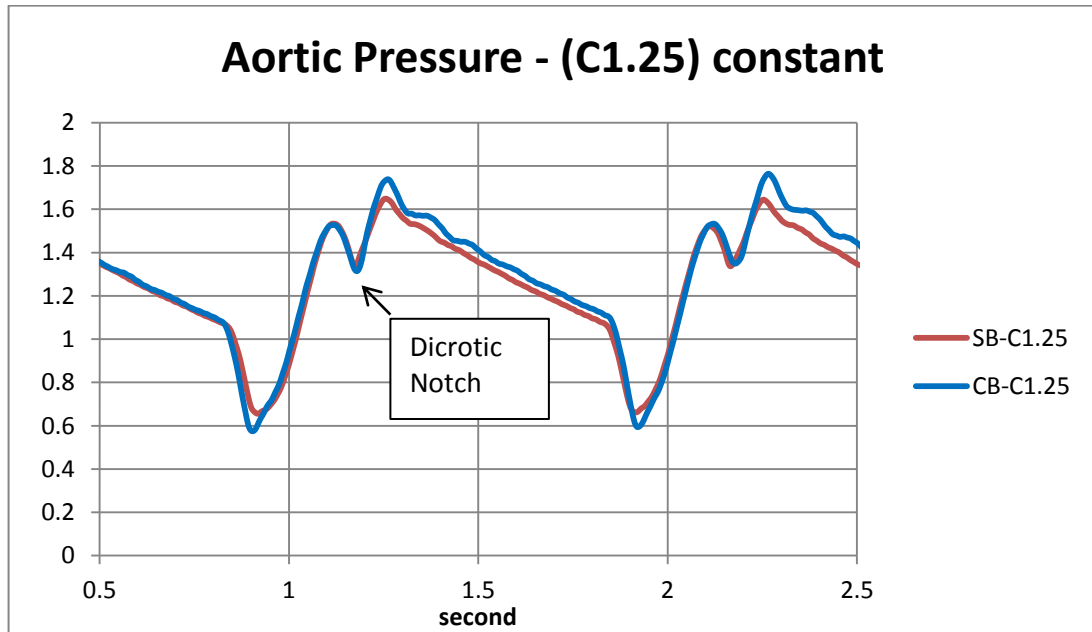
Figure 4-105: Aortic pressure waveform with fixed arterial waveform and varied balloon pump type

Statistical analysis was used to determine whether or not any effect from the experimental factors on aortic systolic and end-diastolic pressure is significant. The means and SDS for AoPmax of each combination are tabulated in Table 4-60.

Table 4-60 : The mean and SD (in brackets) of AoPmax change involving DeviceDesign and Arterial Compliance factor

AoPmax		Device Design		Row Mean
		SB	CB	
Art. Compliance	C2.5	1.32 (3.13)	1.53 (4.08)	*1.42*
	C1.25	2.07 (2.05)	2.10 (4.83)	*2.08*
Column Mean		*1.69*	*1.81*	*1.75*

The overall effect of both Arterial Compliance and Device Design factor on AoPmax in assisted circulation was a minimal 1.75% increase (range: 1.32% to 2.1%). There was little difference between the levels in row and column mean. Statistical analysis was carried out to determine

statistical significance of the result. A non-parametric SRH test was used to analyse the 2 x 2 factorial experimental data; the result is tabulated in Table 4-61.

Table 4-61: SRH table for the AoPmax

Source	P-value
DeviceDesign	0.016
ArtCompliance	0.016
DeviceDesign ×ArtCompliance	0.322

The result showed in assisted circulation, both Device Design and Arterial Compliance had a significant main effect on the QCorMean percentage difference (p < 0.05); however, the interaction between those two experimental factors was not significant (p = 0.332).
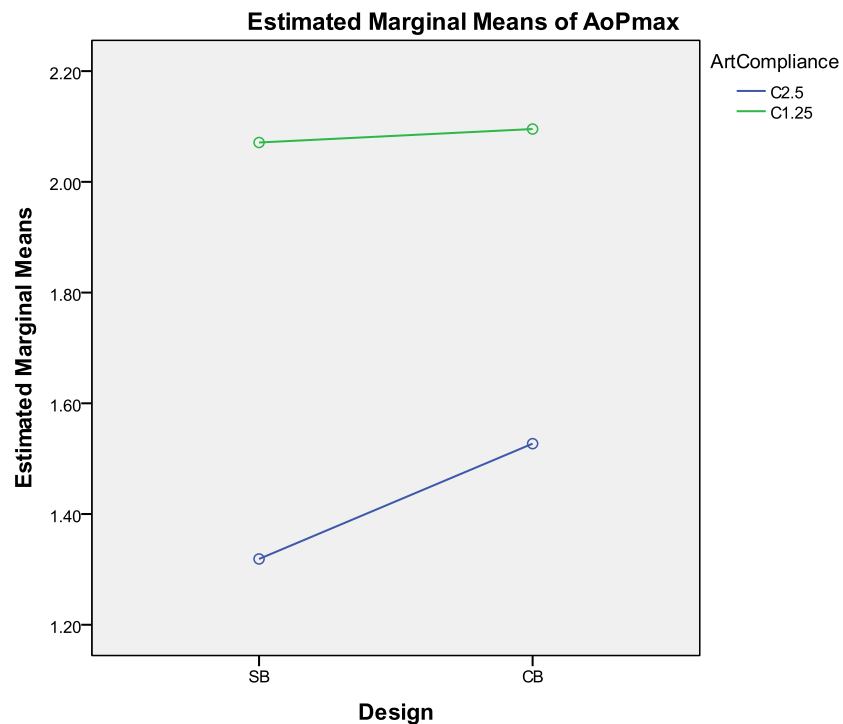
Figure 4-106: Means of each combination of a 2 x 2 factorial experiment

Figure 4-106 illustrates the means of each combination for DeviceDesign and Arterial Compliance factors. The CB type consistently yielded higher AoPmax mean value, while in lower arterial compliance condition (C1.25) higher AoPmax mean value was yielded.

However, this result contradicts counterpulsation device such as IABP effect on AoPmax, where it should have decreased compared to non-assisted circulation. The consistent and significant AoPmax percentage increase across all combinations suggested that the effect of CIMS balloon pump at the ascending aorta was unable to decrease aortic systolic pressure. However, the effect of slightly increased AoPmax might not be detrimental to the HF patient condition.

4.4.1.4 Aortic End-Diastolic Pressure (AoEDP)

The means and standard deviations (SD) in percentage of aortic end-diastolic pressure (AoEDP) are tabulated in Table 4-62.

Table 4-62: The means and SDs (in brackets) of AoEDP augmentation from Arterial Compliance and DeviceDesign factor

AoEDP		DeviceDesign		Row Mean
		SB	CB	
Arterial Compliance	C2.5	-2.45 (3.70)	-3.15 (4.80)	*-2.80*
	C1.25	-13.24 (4.26)	-16.48 (7.67)	*-14.86*
Column Mean		*-7.85*	*-9.81*	*-8.83*

Contrary to the previous result, (4.4.2.3 AoPmax), the overall effect of Device Design and Arterial Compliance factor, when CIMS balloon pump was activated, was a reduction of the mean value of AoEDP at -8.83% (range: -16.48% to -2.45%). The greatest AoEDP reduction was from the combination of (CB – C1.25) at -16.48%. The mean difference for column was small, but row mean difference was quite big. To determine whether the differences were significant or due to chance, further statistical analysis was performed.

Table 4-63 : SRH table for 2 x 2 factorial experiment

Source	p-value
DeviceDesign	0.01
ArtCompliance	3.13×10^{-45}
DeviceDesign × ArtCompliance	0.308

The non-parametric SRH test was used to analyse the 2 x 2 factorial experiment data, Table 4-63 tabulates the result. There was a significant main effect for both the Device Design and Arterial Compliance factor ($p < 0.05$). However, the interaction between those experimental factors yielded no significance effect ($p = 0.308$).

All means for each combination of the two factors reported AoEDP reduction compared to non-assisted circulation, and illustrated in Figure 4-107. This suggests that under the two experimental factors, Device Design and Arterial Compliance, considerable afterload reduction can be achieved for all combinations.
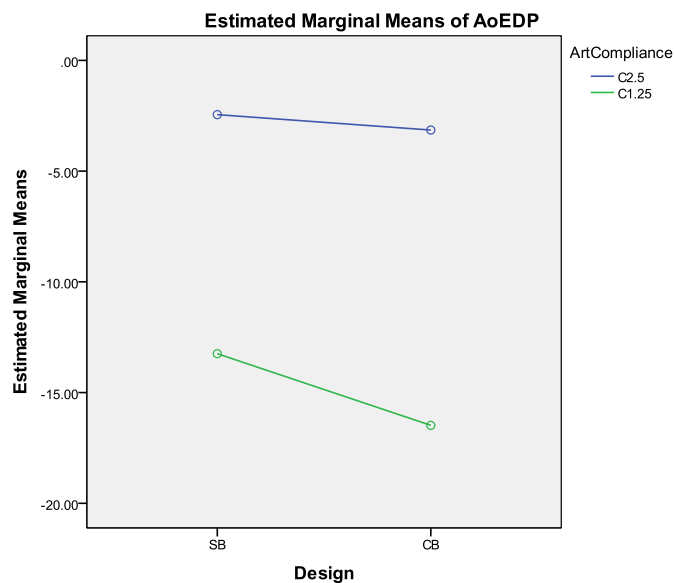
Figure 4-107 : The mean for aortic end-diastolic pressure (AoEDP)

Since there was no interaction between the experimental factors, each experimental factor is independent; for example, CB type balloon pump always yielded greater AoEDP reduction for both arterial compliance levels. Likewise, the low arterial compliance (C1.25) always yielded greater AoEDP reduction compared to high arterial compliance, C2.5, regardless of which type of the balloon pump used.

These findings suggested that for HF patient cohort, the greatest reduction of afterload can be achieved by having an optimised balloon pump design, regardless of patient's vasculature compliance. Also, the effect of arterial compliance must not be dismissed, since the difference between means of C2.5 and C1.25 was quite substantial as shown in Table 4-62. The best combination for AoEDP reduction was CB – C1.25.

4.4.1.5 Correlation

dP vs. CO

A correlation test revealed that CO and dP were significantly related, r_S = .684, N = 360, p < 0.01, two-tails. This shows that the higher the dP value, the CO increased as well although no causation is implied. The coefficient of determination, R^2 = 0.468, meaning 46.8% of variation in CO can be attributed to dP and vice versa.

dP vs. QcorMean

The association between dP and LCA perfusion was also significant r_S = .557, N = 360, p < 0.01, two-tails, and the coefficient of determination, R^2 = .31. There was 31% of variation of dP that was associated with QcorMean.

Discussion

Arterial Compliance and Device Design experimental factors were instrumental for the high degree of correlation, and association of dP against cardiac output, and left coronary artery perfusion. The increase of periphery and coronary perfusion is strongly associated with diastolic pressure augmentation with Device Design and Arterial Compliance factor

4.4.2 Discussion

A 2 x 2 two-way factorial experiment of Device Design (2 levels) and Arterial Compliance factors (3 levels) was carried out. With other experimental factors fixed (Timing: B-I, GasVol: 25 mL, Heart

valve: MHV), these experimental factors were deemed highly important since haemodynamics response from this experiment shown to be better compared to previous ones.

This experiment suggested that there were clear evidences that the Device Design and Arterial Compliance factor improved periphery and LCA perfusion, where both response outputs yield greatest output at combination (CB – C1.25). This combination also yielded greatest AoEDP reduction. In contrast, systolic aortic pressure, AoPmax, increased slightly with the highest means at 2.1 % for (CB – C1.25) combination. The implication of this finding for HF patient is at best hypothetical, but the slight increase of the systolic aortic pressure might not be detrimental to the patient, since there would be far greater augmentation from combined effect of significant AoEDP reduction, and increased periphery and LCA blood perfusion.

These findings suggest that CIMS balloon pump at the ascending aorta would benefit greatly with optimised balloon pump design in all vasculature conditions or low arterial condition with any type of the CIMS balloon pump. These findings are compared with existing data in the literature; Table 4-64 tabulates the cardiac output result.

Table 4-64: Comparison of CO augmentation between several published report

	Compliance range [mL/mmHg]	CO augmentation (%)	CO (L/min) (non-assisted)
Present study	1.25 & 2.5	7.6 - 18	3
Papaioannou et al. (2002)	1.05 to 2.62	1 – 7	2.6
Schampaert et al. (2011)	0.9	20	2.4
Ferrari et. al (2005)	2	17	3.4

The effect of varied balloon pump design and arterial compliance, each with more than one level, resulted in CIMS balloon pump yielded a greater CO augmentation compared to Papaioannou's group, but comparable with the results from Schampaert et al. (2011), and Ferrari et al. (2005).

One group published that left coronary artery mean flowrate (LCA) perfusion increased by almost 15% using an IABP in a MCL with a fairly low arterial compliance (C = 0.9 mL/mmHg) (Schampaert et al., 2011); the CIMS balloon pump yielded an increase of 20% for QcorMean with (CB – C1.25) combination. For *in vitro* setting, the effect of CIMS balloon pump at the ascending aorta on periphery and LCA perfusion seemed to be comparable to IABP, and in some cases, was better.

The findings of AoPmax and AoEDP are compared with published *in vitro* experiments using IABP device tabulated in Table 4-65 and Table 4-66.

Table 4-65: Comparison of AoPmax of several IABP studies with CIMS balloon pump

	Compliance range [mL/mmHg]	AoPmax augmentation (%)
Present study (using CB's result)	2.5	1.53 ($\approx$ 1 mmHg)
	1.25	2.1 ($\approx$ 1.8 mmHg)
Papaioannou et al. (2002)	2.62	($\approx$ -10 mmHg)
	1.05	($\approx$ -20 mmHg)
Ferrari et al. (2005)	2	-7.2

Table 4-66: Comparison of AoEDP augmentation between IABP studies with CIMS balloon pump

	Compliance range [mL/mmHg]	AoEDP augmentation (%)
Present study (Using CB result)	2.5	-3.2 ($\approx$ -1.6 mmHg)
	1.25	- 16.5 ($\approx$ -7 mmHg)
Papaioannou et al. (2002)	2.62	($\approx$ -10 mmHg)
	1.05	($\approx$ -20 mmHg)
Schampaert et al. (2011)	0.91	- 16 ($\approx$ - 4 mmHg)
Ferrari et. al (2005)	2	-7.6

Instead of reduction, AoPmax increased when the CIMS balloon pump activated, and this was very different compared to results tabulated in Table 4-65. However, the pressure increase was very small and might not be clinically significant. The reduction of AoEDP due to the CIMS balloon pump activation was comparable to most of the published results in Table 4-66. In both present and Papaioannou's study, even though the magnitude was quite different, it was shown that with decreasing arterial compliance, reduction of AoEDP become greater.

The association of dP with CO, and dP with QcorMean, showed a considerable strength at R^2 = 46.8% and 31%. Despite less than 50%, the correlation of (dP vs. CO) and (dP vs. QcorMean) when arterial compliance and balloon design factor were investigated suggests a very favourable association, and thus could be used for patient status indicator.

4.5   Heart Valve

The effect of different type of aortic heart valve was investigated using two separate factorial experiments differed only on the type of aortic valve either the mechanical (MHV) or bioprosthetic heart valve (BioPHV) (refer to Table 3-9) installed in the MCL. Experimental factors were the Deflation Point (G, I & J) and Arterial Compliance (C2.5 & C1.5) factor making a 2 × 3 factorial experiment, resulting in 6 combinations. Fixed experimental factors were 1) Inflation timing set at dicrotic notch, 2) Helium gas volume was 25 mL and 3) straight body (SB) type balloon pump.

By separating between originally intended one 2 × 3 × 2 to two 2 × 3 factorial experiments, the factorial experiments were easier to do, while still maintaining accuracy of the response outputs. It was hoped that the effect of the CIMS balloon pump counterpulsation with different aortic heart valve can shed light on haemodynamic performance differences.

4.5.1   Mechanical Heart Valve (MHV)

In this subchapter, the results of haemodynamic performance due to Deflation Point and Arterial Compliance factors while using mechanical heart valve (MHV) are presented. Three series of 2 × 3 factorial experiments were carried out and the measured data was analysed.

4.5.1.1 Cardiac Output (CO)

Figure 4-108 illustrates the pulsatile aortic flowrate with fixed balloon deflation timing (BI) and varied arterial compliance (C2.5 & C1.25). No prominent difference can be detected except for a higher magnitude in systole by flowrate BI − C1.25. Mean flowrate (i.e. cardiac output), before and after balloon activation, is used to calculate percentage difference, and used for statistical analysis.
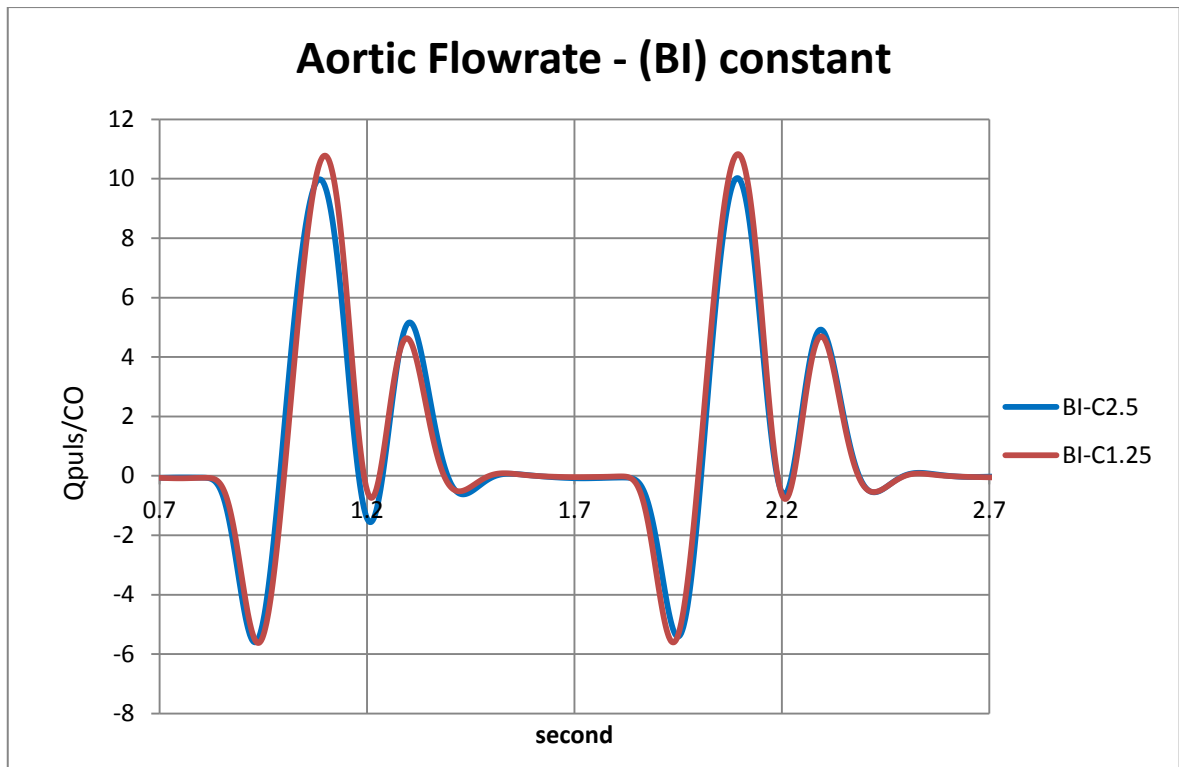
Figure 4-108 : The aortic flowrate of MHV experiment with fixed deflation timing and varied arterial compliance (the ordinate is instantaneous flow/non-assisted C.O.)

Table 4-67 tabulates the mean value and standard deviations (SD) for all combinations of Arterial Compliance and Deflation Point factor with mechanical heart valve (MHV) installed in the MCL.

Table 4-67: Mean values and SDs (in brackets) for MHV experiment

CO		Deflation Point			Row Mean
		BG	BI	BJ	
Arterial Compliance	C2.5	6.30 (1.18)	6.23 (0.80)	5.34 (2.95)	*5.96*
	C1.25	9.69 (1.10)	11.28 (1.09)	10.13 (1.67)	*10.37*
Column Mean		*7.99*	*8.76*	*7.74*	*8.16*

The grand mean value of CO augmentation was a considerable 8.16% (range: 5.34% to 11.28%), with the highest output by combination (BI – C1.25). There mean differences in column mean is low, but there is an increase of nearly two fold at row mean. To determine whether the mean differences between groups were significant or not, statistical test was carried out.

Table 4-68: SRH test result for MHV experiement

Source	P-value
ArtCompliance	1.275×10^{-77}
DeflationPoint	0.003
ArtCompliance×DeflationPoint	0.008

Table 4-68 reports the SRH result for the two-way factorial experiment. Both experimental factors showed significant main effect ($p < 0.05$), and the interaction between the factors was also significant ($p < 0.05$). Further post-hoc test was carried out to determine significance of mean differences in Deflation Point factor. Table 4-69 tabulates the post-hoc Nemenyi test result.

Table 4-69: Nemenyi test result for Deflation Point factor

	vs.	(Rb-Ra)	SE	q	q(0.05,∞ ,3)	Result	Significant
BI	BJ	9019.8	2093.3466	4.309	3.314	Reject H_0	YES
BI	BG	8346.6	2093.3466	3.987	3.314	Reject H_0	YES
BG	BJ	673.2	2093.3466	0.322	3.314	Accept H_0	

The mean differences of (BI vs. BJ), and (BI vs. BG) were significant, but not of (BG vs. BJ).This suggests that point BI was the most prominent compared to the other two points.
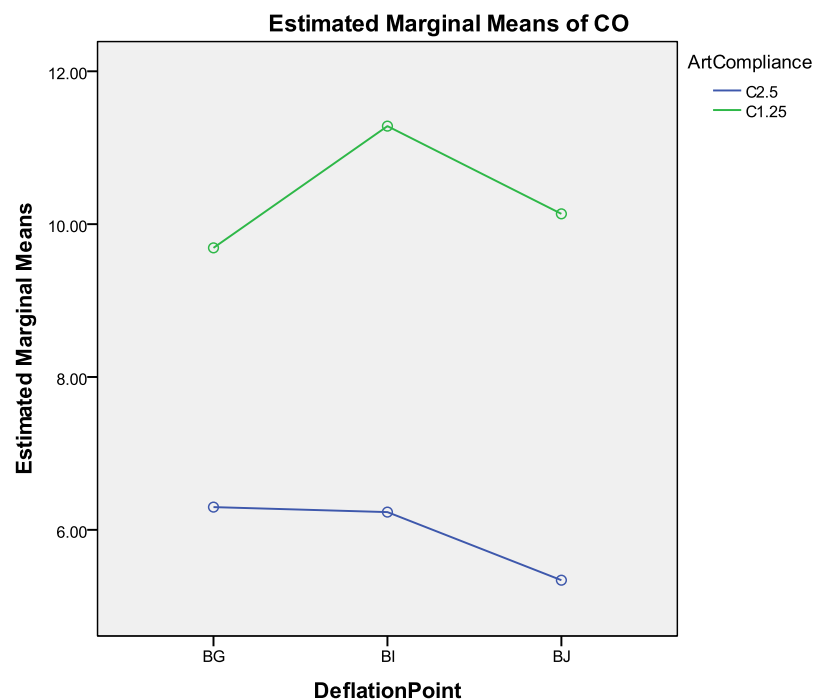
Figure 4-109 : Mean value for all combinations of experimental factors

Figure 4-109 illustrates the CO's mean value for all combinations of both experimental factors. The output by low arterial compliance level, C1.25, surpassed mean value from C2.5 results for every level in Deflation Point factor; while the output of point BI is higher than the other two points especially when in low arterial compliance. This finding supports combination (C1.25 – BI) selection as the optimum yield point.

This section finding reinforces previous subchapters finding that the effect of arterial compliance on CO augmentation was significant. The augmentation of systemic perfusion when MHV was implanted yield better result in low arterial compliance compared to high arterial compliance. Also, the similar finding of combination B-I yielding greatest output also reinforces the findings in TIMING experiment, where optimum balloon inflation and deflation timing is combination B-I.

4.5.1.2 Left Coronary Artery Mean Flowrate (QcorMean)

The effect of fixed deflation point and different arterial compliance on pulsatile LCA flowrate is illustrated in Figure 4-110. The combination BI – C1.25 waveform is quite different in magnitude compared to BI – C2.5 at every positive peak. To determine whether this also translates to meaningful differences between all six combinations, statistical analysis was carried out.
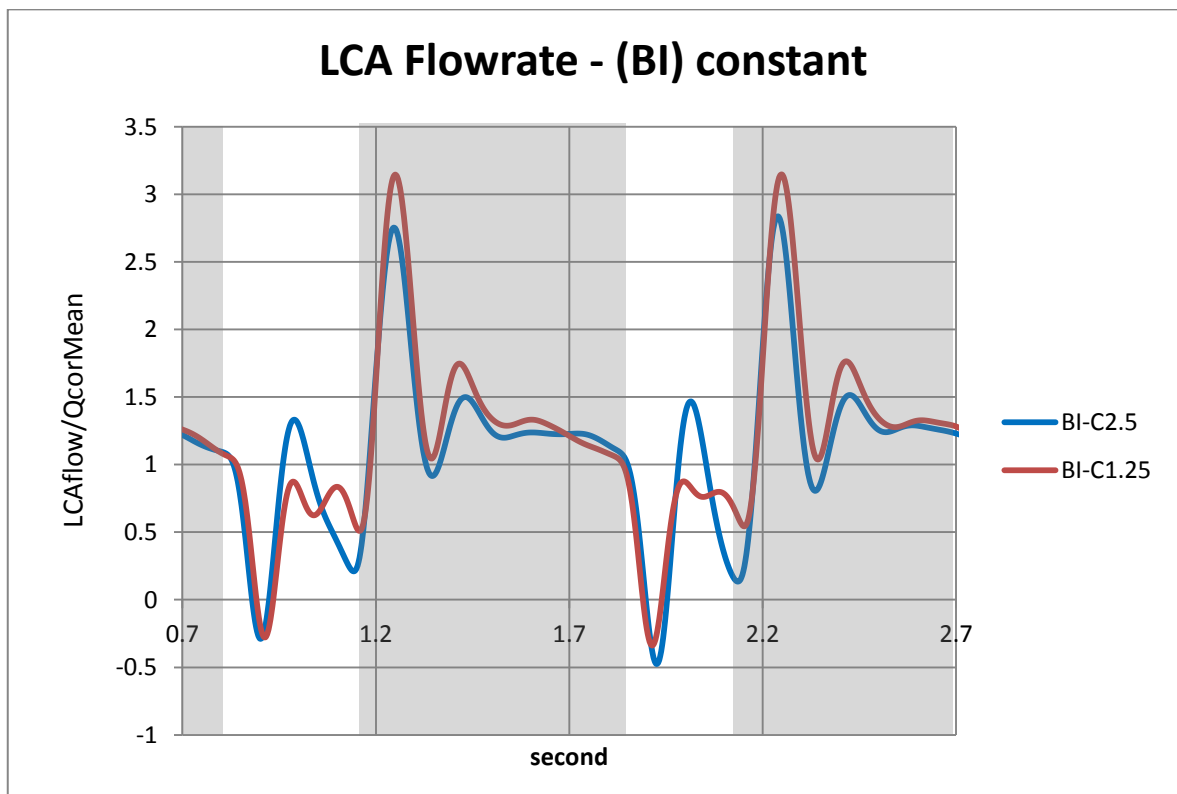
Figure 4-110: The effect of different arterial compliance while the deflation timing is fixed. . Grey areas indicate diastole period (the ordinate is LCA flowrate/non-assisted mean LCA flowrate)

The means and SDs for all combinations of two experimental factors on QcorMean, are tabulated in Table 4-70.

Table 4-70: Means and SDs of QcorMean augmentation

QcorMean		Deflation Point			Row Mean
		BG	BI	BJ	
Arterial Compliance	C2.5	9.37 (0.70)	11.82 (0.71)	9.37 (1.96)	*10.19*
	C1.25	16.37 (1.17)	19.29 (0.97)	16.98 (2.64)	*17.55*
Column Mean		*12.87*	*15.56*	*13.18*	*13.87*

The grand mean value due the treatment of two experimental factors on QcorMean in assisted flow was a reasonable augmentation of 13.87% (range = 9.37% to 19.29%). The mean differences at both row and column mean are apparent; statistical test was carried out to determine the significance of the results.

Table 4-71: SRH test result for QcorMean in the 2 x 3 two-way factorial MHV experiment

Source	P-value
ArtCompliance	1.117×10^{-87}
DeflationPoint	4.56×10^{-15}
ArtCompliance × DeflationPoint	0.395

Table 4-71 tabulates the non-parametric SRH test result; both experimental factors showed significant main effect (p < 0.001), but not the interaction between them (p = 0.395).

Since the Deflation Point factor was shown to exhibit significant main effect, further post-hoc test was carried out to determine which mean difference was significant.

Table 4-72: Nemenyi test result for Deflation timing factor

	vs.	(Rb-Ra)	SE	q	q(0.05,∞,3)	Result	significant
BI	BG	22368.6	2093.3466	10.686	3.314	Reject H_0	YES
BI	BJ	18855	2093.3466	9.007	3.314	Reject H_0	YES
BJ	BG	3513.6	2093.3466	1.678	3.314	Accept H_0	

From Nemenyi test result in Table 4-72, only the mean difference of (BI vs. BG), and (BI vs. BJ) were found to be significant, but not (BG vs. BJ); this suggests that point (B-I) was the pivotal level as clearly illustrated in Figure 4-111.
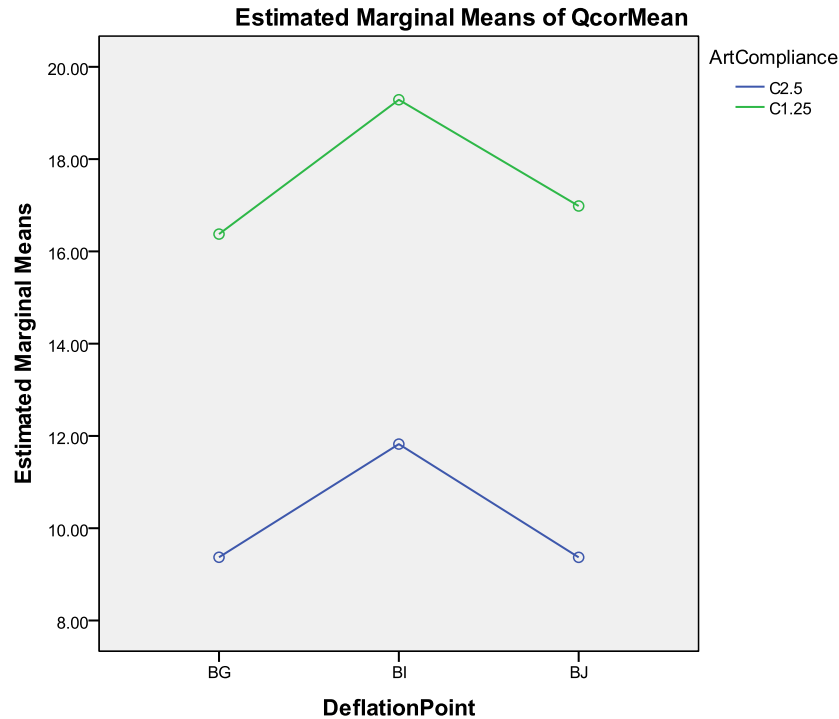
Figure 4-111: Plot of mean value for all combination of Arterial Compliance and Deflation Point factors

The effect of two experimental factors, Arterial Compliance (low and high) and Deflation Point (early, safe and late) on the mean value of QcorMean percentage increase was quite substantial. The highest output was from combination (BI – C1.25). This follows cardiac output (CO) result in previous subchapter (4.5.1.2), where highest yield was also by combination (BI – C1.25). The CIMS balloon deflation set just when the aortic valve was opening i.e. deflation point (I) combined with dicrotic notch inflation (point B) strongly give credence to TIMING experiment finding (subchapter 4.2).

Heart failure patients implanted with MHV due to possible causes such as valve incompetence, and/or heart valve disease, may benefit from the implantation of CIMS balloon pump as the coronary perfusion would show a significant augmentation from these two experimental factors, especially patients with low arterial compliance.

4.5.1.3 Aortic Systolic Pressure (AoPmax)

The effect of fixed (deflation timing) and varied (arterial compliance) factor is illustrated in Figure 4-112. Lower compliance level (C1.25) proves to yield larger pressure range compared to high compliance level.
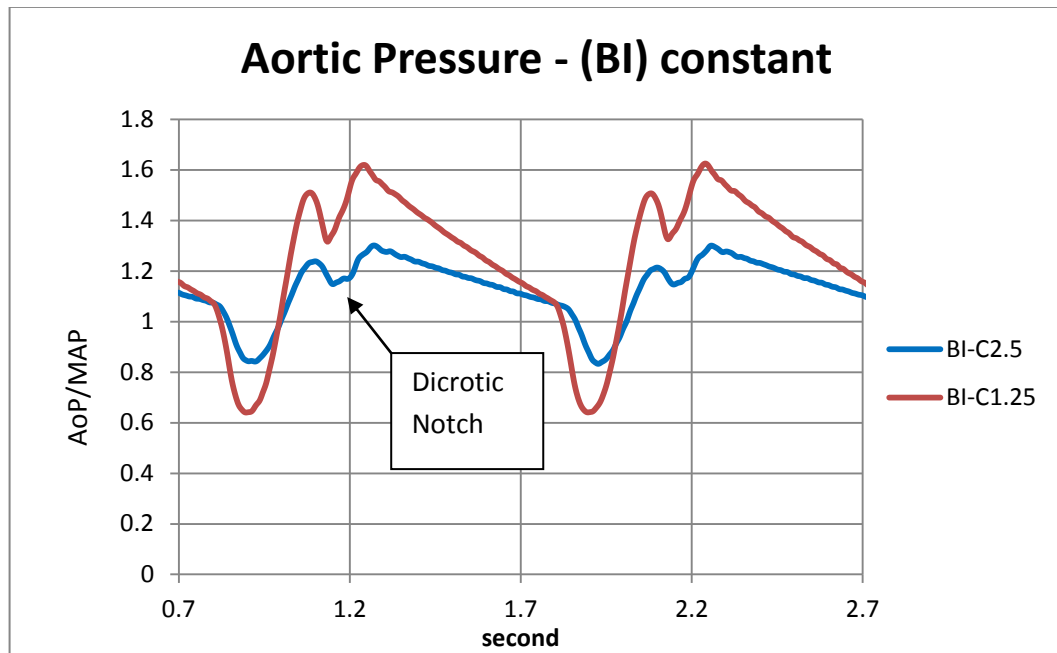
Figure 4-112: Aortic pressure waveform when deflation timing is fixed and arterial compliance is varied (The ordinate is aortic pressure/non-assisted MAP)

Table 4-73 tabulates the means and standard deviations of AoPmax augmentation percentage for all combinations of Arterial Compliance and Deflation Point factor.

Table 4-73: AoPmax means and SDs for Arterial Compliance Deflation Point factors

AoPmax		Deflation Point			Row Mean
		BG	BI	BJ	
Arterial Compliance	C2.5	1.10 (1.54)	1.19 (1.00)	-0.92 (3.23)	*0.46*
	C1.25	2.19 (1.16)	2.84 (1.28)	0.65 (2.52)	*1.89*
Column Mean		*1.64*	*2.01*	*-0.13*	*1.17*

The grand mean value is a minimal 1.17 % (range = -0.92 % to 2.84 %), and while there are obvious differences in row and column mean, they were small; to ascertain that the differences were significant, statistical test was carried out.

Table 4-74: SRH test result of 2 x 3 two-way factorial experiment

Source	P-value
ArtCompliance	5.44×10^{-18}
DeflationPoint	5.7×10^{-11}
ArtCompliance × DeflationPoint	0.027

The non-parametric SRH test, an equivalent of two-way ANOVA with replication was used. Table 4-74 reports that both experimental factors, and the interaction were all statistically significant ($p < 0.05$). Post-hoc test was carried out for Deflation Point factor to determine which level contributed to the statistical significance.

Table 4-75: Nemenyi test result for the Deflation Point factor

vs.		(Rb-Ra)	SE	q	q(0.05,∞,3)	Result	significant
BI	BJ	19740.6	2093.3466	9.430	3.314	Reject H_0	YES
BI	BG	5644.8	2093.3466	2.697	3.314	Accept H_0	
BG	BJ	14095.8	2093.3466	6.734	3.314	Reject H_0	YES

Table 4-75 reports statistically significant mean differences were of (BI vs. BJ) and (BG vs. BJ), but not between mean of (BG vs. BI). This suggests that point BJ was different from the other two as illustrated in Figure 4-113.

The supposed reduction of AoPmax was also not achieved from this round of experiment. Both experimental factors, Arterial Compliance and Deflation Point, failed to reduce the mean value of AoPmax except for one combination (C2.5 – BJ); even the grand mean value of AoPmax increased albeit a small percentage (1.17%).
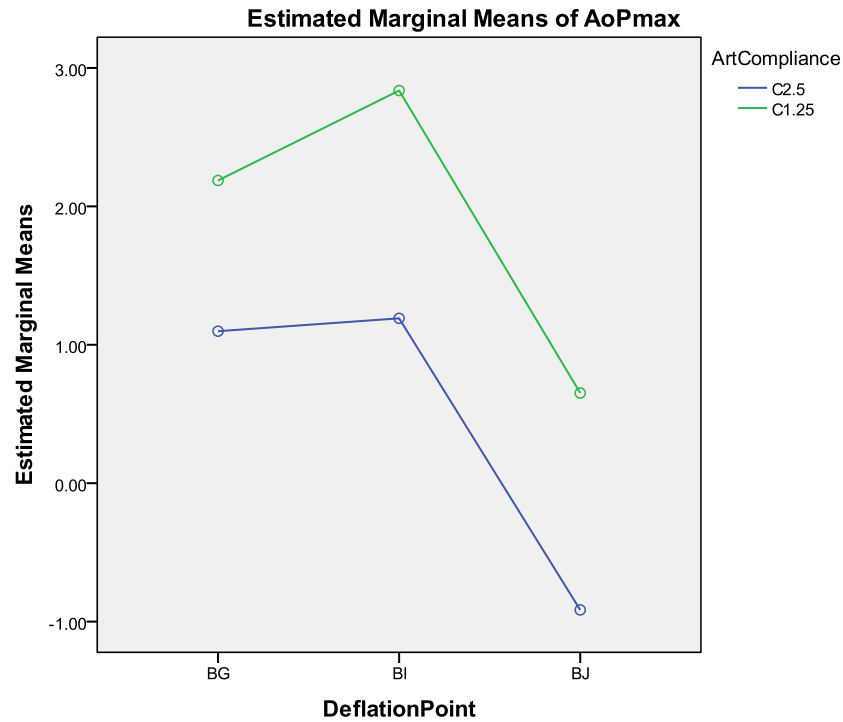
Figure 4-113: Mean value for all combinations of Arterial Compliance and Deflation Point factors

In term of AoPmax reduction, the high arterial compliance (C2.5) yielded better result compared to C1.25. This result contradicted the findings of previous subchapters (e.g. 4.5.1.2), where combination (C1.25 – BI) was the greatest output.

As discussed in previous subchapters, although from this finding, the augmentation effect of CIMS balloon pump on AoPmax reduction contradicted the effect of IABP, the magnitude was small enough to be considered as inconsequential to the workload of the heart. The myocardium workload is more affected by the reduction of afterload from reduction of AoEDP.

4.5.1.4 Aortic End-Diastolic Pressure (AoEDP)

The results of AoEDP due to activation of CIMS balloon pump are tabulated in Table 4-76.

Table 4-76: Means and SDs of AoEDP for all combinations of experimental factors

AoEDP		Deflation Point			Row Mean
		BG	BI	BJ	
Arterial Compliance	C2.5	-2.02 (1.66)	-3.44 (1.13)	-2.88 (4.55)	*-2.78*
	C1.25	-11.13 (1.81)	-13.34 (1.89)	-13.83 (3.98)	*-12.77*
Column Mean		*-6.57*	*-8.39*	*-8.36*	*-7.77*

Due to Arterial Compliance and Deflation Point factors, the grand mean of AoEDP reduction was a reasonable reduction at -7.77% (range = -13.83% to -2.02%). The mean difference at row mean is considerably bigger compared to that of column mean. Statistical test was used to determine whether the mean difference between levels and factors were significant or due to chance only.

Table 4-77: SRH test result for AoEDP response output

Source	P-value
ArtCompliance	$4.157×10^{-86}$
DeflationPoint	$1.869×10^{-5}$
ArtCompliance × DeflationPoint	0.598

The non-parametric SRH test, equivalent to two-way ANOVA with replication, was used and the result is tabulated in Table 4-77. Both experimental factors show significant main effect (p < 0.001) but not the interaction between them (p = 0.598). Further post-hoc test was done on Deflation Point factor to determine which mean difference was significant. The Nemenyi test was used and Table 4-78 tabulates the results.

Table 4-78: Nemenyi test result for Deflation Point factor

	vs	(Rb-Ra)	SE	q	q(0.05,∞,3)	Result	significant
BG	BJ	12088.8	2093.3466	5.775	3.314	Reject H_0	YES
BG	BI	11838.6	2093.3466	5.655	3.314	Reject H_0	YES
BI	BJ	250.2	2093.3466	0.120	3.314	Accept H_0	

The mean differences of (BG vs. BJ) and (BG vs. BI) were significant, while there was no significance difference between (BI vs. BJ), suggesting output from point (B-I) and (B-J) can be

considered similar; but the mean difference with point B-G was significantly different. Figure 4-114 illustrates the mean value of each combination.
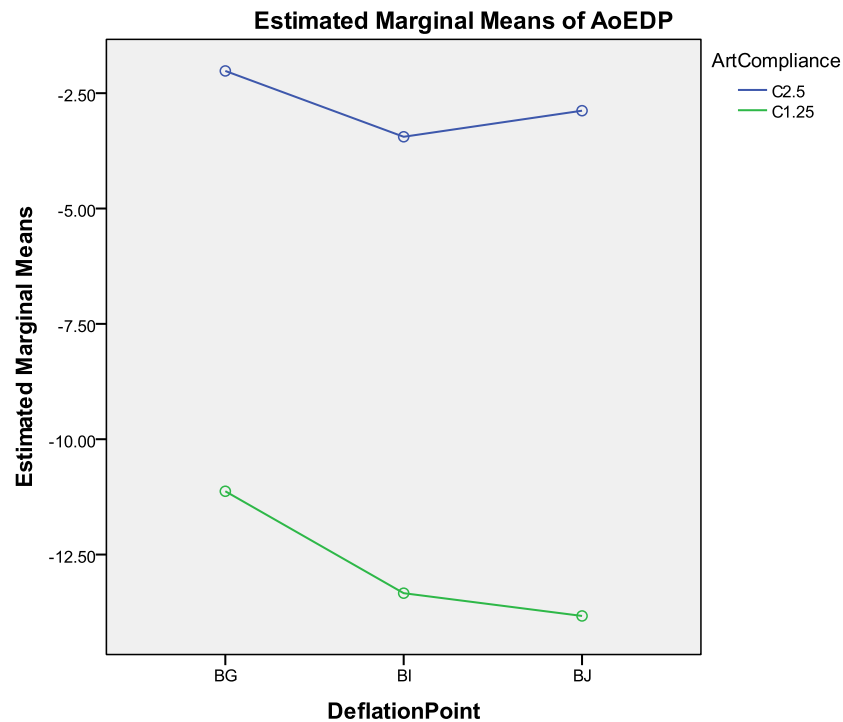
Figure 4-114: AoEDP mean value for all combination of two experimental factors

The reduction of aortic end-diastolic pressure (AoEDP) is essential to lessen myocardium workload. The combination of Arterial Compliance and Deflation Point factor which made up the 2 x 3 factorial experiment, using MHV in the MCL, reported considerable effect yielding AoEDP reduction to -13 %.

The effect of Arterial Compliance factor was significant in reducing AoEDP, with low arterial compliance yielded better result compared to high arterial compliance level. Since most of HF patient are from older generation with low arterial compliance, secondary to stiff vasculature, this finding suggested that CIMS balloon pump augmentation effect can be maximised.

The effect of Deflation Point factor was also significant with the deflation timing set after the aortic valve was opening contributed statistically different than early deflation. Although the greatest reduction of AoEDP was from combination (BJ – C1.25), since (B-I vs. B-J) was found to be statistically similar, the optimum output could be (BI – C1.25), which is the same optimum combination for periphery and coronary perfusion result previously reported.

4.5.1.5 Correlation

dP vs. CO

There was a definite significant positive association between dP and CO under Arterial Compliance and Deflation Point factor when MHV was used in the MCL, r_S =.253, N = 540, p < 0.01, two-tails. Increase of dP, the diastolic pressure augmentation indicator, was shown to be associated with increase in peripheral circulation; however, the magnitude of association was small, since the coefficient of determination was R^2 = 0.064. This means that only 6.4 % of variation in CO can be attributed to dP. From this experiment, it is suggested that the increased diastolic pressure have weak association with increased peripheral blood perfusion.

dP vs. QcorMean

Correlation test was carried out and there was a significant positive correlation between dP and the amount of augmentation to left coronary artery circulation, r_S = .447, N = 540, p < .001, two-tails. The magnitude of the association was considerably moderate, since correlation of determination, R^2 = 0.199, i.e. ≈ 20% of QcorMean variation can be attributed to dP and vice versa. Compared to the above result, there was quite a strong indication of association between augmented diastolic pressure with LCA perfusion.

Discussion

The correlation between dP vs. CO and dP vs. QcorMean were both significant, however the degree of association between variables was small. These results suggested that there are other experimental factors better associated with peak aortic diastolic pressure, periphery and coronary perfusion.

4.5.2   Bioprosthetic Heart Valve (BioPHV)

Experimental results as previous subchapter, affected by Arterial Compliance and Deflation Point factors, using bioprosthetic valve (BioPHV) in the MCL are presented hereinafter.

4.5.2.1 Cardiac Output (CO)

The effect of fixed deflation point and different arterial compliance of two pulsatile aortic flowrate is illustrated in Figure 4-115. Only minor differences in magnitude between waveforms were detected; generally combination BI – C1.25 recorded higher peak in systole. Mean of the aortic flowrate is used for statistical analysis.
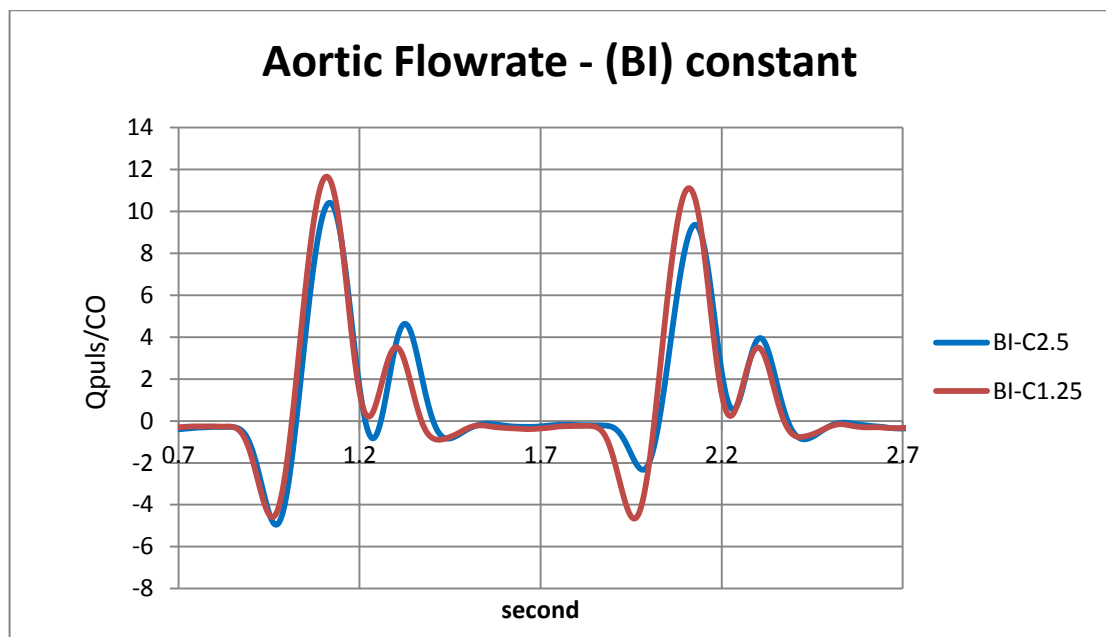
Figure 4-115: Aortic flowrate with fixed deflation point and varied arterial compliance levels (the ordinate is instantaneous flow/non-assisted C.O.)

The means and standard deviations (SD) of cardiac output (CO) for all combinations of Arterial Compliance and Deflation Point factors are tabulated in Table 4-79.

Table 4-79: CO mean values and SD (in brackets) for all combinations of Arterial Compliance and Deflation Point

CO		Deflation Point			Row Mean
		BG	BI	BJ	
Arterial Compliance	C2.5	5.58 (2.11)	4.20 (1.97)	3.35 (1.68)	*4.38*
	C1.25	8.49 (2.08)	6.31 (1.61)	5.77 (1.69)	*6.86*
Column Mean		*7.04*	*5.26*	*4.56*	*5.62*

The grand mean value due to CIMS balloon pump activation under the two experimental factors on CO augmentation percentage was minimal at 5.62% (range: 4.20% to 8.49%). The mean differences between levels in both row and column mean are not far apart. Appropriate statistical test was carried out to ascertain the significance of mean differences.

Table 4-80: The ANOVA test result

Source	P-value
ArtCompliance	0
DeflationPoint	0
ArtCompliance × DeflationPoint	0.124

Contrary to previous results, the data for cardiac output had equal variance, and adhered to normality assumption. Thus ANOVA test was used. The two-way 2 × 3 ANOVA result computed using SPSS software is tabulated in Table 4-80, and shows that both experimental factors, Arterial Compliance and Deflation Point had significant main effect ($p < 0.001$); however the interaction between the factors was not significant ($p = 0.124$). Post-hoc test was carried out on Deflation Point factor to ascertain which level contributed to the significance of the factor.

Table 4-81 : Post-hoc Tukey HSD test for Deflation Point factor

	vs	Mean Difference	Std. Error	Significance ($\alpha = 0.05$)
BG	BI	1.7811	.19699	YES
BG	BJ	2.4778	.19699	YES
BI	BG	-1.7811	.19699	YES
BI	BJ	.6967	.19699	YES
BJ	BG	-2.4778	.19699	YES
BJ	BI	-.6967	.19699	YES

Table 4-81 tabulates the simplified Tukey HSD post-hoc test result where all three levels in Deflation Point factor showed significant differences between each other at significant level of α = 0.05. Figure 4-116 illustrates the mean value of combinations to facilitate understanding.
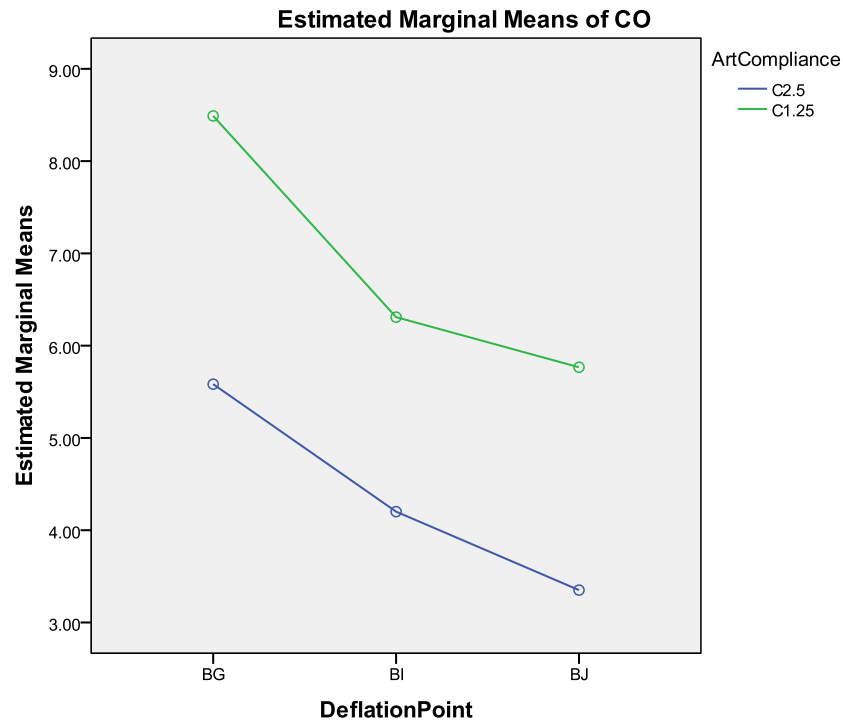
Figure 4-116: CO mean value for all combination with BioPHV

Later balloon deflation decreased cardiac output (CO) mean value with significant difference amongst deflation points, and that difference enhanced by arterial compliance in the MCL; low arterial compliance (C1.25) yielded higher response output compared to high compliance level (C2.5). The greatest CO yield was from combination (BG – C1.25) at almost 8.5% of augmentation, as a comparison the MHV result of combination (BI – C1.25) was at 11%.

When BioPHV was used in the MCL, the grand mean was 5.62% (range: 3.35% to 8.49%). The range overlapped with the MHV result above (4.5.1.1 Cardiac Output (CO)). By timing the CIMS balloon pump deflation prior to systole, instead of deflating the balloon pump at early systole, haemodynamic response would be better for the BioPHV implanted patients.

4.5.2.2 Left Coronary Artery Mean Flowrate (QcorMean)

The effect of varied arterial compliance with fixed deflation timing is not prominent except for minor differences between two LCA flowrate waveforms as illustrated in Figure 4-117.
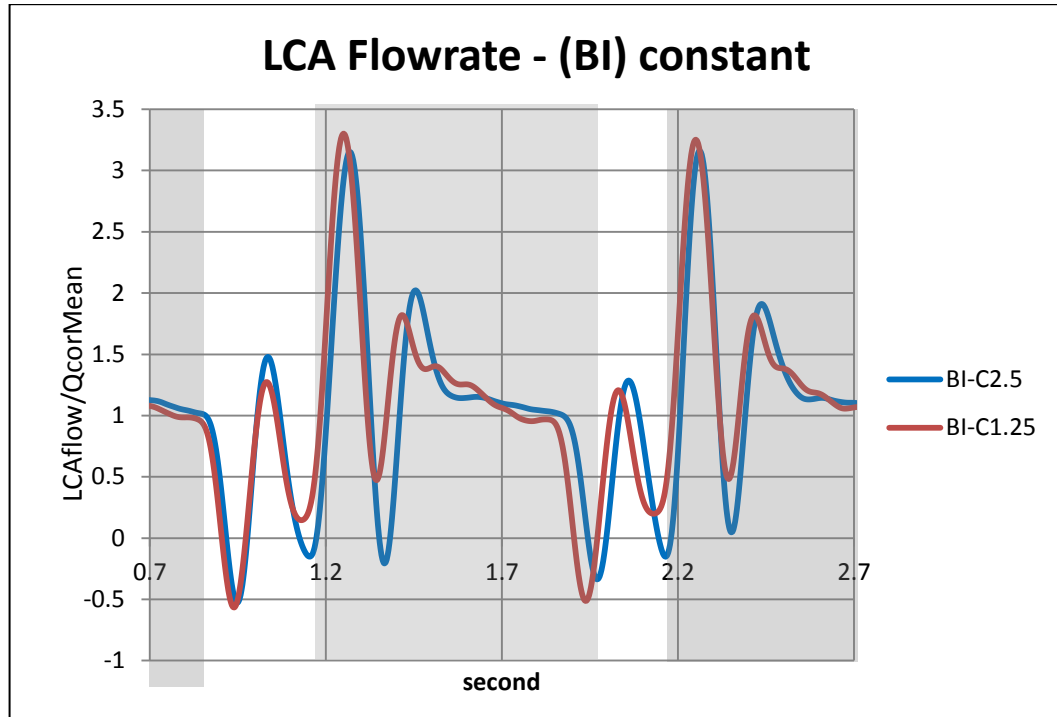
Figure 4-117: The effect of varied arterial compliance with fixed deflation point on LCA waveforms. Grey areas indicate diastole period (the ordinate is LCA flowrate/non-assisted mean LCA flowrate)

The mean flowrate was calculated for both non-assisted and assisted circulation and the percentage difference is used for statistical analysis. The augmentation effect on LCA blood perfusion is tabulated in Table 4-82. The mean values and standard deviations (SD) are from combinations of Arterial Compliance and Deflation Point factors.

Table 4-82: Mean values and SDs (in brackets) of QcorMean for all combinations of Arterial Compliance and Deflation Point factors

QcorMean		Deflation Point			Row Mean
		BG	BI	BJ	
Art. Compliance	C2.5	7.79 (1.31)	4.33 (1.21)	3.52 (1.32)	*5.21*
	C1.25	13.00 (0.82)	10.04 (1.34	8.56 (0.91)	*10.54*
Column Mean		*10.39*	*7.19*	*6.04*	*7.87*

The grand mean value of the augmented QcorMean was 7.87% (range = 3.52% to 13%). There was a two-fold increase at row mean, as well as gradual reduction as the deflation point were shifted later in the cardiac cycle in column mean. Statistical analysis was used to determine whether those mean differences were statistically significant or not.

Table 4-83: SRH test result for QcorMean data

Source	P-value
ArtCompliance	6.322×10^{-74}
DeflationPoint	2.507×10^{-30}
ArtCompliance × DeflationPoint	0.278

Table 4-83 tabulates the SRH test result; there was significant main effect for both experimental factors ($p < 0.001$), but not the interaction between them ($p = 0.278$). Since Deflation Point factor yield significant main effect, further post-hoc test was carried out to determine significance of mean differences between levels.

Table 4-84: Nemenyi test result for Deflation Point factor

	vs.	(Rb-Ra)	SE	q	q(0.05,∞,3)	Result	significant
BG	BJ	33697.8	2093.3466	16.098	3.314	Reject H_0	YES
BG	BI	23511.6	2093.3466	11.232	3.314	Reject H_0	YES
BI	BJ	10186.2	2093.3466	4.866	3.314	Reject H_0	YES

Table 4-84 tabulates the post-hoc Nemenyi test result, and all three levels were significantly different from each other ($p < 0.05$); Figure 4-118 illustrating mean value for each combination facilitates visual understanding.

Estimated Marginal Means of QcorMean
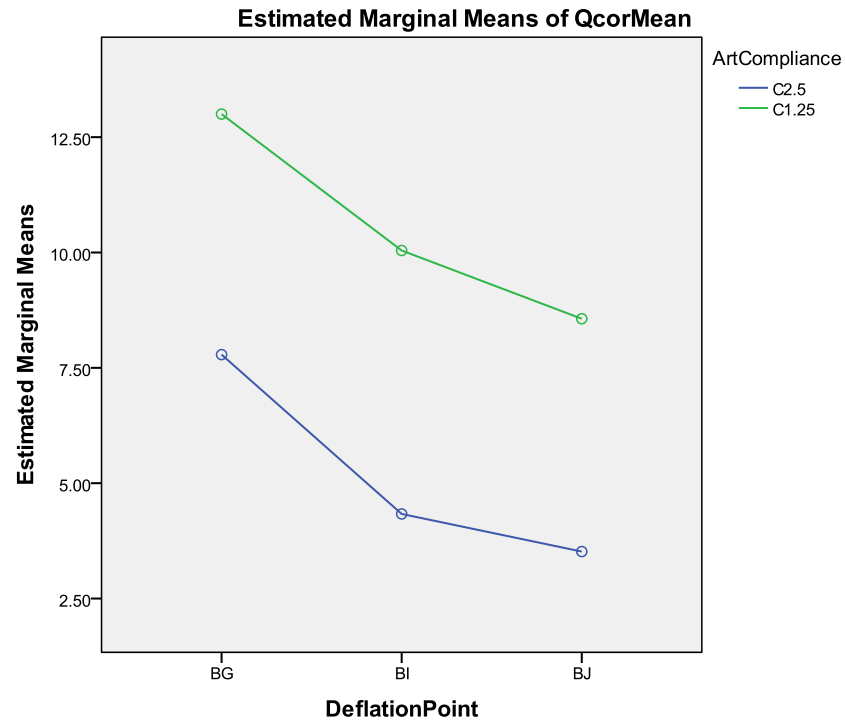
Figure 4-118: Mean vale for all combinations of experimental factors

The low arterial compliance condition yielded higher QcorMean mean value compared to the high compliance condition across all Deflation Point levels; and the decreasing trend from early to later deflation point was similar for both C1.25 and C2.5 level. Greatest yield was from combination (C12.5 – BG) at 13%. These trends are similar to the CO response output reported above (4.5.1.1).

These findings suggest patient with bio-prosthetic heart valve implanted with the CIMS balloon pump would receive optimal support if the balloon pump deflates before the aortic valve opens and possibly greater if the patient has low arterial compliance vasculature.

4.5.2.3 Aortic Systolic Pressure (AoPmax)

The effect of varied arterial compliance levels and fixed deflation point on aortic pressure is illustrated in Figure 4-119.
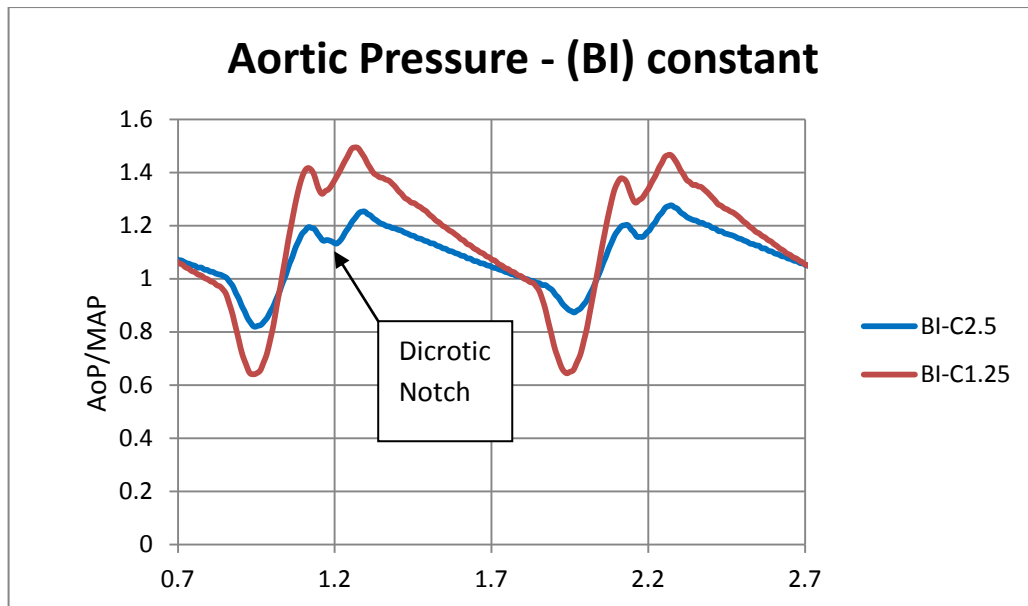
Figure 4-119: The aortic pressure with effect of two different levels of arterial compliance and fixed deflation point (The ordinate is aortic pressure/non-assisted MAP)

The range of aortic pressure is larger by the low arterial compliance waveform compared to the other one. The systolic and end-diastolic pressure is used for statistical analysis. The means and standard deviations for AoPmax augmentation due to the Arterial Compliance and Deflation Point factors are tabulated in Table 4-85.

Table 4-85 : AoPmax means and SD (in brackets) for all combinations

AoPmax		Deflation Point			Row Mean
		BG	BI	BJ	
Art. Compliance	C2.5	0.83 (1.87)	-2.39 (2.70)	-4.53 (2.12)	*-2.03*
	C1.25	1.37 (1.46)	-2.86 (2.46)	-4.24 (2.03)	*-1.91*
Column Mean		*1.10*	*-2.62*	*-4.39*	*-1.97*

The grand mean of the aortic systolic pressure (AoPmax) augmentation effect from the two experimental factors was a small reduction at -1.97 % (range = -4.53 % to 1.37 %). Column and row means are all minimal except for column BJ. Statistical analysis was performed to determine whether mean differences were statistically significant or occurred due to chance.

Table 4-86: SRH test result for the 2 x 3 factorial experiment

Source	P-value
ArtCompliance	0.695
DeflationPoint	1.5×10^{-64}
ArtCompliance ×DeflationPoint	0.247

The non-parametric SRH test, equivalent to two-way ANOVA with replication, was used to analyse the 2 x 3 factorial experiment data; Table 4-86 reports that only Deflation Point factor was found to yield significant main effect (p < 0.001). Since the Deflation Point factor showed significant main effect, further post-hoc test was carried out to determine which mean difference between levels was significant.

Table 4-87: Nemenyi test result for Deflation Point factor

vs		(Rb-Ra)	SE	q	q(0.05,∞,3)	Result	significant
BG	BJ	49644	2093.3466	23.715	3.314	Reject H_0	YES
BG	BI	33964.2	2093.3466	16.225	3.314	Reject H_0	YES
BI	BJ	15679.8	2093.3466	7.490	3.314	Reject H_0	YES

The Nemenyi test result tabulated in Table 4-87 shows all levels were significantly different from each other. Figure 4-120 illustrates the mean values of combinations in this experiment.
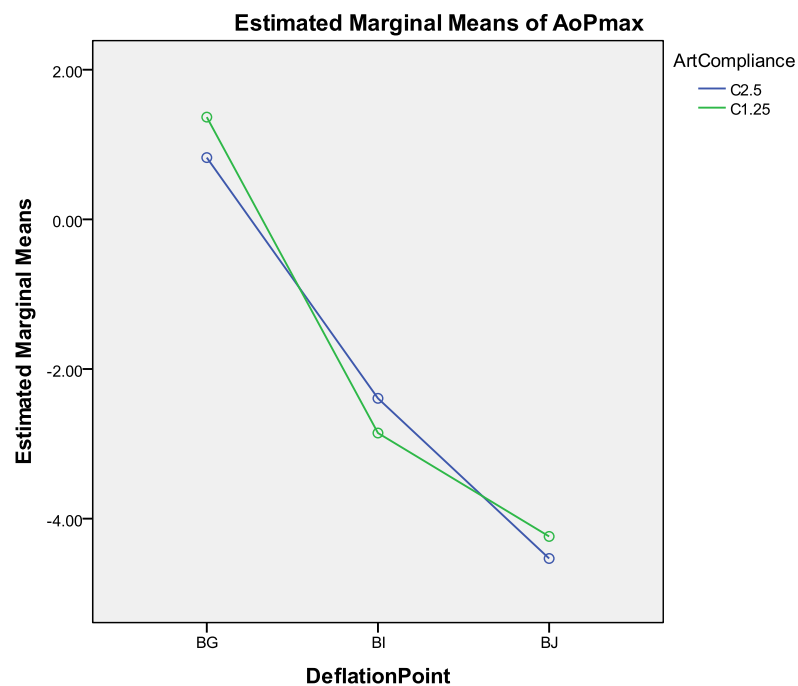
Figure 4-120: Plot of mean values for all combinations of two experimental factors

Figure 4-120 illustrates the mean values of AoPmax, and the obvious trend is dramatic reduction of AoPmax's mean value for both levels of Arterial Compliance as the deflation point shifted to the right i.e. later in the cardiac cycle. The decreasing output trend was similar to previous results, but differs by the fact that using bioprosthetic aortic valve, aortic systolic pressure is not affected by arterial compliance factor.

Patient implanted with bio-prosthetic heart valve and the CIMS balloon pump might not benefit from AoPmax reduction as demonstrated from this experiment, although deflation point past systole (point J) somehow decreased AoPmax, but only minimal at around -4 %. At point B-I (optimum point from most experiments) it was revealed that AoPmax was reduced to around -2.6%, a very minimal reduction that may or may not have clinical significance.

4.5.2.4 Aortic End-Diastolic Pressure (AoEDP)

The mean values and SD for AoEDP due to influence from two experimental factors are presented in Table 4-88.

Table 4-88: AoEDP mean values and SDs (in brackets) for all combinations from two experimental factors

AoEDP		Deflation Point			Row Mean
		BG	BI	BJ	
Art. Compliance	C2.5	-2.93 (1.67)	-3.96 (3.76)	-4.09 (4.48)	*-3.66*
	C1.25	-14.30 (3.17)	-16.38 (3.25)	-9.36 (7.63)	*-13.35*
Column Mean		*-8.61*	*-10.17*	*-6.73*	*-8.50*

The reduction of aortic end-diastolic pressure (AoEDP) by two different experimental factors, Arterial Compliance and Deflation Point yielded a favourable grand mean value of -8.50 % (range : -16.38 % to -2.93 %). The highest yield output was from combination (BI − C1.25) at -16.4%. Statistical analysis was performed to ascertain whether the mean differences were significant or occurred due to chance.

Table 4-89: Non-parametric SRH test result for 2 x 3 two way factorial experiment

Source	P-value
ArtCompliance	2.034×10^{-61}
DeflationPoint	01×10^{-4}
ArtCompliance × DeflationPoint	1.233×10^{-7}

As tabulated in Table 4-89, both experimental factors show significant main effect, and also the interaction between them ($p < 0.001$). Post-hoc test was performed on Deflation Point factor to ascertain which mean difference amongst levels was significant.

Table 4-90: The Nemenyi test result for Deflation Point factor

	vs.	(Rb-Ra)	SE	q	q(0.05,∞,3)	Result	significant
BJ	BI	12569.4	2093.3466	6.004	3.314	Reject H_0	YES
BJ	BG	4851	2093.3466	2.317	3.314	Accept H_0	
BG	BI	7718.4	2093.3466	3.687	3.314	Reject H_0	YES

The post-hoc Nemenyi test for Deflation Point factor in Table 4-90 shows that only the mean differences of (BJ vs. BI) and (BG vs. BI) was significant at 5% level, suggesting response output at point BG and BJ was similar, with point BI is the prominent output.
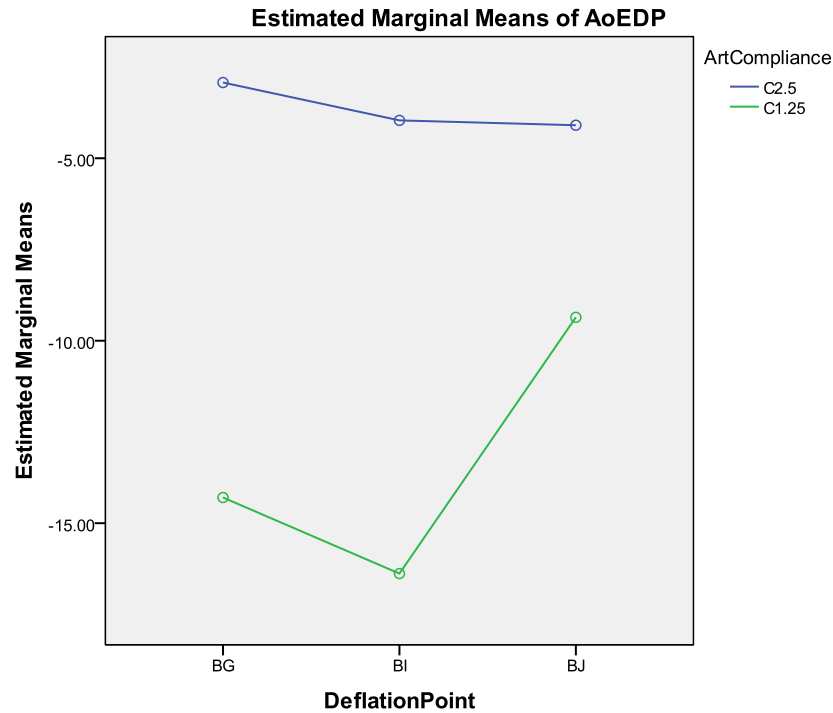
Figure 4-121: The mean value for all combinations of experimental factors

The reduction of aortic end-diastolic pressure (AoEDP), when influenced by the Arterial Compliance and Deflation Point factor, was a grand mean of -8.50 %. There was a significant mean difference of almost 10 mmHg between the levels of Arterial Compliance, as reported in Table 4-88. Low arterial compliance yielded greater AoEDP reduction, thus reducing the amount of resistance the heart has to overcome during systole. The effect of deflation timing was significant, but the effect was more pronounced when at low compliance rather than at high compliance level. From Figure 4-121, highest reduction was at point (BI) when compliance level is C1.25, while at high arterial compliance, (C2.5), mean differences were not significant.

From these results, it was suggested that afterload reduction is highly probable with bioprosthetic heart valve especially if the patient's vasculature is stiff and if the optimum inflation/deflation timing was chosen. Both MHV and BioPHV, in term of AoEDP reduction magnitude, can be suggested to be comparable since greatest AoEDP reduction was from combination (C1.25 – BI).

4.5.2.5 Correlation

The association of pressure difference (dP) between peak aortic diastolic pressure (PADA) and aortic systolic pressure (AoPmax), with peripheral and LCA perfusion was investigated using correlation test. The results are presented below.

dP vs. Cardiac Output

There was a significant positive correlation between dP and CO, r = .179, N = 540, p < .001, two tails; however, the magnitude of the association was small as demonstrated by the coefficient of determination, R^2 = 0.032, meaning that only 3.2% of CO data variations were caused by dP and vice versa. The association between these two factors is significant but it was small.

dP vs. QcorMean

There was a positive association between dP and augmentation of blood perfusion to the LCA, r_S = .177, N = 540, p < .001, two tails. However, only a small amount of variation of QcorMean mean value was attributed to dP since R^2 = 0.031, meaning the variations between the dependent variables was only a minimal 3.1 %.

Discussion

There were significant associations of (dP and CO), and (dP and QcorMean). However, the degrees of association between the response outputs were low at less than 5%. Diastolic pressure augmentation involving these experimental factors may not indicate increased CO and QcorMean.

4.5.3 Discussion

The original intention was to compare two different types of heart valve's effect on the MCL circulation when deflation timing and arterial compliance levels were varied i.e. a three-way factorial experiment (heart valve type vs. deflation timing vs. arterial compliance). However, since there could be a possibility of increased experimental error due to randomised heart valve swap; a decision was taken, to avoid excessive experimental or handling error from creeping into the data recorded, by splitting the three-way factorial design experiment into two (2) two-way

factorial experiments instead; one for the mechanical heart valve (MHV), and the other for bioprosthetic heart valve (BioPHV).

Each of the two-way factorial design experiment comprised of two experimental factors, the Arterial Compliance (C2.5 & C1.25), and Deflation Point (G, I & J) factors. The discussion hereafter compares the response output from both heart valves. Table 4-91 tabulates summary of the grand mean values, its range of response outputs, maximum output combinations and its values from both types of heart valve.

Table 4-91: Grand mean and range (in brackets), maximum output value and corresponding combination of each response output for both heart valve types

Response Output		MHV	BIOPHV
CO	grand mean	8.16%	5.62%
	range	[5.34% to 11.28%]	[3.35% to 8.49%]
	best combination maximum value	(BI – C1.25) 11.3%	(BG – C1.25) 8.5%
QcorMean	grand mean	13.87%	7.87%
	range	[9.37% to 19.29%]	[3.52% to 13%]
	best combination maximum value	(BI – C1.25) 19.3%	(BG – C1.25) 13%
AoPmax	grand mean	1.17%	-1.97%
	range	[-0.92% to 2.84%]	[-4.53% to 1.37%]
	best combination maximum value	(BJ – C2.5) - 1%	(BJ – C2.5) -4.5%
AoEDP	grand mean	-7.77%	-8.50%
	range	[-13.83% to -2.02%]	[-16.38% to -2.93%]
	best combination maximum value	(BI – C1.25) -13.3%	(BI – C1.25) -16.4%

Cardiac Output

Heart failure (HF) patients suffer diminished cardiac output (CO) from a normal range of 5 – 6 L/min, to around 3.0 – 4.0 L/min. The MCL simulated HF level perfusion at CO = 3.0 L/min, and activation of CIMS balloon pump augmented the systemic circulation shown in Table 4-91.

The grand mean value yielded by both types of heart valve was different although there were some overlaps in the range. The magnitude difference of the maximum yield from both aortic heart valves was small ; in both instances, maximum yield was from low arterial compliance

condition, only differed at either just after aortic valve opened (BI), or before aortic valve opened (BG).

The amount of peripheral blood perfusion augmentation by the CIMS balloon pump was small; the greatest output from either type was an improvement of approximately 10%. It can be suggested that the effect of aortic heart valve type on CO yield output was not prominent, and a surgeon contemplating the CIMS balloon implantation could do so without concern over aortic heart valve selection, since flow augmentation was affected more by other factors such as vasculature condition and/or balloon pump design (refer to subchapter 4.4).

Left coronary artery (LCA) mean flowrate

The augmentation of myocardial flow is one of the priorities for CIMS balloon pump activation, since that increases oxygen supply to the heart. LCA flow augmentation was reported for both types of heart valve, although the grand mean value yielded by the MHV was higher as tabulated in Table 4-91; even the range exhibited by MHV is higher compared to BioPHV.

A similar trend detected from QcorMean result of MHV and BioPHV experiments was the combination that yielded the greatest QcorMean output which also yielded optimum CO augmentation. For MHV, the combination was (BI– C1.25); while for BioPHV, the optimum combination was (BG – C1.25). LCA flow was augmented far more optimum in low arterial compliance condition, while the deflation timing that was optimum for both response outputs (CO and QcorMean) was before aortic heart valve leaflet opened completely (point BJ).

There was a considerable QcorMean augmentation from both heart valves type, although MHV yielded greater output compared to BioPHV. It can be suggested that the differences from structural construct of heart valve proximal to the LCA circulation might have caused the differences. Regardless, the favourable increase of QcorMean can be considered a positive aspect in increasing myocardium oxygen supply.

Aortic Systolic Pressure

In Table 4-91, the reduction of AoPmax was better executed by BioPHV compared to MHV, which was indicated by AoPmax's grand mean value. Almost all AoPmax mean value from BioPHV experiment recorded reduction compared to non-assisted circulation with the greatest AoPmax

reduction was combination (BJ – C2.5). As for MHV, only one combination yielded pressure reduction (BJ – C2.5).

Later deflation point was prominent in both MHV and BioPHV for aortic systolic pressure reduction while arterial compliance had no significant effect for BioPHV. Although the reduction of AoPmax was recorded, the percentage of reduction due to varied arterial compliance and balloon deflation points either by BioPHV, and especially MHV was small; as such most probably no adverse effect on the myocardium workload.

Aortic End-Diastolic Pressure

The reduction of aortic end-diastolic pressure (AoEDP) is important since the reduced aortic pressure prior to systole is hypothesised to reduce myocardium afterload.

There were similar trends between MHV and BioPHV. The arterial compliance was significant in both experiments, and mean difference between levels were also quite large. Both types yielded greatest AoEDP reduction when the arterial compliance was set to low. The average percentages of AoEDP reductions from C1.25 level were -12.77% and -13.35% for MHV and BioPHV respectively. These values are close to each other, although no statistical comparison was done.

With regards to the Deflation Point factor, the trend was different. When the MCL was fitted with MHV, later deflation timing reduced AoEDP mean value considerably, with point (BI) and (BJ) statistically similar. However, in MCL fitted with a BioPHV, the maximum reduction occurred only at point (BI). These bring the same combination for AoEDP reduction for both heart valve types at (BI – C1.25).

With manipulation of three experimental factors (heart valve, arterial compliance & deflation timing), AoEDP reduction was shown to be significant. It can be suggested that afterload would be reduced as well, thus would lead to myocardium workload reduction; especially if the patient has a low compliance vasculature, and optimum timing was chosen regardless of the type of aortic heart valve chosen.

Correlation

Table 4-92 summarises the correlation test result. The coefficient of correlation, r or r_S, and coefficient of determination, R^2, are tabulated for each heart valve type.

Table 4-92: Summary of MHV and BioPHV's correlation test result. Magnitude of variation between variables are shown in brackets

Correlation Summary		MHV	BioPHV
dP vs. CO	*r*	0.253	0.179
	R^2	0.064 (6.4%)	0.032 (3.2%)
dP vs. QcorMean	*r*	0.447	0.177
	R^2	0.199 (≈20%)	0.031 (3.1%)

There was minimal association between diastolic pressure augmentation dP with CO, and dP with QcorMean, except the association of dP with QcorMean when MHV was implanted in the MCL at a moderate 20%. That result might be attributed to the structural rigidity of the MHV's metallic bileaflet and the confounding effect of CIMS balloon pump being near to the MHV.

The low association of dP with flowrate variables tabulated in Table 4-92 suggested that under experimental factors of deflation timing, arterial compliance and heart valve types, the diastolic augmentation would not indicate clearly increased periphery and coronary perfusion.

Overall Finding

Gathering all the findings, it can be suggested that types of artificial heart valve, either a mechanical or bio-prosthetic, is not a contraindication of the CIMS balloon pump. Bio-prosthetic heart valve is implanted mostly in older population, although no significant difference in survival compared to MHV was reported (Asimakopoulos et al., 1997). Bio-prosthetic heart valve durability was less than MHV but there was no need for an anti-coagulation medication such as Warfarin, and this might be favoured with CIMS balloon pump implantation, where balloon inflation and deflation occluded the aorta.

4.6   Overall Discussion

The objective of these experiments was to investigate the haemodynamic performance due to the CIMS balloon pump activation, and the optimum combination for response output. Since the CIMS balloon pump has no precedent, a comparison is made with existing results from IABP or similar counterpulsation device available in the literature.

Table 4-93 tabulates the list of experiments carried out and the experimental factors involved. The factorial experimental method was used in this study, thus two experimental factors were combined (cross-hatched cells), while the others were fixed (non-shaded cells).

Table 4-93: The experimental factors used in these experiments. For each column, the varied factors are cross-hatch cells, while fixed factors are non-shaded cells. GasVol: Helium gas volume, Art.Comp: arterial compliance.

Types of experiment		TIMING	GasVOL	COMPLIANCE	MHV	BioPHV
Experimental Factor	Inflation	**A,B,C**	B	B	B	B
	Deflation	**G,H,I,J**	I	I	G,I,J	G,I,J
	GasVOL	V25	**V20,V25,V30**	V25	V25	V25
	Device Design	SB	**SB,CB**	**SB,CB**	SB	SB
	Arterial Compliance	C2.5	C2.5	**C1.25,C2.5**	**C1.25,C2.5**	**C1.25,C2.5**

Table 4-94 tabulates the grand mean value and ranges for all experiments in this chapter. The best in term of increase or reduction grand mean cell in a row is the red cell, the blue cell is the least useful, while the green cell is for the middle ones.

Table 4-94: Grand mean values and ranges for every experiment carried out. (red cell: best output, green: middle, blue: least best output)

Overall Finding		TIMING	GasVol	COMPLIANCE	MHV	BioPHV
CO	Grand Mean	5.52%	8.12%	12.92%	8.16%	5.62%
	range	(3.90% to 7.07%)	(5.12% to 11.52%)	(7.56% to 18.03%)	(5.34% to 11.28%)	(4.2% to 8.49%)
QcorMean	Grand Mean	9.14%	9.83%	16.45%	13.87%	7.87%
	range	(7.48% to 10.43%)	(5.34% to 15.6%)	(12.02% to 20.5%)	(9.37% to 19.29%)	(3.52% to 13%)
AoPmax	Grand Mean	-0.20%	0.94%	1.75%	1.17%	-1.97%
	range	(-2.28% to -1.7%)	(-0.68% to 2.41%)	(1.32% to 2.1%)	-0.92 % to 2.84 %	-4.53 % to 1.37 %
AoEDP	Grand Mean	-2.86%	-1.77%	-8.83%	-7.77%	-8.50%
	range	(-3.58% to -2.24%)	(-4.08% to -0.06%)	(-16.5% to -2.5%)	(-13.8% to -2.02%)	(-16.38% to -2.93%)

Discussion on each response output from those five experiments is presented.

4.6.1   Cardiac Output (CO)

Table 4-94 tabulates the grand mean values vary from just over 5 % up to almost 13 %. The highest grand mean value (12.9 %) was reported from the COMPLIANCE experiment, conducted with Device Design and Arterial Compliance factors while the lowest was from the TIMING experiment. The highest mean value was also from the COMPLIANCE experiment at 18% (combination of CB – C1.25), and the lowest mean value was from the TIMING experiment at 3.9 % (combination of C – G).

From the TIMING experiment, in term of CO yield result, the optimum timing for balloon inflation was at dicrotic notch (point B), and deflation timing was best when the balloon was deflated when systole just starting (point I). The optimised timing (B-I) was chosen as the fixed experimental factor for other experiments. The low yield from the TIMING experiment suggested that other factors than deflation/inflation timing was much more influential for CO augmentation.

The CO augmentation can be suggested to be minimal across all conducted experiments except COMPLIANCE experiment that yielded highest response output when arterial compliance and balloon pump design level was varied. Much research has been conducted associating the

beneficial effect of stiff vasculature for counterpulsation based LVAD especially the IABP (Papaioannou et al., 2002, Papaioannou et al., 2004). The encouraging result from the COMPLIANCE experiment suggested that CIMS balloon pump would also be the same, and it can also be suggested that device design has a considerable effect on flow augmentation. The GasVOL experiment showed that varied balloon pump design and Helium gas volume level also yielded favourable output,thus supporting the effect of balloon pump design.

It is interesting to note that the greatest output were from the optimum combination of low arterial compliance and CB type body balloon pump. The low arterial compliance augmented the blood pressure by way of increased pressure wave amplification and thus blood perfusion. The design of the CB type balloon pump, which had an extra space and thin silicone membrane allowing some degree of innate compliance might have increased the amount of water pushed out in diastole, and thus increasing systemic perfusion. Similar counterpulsation device such as the para-aortic counterpulsation device (PACD) seems to increase the amount of blood stored in the ascending aorta before pushing it out at diastole and works well irrespective of arterial compliance level and volumetric capacity of the device (Nanas et al., 1997, Charitos et al., 1998, Terrovitis et al., 2003).

4.6.2 Left Coronary Artery Mean Flowrate (QcorMean)

From Table 4-94, the highest grand mean value of QcorMean augmentation was yielded by COMPLIANCE experiment followed by MHV, TIMING and GASVOL experiment. The BIOPHV experiment reported the lowest yield in term of grand mean value. The highest mean value was 20.5 % (combination C1.25 − CB), from COMPLIANCE experiment, which is similar to the CO pattern discussed above. The combination of low arterial compliance and CB type balloon pump resulted in a far greater augmentation to the LCA perfusion compared to any other experimental factors.

Another experimental factor optimising QcorMean augmentation was the type of aortic heart valve. The MHV experiment, combination of arterial compliance, deflation point, and mechanical heart valve factor, yielded a reasonable result where the highest output was 19.29% (combination of C1.25 − BI), quite similar to COMPLIANCE's experiment output. It should be pointed out that, except for BIOPHV experiment, all other experiments were conducted with MHV as the fixed

experimental factor. Hence, it can be argued that mechanical heart valve would not be a contraindication for CIMS device.

For HF patient, augmentation of blood perfusions to the coronary arteries increases myocardium oxygen supply, also increases the ratio between myocardium oxygen supply and demand i.e. EVR value, allowing myocardium to function better, especially for patients suffering ischaemic heart failure (Williams et al., 1982). The increased myocardium blood perfusion coupled with decreased end-diastolic pressure (discussed below) would lead to increased cardiac function of the heart as a whole.

A LVAD wrapped around the ascending aorta, the EABP (C-Pulse™; Sunshine Heart Inc., Sydney, Australia), may provide an objective comparison. The total coronary artery flow increased by 11 % (1: 1 ratio) both from EABP and IABP activation at the ascending and descending aorta respectively (Davies et al., 2005), while the CIMS balloon pump, augmenting left coronary artery, reported augmentation range across all experiments at 3.5 % to 21%. The comparison between these studies suggests that CIMS balloon pump may perform better with an improved balloon pump design.

If the percentage augmentation of LCA flowrate is expressed in mL, then the highest yield was 0.23 mL/beat (20% of 67 mL/min), a small increase; however, since the amount of displaced blood volume to coronary arteries due to IABP activation *in vitro* is also small at 3.8% = ≈1.5 mL/beat (Kolyva et al., 2010b), with future improved CIMS balloon design, coronary arteries perfusion should improve as well.

4.6.3   Aortic Systolic Pressure (AoPmax)

The activation of counterpulsation device such as the IABP is supposed to reduce both aortic systolic pressure (AoPmax) and end-diastolic pressure (AoEDP) (Quall, 1993b), as demonstrated by several studies (Kolyva et al., 2009, Niederer and Schilt, 1988, Ferrari et al., 2005a).

In the present study, the grand mean values for all experiments conducted were found to be small (range: -4.53 % to 2.84 %). The highest reduction for AoPmax was from BioPHV experiment followed by TIMING experiment. On the contrary, the other three experiments reported a minimal AoPmax increase.

The BioPHV experiment reported highest grand mean reduction of AoPmax, and also the highest reduction was -4.53 % from BioPHV's combination (BJ – C2.5), although it was statistically similar to (BJ – C1.25) combination.

One study using a cuff wrapped around the ascending aorta reported no significant differences of assisted AoPmax compared to non-assisted circulation (Furman et al., 1970). Another clinical study also showed no discernible mean differences between non-assisted and assisted circulation when using extra aortic balloon pump (EABP) at 1:1 ratio, although at 1:2 ratio there might be statistical significance (Legget et al., 2005). The result from Legget's study is reproduced in Table 4-95.

Table 4-95 : Aortic systolic pressure reproduced from Legget et. al (2005). Values listed are mean (standard error)

	Baseline (n = 6)	1 : 1 (n = 6)	1 : 2 (n = 5)
Systolic blood pressure [mmHg]	112 (5.4)	112 (7.0)	103 (11.9)

From Table 4-95, no discernible difference was measured for AoPmax value at 1:1 ratio, thus result from present study is comparable and might not be detrimental, also it can be suggested that since the changes were minimal, the effect from the CIMS balloon pump on AoPmax might pose no clinical significance.

4.6.4   Aortic End-Diastolic Pressure (AoEDP)

Afterload reduction from decreased AoEDP is an important objective of CIMS balloon pump. During diastole, the LV wall undergoes isovolumetric contraction; the amount of myocardial tension build up in diastole depends on two factors, 1) arterial pressure and 2) ventricular radius, expressed by the Laplace equation. The reduction of arterial pressure just before LV contraction render less myocardial tension and thus the amount of myocardium work lessens. Also, reduced myocardial tension would decrease the tension time index (TTI) value.

The result tabulated in Table 4-94 showed that CIMS balloon pump invariably reduced the AoEDP across all tested experimental factors. The grand mean value has a wide range; the greatest reduction was -8.83% from COMPLIANCE experiment up to -1.77% from GasVol experiment. The

greatest mean value from all experiments was -16.48%, from COMPLIANCE experiment (combination C1.25 – CB), followed by BIOPHV experiment at -16.38% (combination C1.25 – BI). The COMPLIANCE and BIOPHV experiments shared an identical experimental factor which was the Arterial Compliance factor at C1.25 level. Thus, from these experiments it is suggested that afterload reduction can be achieved if arterial compliance of the patient is low.

There have been studies reporting the reduction of AoEDP with improved LV function, and with the combined effect of reduced AoEDP and increased LCA perfusion, myocardium workload can be lessened, which should be reflected by increased EVR value (presented in subchapter 4.6.7), by way of reduced TTI value. The IABP was shown to alleviate angina in patients due to decreased myocardial oxygen consumption from decreased afterload (Williams et al., 1982). A short term *in vivo* study onto 6 patients using C-Pulse LVAD reported that the myocardium wall stress was reduced by 31% when end-diastolic aortic pressure was reduced by only -3.3% (Legget et al., 2005), and when C-Pulse LVAD was implanted chronically into a patient, a moderate haemodynamic improvement with almost 55% of cardiac output increase compared to pre-implantation was recorded. The patient improved from NYHA Class IV to III at 6 months indicating myocardium recovery (Mitnovetski et al., 2008). Present study showed the CIMS balloon pump managed to decrease AoEDP favourably in *in vitro* setting.

4.6.5 Correlation

The correlations between dP and blood perfusion to peripheral and LCA circulation were investigated to determine whether there was any association between them. The pressure difference, dP, is the ratio between diastolic aortic pressure increase against aortic systolic pressure, AoPmax. Since AoPmax was shown to change very minimal after CIMS balloon pump augmentation, dP can be assumed to represent peak aortic diastolic pressure (PADA) as well. In Table 4-96, the results of correlation coefficient, *r* and coefficient of determination, R^2, are tabulated.

Table 4-96: The correlation coefficient and coefficient of determination results (red cell: best output, green: middle, blue: least best output)

Variable Correlation		Timing	Gas Vol	Compliance	MHV	BioPHV
dP vs. CO	r	0.171	0.447	0.684	0.253	0.179
	R^2	2.9%	22.8%	46.8%	6.4%	3.2%
dP vs. QcorMean	r	0.206	0.705	0.557	0.447	0.177
	R^2	4.2%	49.7%	33.3%	20%	3.1%

(All *r* reported $p < 0.01$, two tails)

All association between the dependent variables were shown to be statistically significant ($p < 0.01$, two-tails). The coefficient of determination, R^2, allows for comparison between cells in the above table as it quantifies the strength of the particular association between variables.

There were minimal variations of between dP and CO from TIMING, MHV and BioPHV experiments. However, COMPLIANCE and GASVOL experiment showed quite a considerable magnitude of variation. Those experiments shared a common Device Design factor. The CB design was able to push more fluid in diastole, and this might have increased the amount of diastolic flowrate, thus increasing association between PADA and CO.

It was a slightly different story between dP and QcorMean. There were considerable variation between dP and QcorMean from GASVOL, COMPLIANCE and MHV experiments, but minimal from other experiments. The common experimental factors were Device Design and Arterial Compliance factors as tabulated in Table 4-93. Judging from the results in Table 4-96, the association was highest when balloon pump design factor was coupled with a greater amount of Helium gas.

The original intention was to find out whether pressure difference between AoPmax and diastolic aortic pressure augmentation (PADA), dP, can be used as an indicator of increased periphery and coronary perfusion. Correlation test was used; the results obtained in the form of *r* and R^2 showed interesting outcomes. The association of increased aortic diastolic pressure with perfusions (periphery and coronary) were only strong if certain factors involved. Those were arterial compliance, device design, and Helium gas volume. Other experimental factors such as variation of inflation and deflation timing, and types of aortic heart valve have a minor effect on the association. Thus, for a physician or device operator, dependence on peak aortic diastolic augmentation (PADA) pressure to indicate increased perfusion may not be enough, rather other

physical indicator of the patient should be taken into account to determine the effectiveness of the CIMS balloon pump counterpulsation.

4.6.6   The Effect of Experimental Factors

There are various studies investigating biological and mechanical factors affecting the performance of counterpulsation device especially the IABP and others e.g. EABP such as arterial compliance, heart rate, blood pressure, position of the device, balloon volume and balloon inflation/deflation timing; the most prominent factors suggested are the arterial compliance (Papaioannou et al., 2002, Papaioannou and Stefanadis, 2005).

The present study also investigated the effect of arterial compliance, balloon pump inflation/deflation timing, types of heart valve, amount of Helium gas used, and adding balloon pump design as a possible factor. The experiments were conducted using factorial design method to allow a better understanding on multifactor interaction. From the results, it can be suggested with high probability that arterial compliance is a prominent factor, and if coupled with other experimental factor such as balloon device design, a very favourable haemodynamic augmentation can be achieved.

On its own, balloon pump inflation and deflation timing has a moderate effect on response output; also the amount of Helium gas volume was shown to be an important factor for LCA augmentation, especially when coupled with Device Design factor.

The mechanism of how counterpulsation induce flow and pressure augmentation is rarely discussed, only the effect and clinical relevance to blood perfusion and myocardium workload. An attempt using wave intensity analysis (WIA) managed to explain the mechanism of IABP counterpulsation by attributing Backward Compression Wave to balloon inflation, and Backward Expansion Wave to balloon deflation (Kolyva et al., 2009). Although Kolyva et al. *in vivo* study did not discuss the effect of arterial compliance to WIA, its influence would surely be substantial. The WIA method would also be useful to determine qualitatively the CIMS balloon pump design effect.

Device Design Factor, SB vs. CB

Device Design factor which comprised of a straight body and a compliant body type balloon pump is a novel idea which has never been tested in counterpulsation setting. The CB type balloon pump was shown to excel in haemodynamics augmentation compared to SB type.

The effect of CB type balloon pump on haemodynamic augmentation is demonstrated in several experiments presented in this chapter. The design of the CB type that employed thin silicone membrane and an extra cylindrical space gave extra static compliance, although small at 0.11 mL/mmHg (refer to Appendix D-2), has managed to yield greater output compared to SB type balloon pump.

However, it must be noted that the experiments conducted were not designed to specifically identify the reason for improvement by the CB type compared to the SB type balloon pump. Some explanation that could be offered is the extra space surrounding the silicone membrane; the extra space afforded in the CB type balloon pump could facilitate faster silicone membrane expansion and deflation by the Helium gas. However, there is no scientific evidence to support this hypothesis. Another confounding factor is the thin silicone membrane; it allows expansion during systole to accommodate more fluid, this might have been the factor augmenting pressure and flowrate of systemic and coronary circulation. The silicone membrane thickness was 0.5 mm (SB type balloon pump was of 1.0 mm). A thinner silicone membrane would allow for faster inflation and deflation. Again, the effect of different thickness of silicone membrane was not investigated.

These confounding factors make it difficult to specify the true reason of the CB type balloon pump effectiveness with respect to the SB alternative, especially in term of aortic pressure reduction prior to systole (i.e. afterload). There might be relationships between these factors which can be ascertained using regression analysis method.

Even though static compliance test were conducted (refer to Appendix D), whether that means during balloon pump activation the compliance remains as it is, or the static compliance effect is nullified can not be answered with certainty.

4.6.7 CIMS Balloon Pump Effect on Endocardial Viability Ratio (EVR)

Since previous subchapters suggest the greatest flow augmentation and end-diastolic pressure reduction is achieved in the TIMING experiment, EVR values were calculated for the TIMING

experiment data only. The effect on myocardial oxygen supply and demand can be quantified by the endocardial viability ratio (EVR - a counterpulsation performance index). The effect of balloon pump activation on EVR value was investigated.

Balloon inflation in diastole caused sudden aortic pressure increase, thus augmenting coronary and systemic flow. Increase in coronary flow is also indicative of increased myocardial oxygen supply. At the end of diastole balloon deflation reduces resistance to blood flow from the left ventricle allowing systolic ejection, and this reduces the amount of work which the myocardium has to generate equating to reduced oxygen consumption. Figure 4-122 illustrates the effect of balloon inflation/deflation on the aortic and left ventricular pressures as measured in the MCL.
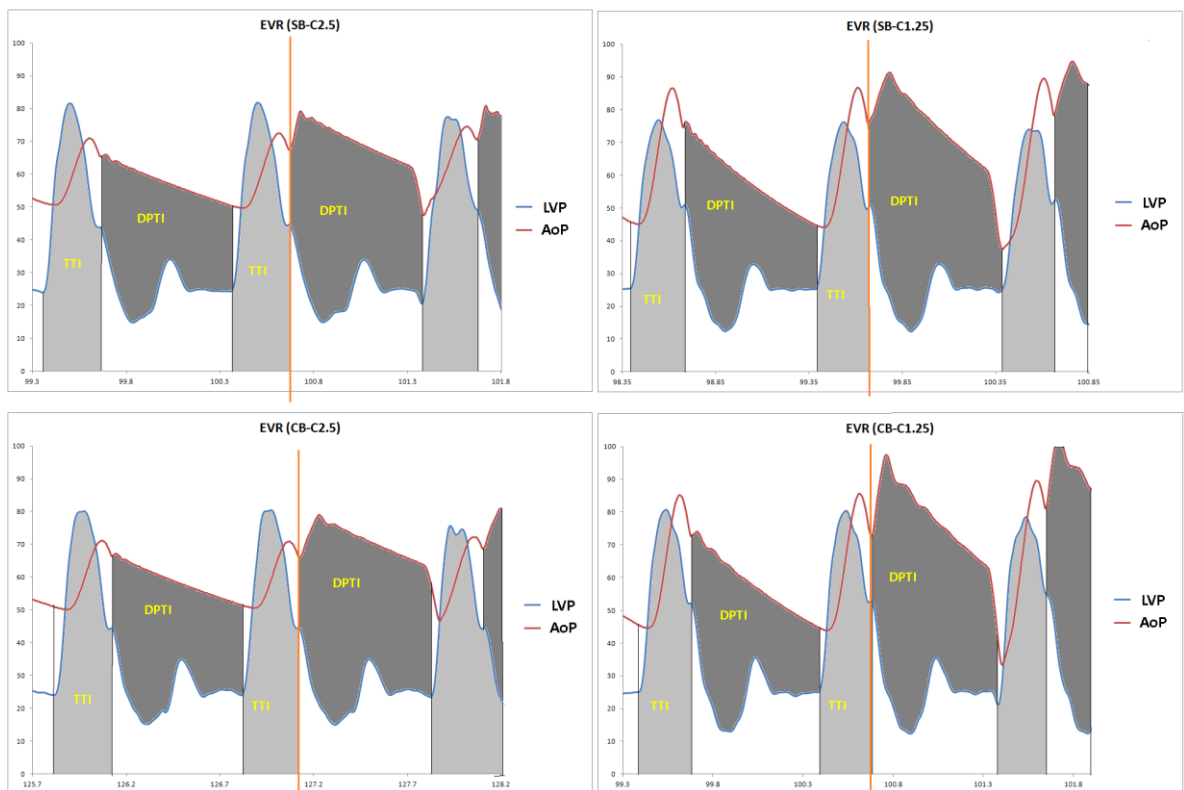
Figure 4-122: A sample of TTI and DPTI for four combinations from Device Design (SB or CB) and Arterial Compliance factors (1.25 or 2.5) before and after balloon activation. The light grey shade is the tension time index (TTI), while the dark grey shade is the diastolic pressure time index (DPTI). TTI decreased a little bit while DPTI increased thus increasing EVR value. (LVP: Left Ventricular Pressure, AoP: Aortic Pressure)

An example of differences between TTI and DPTI is tabulated in Table 4.1, while the EVR results for each type of balloon design are shown in Table 4-98 and Table 4-99.

Table 4-97: The TTI and DPTI value of one experiment (factorial experiment: SB & C2.5)

Myocardial oxygen supply/demand		TTI	DPTI	EVR
Non-assisted	Average	3733.41	5003.03	
	SD	64.99	119.99	
	SE	14.53	26.83	
	Ratio			1.34
Assisted	Average	3676.35	6457.74	
	SD	87.27	119.99	
	SE	19.51	26.83	
	Ratio			1.76
Statistical Analysis	% difference	-1.53	29.08	31.1
	Student t-test	p < 0.05	p < 0.05	

Student t-test was carried out for both TTI and DPTI data; even though DPTI data variance was not homogenous, the normality assumption was met. There were significance differences between non-assisted and assisted circulation for both TTI and DPTI (p < 0.05); however, the percentage change of TTI was small at -1.5%. The change in DPTI value was greater at 29%, thus increasing EVR value by 31%.

Next, the comparison of EVR value between different levels of arterial compliance for both types of balloon pump is presented.

Table 4-98: The endocardial viability ratio (EVR) of SB design for both levels of arterial compliance. The EVR is presented as mean ± standard deviation. *Both C2.5 and C1.25 columns were tested using the Mann-Whitney test

EVR (Straight Body -SB)	Arterial Compliance	
	C2.5	C1.25
Non-assist	1.28 ± 0.07	1.25 ± 0.09
Assist	1.70 ± 0.1	2.01 ± 0.11
Percentage of difference (Ratio)	33 % (1.33)	61% (1.61)
p-value*	p < 0.001	p < 0.001

Table 4-99: The endocardial viability ratio (EVR) of CB design for both levels of arterial compliance. The EVR is presented as mean ± standard deviation. *: Both C2.5 and C1.25 columns were tested using the Mann-Whitney test

EVR (Compliant Body - CB)	Arterial Compliance	
	C2.5	C1.25
Non-assist	1.19 ± 0.04	1.18 ± 0.04
Assist	1.71 ± 0.11	2.06 ± 0.17
Percentage of difference (Ratio)	43 % (1.43)	74.5% (1.74)
p-value*	p < 0.001	p < 0.001

There were significant mean differences (p < 0.001) between EVR for non-assist and assisted circulations for all combinations. The activation of the CIMS balloon pump had a considerable effect increasing the EVR values, thus on (simulated) myocardial oxygen supply and demand.

Further comparison between both experimental factors (Device Design and Arterial Compliance) was carried out using a factorial analysis method. The percentage difference of EVR value between non-assisted and assisted circulation was used for analysis purposes using similar methods as in previous chapters. Figure 4-123 illustrates the mean of each combination, while Table 4-100 tabulates the mean and standard deviation of each combination's percentage difference of EVR value.
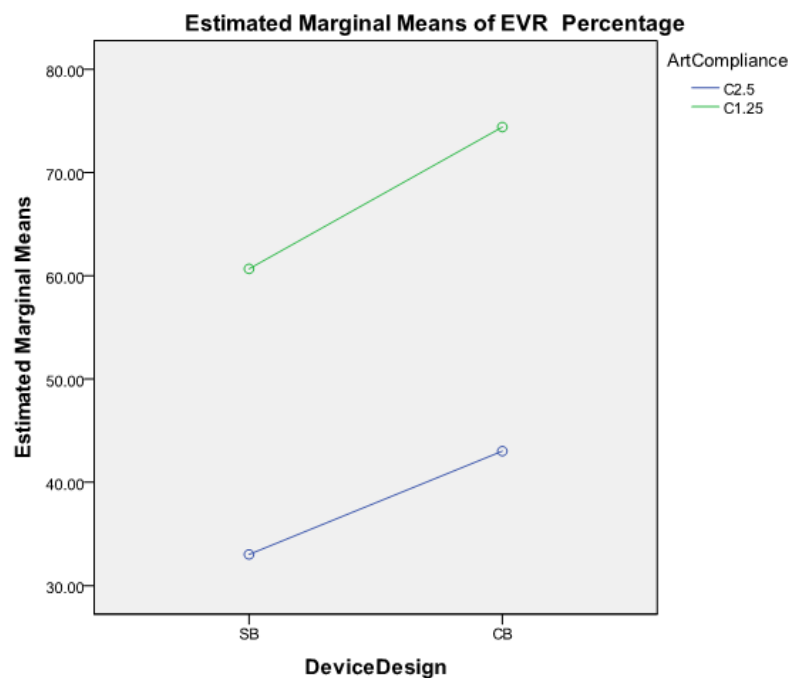
Figure 4-123: The means of EVR percentage difference

There are noticeable differences between combinations, especially between low and high arterial compliance. The means and standard deviations for each combination are tabulated in Table 4-100.

Table 4-100: The mean and standard deviation in EVR percentage difference before and after balloon activation

Endocardial Viability Ratio (EVR)		Arterial Compliance		Row Mean
		C2.5	C1.25	
Device Design	SB	33 ±7.5	61 ± 4.6	*46.8*
	CB	43 ± 8.5	74 ± 13.3	*58.7*
Column mean		*38*	*67.5*	*50.7*

With CIMS balloon activation, the EVR percentage yields a grand mean of almost 51% (range: 33% to 74%). The row mean for SB and CB design shows a difference of approximately 11%, while there is a much greater mean difference between low and high arterial compliance. Yet again, the combination of CB – C1.25 yields the greatest percentage of EVR increase. The mean differences were tested for significance using the SRH methods described in chapter 3 and employed in previous subchapters.

Table 4-101: The statistical SRH test result for EVR

Experimental factor	p- value
Device Design	9.1×10^{-6}
Arterial Compliance	4.1×10^{-39}
Device Design × Arterial Compliance	p = 0.99

Table 4-101 tabulates the p-value from the SRH test of each experimental factor and the interaction between them; in both experimental factors, there is significant difference between means (p < 0.001), but not the interaction between them (p = 0.99).

Discussion

The endocardial viability ratio (EVR) is a suitable performance index for the counterpulsation method; it has been shown to be able to estimate the myocardial oxygen supply and demand ratio quite accurately (Philips et al., 1975). The result of the present study is compared with *in vivo* and *in vitro* studies tabulated in Table 4-102.

Table 4-102: Endocardial viability ration (EVR) values from present and other counterpulsation device studies.

Researcher	Device	EVR (% increase)
present study (C = 1.25 and 2.5 mL/mmHg)	CIMS balloon pump (*in vitro*)	33 % to 74 %
(Cmolik et al., 2001)	IABP (*in vivo*)	16 %
(Terrovitis et al., 2003)	IABP (*in vivo*)	50 %
	PACD (*in vivo*)	70 %
(Utoh et al., 1993)	EPAD (*in vivo*)	20 %
(Ferrari et al., 2011) (C = 1.8 and 2.5 mL/mmHg)	IABP (*in vitro*)	42 % and 57 %
(Lu et al., 2011)	IABP (*in vivo*)	40 %
	PABP (*in vivo*)	46 %

Table 4-102 shows EVR improvement due to CIMS balloon pump activation in the MCL is comparable with results published in other studies. The most similar setting is with the in vitro study of Ferrari et al. (2011), which had the same arterial compliance condition. In high arterial compliance, IABP performed better than CIMS, while the CIMS balloon pump performed better in low arterial compliance.

The results presented here suggest that arterial compliance and device design play significant roles independently; where the contribution from column C1.25 and row CB yielded the greatest percentage increase in column and row respectively. Consequently, the combination of CB – C1.25, yielded the greatest EVR improvement at 74 %. When compared with results in Table 4-102, CIMS result is better than IABP (50%), and comparable with a para-aortic counterpulsation device (PACD) (70%) of similar volume displacement (30 mL) (Terrovitis et al., 2003).

The differences between combinations can be further scrutinised by referring to Figure 4-122; where the increase in EVR values, as tabulated in Table 4-98 and Table 4-99, is attributed to bigger DPTI value in the numerator, while the TTI values decrease a little. Diastolic augmentation from CIMS balloon activation has increased the DPTI value which represents myocardial oxygen supply. The near constant TTI value can be attributed to the MCL characteristics used in this study. Although the MCL is able to simulate haemodynamics characteristics of systemic and left coronary artery circulation accurately, the MCL cannot simulate the Frank-Starling mechanism accurately, where any changes in the preload and afterload affect the intraventricular pressure and ejection fraction. As tabulated in Table 4-97, TTI did decrease in assisted circulation, although small ($\approx$ -1 to -2%), due to decreased aortic root pressure pre-systole. The EVR values recorded from this study exceeded a value of 1.0 (range: 1.18 to 1.28) i.e. the minimal necessary balance of supply versus demand in the myocardium; although the range of EVR values pre-assist published in the literature tabulated in Table 4-102 have a range from 0.86 to 1.29. The higher than 1.0 value may be attributed to the shape of left ventricular pressure waveform generated by the MCL used.

The increased aortic pressure in diastole is an important factor for increased coronary flow (Green and Hutton, 1999, Geven et al., 2004). In the COMPLIANCE subchapter (at section 4.4.1.2) the left coronary artery mean flowrate increase by a grand mean of 16.5 % (range: 12 to 21 %). Although as discussed earlier (2.5.3 Intra Aortic Balloon Pump) increased aortic diastolic pressure from balloon pump activation may not be translated to increased coronary flowrate consequently the myocardial oxygen supply, EVR can still be considered as a suitable performance index to indicate myocardial oxygen supply.

The CIMS balloon pump has demonstrated the capability of increasing myocardial oxygen supply/demand ratio, and is thus a favourable candidate as a mechanical heart assist device for heart failure patients, as indicated in Chapter 2.

4.7   Conclusion

There was an optimised timing for balloon inflation/deflation. The inflation point for the CIMS balloon pump at the ascending aorta was similar to IABP i.e. at dicrotic notch, but the deflation point was slightly later after aortic valve was opened. This timing combination also proved to be significant when combined with other experimental factors. From the results it was concluded that the CIMS balloon pump yielded its best haemodynamic response with regards to periphery and coronary perfusion as well as afterload reduction when stiff vasculature was set in the MCL, and when compliant body type balloon pump was used, for example cardiac output was increased to almost 20%, left coronary perfusion mean flowrate too was increased by 20%, while flow resistance in the form of aortic end-diastolic pressure was reduced by 16%. Aortic systolic pressure changes were minimal from all experiments, hence the small changes in AoPmax was hypothesised as clinically insignificant.

These findings reinforce the known effect of arterial compliance but also add the influence of balloon innate compliance to optimise counterpulsation effect at the ascending aorta.

The trends between MHV and BioPHV were different especially on which deflation point yielding optimum augmentation. Perfusion augmentation for MHV was optimised at dicrotic notch for inflation and deflates at early systole, while BioPHV differed at earlier deflation point. Overall, the performance of MHV was better compared to BioPHV.

With regards to correlation between diastolic augmentation pressure, dP and CO and QcorMean, there were definitely significant correlations in all experiments, but the association was only stronger when arterial compliance and balloon pump innate compliance were the prominent factors.

The effect of CIMS balloon activation on myocardial perfusion as indicated by the endocardial viablitiy ratio (EVR) was shown to be favourable. Depending on the combination of the experimental factors, the EVR value increased by 33% to 74%; where diastolic augmentation

contributed more to EVR value increase compared to systolic unloading. Systolic unloading decreased by -1% to -2%, while diastolic augmentation increased by 29%.

Chapter 5   Haemodynamics of the CIMS Balloon Pump

This chapter presents results from two experiments to determine the effect of balloon deflation on the aortic heart valve: a flow visualization experiment, and pressure/flow experiment.

5.1   Flow Visualisation

It was observed that the valve opened somewhat earlier when the CIMS balloon pump was activated. It was hypothesised that this was due to an earlier positive pressure gradient across the aortic heart valve. To determine whether that observation was correct or not, flow visualisation experiments were carried out.

A simple set up and some modifications on the human mock circulatory loop (MCL) were done to enable flow visualisation - as presented in Chapter 3. The intention of the flow visualisation experiment was to record the sequence of valve leaflet opening when subjected to balloon inflation and deflation activity. The MCL was turned on and set to heart failure (HF) condition with these settings: arterial compliance = 2.5 mL/mmHg, balloon inflation/deflation = point (B-I) and mechanical aortic heart valve (MHV). The MCL was varied with two heart rates modes: 60 beats/min and 54 beats/min. The video recording was at 30 fps (frame per seconds).

5.1.1   Valve Opening Time

Figure 5-124 illustrates a square wave, and the measured pressure and pulsatile flowrate waveforms. The square wave signal (LVSquareWave) is the signal sent to the pressure regulator allowing compressed air into the left ventricular (LV) chamber thus initiating systole. The LVSquareWave is also sent to a red LED as an analog signal to illuminate the LED during systole. There is a time lag of around 0.3 s between the square wave and the response from pressure and flow rate whilst pressure accumulates in the LV chamber; the MCL was built with an air gap in the LV chamber allowing compressed air to escape which, in diastole, allowed passive filling but which, in systole, required longer time to initiate contraction.
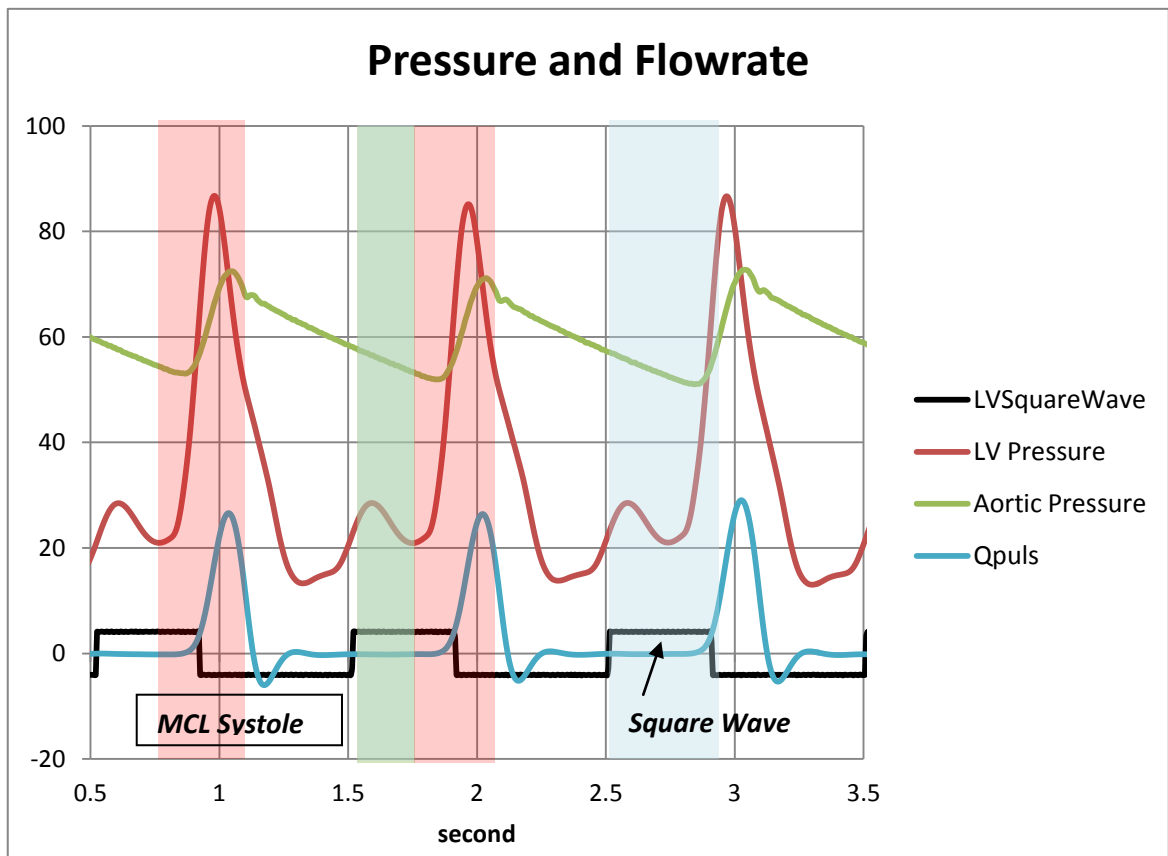
Figure 5-124: Square wave sent to pressure regulator, and the red LED precedes left ventricular sac contraction and fluid outflow from the LV chamber. The red band indicates MCL systole (LV sac contraction), blue band indicates square wave activation, while the greenband indicates the time lag between red and blue band.

Table 5-103: List of videos taken (fps: frame per seconds)

Non-assisted	Assisted
60 beats/min (T = 1 s) , 30 fps	60 beats/min (T = 1 s), 30 fps
54 beats/min (T = 1.1 s), 30 fps	54 beats/min (T = 1.1 s), 30 fps

As tabulated in Table 5-103, four different video recordings were taken. From each video recording, 10 seconds of 60 beats/min video were cut and converted into still images (300 images) for analysis purpose. For the 54 beats/min video, the cardiac cycle time is 10% longer than 60 beats/min (T = 1.1 second), so 330 still images were converted from the video. Examples of the still images from 60 beats/min video are given in Figure 5-125 and Figure 5-126 for assisted and non-assisted circulation respectively.

The low frame rate (30 fps) of the video recording means that there is an error of up to ± 0.033 seconds in establishing precisely when an event occurred. Since this experiment was conducted to identify the possibility of premature valve opening, the error between images is tolerated.
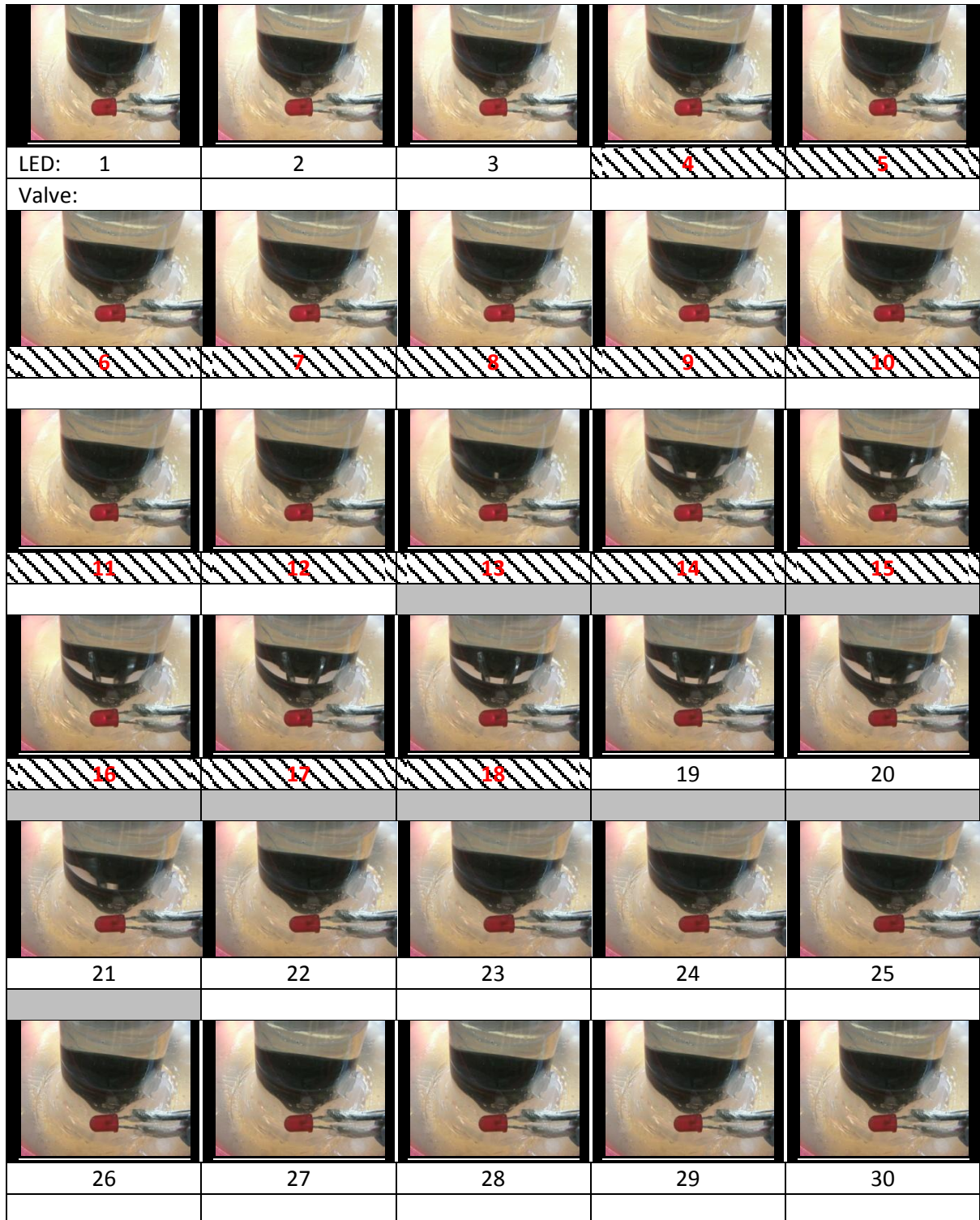
Figure 5-125: Filmstrip of one second worth of 60 beats/min video for non-assisted circulation; the cross-hatch panels indicate that the red LED is illuminated, while the grey-shaded panels indicate valve leaflet is open.

Figure 5-125 illustrates the still images taken of one cardiac cycle of 60 beats/min in non-assisted circulation as an example. In panel number 4, the red LED illuminates which continues to panel number 18 indicated by the panel cross-hatching. This translates into a period of 0.5 seconds. The pressure accumulates in the LV chamber and when LV pressure exceeds aortic pressure, the mechanical valve leaflet opens up a few milliseconds later at panel number 13 as indicated by the grey-shaded panel, continuing to panel number 21. This means that the period for which the valve open was 0.3 seconds. The panels between LED first illuminated (number 4) and valve opening (number 13) yielded an additional 0.3 seconds. This is an important indicator of valve opening time, since LED illumination time and duration is constant. Any effect of balloon deflation would change the duration between LED first illuminated and valve opening.

26	27	28	29	30
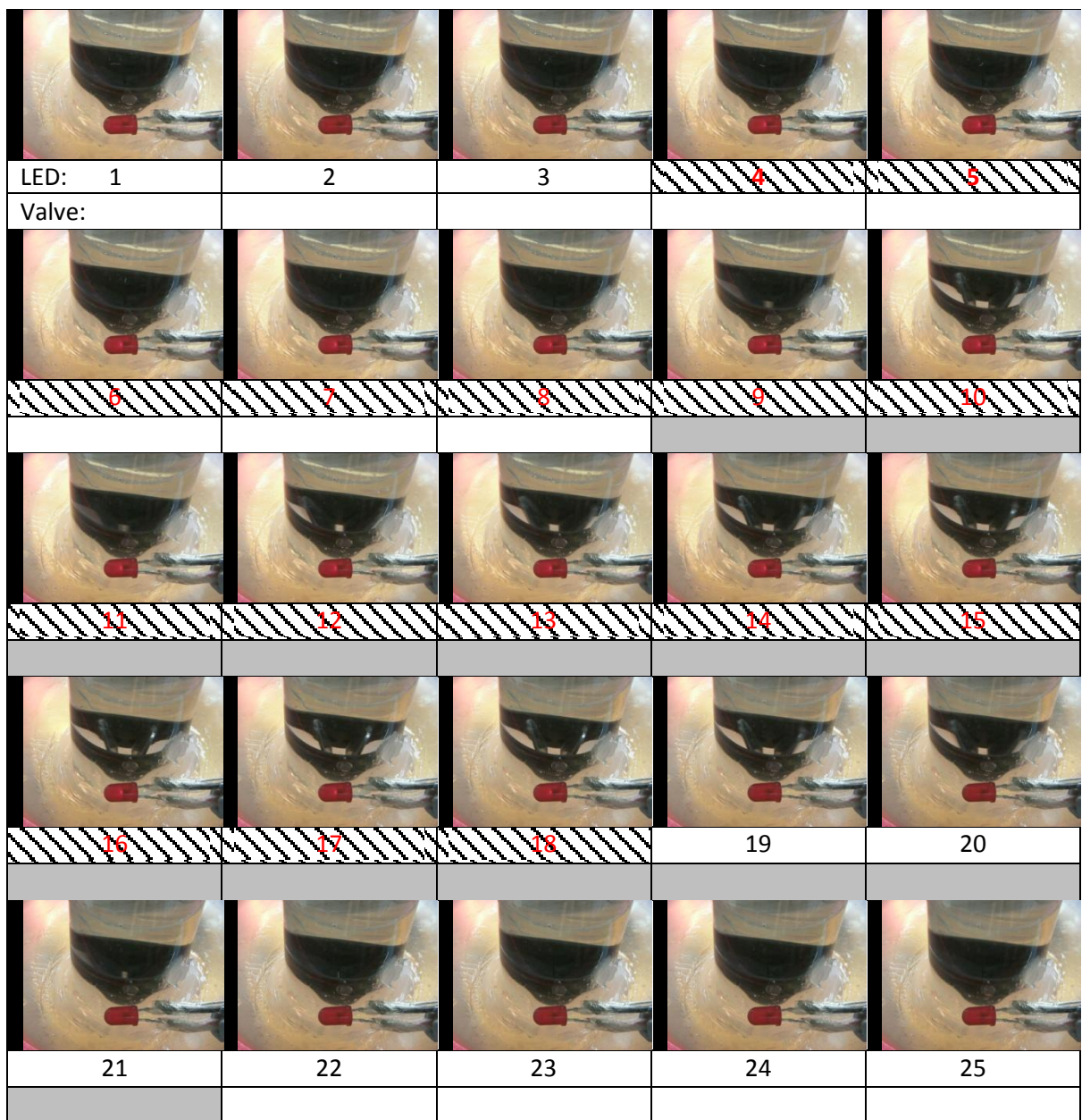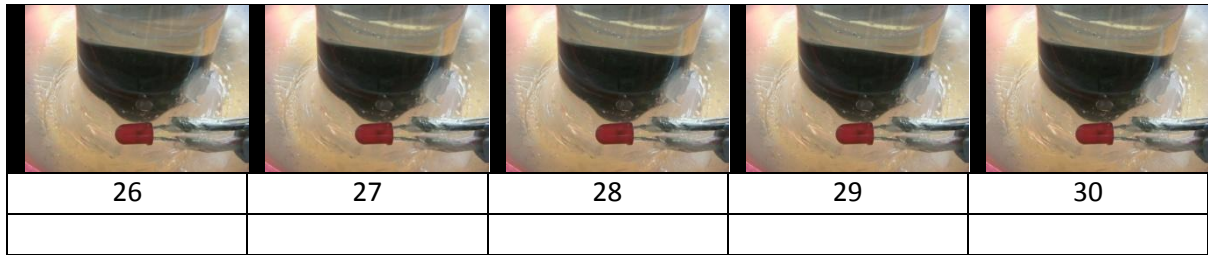
Figure 5-126: Filmstrip of one second worth of 60 beats/min video in assisted circulation. The cross-hatch panels indicate that the red LED is illuminated, while the grey-shaded panels indicate that the valve is open.

Figure 5-126 illustrates an example of the valve opening sequence with CIMS balloon pump activation and 60 beats/min heart rate. The red LED is illuminated first at panel number 4 until panel number 18. Due to the CIMS balloon pump activation, the valve opens earlier at panel number 9 and is closed at panel 22; meaning the valve was opened for 13 panels, which translates to 0.43 seconds. The duration is longer than in the non-assisted circulation example of Figure 5-125 at 0.3 seconds.

All ten seconds worth of images from videos of 60 beats/min and 54 beats/min were manually counted. The duration of red LED illuminated, the duration of valve opened, and the time difference (Δt) between those durations was computed. The time difference would indicate clear evidence of earlier valve opening with activation of the CIMS balloon pump. The results are presented in subchapter 5.2.2.

5.1.2   Statistical Analysis

Table 5-104 tabulates the results of still picture analysis of 60 beats/min and 54 beats/min video. The period of red LED illumination, the time period from red LED illuminated to valve opening (Δt), and the opening duration of the valve are tabulated.

Table 5-104: The results of 60 beats/min and 54 beats/min for non-assisted and assisted circulation. Δt: The time duration from LED turned ON until the aortic heart valve open. Unit is in second (s)

Heart Rate		LED On Period	Δt	Valve Open Duration
60 bpm	Non-assisted	0.50±0	0.30±0	0.30±0.02
	Assisted	0.50±0	0.20±0.04	0.39±0.05
54 bpm	Non-assisted	0.54±0.04	0.34±0.02	0.29±0.02
	Assisted	0.57±0.03	0.25±0.02	0.38±0.02

Statistical tests were used to discern whether mean differences between assisted and non-assisted circulation were significant or not. However, there are two assumptions that need to be fulfilled: homogeneity of variance, and normality of data distribution. If both were fulfilled (i.e. p-value > 0.05) a parametric type Student t-test was used, if not a non-parametric type Mann-Whitney test was used. Although Student t-test may tolerate non-homogenous data distribution i.e. unequal variance, non-normality is not tolerated. Table 5-105 tabulates the statistical data and results of 60 beats/min and 54 beats/min.

The hypothesis for these statistical tests is:

H_O = There is NO mean difference between non-assisted and assisted circulation.

Table 5-105: The statistical results of 60 beats/min and 54 beats/min. All four variables were tested using Mann-Whitney test. *Δt:* Duration of time between red LED illuminated and valve opening.

Statistical Result		60 beats/min		54 beats/min	
		Δt	Valve Open Duration	*Δt*	Valve Open Duration
Mean difference (Assist – Non-assist)		-0.10	0.09	-0.10	0.09
Normality (Shapiro-Wilk test)	Non-assist	constant	$p < 0.05$	$p < 0.05$	$p < 0.05$
	Assist	$p = 0.073$	$p = 0.138$	$p < 0.05$	$p < 0.05$
Equality of variance		$p < 0.05$	$p < 0.05$	$p = 0.115$	$p = 0.869$
p –value		$p < 0.001$	$p < 0.001$	$p < 0.001$	$p < 0.001$

Statistical results show that the activation of the CIMS balloon pump at the ascending aorta increases the valve opening period (all $p < 0.001$), due to the earlier valve opening prior to systole as shown by *Δt* results (all $p < 0.001$). Discussion of the implications of this result is presented at the end of this chapter.

5.2 Pressure Difference across the Aortic Heart Valve

The haemodynamics of balloon inflation and deflation is discussed further in this subchapter. In the previous subchapter, balloon deflation prior to systole was shown to cause the valve to open earlier. The early valve opening allows for longer valve opening as demonstrated by the statistical analysis.

5.2.1 Non-assisted circulation

What occurred during a cardiac cycle in the ascending aorta of the MCL during non-assisted circulation is illustrated in Figure 5-127. During systole, i.e. LV sac contraction, once the left ventricular pressure (LVP) exceeds the aortic pressure, the heart valve opens. As time passes, LVP decreases and once the aortic pressure exceeds LVP, the valve closes (i.e. diastole starts). A small volume of downstream fluid flows back into the aortic root area, which closes the valve; the small volume of retrograde flow which continues during diastole comprises coronary perfusion and leakage flow through the (mechanical) heart valve.
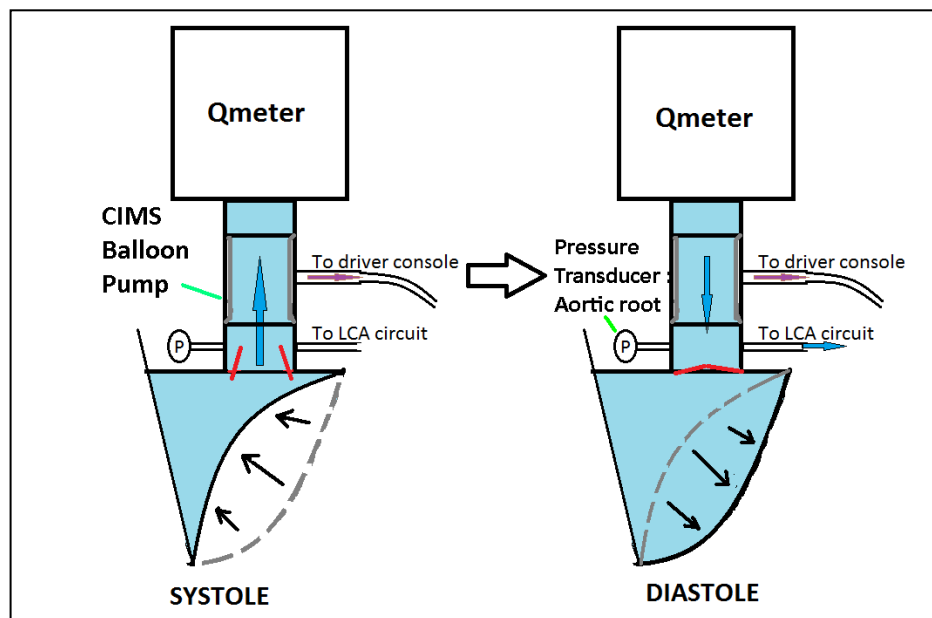
Figure 5-127: Flow in the ascending aorta of the MCL in systole and diastole in non-assisted circulation. There is a pressure transducer for aortic root pressure measurement and a flow meter (Qmeter) just distal of the CIMS balloon which is not activated in non-assisted flow.

The valve closing can also be traced using pressure difference between LVP and aortic root pressure (AoRootP), defined as *ΔProot* as defined in Eq. 5.1. Pressure difference between LVP and aortic pressure (AoP) is defined as *ΔPaorta*, and expressed in Eq. 5.2.

$$\Delta Proot = LVP - AoRootP \qquad\qquad 5.1$$

$$\Delta Paorta = LVP - AoP \qquad\qquad 5.2$$

The aortic root pressure (AoRootP) was measured distal to the aortic heart valve (refer to Figure 5-127). An example of LVP, AoRootP, AoP, pulsatile flowrate (Qpuls), *ΔPaorta,* and *ΔProot* is illustrated in Figure 5-128. Those waveforms were constructed from the average of 30 samples to eliminate beat-to-beat variability.
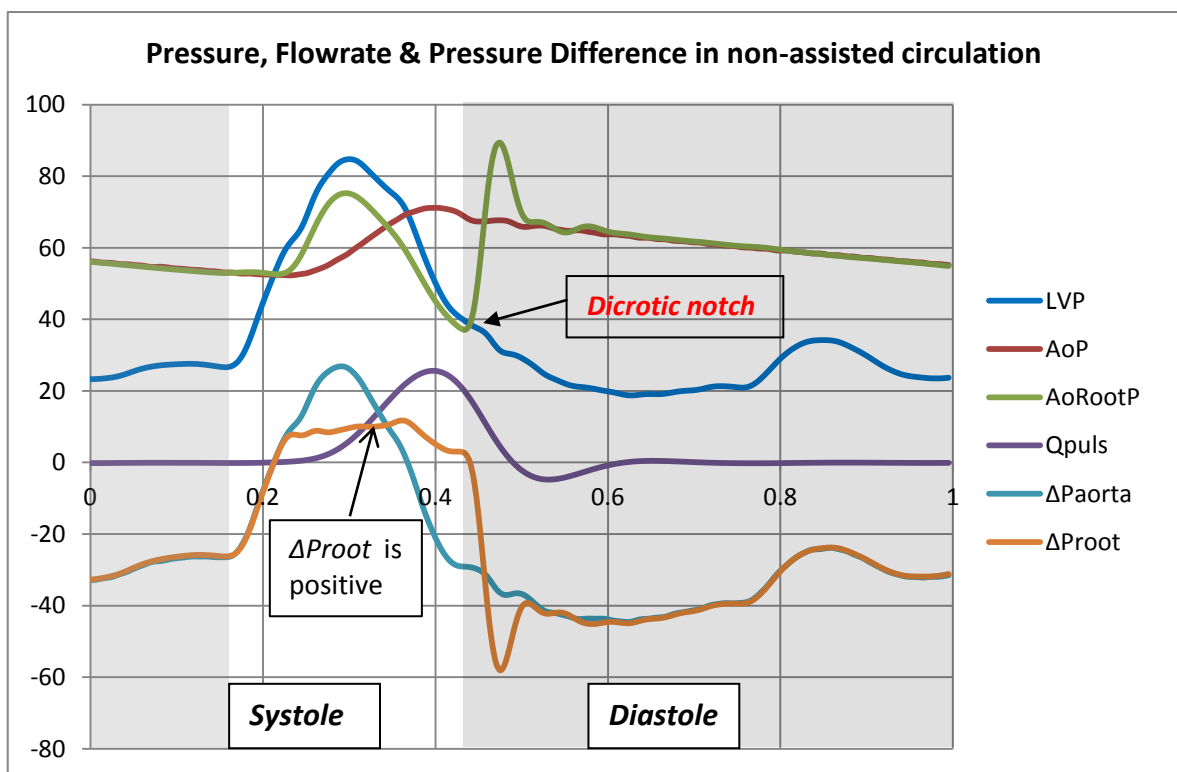
Figure 5-128: Left ventricular pressure (LVP), aortic pressure (AoP), aortic root pressure (AoRootP), pressure difference across the aortic heart valve (*ΔProot*), pressure difference between LVP and AoP (*ΔPaorta*), and aortic flowrate (Qpuls). Systole is defined as the LV sac contraction duration. Diastole starts when aortic valve closes, indicated by the dicrotic notch. Gray shaded area indicates diastole period.

The positive pressure difference across the heart valve at the aortic root, *ΔProot*, caused flow from the LV sac in to the aorta of the MCL; once *ΔProot* exceeds zero, aortic flow starts. The aortic flow continues to peak and decreases during *ΔProot* is positive, indicated in Figure 5-128. Once the zero threshold is crossed, the aortic valve closes, which can be seen from the sudden aortic pressure increase, known as the dicrotic notch. The dicrotic notch exhibited by AoRootP differs to

the one by AoP; this is due to the lack of local compliance at the aortic root. The sudden increase of AoRootP after the dicrotic notch is due to mechanical 'ringing' unique to mechanical heart valves. The aortic flow also decreases due to loss of momentum after the dicrotic notch but still has forward flow; the aortic flow then changes direction becoming negative flow (backward) before stopping (although leakage flow due to mechanical heart valve still occurs (but is very small)).

5.2.2   Assisted circulation

Inflation of CIMS balloon pump causes two distinct effects on the regions proximal and to the CIMS balloon pump as illustrated in Figure 5-129 (at early diastole). For the distal region, fluid is pushed downstream (forward flow), while the aortic root region receives backward flow. On deflation, pressure within the lumen of the CIMS device is lower than in the proximal and distal regions. The pressure differences cause forward flow (from the aortic root), and backward flow (through the aortic flow sensor). The effect of balloon activation is illustrated in Figure 5-130.
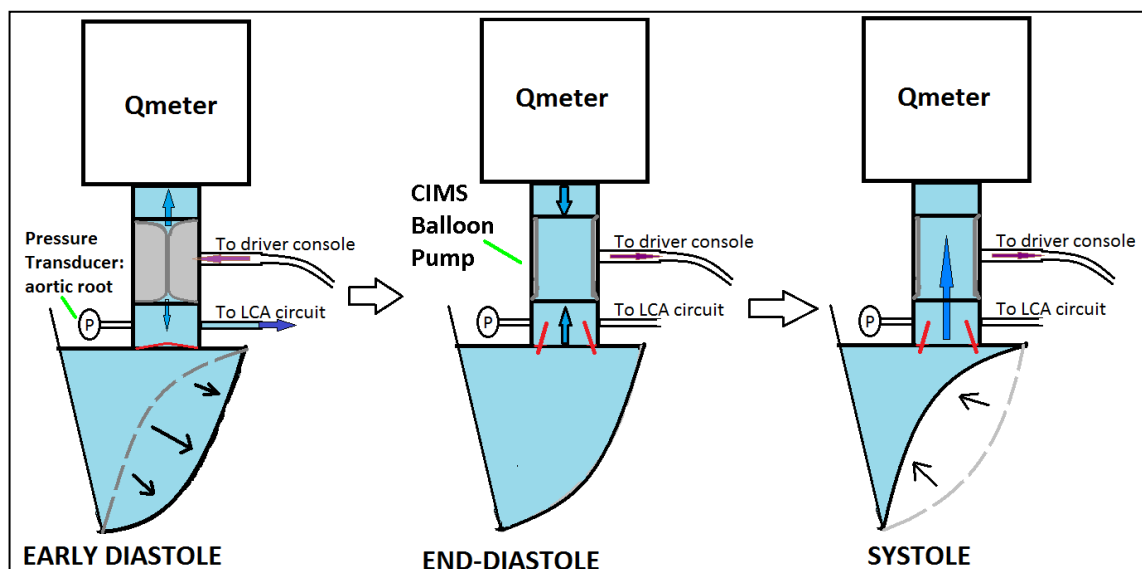
Figure 5-129: Balloon pump inflation in early diastole caused increased aortic root pressure and LCA perfusion at the aortic root, while distal to the CIMS balloon pump, aortic pressure increased and fluid was pushed downstream. In end-diastole, due to balloon deflation, pressure within the CIMS balloon pump decreased, thus inducing forward and backward flow.
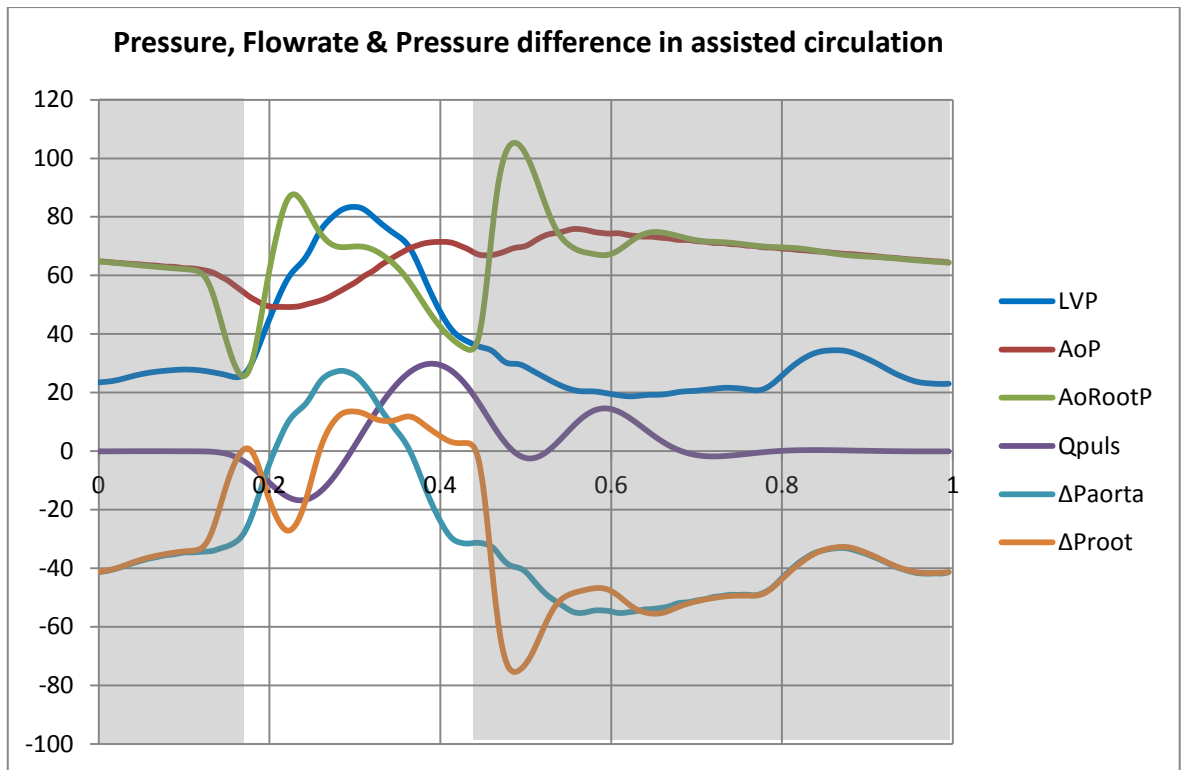
Figure 5-130: Pressures, pressure differences, and aortic flowrate of assisted circulation. AoP and AoRootP decreased prior to LV sac contraction.

Further discussion on the effect of the CIMS balloon pump activation on aortic root region is presented below in 5.2.3.

5.2.2.1 Aortic Root Region – Proximal to the CIMS Balloon Pump

It has been shown in a previous subchapter (5.1 Flow Visualisation) that the CIMS balloon pump deflation caused earlier valve opening. The sudden deflation causes decreased pressure distal to the aortic heart valve, and proximal to CIMS balloon pump in the ascending aorta of the MCL i.e. in the aortic root. Figure 5-131 illustrates pressure waveforms affected by balloon deflation.
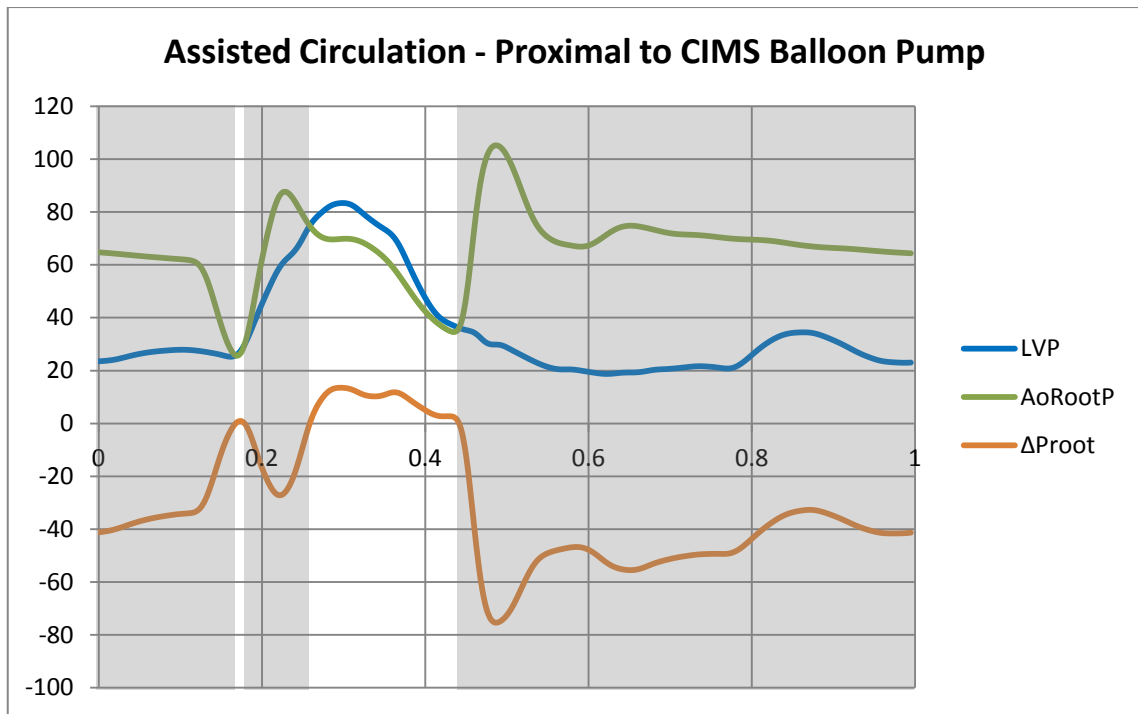
Figure 5-131: The LVP, aortic root pressure, and *ΔProot* in assisted circulation. Grey areas indicate region where *ΔProot* is less than zero.

Figure 5-131 illustrates waveforms of LVP, AoRootP and *ΔProot* in assisted circulation. The aortic flowrate waveform is not included; the reasons are:

1) in early-diastole, since the CIMS balloon pump occludes the ascending aortic part of MCL; aortic flowrate measured distal of the CIMS balloon pump is not representative of actual occurrence at the aortic root region,

2) in end-diastole, the effect of balloon deflation causes a negative pressure region at the CIMS balloon pump. As illustrated in Figure 5-129, backward flow that occurred might be bidirectional i.e. towards the CIMS balloon pump from the aortic root and region distal to the CIMS balloon pump.

The deflation prior to systole increases *ΔProot* until *ΔProot* rises slightly over the zero baseline, before *ΔProot* decreases drastically due to AoRootP sudden increase. The AoRootP increases rapidly after the pre-systole decrease, with values greater than LVP, until it reaches a peak. Consequently, the *ΔProot* increases exceeding zero. The difference between *ΔProot* of non-assisted and assisted circulation is illustrated in Figure 5-132.
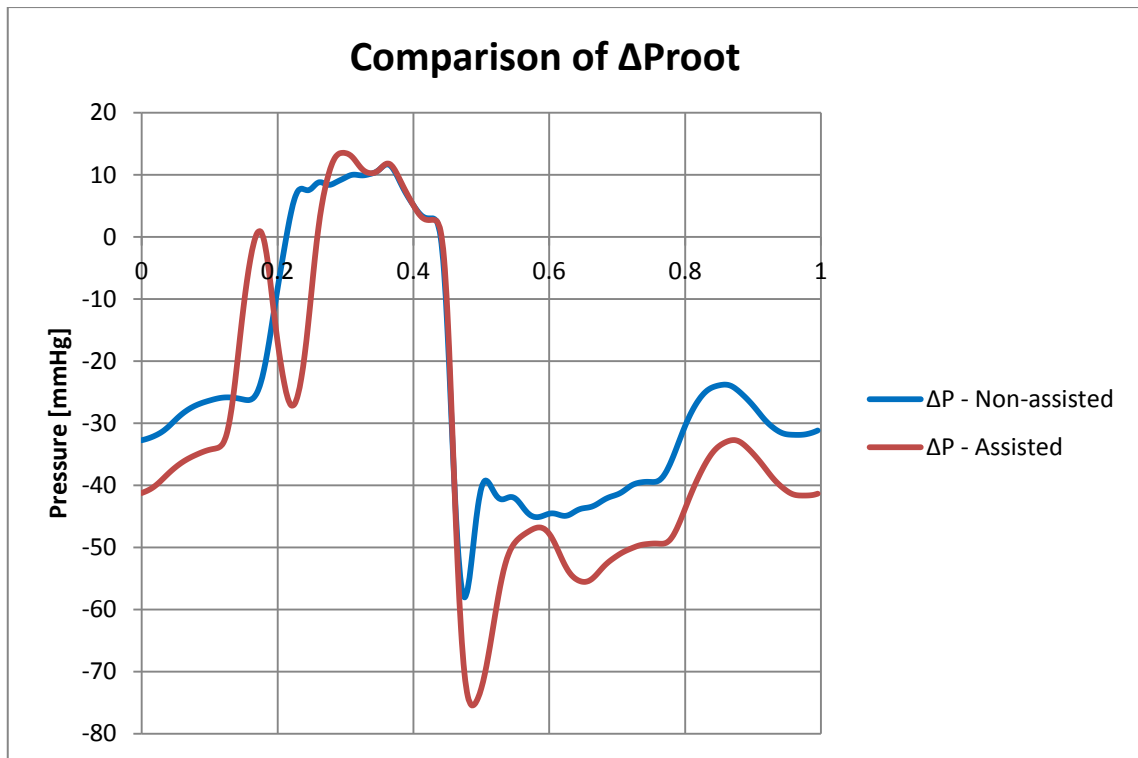
Figure 5-132: The *ΔProot* of non-assisted and assisted circulation for combination (B-I). Assisted circulation has greater magnitudes when *ΔProot* is less than zero.

The effect of balloon inflation in diastole was shown to increase *ΔProot* compared to non-assisted circulation. The effect of different balloon deflation at end-diastole is presented below.

5.2.3 Different Balloon Deflation Timing

The effect of the CIMS balloon deflation prior to systole has been shown to cause earlier valve opening. The effect of different balloon deflation timing on *ΔProot* is presented here.

Three sets of data with different balloon deflation timings (B-G, B-I, & B-J) were analysed for non-assisted and assisted circulation. Combination B-G means that the CIMS balloon was set for early deflation, B-I was set at optimum (just after valve was opened), and B-J was a late deflation. Fixed experimental factors were high arterial compliance (C2.5), 25 mL of Helium Gas, and SB type balloon pump. The results of non-assisted and assisted circulation are illustrated in Figure 5-133 and Figure 5-134 respectively. The data have been synchronised to eliminate time lag between waveforms.
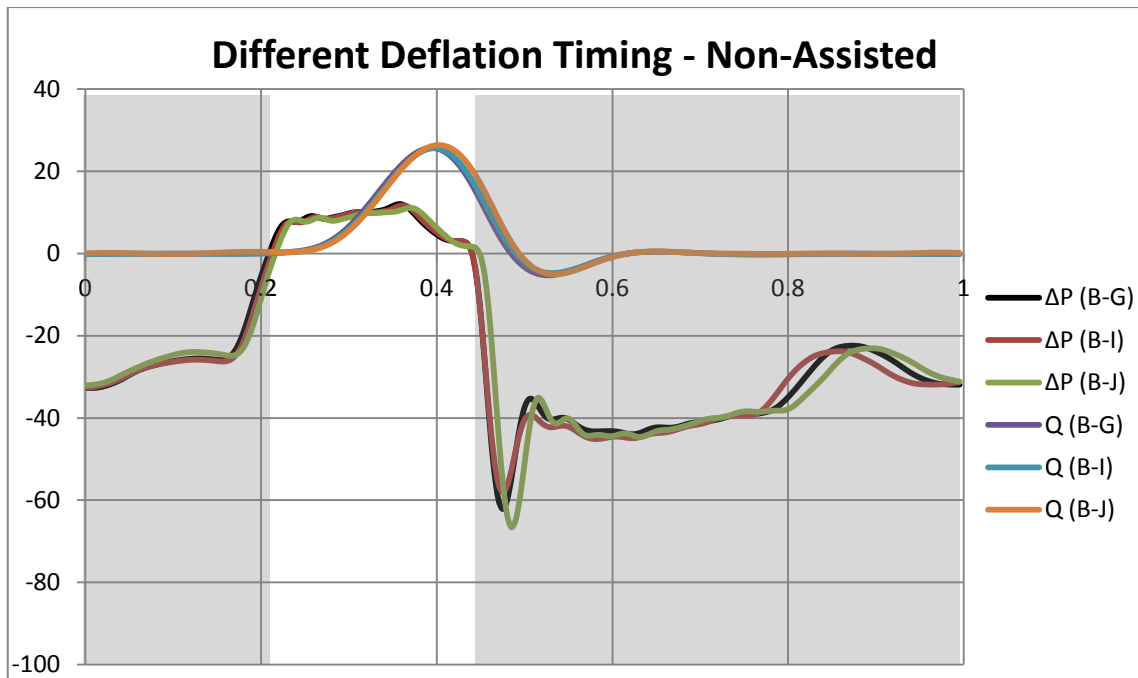
Figure 5-133: Flowrates and *ΔProot* for varying deflation timing in non-assisted circulation

No prominent difference can be detected from aortic flowrate and *ΔProot* waveforms illustrated in Figure 5-133. Once *ΔProot* exceeds zero, aortic flow starts, and when *ΔProot* become less than zero, valve closes and aortic flow starts to decline before stopping in diastole. The time *ΔProot* becomes greater than zero is also similar at around 0.21 seconds.
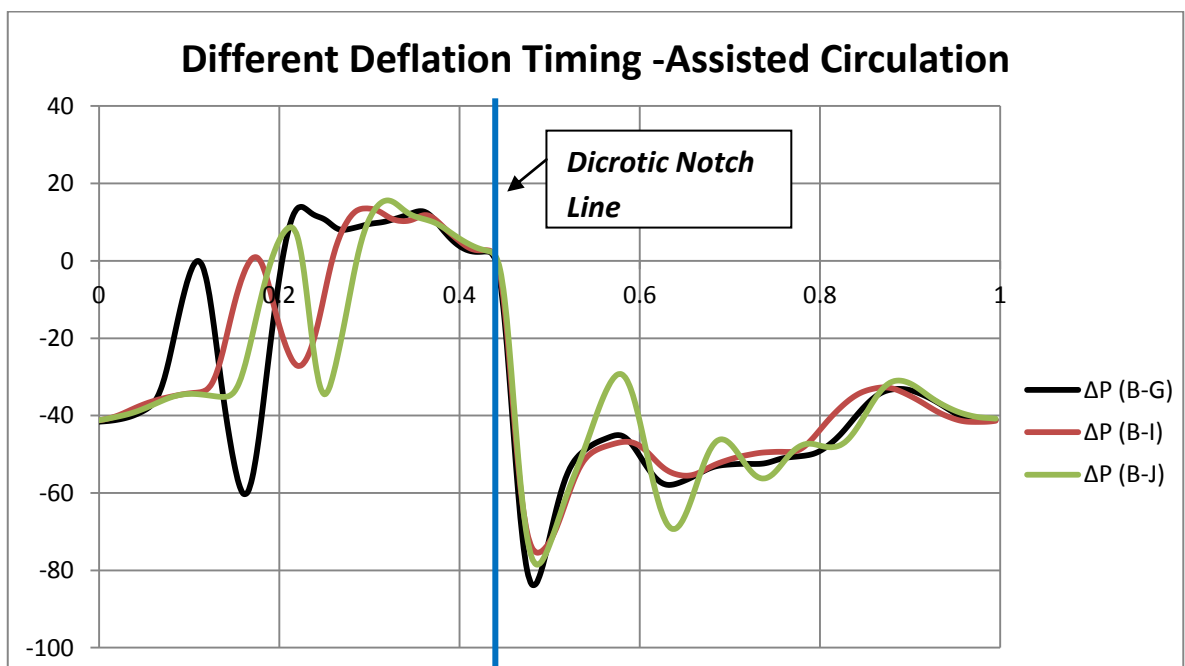
Figure 5-134: Pressure difference across the aortic heart valve, *ΔProot*, for varying deflation timing in non-assisted circulation

However, the effect of varying deflation timing can be seen clearly in Figure 5-134. Earlier deflation (B-G) is the first waveform; it exhibits a peak before decreasing drastically. The next waveform is B-I, followed by the B-J waveform. Compared with the other two waveforms, the peak of B-J waveforms exceeded zero (around 8 mmHg). In diastole (period after dicrotic notch), ΔP (B-J) waveform exhibits slightly different shape compared to the other two.

Combination B-G reaches its initial peak around 0.11 seconds, followed by B-I at 0.17 seconds, and finally B-J, at 0.19 seconds, crosses zero baseline before reaching the peak at 0.21 seconds. The pressure difference, *ΔProot,* becomes negative at a similar time in the cardiac cycle.

The rapid decrease past first peak for *ΔProot* is prominent especially by combination B-G. The other two combinations are not as severe as B-G waveform. This difference was contributed by higher AoRootP, compared to LVP, when valve was opened too early; possibly due to mechanical valve bounce.

What these observations suggested is that valve opening occurred earlier due to balloon pump deflation. The effect of earlier deflation shows *ΔProot* reaches a peak, although the rapid decrease might point to a conjecture that the heart valve was opened and closed in a rapid succession. However, the result from flow visualisation experiment did not support that conjecture. Earlier *ΔProot* peak means earlier valve opening, and remains open until the end of systole. The valve opening time was shown to be longer due to the CIMS balloon pump deflation (combination B-I). Thus, valve opening time of combination B-G would be longer than B-I, while combination B-J would be shorter and possibly no difference compared to non-assisted circulation. More is discussed in subchapter 5.4.

5.3 Net Flow Volume

At the ascending aorta of the MCL, the decreased pressure due to balloon deflation affected aortic fluid flow by causing backward flow prior to systole as illustrated in Figure 5-135. The effect of diastolic augmentation that pushes fluid downstream (forward flow) is negated by the backward flow prior to systole.
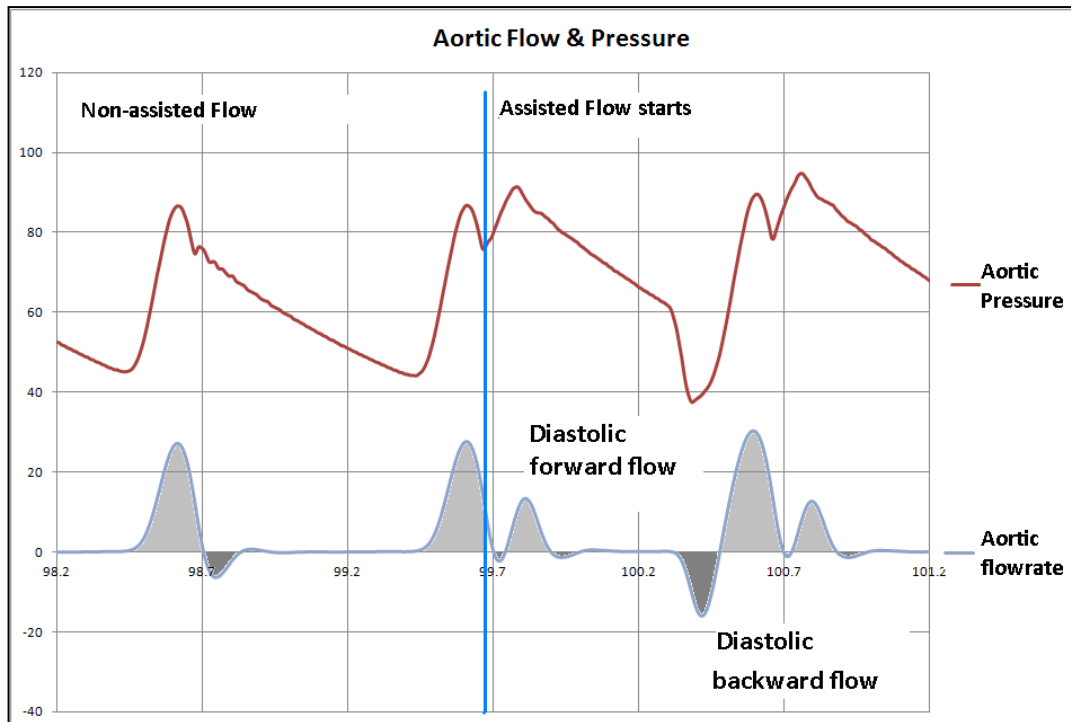
Figure 5-135: The effect of balloon inflation caused positive spike at aortic flow (forward flow- light grey shade), while balloon pump deflation caused negative spike (backward flow- dark grey shade)

The hypothesis was that the increase in cardiac output is essentially the net amount of fluid pushed downstream in diastole. As illustrated in Figure 5-135, in non-assisted circulation, backward flow (dark grey shaded area) in early-diastole is the sum of mechanical heart valve leakage flow, heart valve closing flow, and coronary artery flow. On the contrary, in assisted circulation, the amount of backward flow in early-diastole is lesser; however, the backward flow area at end-diastole prior to LV contraction increases, due to balloon pump deflation. Due to decreased flow resistance at the aortic root, forward flow area in assisted circulation is also fractionally greater compared to non-assisted circulation.

Data from one experiment[45] was used to verify the validity of the hypothesis. The fluid volume of forward and backward flow of 30 samples (non-assisted & assisted) was calculated by computing the integral of shaded areas; the results are tabulated in Table 5-106. Any data point greater than zero is considered forward flow, while data points less than zero are considered backward flow.

---

[45] The mock loop was set to HF condition, arterial compliance set at high (C2.5), mechanical heart valve, optimum timing (B-I combination), optimum Helium gas volume (25 mL), and SB type balloon pump.

Table 5-106: Statistical results of non-assist and assisted circulation. CO: Cardiac Output. *: Kolmogorov-Smirnov test; **: Levene's test.

Aortic Flow	Stat.	Forward aortic flow (L/min)	Forward Volume (mL/beats)	Backward aortic Flow (L/min)	Backward Volume (mL/beats)	Net Forward Volume (mL/beats)	CO (L/min)
Non-assist	Average	3.50	58.34	-0.46	-7.60	50.74	3.04
	SD	0.18	3.07	0.04	0.60	2.99	0.18
	SE	0.02	0.39	0.00	0.08	0.38	0.02
Assist	Average	4.85	80.81	-1.63	-27.22	53.60	3.22
	SD	0.12	1.98	0.10	1.61	2.45	0.15
	SE	0.01	0.25	0.01	0.20	0.31	0.02
Statistical Analysis	Percentage difference	38.5	38.5	258.1	258.1	5.6	5.6
	Normality assumption *	$p > 0.05$	$p > 0.05$	$p > 0.05$	$p > 0.05$	$p > 0.05$	$p > 0.05$
	Equality of variance**	0.08	0.08	0.01	0.01	0.125	0.125
	Student t-test	$p < 0.001$	$p < 0.001$	$p < 0.001$	$p < 0.001$	$p < 0.001$	$p < 0.001$

The data distribution adhered to normality assumption ($p > 0.05$), thus Student t-test was employed. Although some variables exhibited non-homogenous variance, Student t-test can accommodate some deviation of variance.

Both forward and backward fluid volume showed a significant increase ($p < 0.001$) after balloon inflation. The positive flow SV was increased by 22.47 mL; however, due to balloon deflation, the backward flowrate SV also increased by 19.6 mL. The net fluid volume (forward – backward) per beat was 2.86 mL (22.47 – 19.6 mL), this is reflected in the increasing cardiac output (CO) of assisted circulation significantly by almost 6% ($p < 0.001$).

5.4   Discussion

It was hypothesised that sudden deflation prior to LV contraction caused early valve opening (as observation had suggested). Flow visualisation and pressure/flow experiments were conducted to verify that hypothesis.

Flow visualization experiments were conducted to determine whether the valve leaflet opened longer when CIMS balloon pump was activated. The statistical analysis reported that the valve leaflet opening time increased significantly between assisted and non-assisted circulation. Thus, balloon pump deflation prior to valve leaflet opening is suggested to cause early valve opening.

The pressure difference across the aortic heart valve, $\Delta Proot$, indicates which direction fluid flows. Positive $\Delta Proot$ means that left ventricular pressure (LVP) is greater than aortic root pressure (AoRootP), thus initiating forward flow into the ascending aorta. Negative $\Delta Proot$ means that AoRootP is greater than LVP; this causes the aortic heart valve to close. In non-assisted circulation, the aortic valve opens when $\Delta Proot$ is greater than zero due to LV sac contraction. However, in assisted circulation, with the CIMS balloon pump activation, sudden deflation prior to systole caused aortic root pressure to decrease, rendering a positive pressure gradient; which opens the aortic valve early.

The effect of different deflation timing on $\Delta Proot$ was analysed. It was shown that earlier balloon deflation caused $\Delta Proot$ to become greater than zero momentarily at an earlier time in the cardiac cycle compared to non-assisted circulation. This finding corroborated the outcome of flow visualisation experiment; that the aortic valve opens earlier in assisted circulation due to the CIMS balloon pump deflation.

After the initial positive peak, $\Delta Proot$ decreased rapidly due to increased aortic root pressure, which was greater than LVP. It was not until a few milliseconds later that $\Delta Proot$ again exceeded zero, when LVP became greater than AoRootP, as LV sac contraction occurred. From the flow visualisation experiment, it was shown that the aortic valve opens continuously from the initial $\Delta Proot$ peak. However, since there was a 0.033 seconds variance between images, it is probable that the negative $\Delta Proot$ period after the first positive peak causing the aortic valve to open might not have been captured. A high-speed video recorder with at least 1000 fps (0.001 seconds interval between images) might be able to capture the valve opening and closing sequence more accurately.

The diastolic augmentation on systemic circulation of MCL increased forward flow, while balloon deflation prior to systole drew fluid into the balloon pump region. In this exercise, the net stroke volume increased CO by 5.9 %. One intriguing finding of this study was the amount of backward flow volume ($\approx$27 mL), which was greater than the amount of balloon pump displacement ($\approx$25 mL). However, since positive stroke volume in assisted circulation was 81 mL (non-assist: 58 mL), the net volume was greater than zero, thus contributed to increased cardiac output percentage.

Several *in vivo* studies report the effect of counterpulsation on aortic flow. An *in vivo* study reported qualitatively the backward flow when an EABP was implanted in pigs (Davies et al., 2005). Another study comparing the effect of counterpulsation at various places in the aorta also reported that backward flow towards coronary arteries occurred when an IABP and several types of end-to-side anastomosis type balloon pumps were activated, but again, only qualitative results (Furman et al., 1970). The implantation of an extra-aortic counterpulsation device (EACD) on the ascending aorta of a sheep showed that deflation of EACD prior to systole induced sudden retrograde flow although the retrograde flow was " eliminated as LV ejection begins" (Zelano et al., 1992).

The sudden reduction of the aortic end-diastolic pressure was attributed as the reason LV work decreased as indicated by TTI reduction (Zelano et al., 1992), however, none of the above studies quantify the effect of balloon deflation on valve leaflet opening. This study further suggested that balloon deflation distal to aortic heart valve will not only decrease aortic end-diastolic pressure, but also induce earlier valve opening.

5.5   Conclusion

The flow visualisation experiment, and further analysis on the pressure difference across the aortic valve have shown that the CIMS balloon deflation induced earlier valve opening. The CIMS balloon deflation at end-diastolic period not only caused earlier valve opening, it also reduced aortic end-diastolic pressure, thus decreasing flow resistance in systole. The pressure difference across the aortic valve, *ΔProot,* momentarily exceeded zero baseline in diastole from sudden aortic root pressure reduction due to the CIMS balloon pump deflation. That caused earlier valve opening.

The cardiac output increase in assisted circulation was due to net forward flowrate and backward flowrate. The net forward volume per beat was small (≈ 6 %), yet still statistically significant.

Chapter 6   Conclusion and Future Works

The conclusion and suggested future work from this study is presented.

6.1   Conclusion

In the current market there is an opportunity for cheap, affordable chronic cardiac assist devices. The CIMS device was conceptualised to fill in that gap, and this study was conceived to test the effectiveness of that concept. A pressure/flow factorial experiments and flow visualisation experiments were carried out. Statistical analysis was performed and the results are presented in Chapter 4 and Chapter 5; from those results, several conclusions can be drawn.

The CIMS balloon pump activation augmented peripheral and left coronary circulation, as well as reduction of the aortic end-diastolic pressure. The systolic aortic pressure changes were small across all experiments, so it was hypothesised that the small difference may not be clinically detrimental. The changes brought by counterpulsation technique depended on several factors, but the most prominent ones was the effect of arterial compliance. In low arterial compliance setting, for example, cardiac output was augmented by 15%, while left coronary artery mean flowrate was increased by 19%; but when the effect of device innate compliance is added, then CO increased to 20% while QcorMean increased to 21% (with CB type balloon pump). Clearly, other experimental factor also significantly affects the output.

Resistance to left ventricular flow output is measured by reduction of aortic end-diastolic pressure (AoEDP), caused by balloon deflation prior to LV systole. The greatest mean reduction (≈ -9%) was also when arterial compliance factor was coupled with balloon innate compliance factor. The reduction of myocardial work due to decreased AoEDP cannot be quantified, since the MCL was not equipped with a suitable measurement device. For example, the C-Pulse LVAD managed to reduce LV wall stress to -31%, indicating reduced afterload, although AoEDP reduction was a mere -3% (Legget et al., 2005), thus the implanted CIMS balloon pump would probably achieve the same level, if not better afterload reduction, consequently less myocardial work.

The measure of increased myocardial perfusion can be expressed using endocardial viability ratio (EVR). Activation of the CIMS balloon pump increased the EVR value between 33% and 74% (depending on experimental factor combination), indicating that myocardial perfusion would improve favourably with the CIMS balloon pump. The systolic unloading decreased by just 1% to

2%, while the diastolic augmentation increased by 29%. The myocardial function improvement clearly can be achieved by the CIMS balloon pump.

The effect of balloon pump deflation just before systole caused sudden pressure reduction; and since the CIMS balloon pump is placed just after the aortic heart valve, earlier valve opening occurred as shown in Chapter 5. A flow visualisation experiment and factorial experiments were conducted to detect any effect from balloon pump deflation on the aortic heart valve. The prolonged opening time due to the CIMS balloon pump activation was confirmed statistically ($p < 0.001$) from flow visualisation experiment. Also, from analysis of $\Delta Proot$, the pressure difference across the aortic heart valve, it was shown that $\Delta Proot$ momentarily exceeded zero baseline prior to systole, thus validating the hypothesis of early valve opening.

6.2   Suggested Future Works

The CIMS balloon pump has demonstrated flow and pressure augmentation under various experimental factors. In terms of myocardium workload, an inference of possible workload decrease was suggested by the aortic end-diastolic pressure reduction, since the MCL was not equipped with suitable instrument and hardware to determine changes in myocardium workload. Future modifications on MCL is suggested to incorporate appropriate hardware and/or suitable algorithm e.g. the time-varying elastance model (Suga and Sagawa, 1974), or the one-fiber heart model (Arts et al., 1991, Cox et al., 2009).

A comparison between the CIMS balloon pump and the IABP is definitely a good direction for future works. Some modifications naturally have to be carried out to allow IABP placement in the MCL. Possible research question would be the effect of balloon pump on the aortic heart valve, and the influence on flow haemodynamics. Factorial design experiment comparing between types of mechanical heart assist device (CIMS vs. IABP), CIMS balloon device design (SB & CB), and arterial compliance (high and low) could yield interesting results.

The question of how exactly did the CIMS balloon pump augmentation affect aortic, coronary artery flowrate and intravascular pressure could be answered by using the Wave Intensity Analysis (WIA) technique. Several studies could be used as a reference (Feng and Khir, 2007, Biglino et al., 2008, Kolyva et al., 2009).

The effect of balloon inflation and deflation on the aortic heart valve haemodynamics would be an interesting study; since it was shown that $\Delta Proot$ due to balloon inflation has increased in diastole.

Another important future work is the exact reason for the observed higher efficacy of the CB type balloon pump when compared to the SB type balloon pump. By separating the effect of various confounding factors as discussed in section 4.7, using factorial experiment method, the prominent factor contributing difference in performance could be determined.

The next step forward for the CIMS balloon pump is its development into an *implantable prototype*. Further work must be carried out to achieve biomaterial status on the balloon pump and the percutaneous driveline; after which a clinical *in vivo* animal study may be conducted, before progressing further to human patient as per regulations laid out by relevant authority (e.g. the Food and Drug Administration (FDA) in the USA; while in the Europe, CE mark for approved biomedical devices is awarded under Medical Device Directives by the European Commission (EC)).

References

(WHO), W. H. O. 1977. *Manual of the international statistical classification of diseases, injuries, and causes of death, Volume 1,* Geneva, World Health Organization.

ADAMS, K. F. & ZANNAD, F. 1998. Clinical definition and epidemiology of advanced heart failure. *American heart journal,* 135**,** S204-15.

AKUTSU, T. & KOLFF, W. J. 1958. Permanent Substitutes for Valves and Hearts. *ASAIO Journal,* 4.

AKYUREKLI, Y., TAICHMAN, G. C. & KEON, W. J. 1980. Effectiveness of intra-aortic balloon counterpulsation on systolic unloading. *Canadian journal of surgery. Journal canadien de chirurgie,* 23**,** 122-6.

ARTS, T., BOVENDEERD, P. H., PRINZEN, F. W. & RENEMAN, R. S. 1991. Relation between left ventricular cavity pressure and volume and systolic fiber stress and strain in the wall. *Biophysical Journal,* 59**,** 93-102.

ASIMAKOPOULOS, G., EDWARDS, M.-B. & TAYLOR, K. M. 1997. Aortic Valve Replacement in Patients 80 Years of Age and Older : Survival and Cause of Death Based on 1100 Cases: Collective Results From the UK Heart Valve Registry. *Circulation,* 96**,** 3403-3408.

ASSOCIATION, C. C. N. Y. H. 1964. Diseases of the heart and blood vessels. Nomenclature and criteria for diagnosis. 6 ed. Boston: Little, Brown and Co.

BARNARD, C. N. 1967. The operation. A human cardiac transplant: an interim report of a successful operation performed at Groote Schuur Hospital, Cape Town. *South African medical journal = Suid-Afrikaanse tydskrif vir geneeskunde,* 41**,** 1271-4.

BASKETT, R. J. F., GHALI, W. A., MAITLAND, A. & HIRSCH, G. M. 2002. The intraaortic balloon pump in cardiac surgery. *The Annals of Thoracic Surgery,* 74**,** 1276-1287.

BASKETT, R. J. F., O'CONNOR, G. T., HIRSCH, G. M., GHALI, W. A., SABADOSA, K. A., MORTON, J. R., ROSS, C. S., HERNANDEZ, F., NUGENT, W. C., LAHEY, S. J., SISTO, D., DACEY, L. J., KLEMPERER, J. D., HELM, R. E. & MAITLAND, A. 2005. The preoperative intraaortic balloon pump in coronary bypass surgery: A lack of evidence of effectiveness. *American Heart Journal,* 150**,** 1122-1127.

BERNE, R. M., LEVY, M. N., KOEPPEN, B. M. & STANTON, B. A. 2004. *Physiology,* St. Louis, Missouri, Mosby.

BIGLINO, G., WHITEHORNE, M., PEPPER, J. R. & KHIR, A. W. 2008. Pressure and flow-volume distribution associated with intra-aortic balloon inflation: an in vitro study. *Artificial organs,* 32**,** 19-27.

BIRKS, E. J., GEORGE, R. S., HEDGER, M., BAHRAMI, T., WILTON, P., BOWLES, C. T., WEBB, C., BOUGARD, R., AMRANI, M., YACOUB, M. H., DREYFUS, G. & KHAGHANI, A. 2011. Reversal of Severe Heart Failure With a Continuous-Flow Left Ventricular Assist Device and Pharmacological Therapy / Clinical Perspective. *Circulation,* 123**,** 381-390.

BIRKS, E. J., TANSLEY, P. D., HARDY, J., GEORGE, R. S., BOWLES, C. T., BURKE, M., BANNER, N. R., KHAGHANI, A. & YACOUB, M. H. 2006. Left ventricular assist device and drug therapy for the reversal of heart failure. *The New England journal of medicine,* 355**,** 1873-84.

BONOW, R. O., MANN, D. L., BRAUNWALD, E., ZIPES, D. P. & LIBBY, P. 2011. *Braunwald's Heart Disease: A Textbook of Cardiovascular Medicine*, Saunders/Elsevier.

BROWER, G. L., GARDNER, J. D., FORMAN, M. F., MURRAY, D. B., VOLOSHENYUK, T., LEVICK, S. P. & JANICKI, J. S. 2006. The relationship between myocardial extracellular matrix remodeling and ventricular function. *European journal of cardio-thoracic surgery : official journal of the European Association for Cardio-thoracic Surgery,* 30**,** 604-10.

BURTON, A. C. 1972. *Physiology and Biophysics of the Circulation,* Chicago, Year Book Medical Publishers.

BURTON, C. 1954. Relation of Structure of the Wall. *Physiological Review,* 34**,** 619-642.

CARDIOLOGY, T. T. F. O. H. F. O. T. E. S. O. 1995. Guidelines for the diagnosis of heart failure. *Heart Failure.*

CARREL, A. & LINDBERGH, C. A. 1935. The Culture of Whole Organs. *Science,* 81**,** 621-623.

CASSOT, F., MORVAN, D., ISSARTIER, P. & PELISSIER, R. 1985. New versatile physical model fitting the systemic circulation accurately. *Medical & Biological Engineering & Computing,* 23**,** 511-516.

CHARITOS, C. E., NANAS, J. N., KONTOYIANNIS, D. A., NANAS, S. N., STAMATOPOULOS, G. Z., RAPTI, A. C., STAMATELOPOULOS, S. F. & MOULOPOULOS, S. D. 1998. The efficacy of the high volume counterpulsation technique at very low levels of aortic pressure. *J Cardiovasc Surg (Torino),* 39**,** 625-632.

CHEUNG, A. T., SAVINO, J. S. & WEISS, S. J. 1996. Beat-to-beat augmentation of left ventricular function by intraaortic counterpulsation. *Anesthesiology,* 84**,** 545-554.

CLAUSS, R. H., BIRTWELL, W. C., ALBERTAL, G., LUNZER, S., TAYLOR, W. J., FOSBERG, A. M. & HARKEN, D. E. 1961. Assisted circulation. I. The arterial counterpulsator. *The Journal of thoracic and cardiovascular surgery,* 41**,** 447-58.

CMOLIK, B. L., THOMPSON, D. R., SHERWOOD, J. T., GEHA, A. S. & GEORGE, D. T. 2001. Increased coronary artery blood flow with aortomyoplasty in chronic heart failure. *Ann Thorac Surg,* 71**,** 284-289.

COCKCROFT, J. R., WILKINSON, I. A. N. B. & WEBB, D. J. 1997. Age , arterial stiffness and the endothelium. *Pharmacology,* 26-S4**,** 53-60.

CODD, M. B., SUGRUE, D. D., GERSH, B. J. & MELTON, L. J. 1989. Epidemiology of idiopathic dilated and hypertrophic cardiomyopathy. A population-based study in Olmsted County, Minnesota, 1975-1984. *Circulation,* 80**,** 564-72.

COHEN, M., URBAN, P., CHRISTENSON, J. T., JOSEPH, D. L., FREEDMAN, R. J., MILLER, M. F., OHMAN, E. M., REDDY, R. C., STONE, G. W. & FERGUSON, J. J. 2003. Intra-aortic balloon counterpulsation in US and non-US centres: results of the Benchmark® Registry. *European heart journal,* 24**,** 1763-1770.

COPELAND, J. G., SMITH, R. G., ARABIA, F. A., NOLAN, P. E., SETHI, G. K., TSAU, P. H., MCCLELLAN, D. & SLEPIAN, M. J. 2004. Cardiac Replacement with a Total Artificial Heart as a Bridge to Transplantation. *New England Journal of Medicine,* 351**,** 859-867.

CORNHILL, J. F. 1977. An aortic-left ventricular pulse duplicator used in testing prosthetic aortic heart valves. *The Journal of thoracic and cardiovascular surgery,* 73**,** 550-8.

COWIE, M. R. 2000. Survival of patients with a new diagnosis of heart failure: a population based study. *Heart,* 83**,** 505-510.

COX, L. G. E., LOERAKKER, S., RUTTEN, M. C. M., DE MOL, B. A. J. M. & VAN DE VOSSE, F. N. 2009. A Mathematical Model to Evaluate Control Strategies for Mechanical Circulatory Support. *Artificial Organs,* 33**,** 593-603.

CURTIS, S. L., ZAMBANINI, A., MAYET, J., MCG THOM, S. A., FOALE, R., PARKER, K. H. & HUGHES, A. D. 2007. Reduced systolic wave generation and increased peripheral wave reflection in chronic heart failure. *American Journal of Physiology - Heart and Circulatory Physiology,* 293**,** H557-H562.

DANDEL, M., WENG, Y., SINIAWSKI, H., POTAPOV, E., DREWS, T., LEHMKUHL, H. B., KNOSALLA, C. & HETZER, R. 2008. Prediction of cardiac stability after weaning from left ventricular assist devices in patients with idiopathic dilated cardiomyopathy. *Circulation,* 118**,** S94-105.

DANDEL, M., WENG, Y., SINIAWSKI, H., POTAPOV, E., LEHMKUHL, H. B. & HETZER, R. 2005. Long-term results in patients with idiopathic dilated cardiomyopathy after weaning from left ventricular assist devices. *Circulation,* 112**,** I37-45.

DAVIES, A. N., PETERS, W. S., SU, T., SULLIVAN, C. E., PERKIDIDES, T., MILSOM, F. P. & WHITE, G. 2005. Extra-ascending aortic versus intra-descending aortic balloon counterpulsation-effect on coronary artery blood flow. *Heart, Lung and Circulation,* 14**,** 178-86.

DAVIES, J. E., WHINNETT, Z. I., FRANCIS, D. P., MANISTY, C. H., AGUADO-SIERRA, J., WILLSON, K., FOALE, R. A., MALIK, I. S., HUGHES, A. D., PARKER, K. H. & OTHERS 2006. Evidence of a dominant backward-propagating" suction" wave responsible for diastolic coronary filling in humans, attenuated in left ventricular hypertrophy. *Circulation,* 113**,** 1768.

DAVILA, J. C., TROUT, R. G., SUNNER, J. E. & GLOVER, R. P. 1956. A simple mechanical pulse duplicator for cinematography of cardiac valves in action. *Annals of surgery,* 143**,** 544-51.

DEBAKEY, M. E. 1971. Left ventricular bypass pump for cardiac assistance: Clinical experience. *The American Journal of Cardiology,* 27**,** 3-11.

DEBAKEY, M. E. 2003. John Gibbon and the heart-lung machine: a personal encounter and his import for cardiovascular surgery. *The Annals of Thoracic Surgery,* 76**,** S2188-S2194.

DENOLIN, H., KUHN, H., KRAYENBUEHL, H. P., LOOGEN, F. & REALE, A. 1983. The definition of heart failure. *European heart journal,* 4**,** 445-8.

DIPLA, K., MATTIELLO, J. A., JEEVANANDAM, V., HOUSER, S. R. & MARGULIES, K. B. 1998. Myocyte recovery after mechanical circulatory support in humans with end-stage heart failure. *Circulation,* 97**,** 2316-22.

DONOVAN, F. M. 1975. Design of a hydraulic analog of the circulatory system for evaluating artificial hearts. *Biomaterials, medical devices, and artificial organs,* 3**,** 439-49.

DOWNEY, J. M. & KIRK, E. S. 1975. Inhibition of coronary blood flow by a vascular waterfall mechanism. *Circulation research,* 36**,** 753-60.

DU BOIS, D. & DU BOIS, E. F. 1916. CLINICAL CALORIMETRY: TENTH PAPER A FORMULA TO ESTIMATE THE APPROXIMATE SURFACE AREA IF HEIGHT AND WEIGHT BE KNOWN. *Archives of Internal Medicine,* XVII**,** 863-871.

DURAN, C. G., GUNNING, A. J. & MCMILLAN, T. 1964. A Simple Versatile Pulse Duplicator. *Thorax,* 19**,** 503-6.

DZAU, V. J. & SAFAR, M. E. 1988. Large conduit arteries in hypertension: role of the vascular renin-angiotensin system. *Circulation,* 77**,** 947-54.

ERIKSSON, H., SVÄRDSUDD, K., LARSSON, B., OHLSON, L. O., TIBBLIN, G., WELIN, L. & WILHELMSEN, L. 1989. Risk factors for heart failure in the general population: the study of men born in 1913. *European heart journal,* 10**,** 647-56.

FEDERMANN, M. & HESS, O. M. 1994. Differentiation between systolic and diastolic dysfunction. *European heart journal,* 15 Suppl D**,** 2-6.

FENG, J. & KHIR, A. Determination of wave intensity in flexible tubes using measured diameter and velocity. Engineering in Medicine and Biology Society, 2007. EMBS 2007. 29th Annual International Conference of the IEEE, 2007. IEEE, 985-988.

FERGUSON, J. J., COHEN, M., FREEDMAN, R. J., STONE, G. W., MILLER, M. F., JOSEPH, D. L. & OHMAN, E. M. 2001. The current practice of intra-aortic balloon counterpulsation: results from the Benchmark Registry. *Journal of the American College of Cardiology,* 38**,** 1456-62.

FERRARI, G., DE LAZZARI, C., KOZARSKI, M., CLEMENTE, F., GÓRCZYNSKA, K., MIMMO, R., MONNANNI, E., TOSTI, G. & GUARAGNO, M. 2002. A hybrid mock circulatory system: Testing a prototype under physiologic and pathological conditions. *ASAIO journal,* 48**,** 487.

FERRARI, G., DE LAZZARI, C., MIMMO, R., AMBROSI, D. & TOSTI, G. 1994. Mock circulatory system for in vitro reproduction of the left ventricle, the arterial tree and their interaction with a left ventricular assist device. *Journal of medical engineering & technology,* 18**,** 87-95.

FERRARI, G., KHIR, A. W., FRESIELLO, L., DI MOLFETTA, A. & KOZARSKI, M. 2011. Hybrid Model Analysis of Intra-Aortic Balloon Pump Performance as a Function of Ventricular and Circulatory Parameters. *Artificial Organs,* 35**,** 902-911.

FERRARI, G., KOZARSKI, M., DE LAZZARI, C., CLEMENTE, F., MEROLLI, M., TOSTI, G., GUARAGNO, M., MIMMO, R., AMBROSI, D. & GLAPINSKI, J. 2001. A hybrid (numerical-physical) model of the left ventricle. *The International journal of artificial organs,* 24**,** 456-62.

FERRARI, G., KOZARSKI, M., DE LAZZARI, C., GORCZYNSKA, K., TOSTI, G. & DAROWSKI, M. 2005a. Development of a hybrid (numerical-hydraulic) circulatory model: prototype testing and its response to IABP assistance. *The International journal of artificial organs,* 28**,** 750-9.

FERRARI, G., KOZARSKI, M., LAZZARI, C. D. E., DAROWSKI, M. & TOSTI, G. 2005b. Development of Hybrid (Numerical-Physical) Models of the Cardiovascular System : Numerical-Electrical and Numerical Hydraulic. *Biocybernatics and Biomedical Engineering,* 25**,** 3-15.

FIELD, A. P. 2009. *Discovering statistics using SPSS: (and sex and drugs and rock 'n' roll),* London, SAGE.

FRAZIER, O. H., BENEDICT, C. R., RADOVANCEVIC, B., BICK, R. J., CAPEK, P., SPRINGER, W. E., MACRIS, M. P., DELGADO, R. & BUJA, L. M. 1996. Improved left ventricular function after chronic left ventricular unloading. *The Annals of thoracic surgery,* 62**,** 675-81; discussion 681-2.

FRAZIER, O. H. & JACOB, L. P. 2007. Small Pumps for Ventricular Assistance: Progress in Mechanical Circulatory Support. *Cardiology Clinics,* 25**,** 553-564.

FRAZIER, O. H. & MYERS, T. J. 1999. Left ventricular assist system as a bridge to myocardial recovery. *The Annals of thoracic surgery,* 68**,** 734-41.

FRAZIER, O. H., ROSE, E. A., OZ, M. C., DEMBITSKY, W., MCCARTHY, P., RADOVANCEVIC, B., POIRIER, V. L. & DASSE, K. A. 2001. Multicenter clinical evaluation of the HeartMate vented electric left ventricular assist system in patients awaiting heart transplantation. *The Journal of thoracic and cardiovascular surgery,* 122**,** 1186-95.

FREED, P. S., WASFIE, T., BAR-LEV, A., HAGIWARA, K., VEMURI, D., VAUGHAN, F., BERNSTAM, L., GRAY, R., BERNSTEIN, I. & KANTROWITZ, A. 1985. Long-Term Percutaneous Access Device. *ASAIO journal,* 31.

FURMAN, S., ATTAI, L. & PARKER, B. 1970. Cardiac support by periaortic diastolic augmentation. *New York state journal of medicine,* 70**,** 1964-9.

GAILLARD, E., GARCIA, D., KADEM, L., PIBAROT, P. & DURAND, L. G. Impact of aortic valve stenosis on left coronary artery flow: An in vitro study. *In:* SLOTEN, J., VERDONCK, P., NYSSEN, M. & HAUEISEN, J., eds. IFMBE Proceedings 22, 2009. Springer Berlin Heidelberg, 1922-1925.

GEVEN, M. C., BOHTE, V. N., AARNOUDSE, W. H., VAN DEN BERG, P. M., RUTTEN, M. C., PIJLS, N. H. & VAN DE VOSSE, F. N. 2004. A physiologically representative in vitro model of the coronary circulation. *Physiol Meas,* 25**,** 891-904.

GIBBON, J. H. 1954. Application of a mechanical heart and lung apparatus to cardiac surgery. *Minnesota medicine,* 37**,** 171-85; passim.

GLYNN, R. J., CHAE, C. U., GURALNIK, J. M., TAYLOR, J. O. & HENNEKENS, C. H. 2000. Pulse pressure and mortality in older people. *Archives of internal medicine,* 160**,** 2765-72.

GOLDACRE, M. J., MANT, D., DUNCAN, M. & GRIFFITH, M. 2005. Mortality from heart failure in an English population, 1979-2003: study of death certification. *Journal of epidemiology and community health,* 59**,** 782-4.

GOOD, M. 2006. *The Design of a Mock Circulatory Flow Loop to Test Cardiac Devices.* MSc. Msc. thesis, Nottingham University.

GREEN, D. & HUTTON, P. 1999. Coronary circulation. *Current Anaesthesia & Critical Care,* 10**,** 70-76.

GREGORY, S., TIMMS, D., PEARCY, M. J. & TANSLEY, G. 2009. A naturally shaped silicone ventricle evaluated in a mock circulation loop: a preliminary study. *Journal of medical engineering & technology,* 33**,** 185-91.

GUYTON, A. C. & HALL, J. E. 2006. *Textbook of Medical Physiology,* Philadelphia, PA, Elsevier.

HAYWARD, C. S., PETERS, W. S., MERRY, A. F., RUYGROK, P. N., JANSZ, P., O'DRISCOLL, G., LARBALESTIER, R. I., SMITH, J. A., HO, B., LEGGET, M. E. & MILSOM, F. P. 2010. Chronic extra-aortic balloon counterpulsation: First-in-human pilot study in end-stage heart failure. *The Journal of Heart and Lung Transplantation,* 29**,** 1427-1432.

HETZER, R., MÜLLER, J., WENG, Y., WALLUKAT, G., SPIEGELSBERGER, S. & LOEBE, M. 1999. Cardiac recovery in dilated cardiomyopathy by unloading with a left ventricular assist device. *The Annals of thoracic surgery,* 68**,** 742-9.

HILDEBRAND, D. K., WU, Z. J., MAYER, J. E. & SACKS, M. S. 2004. Design and hydrodynamic evaluation of a novel pulsatile bioreactor for biologically active heart valves. *Annals of biomedical engineering,* 32**,** 1039-49.

HO, K. K., ANDERSON, K. M., KANNEL, W. B., GROSSMAN, W. & LEVY, D. 1993a. Survival after the onset of congestive heart failure in Framingham Heart Study subjects. *Circulation,* 88**,** 107-15.

HO, K. K. L., PINSKY, J. L., KANNEL, W. B. & LEVY, D. 1993b. The epidemiology of heart failure: the Framingham Study. *Journal of the American College of Cardiology,* 22**,** A6-A13.

HUNT, S. A. 1998. Current Status of Cardiac Transplantation *JAMA: The Journal of the American Medical Association* 280 1692-1698.

HUNT, S. A., BAKER, D. W., CHIN, M. H., CINQUEGRANI, M. P., FELDMAN, A. M., FRANCIS, G. S., GANIATS, T. G., GOLDSTEIN, S., GREGORATOS, G., JESSUP, M. L., NOBLE, R. J., PACKER, M., SILVER, M. A., STEVENSON, L. W., GIBBONS, R. J., ANTMAN, E. M., ALPERT, J. S., FAXON, D. P., FUSTER, V., JACOBS, A. K., HIRATZKA, L. F., RUSSELL, R. O. & SMITH JR, S. C. 2001. ACC/AHA guidelines for the evaluation and management of chronic heart failure in the adult: executive summary: A report of the american college of cardiology/american heart association task force on practice guidelines (committee to revise the 1995 guidel. *Journal of the American College of Cardiology,* 38**,** 2101-2113.

JARON, D., MOORE, T. & HE, P. 1985. Control of intraaortic balloon pumping: Theory and guidelines for clinical applications. *Annals of Biomedical Engineering,* 13**,** 155-175.

JEEVANANDAM, V., JAYAKAR, D., ANDERSON, A. S., MARTIN, S., PICCIONE JR., W., HEROUX, A. L., WYNNE, J., STEPHENSON, L. W., HSU, J., FREED, P. S. & KANTROWITZ, A. 2002. Circulatory Assistance With a Permanent Implantable IABP: Initial Human Experience. *Circulation,* 106**,** I-183-188.

JIANG, H., OGDEN, L. G., BAZZANO, L. A., VUPPUTURI, S., LORIA, C. & WHELTON, P. K. 2001. Risk factors for congestive heart failure in US men and women: NHANES I Epidemiologic Follow-up Study. *Archives of internal medicine,* 161**,** 996-1002.

KANTROWITZ, A. 1953. Experimental augmentation of coronary flow by retardation of the arterial pressure pulse. *Surgery,* 34**,** 678-87.

KANTROWITZ, A. 1987. Moments in history. Introduction of left ventricular assistance. *ASAIO transactions / American Society for Artificial Internal Organs,* 33**,** 39-48.

KANTROWITZ, A., CARDONA, R. R. & FREED, P. S. 1992. Percutaneous intra-aortic balloon counterpulsation. *Crit Care Clin,* 8**,** 819-37.

KANTROWITZ, A., TJONNELAND, S., FREED, P. S., PHILLIPS, S. J., BUTNER, A. N. & SHERMAN, J. L. 1968. Initial clinical experience with intraaortic balloon pumping in cardiogenic shock. *JAMA : the journal of the American Medical Association,* 203**,** 113-8.

KATO, R., ISHIHARA, H., SOBUE, T. & YOKOTA, M. 1996. Correlation between left ventricular contractility and relaxation in patients with idiopathic dilated cardiomyopathy. *Clinical Cardiology,* 19**,** 413-418.

KERN, M. J., AGUIRRE, F. & BACH, R. 1993. Augmentation of Coronary Blood Flow by Intra-aortic Balloon Pumping in Patients After Coronary Angioplast. *Circulation,* 87**,** 500-511.

KHIR, A. W. & PARKER, K. H. 2005. Wave intensity in the ascending aorta : effects of arterial occlusion. *Journal of Biomechanics,* 38**,** 647-655.

KHIR, A. W., PRICE, S., HENEIN, M. Y., PARKER, K. H. & PEPPER, J. R. 2003. Intra-aortic balloon pumping: effects on left ventricular diastolic function. *European Journal of Cardio-Thoracic Surgery,* 24**,** 277-282.

KIRKLIN, J. K. & NAFTEL, D. C. 2008. Mechanical circulatory support: registering a therapy in evolution. *Circulation. Heart failure,* 1**,** 200-5.

KIRKLIN, J. K., NAFTEL, D. C., STEVENSON, L. W., KORMOS, R. L., PAGANI, F. D., MILLER, M. A., ULISNEY, K. & YOUNG, J. B. 2008. INTERMACS database for durable devices for circulatory support: first annual report. *The Journal of heart and lung transplantation : the official publication of the International Society for Heart Transplantation,* 27**,** 1065-72.

KLABUNDE, R. E. 1998. *Cardiovascular Physiology Concepts* [Online]. Available: www.cvphysiology.com [Accessed 19 June 2010].

KLABUNDE, R. E. 2005. *Cardiovascular Physiology Concept,* Baltimore, Philadelphia, Lippincot Williams & Wilkins.

KLEPINSKI, R. 2006. FDA Medical Device Requirements. *In:* KUTZ, M. (ed.) *Biomedical Engineering and Design Handbook , Volume 2.* 2nd ed.: McGraw-Hill.

KLOTZ, S., BARBONE, A., REIKEN, S., HOLMES, J. W., NAKA, Y., OZ, M. C., MARKS, A. R. & BURKHOFF, D. 2005. Left ventricular assist device support normalizes left and right ventricular beta-adrenergic pathway properties. *J Am Coll Cardiol,* 45**,** 668-76.

KNIERBEIN, B., REUL, H., EILERS, R., LANGE, M., KAUFMANN, R. & RAU, G. 1992. Compact mock loops of the systemic and pulmonary circulation for blood pump testing. *The International journal of artificial organs,* 15**,** 40-8.

KOENIG, S. C., PANTALOS, G. M., GILLARS, K. J., EWERT, D. L., LITWAK, K. N. & ETOCH, S. W. 2004. Hemodynamic and pressure-volume responses to continuous and pulsatile ventricular assist in an adult mock circulation. *Asaio J,* 50**,** 15-24.

KOLFF, W. J. 1959. Mock circulation to test pumps designed for permanent replacement of damaged hearts. *Cleveland Clinic quarterly,* 26**,** 223-6.

KOLYVA, C., BIGLINO, G., PEPPER, J. R. & KHIR, A. W. 2010a. A Mock Circulatory System With Physiological Distribution of Terminal Resistance and Compliance: Application for Testing the Intra-Aortic Balloon Pump. *Artificial organs*.

KOLYVA, C., PANTALOS, G. M., GIRIDHARAN, G. A., PEPPER, J. R. & KHIR, A. W. 2009. Discerning aortic waves during intra-aortic balloon pumping and their relation to benefits of counterpulsation in humans. *Journal of Applied Physiology,* 107**,** 1497-1503.

KOLYVA, C., PANTALOS, G. M., PEPPER, J. R. & KHIR, A. W. 2010b. How much of the intraaortic balloon volume is displaced toward the coronary circulation? *J Thorac Cardiovasc Surg,* 140**,** 110-116.

KOZAK, L. J., OWINGS, M. F. & HALL, M. J. 2005. National Hospital Discharge Survey: 2002 annual summary with detailed diagnosis and procedure data. *Vital Health Stat.* National Center for Health Statistics.

KOZARSKI, M., FERRARI, G., ZIELIŃSKI, K., GÓRCZYŃSKA, K., PAŁKO, K. J., TOKARZ, A. & DAROWSKI, M. 2008. A new hybrid electro-numerical model of the left ventricle. *Computers in biology and medicine,* 38**,** 979-89.

KRABATSCH, T., SCHWEIGER, M., DANDEL, M., STEPANENKO, A., DREWS, T., POTAPOV, E., PASIC, M., WENG, Y.-G., HUEBLER, M. & HETZER, R. 2011. Is bridge to recovery more likely with pulsatile left ventricular assist devices than with nonpulsatile-flow systems? *The Annals of Thoracic Surgery,* 91**,** 1335-40.

KRISHNA, M. & ZACHAROWSKI, K. 2009. Principles of intra-aortic balloon pump counterpulsation. *Continuing Education in Anaesthesia, Critical Care & Pain,* 9**,** 24-28.

LEGENDRE, D., FONSECA, J., ANDRADE, A., BISCEGLI, J. F., MANRIQUE, R., GUERRINO, D., PRAKASAN, A. K., ORTIZ, J. P. & JULIO CESAR, L. 2008. Mock Circulatory System for the Evaluation of Left Ventricular Assist Devices, Endoluminal Prostheses, and Vascular Diseases. *Artificial Organs,* 32**,** 461-467.

LEGGET, M. E., PETERS, W. S., MILSOM, F. P., CLARK, J. S., WEST, T. M., FRENCH, R. L. & MERRY, A. F. 2005. Extra-aortic balloon counterpulsation: an intraoperative feasibility study. *Circulation,* 112**,** I26-31.

LEVICK, J. R. 2003. *An Introduction to Cardiovascular Physiology,* London, Arnold.

LEVIN, H. R., OZ, M. C., CHEN, J. M., PACKER, M., ROSE, E. A. & BURKHOFF, D. 1995. Reversal of chronic ventricular dilation in patients with end-stage cardiomyopathy by prolonged mechanical unloading. *Circulation,* 91**,** 2717-20.

LIOTTA, D., HALL, C. W., HENLY, W. S., COOLEY, D. A., CRAWFORD, E. S. & DEBAKEY, M. E. 1963. Prolonged assisted circulation during and after cardiac or aortic surgery: Prolonged partial left ventricular bypass by means of intracorporeal circulation. *The American Journal of Cardiology,* 12**,** 399-405.

LIU, Y., ALLAIRE, P., WOOD, H. & OLSEN, D. 2005. Design and initial testing of a mock human circulatory loop for left ventricular assist device performance testing. *Artificial organs,* 29**,** 341-5.

LIU, Y., ALLAIRE, P., WU, Y., WOOD, H. & OLSEN, D. 2006. Construction of an artificial heart pump performance test system. *Cardiovascular engineering (Dordrecht, Netherlands),* 6**,** 151-8.

LLOYD-JONES, D., ADAMS, R. J., BROWN, T. M., CARNETHON, M., DAI, S., DE SIMONE, G., FERGUSON, T. B., FORD, E., FURIE, K., GILLESPIE, C., GO, A., GREENLUND, K., HAASE, N., HAILPERN, S., HO, P. M., HOWARD, V., KISSELA, B., KITTNER, S., LACKLAND, D., LISABETH, L., MARELLI, A., MCDERMOTT, M. M., MEIGS, J., MOZAFFARIAN, D., MUSSOLINO, M., NICHOL, G., ROGER, V. L., ROSAMOND, W., SACCO, R., SORLIE, P., STAFFORD, R., THOM, T., WASSERTHIEL-SMOLLER, S., WONG, N. D. & WYLIE-ROSETT, J. 2010. Heart disease and stroke statistics--2010 update: a report from the American Heart Association. *Circulation,* 121**,** e46-e215.

LU, P.-J., LIN, P.-Y., YANG, C.-F. J., HUNG, C.-H., CHAN, M.-Y. & HSU, T.-C. 2011. Hemodynamic and Metabolic Effects of Para- versus Intraaortic Counterpulsatile Circulation Supports. *ASAIO Journal January/February,* 57**,** 19-25.

MADIGAN, J. D., BARBONE, A., CHOUDHRI, A. F., MORALES, D. L., CAI, B., OZ, M. C. & BURKHOFF, D. 2001. Time course of reverse remodeling of the left ventricle during support with a left ventricular assist device. *The Journal of thoracic and cardiovascular surgery,* 121**,** 902-8.

MANCINI, D. & BURKHOFF, D. 2005. Mechanical device-based methods of managing and treating heart failure. *Circulation,* 112**,** 438-48.

MANN, D. L. & BRISTOW, M. R. 2005. Mechanisms and models in heart failure: the biomechanical model and beyond. *Circulation,* 111**,** 2837-49.

MANOLIO, T. A., BAUGHMAN, K. L., RODEHEFFER, R., PEARSON, T. A., BRISTOW, J. D., MICHELS, V. V., ABELMANN, W. H. & HARLAN, W. R. 1992. Prevalence and etiology of idiopathic dilated cardiomyopathy (summary of a National Heart, Lung, and Blood Institute Workshop). *The American Journal of Cardiology,* 69**,** 1458-1466.

MATHERS, C. 2004. *The global burden of disease : 2004 update,* Geneva, World Health Organization.

MAYBAUM, S., MANCINI, D., XYDAS, S., STARLING, R. C., AARONSON, K., PAGANI, F. D., MILLER, L. W., MARGULIES, K., MCREE, S., FRAZIER, O. H. & TORRE-AMIONE, G. 2007. Cardiac improvement during mechanical circulatory support: a prospective multicenter study of the LVAD Working Group. *Circulation,* 115**,** 2497-505.

MCCARTHY, P. M., NAKATANI, S., VARGO, R., KOTTKE-MARCHANT, K., HARASAKI, H., JAMES, K. B., SAVAGE, R. M. & THOMAS, J. D. 1995. Structural and left ventricular histologic changes after implantable LVAD insertion. *The Annals of thoracic surgery,* 59**,** 609-13.

MCDONAGH, T. A., MORRISON, C. E., LAWRENCE, A., FORD, I., TUNSTALL-PEDOE, H., MCMURRAY, J. J. & DARGIE, H. J. 1997. Symptomatic and asymptomatic left-ventricular systolic dysfunction in an urban population. *Lancet,* 350**,** 829-33.

MCDONALD, J. H. 2009. *Handbook of Biological Statistics,* Baltimore, Maryland, Sparky House Publishing.

MCKEE, P. A., CASTELLI, W. P., MCNAMARA, P. M. & KANNEL, W. B. 1971. The natural history of congestive heart failure: the Framingham study. *The New England journal of medicine,* 285**,** 1441-6.

MCMILLAN, I. K. R. 1955. Aortic stenosis; a post-mortem cinephotographic study of valve action. *British heart journal,* 17**,** 56-62.

MCMILLAN, I. K. R., DALEY, R. & MATTHEWS, M. B. 1952. The movement of aortic and pulmonary valves studied post mortem by colour cinematography. *British heart journal,* 14**,** 42-6.

MCMURRAY, J. J. & STEWART, S. 2000. HEART FAILURE: Epidemiology, aetiology, and prognosis of heart failure. *Heart,* 83**,** 596-602.

MEYNS, B. P., NISHIMURA, Y., JASHARI, R., RACZ, R., LEUNENS, V. H. & FLAMENG, W. J. 2000. Ascending versus descending aortic balloon: Pumping: organ and myocardial perfusion during ischemia. *The Annals of thoracic surgery,* 70**,** 1264-1269.

MILLER, G. E. 2006. *Artificial organs,* Morgan & Claypool Publishers.

MILLER, M. A., ULISNEY, K. & BALDWIN, J. T. 2010. INTERMACS (Interagency Registry for Mechanically Assisted Circulatory Support): a new paradigm for translating registry data into clinical practice. *Journal of the American College of Cardiology,* 56**,** 738-40.

MITCHELL, G. F., PARISE, H., BENJAMIN, E. J., LARSON, M. G., KEYES, M. J., VITA, J. A., VASAN, R. S. & LEVY, D. 2004. Changes in arterial stiffness and wave reflection with advancing age in healthy men and women: the Framingham Heart Study. *Hypertension,* 43**,** 1239-45.

MITNOVETSKI, S., ALMEIDA, A. A., BARR, A., PETERS, W. S., MILSOM, F. P., HO, B. & SMITH, J. A. 2008. Extra-Aortic Implantable Counterpulsation Pump in Chronic Heart Failure. *Ann Thorac Surg,* 85**,** 2122-2125.

MOHAN, S. B., PARKER, M., WEHBI, M. & DOUGLASS, P. 2002. Idiopathic dilated cardiomyopathy: a common but mystifying cause of heart failure. *Cleveland Clinic journal of medicine,* 69**,** 481-7.

MORSI, Y. S. 2000. In vitro comparison of steady and pulsatile flow characteristics of jellyfish heart valve. *Journal of Artificial Organs,* 3**,** 143-148.

MOSTELLER, R. 1987. Simplified Calculation of Body-Surface Area. *New England Journal of Medicine,* 317**,** 1098.

MOSTERD, A. & HOES, A. W. 2007. Clinical epidemiology of heart failure. *Heart (British Cardiac Society),* 93**,** 1137-46.

MOULOPOULOS, S. D., TOPAZ, S. & KOLFF, W. J. 1962. Diastolic balloon pumping (with carbon dioxide) in the aorta--a mechanical assistance to the failing circulation. *Am Heart J,* 63**,** 669-675.

MUELLER, J. & WALLUKAT, G. 2007. Patients who have dilated cardiomyopathy must have a trial of bridge to recovery (pro). *Heart failure clinics,* 3**,** 299-315.

MÜLLER, J., WALLUKAT, G., WENG, Y. G., DANDEL, M., SPIEGELSBERGER, S., SEMRAU, S., BRANDES, K., THEODORIDIS, V., LOEBE, M., MEYER, R. & HETZER, R. 1997. Weaning from mechanical cardiac support in patients with idiopathic dilated cardiomyopathy. *Circulation,* 96**,** 542-9.

NANAS, J. N., LOLAS, C. T., CHARITOS, C. E., NANAS, S. N., MARGARI, Z. J., AGAPITOS, E. V. & MOULOPOULOS, S. D. 1996. A valveless high stroke volume counterpulsation device restores hemodynamics in patients with congestive heart failure and intractable cardiogenic shock awaiting heart transplantation. *J Thorac Cardiovasc Surg,* 111**,** 55-61.

NANAS, S. N., NANAS, J. N., CHARITOS, C. E., GOUGOULAKIS, A., MAKARITSIS, K., CHATZIGEORGIOU, J., MOUSSOUTZANI, K., ANASTASIOU-NANA, M. I. & MOULOPOULOS, S. D. 1997. High stroke volume para-aortic counterpulsation device versus centrifugal pump in cardiogenic shock: experimental study. *World J Surg,* 21**,** 318-2l; discussion 322.

NICHOLS, W. W. & O'ROURKE, M. F. 2005. *McDonald's Blood Flow in Arteries,* London, Hodder Arnorld.

NICHOLS, W. W., O'ROURKE, M. F., HARTLEY, C. & MCDONALD, D. A. 1998. *McDonald's blood flow in arteries: theoretical, experimental, and clinical principles,* Arnold.

NIEDERER, P. & SCHILT, W. 1988. Experimental and theoretical modelling of intra-aortic balloon pump operation. *Medical and Biological Engineering and Computing,* 26**,** 167-174.

NORMAN, J. C., BROOK, M. I., COOLEY, D. A., KLIMA, T., KAHAN, B. D., FRAZIER, O. H., KEATS, A. S., HACKER, J., MASSIN, E. K., DUNCAN, J. M., SOLIS, R. T., DACSO, C. C., LUPER, W. E., WINSTON, D. S. & REUL, G. J. 1978. Total support of the circulation of a patient with post-cardiotomy stone-heart syndrome by a partial artificial heart (ALVAD) for 5 days followed by heart and kidney transplantation. *Lancet,* 1**,** 1125-7.

NOSÉ, Y., SCHAMAUN, M. & KANTROWITZ, A. 1963. Experimental use of an electronically controlled prosthesis as an auxiliary left ventricle. *Transactions - American Society for Artificial Internal Organs,* 9**,** 269-274.

OLSEN, D. B. 2000. The history of continuous-flow blood pumps. *Artificial organs,* 24**,** 401-4.

OPIE, L. H., COMMERFORD, P. J., GERSH, B. J. & PFEFFER, M. A. 2006. Controversies in ventricular remodelling. *The Lancet,* 367**,** 356-367.

ORIME, Y., TAKATANI, S., TASAI, K., OHARA, Y., NAITO, K., MIZUGUCHI, K., MAKINOUCHI, K., MATSUDA, Y., SHIMONO, T., GLUECK, J., NOON, G. P. & NOSÉ, Y. 1994. In Vitro and In Vivo Validation Tests for Total Artificial Heart. *Artificial Organs,* 18**,** 54-72.

PANTALOS, G. M., ALTIERI, F., BERSON, A., BOROVETZ, H., BUTLER, K., BYRD, G., CIARKOWSKI, A. A., DUNN, R., FRAZIER, O. H., GRIFFITH, B., HOEPPNER, D. W., JASSAWALLA, J. S., KORMOS, R. H., KUNG, R. T. V., LEMPERLE, B., LEWIS, J. P., PENNINGTON, D. G., POIRIER, V. L., PORTNER, P. M., ROSENBERG, G., SHANKER, R. & WATSON, J. T. 1998. Long-term mechanical circulatory support system reliability recommendation: American Society for Artificial Internal Organs and The Society of Thoracic Surgeons: Long-term mechanical circulatory support system reliability recommendation. *The Annals of Thoracic Surgery,* 66**,** 1852-1859.

PANTALOS, G. M., KOENIG, S. C., GILLARS, K. J., GIRIDHARAN, G. A. & EWERT, D. L. 2004. Characterization of an Adult Mock Circulation for Testing Cardiac Support Devices. *ASAIO Journal,* 50**,** 37-46.

PAPAIOANNOU, T. G., MATHIOULAKIS, D. S., NANAS, J. N., TSANGARIS, S. G., STAMATELOPOULOS, S. F. & MOULOPOULOS, S. D. 2002. Arterial compliance is a main variable determining the effectiveness of intra-aortic balloon counterpulsation: quantitative data from an in vitro study. *Medical engineering & physics,* 24**,** 279-84.

PAPAIOANNOU, T. G., MATHIOULAKIS, D. S., STAMATELOPOULOS, K. S., GIALAFOS, E. J., LEKAKIS, J. P., NANAS, J., STAMATELOPOULOS, S. F. & TSANGARIS, S. G. 2004. New aspects on the role of blood pressure and arterial stiffness in mechanical assistance by intra-aortic balloon pump: in-vitro data and their application in clinical practice. *Artificial organs,* 28**,** 717-27.

PAPAIOANNOU, T. G. & STEFANADIS, C. 2005. Basic principles of the intraaortic balloon pump and mechanisms affecting its performance. *ASAIO journal (American Society for Artificial Internal Organs : 1992),* 51**,** 296-300.

PARKER, K. 2009a. A brief history of arterial wave mechanics. *Medical and Biological Engineering and Computing,* 47**,** 111-118.

PARKER, K. & JONES, C. 1990. Forward and backward running waves in the arteries: analysis using the method of characteristics. *J Biomech Eng,* 112**,** 322-326.

PARKER, K. H. 2009b. An introduction to wave intensity analysis. *Medical & biological engineering & computing,* 47**,** 175-88.

PHILIPS, P., MARTY, A., MIYAMOTO, A. & BREWER, L., 3D 1975. A clinical method for detecting subendocardial ischemia after cardiopulmonary bypass. *J Thorac Cardiovasc Surg,* 69**,** 30-39.

PIESKE, B. 2004. Reverse remodeling in heart failure - fact or fiction? *European Heart Journal Supplements,* 6**,** D66-D78.

PORTNER, P. M., OYER, P. E., MCGREGOR, C. G. A., BALDWIN, J. C., REAM, A. K., WYNER, J., ZUSMAN, D. R. & SHUMWAY, N. E. 1985. First human use of an electrically powered implantable ventricular assist system. *Artificial organs,* 9**,** 36.

QUALL, S. J. 1993a. Basic Principles of IABC. *Comprehensive Intraaortic Balloon Counterpulsation.* 2nd ed. St. Louis, Missouri: Mosby - Year Book, Inc.

QUALL, S. J. 1993b. *Comprehensive Intraaortic Balloon Counterpulsation,* St. Louis, Missouri, Mosby - Year Book Inc.

QUALL, S. J. 1993c. Conventional timing using the arterial pressure waveform. *Comprehensive Intraaortic Balloon Counterpulsation.* 2nd ed. St. Louis, Missouri: Mosby - Year Book Inc.

RAFTERY, E. B., DAYEM, M. K. & MELROSE, D. G. 1968. Mechanical performance of Hammersmith mitral valve prosthesis. *British heart journal,* 30**,** 666-75.

RATNER, B. D. 2004. *Biomaterials science: an introduction to materials in medicine,* London, Elsevier Academic Press.

REMES, J., REUNANEN, A., AROMAA, A. & PYÖRÄLÄ, K. 1992. Incidence of heart failure in eastern Finland: a population-based surveillance study. *European heart journal,* 13**,** 588-93.

REMME, W. J. & SWEDBERG, K. 2001. Guidelines for the diagnosis and treatment of chronic heart failure. *European heart journal,* 22**,** 1527-60.

REUL, H. M. & AKDIS, M. 2000. Blood pumps for circulatory support. *Perfusion,* 15**,** 295-311.

ROBBINS, R. C., BARLOW, C. W., OYER, P. E., HUNT, S. A., MILLER, J. L., REITZ, B. A., STINSON, E. B. & SHUMWAY, N. E. 1999. Thirty years of cardiac transplantation at Stanford university. *The Journal of thoracic and cardiovascular surgery,* 117**,** 939-51.

RODEHEFFER, R. J., JACOBSEN, S. J., GERSH, B. J., KOTTKE, T. E., MCCANN, H. A., BAILEY, K. R. & BALLARD, D. J. 1993. The incidence and prevalence of congestive heart failure in Rochester, Minnesota. *Mayo Clinic proceedings. Mayo Clinic,* 68**,** 1143-50.

ROGERS, J. G., BUTLER, J., LANSMAN, S. L., GASS, A., PORTNER, P. M., PASQUE, M. K. & PIERSON, R. N. 2007. Chronic mechanical circulatory support for inotrope-dependent heart failure patients who are not transplant candidates: results of the INTrEPID Trial. *Journal of the American College of Cardiology,* 50**,** 741-7.

ROSE, E. A., GELIJNS, A. C., MOSKOWITZ, A. J., HEITJAN, D. F., STEVENSON, L. W., DEMBITSKY, W., LONG, J. W., ASCHEIM, D. D., TIERNEY, A. R., LEVITAN, R. G., WATSON, J. T., MEIER, P., RONAN, N. S., SHAPIRO, P. A., LAZAR, R. M., MILLER, L. W., GUPTA, L., FRAZIER, O. H., DESVIGNE-NICKENS, P., OZ, M. C. & POIRIER, V. L. 2001. Long-term use of a left ventricular assist device for end-stage heart failure. *The New England journal of medicine,* 345**,** 1435-43.

ROSENBERG, G., PHILLIPS, W. M., LANDIS, D. L. & PIERCE, W. S. 1981. Design and Evaluation of the Pennsylvania State University Mock Circulatory System. *ASAIO Journal,* 4**,** 41-49.

SAFAR, M. E. & LAURENT, P. 2003. Pulse pressure and arterial stiffness in rats: comparison with humans. *American journal of physiology. Heart and circulatory physiology,* 285**,** H1363-9.

SALES, V. & MCCARTHY, P. 2010. Understanding the C-Pulse Device and Its Potential to Treat Heart Failure. *Current Heart Failure Reports,* 7**,** 27-34.

SALOMAA, V., RILEY, W., KARK, J. D., NARDO, C. & FOLSOM, A. R. 1995. Non–Insulin-Dependent Diabetes Mellitus and Fasting Glucose and Insulin Concentrations Are Associated With Arterial Stiffness Indexes : The ARIC Study. *Circulation,* 91**,** 1432-1443.

SARNOFF, S. J., BRAUNWALD, E., WELCH, G. H., CASE, R. B., STAINSBY, W. N. & MACRUZ, R. 1957. Hemodynamic Determinants of Oxygen Consumption of the Heart With Special Reference to the Tension-Time Index. *American Journal of Physiology -- Legacy Content,* 192**,** 148-156.

SCHAMPAERT, S., VAN'T VEER, M., VAN DE VOSSE, F. N., PIJLS, N. H. J., DE MOL, B. A. & RUTTEN, M. C. M. 2011. In Vitro Comparison of Support Capabilities of Intra-Aortic Balloon Pump and Impella 2.5 Left Percutaneous. *Artificial Organs,* 35**,** 893-901.

SHAH, S. R. 2011. Non-Newtonian Flow of Blood Through an Atherosclerotic Artery. *Research Journal of Applied Sciences,* 6**,** 76-80.

SHARP, M. K. & DHARMALINGHAM, R. K. 1999. Development of a hydraulic model of the human systemic circulation. *Asaio J,* 45**,** 535-540.

SIMON, M. A., WATSON, J., BALDWIN, J. T., WAGNER, W. R. & BOROVETZ, H. S. 2008. Current and future considerations in the use of mechanical circulatory support devices. *Annual review of biomedical engineering,* 10**,** 59-84.

SLAUGHTER, M. S., ROGERS, J. G., MILANO, C. A., RUSSELL, S. D., CONTE, J. V., FELDMAN, D., SUN, B., TATOOLES, A. J., DELGADO, R. M., LONG, J. W., WOZNIAK, T. C., GHUMMAN, W., FARRAR, D. J. & FRAZIER, O. H. 2009. Advanced heart failure treated with continuous-flow left ventricular assist device. *The New England journal of medicine,* 361**,** 2241-51.

STENZ, R. 2006. Intra-aortic balloon counterpulsation. *Anaesthesia & intensive care medicine,* 7**,** 335-336.

STEVENSON, L. W., PAGANI, F. D., YOUNG, J. B., JESSUP, M., MILLER, L., KORMOS, R. L., NAFTEL, D. C., ULISNEY, K., DESVIGNE-NICKENS, P. & KIRKLIN, J. K. 2009. INTERMACS Profiles of Advanced Heart Failure: The Current Picture. *The Journal of Heart and Lung Transplantation,* 28**,** 535-541.

STEVENSON, L. W. & SHEKAR, P. 2005. Ventricular assist devices for durable support. *Circulation,* 112**,** e111-5.

STEWART, S., MACINTYRE, K., HOLE, D. J., CAPEWELL, S. & MCMURRAY, J. J. 2001. More 'malignant' than cancer? Five-year survival following a first admission for heart failure. *European journal of heart failure : journal of the Working Group on Heart Failure of the European Society of Cardiology,* 3**,** 315-22.

SUGA, H. & SAGAWA, K. 1974. Instantaneous pressure-volume relationships and their ratio in the excised, supported canine left ventricle. *Circulation research,* 35**,** 117-26.

SUGAWARA, M., NIKI, K., OHTE, N., OKADA, T. & HARADA, A. 2009. Clinical usefulness of wave intensity analysis. *Medical and Biological Engineering and Computing,* 47**,** 197-206.

TANSLEY, G. D. & RICHENS, D. 2010. *Pulsatile Blood Pump*. United States patent application 12/679,651.

TAYLOR, D. O., EDWARDS, L. B., BOUCEK, M. M., TRULOCK, E. P., DENG, M. C., KECK, B. M. & HERTZ, M. I. 2005. Registry of the International Society for Heart and Lung Transplantation: twenty-second official adult heart transplant report--2005. *The Journal of heart and lung transplantation the official publication of the International Society for Heart Transplantation,* 24**,** 945-955.

TERROVITIS, J. V., CHARITOS, C. E., TSOLAKIS, E. J., DOLOU, P., PIERRAKOS, C. N., SIAFAKAS, K. X. & NANAS, J. N. 2003. Superior performance of a paraaortic counterpulsation device compared to the intraaortic balloon pump. *World journal of surgery,* 27**,** 1311-6.

TIMMS, D., GREGORY, S., HSU, P. L., THOMSON, B., PEARCY, M., MCNEIL, K., FRASER, J. & STEINSEIFER, U. 2010. Atrial versus ventricular cannulation for a rotary ventricular assist device. *Artificial Organs,* 34**,** 714-20.

TIMMS, D., HAYNE, M., MCNEIL, K. & GALBRAITH, A. 2005a. A complete mock circulation loop for the evaluation of left, right, and biventricular assist devices. *Artificial organs,* 29**,** 564-72.

TIMMS, D., HAYNE, M., TAN, A. & PEARCY, M. 2005b. Evaluation of left ventricular assist device performance and hydraulic force in a complete mock circulation loop. *Artificial Organs,* 29**,** 573-580.

TIMMS, D. L., GREGORY, S. D., GREATREX, N. A., PEARCY, M. J., FRASER, J. F. & STEINSEIFER, U. 2011. A compact mock circulation loop for the in vitro testing of cardiovascular devices. *Artificial organs,* 35**,** 384-91.

TRANSPLANT, U. 2008. Transplant Activity in the UK. NHS.

TRAVIS, A. R., GIRIDHARAN, G. A., PANTALOS, G. M., DOWLING, R. D., PRABHU, S. D., SLAUGHTER, M. S., SOBIESKI, M., UNDAR, A., FARRAR, D. J. & KOENIG, S. C. 2007. Vascular pulsatility in patients with a pulsatile- or continuous-flow ventricular assist device. *The Journal of thoracic and cardiovascular surgery,* 133**,** 517-24.

TROST, J. C. & HILLIS, L. D. 2006. Intra-Aortic Balloon Counterpulsation. *The American Journal of Cardiology,* 97**,** 1391-1398.

UNDAR, A. 2004. Myths and truths of pulsatile and nonpulsatile perfusion during acute and chronic cardiac support. *Artificial organs,* 28**,** 439-43.

UNDAR, A. & FRASER, C. D. 2002. The Alphabet of Research on Pulsatile and Nonpulsatile (Continuous Flow) Perfusion During Chronic Support. *Artificial Organs,* 26**,** 812-813.

UNOS, U. N. F. O. S. 2007. The 2007 Annual Report of the U.S. Organ Procurement and Transplantation Network and the Scientific Registry of Transplant Recipients: Transplant Data 1997-2006. Rockville, MD.

UTOH, J., WHALEN, R. L., WILKERSON, B. R., FUKAMACHI, K. & HARASAKI, H. 1993. Chronic in vivo function of a new ventricular assist device: the extracorporeal pulsatile assist device (EPAD). *The International journal of artificial organs,* 16**,** 91-5.

VOHRA, H. A. & ROSIN, M. D. 2004. The intra-aortic balloon pump. *Surgery (Oxford),* 22**,** i-ii.

WESTERHOF, N., LANKHAAR, J.-W. & WESTERHOF, B. E. 2009. The arterial Windkessel. *Medical & biological engineering & computing,* 47**,** 131-41.

WESTERHOF, N., STERGIOPULOS, N. & NOBLE, M. I. M. 2010. *Snapshots of Hemodynamics: An Aid for Clinical Research and Graduate Education*, Springer Verlag.

WHEELDON, D. R. 2003. Mechanical circulatory support: state of the art and future perspectives. *Perfusion,* 18**,** 233-243.

WIETING, D. W., AKERS, W. W., FEOLA, M. & KENNEDY, J. H. 1971. Analysis of a variable volume intra-aortic balloon pump in a mock circulatory system. *Journal of Biomechanics,* 4**,** 37-44.

WILLIAMS, D. O., KORR, K. S., GEWIRTZ, H. & MOST, A. S. 1982. The effect of intraaortic balloon counterpulsation on regional myocardial blood flow and oxygen consumption in the presence of coronary artery stenosis in patients with unstable angina. *Circulation,* 66**,** 593-7.

WILLIAMS, M. R. & OZ, M. C. 2001. Indications and patient selection for mechanical ventricular assistance. *The Annals of thoracic surgery,* 71**,** S86-S91.

WU, Y. I., ALLAIRE, P. J., TAO, G. & OLSEN, D. 2007. Modeling, Estimation, and Control of HUman CIrculatory System With a Left Ventricular Assist Device. *IEEE Transaction on Control System Technology,* 15**,** 754-767.

ZAFEIRIDIS, A., JEEVANANDAM, V., HOUSER, S. R. & MARGULIES, K. B. 1998. Regression of cellular hypertrophy after left ventricular assist device support. *Circulation,* 98**,** 656-62.

ZANNOLI, R., CORAZZA, I. & BRANZI, A. 2009. Mechanical simulator of the cardiovascular system. *Phys Med,* 25**,** 94-100.

ZAR, J. H. 2010. *Biostatistical analysis*, Prentice Hall International.

ZELANO, J. A., KO, W., LAZZARO, R., LAZENBY, W. D., TOPAZ, S., KOLFF, W. J., ISOM, O. W. & KRIEGER, K. H. 1992. Evaluation of an extraaortic counterpulsation device in severe cardiac failure. *The Annals of Thoracic Surgery,* 53**,** 30-36.

APPENDIX

APPENDIX A – Silicone Making

A-1   Silicone Curing Process

Silastic T4 silicone elastomer comes in two parts, a base and a catalyst. The base part and the catalyst part were mixed thoroughly together with a ratio of 10:1 by volume. However, in the process, air bubbles were mixed together as well and needed to be extracted. Air bubbles in the final product will decrease the structural strength not to mention jeopardising the gas impermeability requirement of the CIMS balloon pump. A degassing chamber capable of providing -30 kPa/-1 bar of vacuum was used to extract air bubbles from the silicone mixture. The mixture was left for about 10 minutes; the mixture expanded to about three to five times its original volume (an appropriate mixing container was selected). Once the 10 minutes degassing period was over, the mixture was then checked for any air bubbles. Normally a second air degassing procedure was needed for a further 5 - 10 minutes. Once all air bubbles were extracted, it could then be poured onto whatever mould was prepared beforehand. The time taken for the mixture to cure into a stable and strong silicone elastomer is up to 24 hours, and it was even faster if the mix was subjected to heat for an accelerated curing process.

Figure A-136: Degassing chamber capable of vacuum pressure up to -1 bar or -30 mmHg

Figure A-137: Silastic T4 base
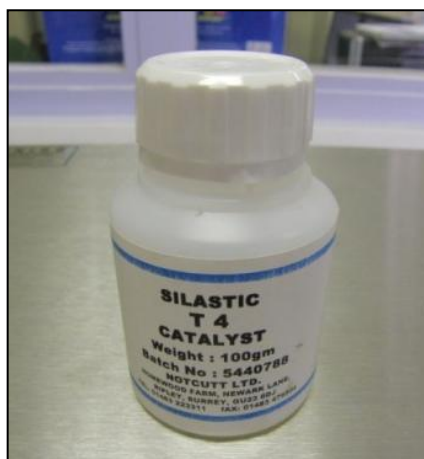
Figure A-138: Silastic T4 catalyst

A-2   Silicone Curing Mould

There are two methods to cure the silicone mixture. The first one was by inserting a rod into a cylindrical hollow aluminium alloy mould. The gap between the centrically fixed rod and the surrounding hollow mould was designed to be 1mm. A silicone based release agent was sprayed onto the aluminium mould surfaces prior silicone mix insertion, to facilitate easier silicone peeling off later on. The silicone mixture was then poured into the mould slowly to allow the silicone to fill up the entire gap. The CAD model of the mould is as per Figure A-139, while the cured cylindrical silicone is shown in Figure A-140.
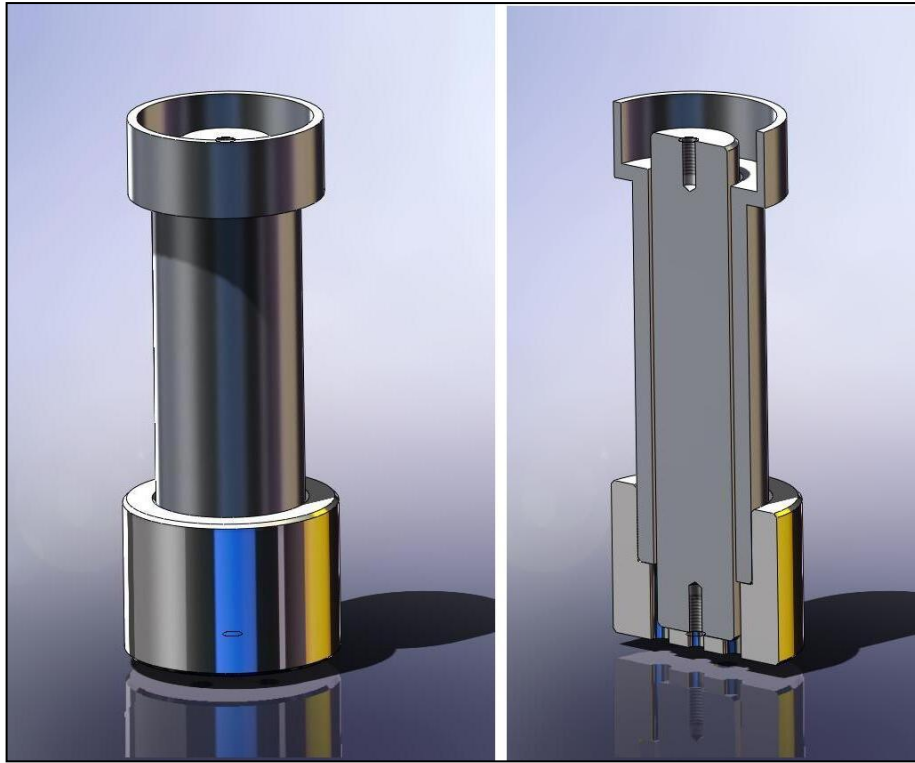
Figure A-139: Aluminium mould use to cure silicone mixture into a cylindrical model. The left side is the assembled parts, while the right figure is showing the cross section of the mould. Silicone is inserted into gap between middle shaft and aluminium cylinder.

The other way was by using a cylindrical rod rotated about its centre axis. After the silicone mixture was ready, it was poured onto the surface of the cylinder; the thickness was manually controlled. Initial cured membrane had a fine thin layer. By repeating the same process, the desired thickness was achieved. The rotational movement of the aluminum cylinder was powered by using a LEGO ™[46] robot employing a worm gear mechanism to provide a rotational speed of eight rotations per minute (rpm). The rotational speed of the aluminium cylinder cannot be too fast as this will prevent the silicone mixture from settling in. However, if the rotation was too slow, gravitational pull will affect the silicone mixture, and the membrane thickness would be compromised, due to silicone dripping resulting in a non-uniform membrane thickness. A careful balance between rotational speed and silicone thickness was achieved after a series of trial and error. This method is suitable to achieve a very thin silicone membrane (≈ 0.2 - 0.4 mm) or multi diameter silicone membranes depending on the mould selected. For the compliant body balloon pump, a thin silicone membrane of ≈ 0.5 mm was cured.

---

[46] LEGO , Billund, Denmark

For the LV silicone sac, the silicone mixture was poured into the mould shown in Figure A-141, and the second part of the mould was inserted into the the first part mould.

Figure A-140: A cylindrical silicone membrane used in the *in vitro* prototype balloon pump

Figure A-141: Mould for the LV silicone sack

A-3   Silicone Silastic T4 Datasheet

Product Information

Moldmaking
Materials *Silastic*® **T-4**
Base/Curing Agent

DOW CORNING

FEATURES

- High strength
- Translucent appearance allows split lines to be cut accurately in block molds
- Low shrinkage and good dimensional stability
- Outstanding release properties
- Medium hardness (40 Shore A) with flexibility and toughness
- Heat-accelerable cure
- Suitable for high-temperature casting
- Two available curing agents: *Silastic* T-4 (standard) and *Silastic* T-4 O (excellent release properties)

COMPOSITION

- Silicone rubber supplied as liquid; cures to flexible silicone elastomer

Moldmaking rubber for prototype design, production tooling and rapid prototyping

APPLICATIONS

Silastic® T-4 Base/Curing Agent is a moldmaking rubber developed for prototype design and production tooling, especially for rapid prototyping applications.

TYPICAL PROPERTIES

Specification Writers: Please contact your local Dow Corning sales office or your Global Dow Corning Connection before writing specifications on this product.

Test	Unit	Result
As Supplied		
Appearance		Translucent liquid
Base Viscosity	cP	70,000
As Mixed – Base and Curing Agent (10:1 by weight)		
Viscosity	cP	37,000
Working Time at 23°C (73°F)	minutes	90 to 120
As Cured – 4 hours at 40°C (104°F)		
Durometer, Shore A	points	40
Tensile Strength	psi	970
Elongation at Break	percent	390
Tear Strength	ppi	150

ISO 34 Cutter (equivalent JIS K6252, DIN53515), Angle nick 1.0 mm.

DESCRIPTION

Silastic T-4 Base/Curing Agent is a two-component material consisting of *Silastic* T-4 Base, which when mixed with *Silastic*® T-4 Curing Agent or *Silastic*® T-4 O Curing Agent cures at room temperature by an addition reaction.

A range of materials can be cast or injected into the cured silicone mold: polyurethane and other reactive resins are materials typically used.

HOW TO USE
Substrate Preparation

The surface of the original should be clean and free of loose material. If necessary, and in particular with porous substrates, use a suitable release agent such as petroleum jelly or PTFE.

Mixing

Weigh 100 parts of *Silastic* T-4 Base and 10 parts of *Silastic* T-4 Curing Agent in a clean container, then mix together until the curing agent is completely dispersed in the base. Hand or mechanical mixing can be used, but do not mix for an extended period of time. Mix sufficiently small quantities to ensure thorough mixing of base and curing agent.

Entrapped air should be removed in a vacuum chamber, allowing the mix to completely expand and then collapse. After a further 1 to 2 minutes under vacuum, the mix should be inspected, and if free of bubbles, then be used. A volume increase of three to five times will occur on vacuum deairing the mixture, so a suitably large container should be used.

APPENDIX B – Statistical Test

B-1   Scheirer-Ray-Hare Test

In the case of ANOVA assumptions cannot be met, the alternative non-parametric test for two-way ANOVA is Scheirer-Ray-Hare (SRH) test. The procedures are:

i.   assemble the original data into ascending order, and assign ranks to replace the original data.

ii.   Perform the standard parametric two-way ANOVA onto the rank-transformed data.

iii.   The new total mean square (MS_{TOTAL}) value for the rank-transformed data is calculated by dividing the Corrected Total value by the degrees of freedom (df).

iv.   Compute the test statistics for each experimental factor and their interaction. The test statistics is defined by H = SS/MS_{TOTAL}. Note that the SS is the sum of squares value obtained from the rank-transformed ANOVA.

v.   The p-value for each factor is computed by using Chi-square distribution using the test-statistics calculated in above procedure and the degrees of freedom.

An example of the SRH test used in this study is tabulated in Table B-109, the experimental factors are Design and Helium gas volume, while the response output is the cardiac output (CO). Table B-107 tabulates the ANOVA results from SPSS program.

Table B-107: The ANOVA result

Source	Type III Sum of Squares	df	Mean Square	F	Sig.
Corrected Model	4.956×10^6	5	991197.480	64.818	.000
Intercept	3.951×10^7	1	3.951×10^7	2583.818	.000
Design	4316589.630	1	4316589.630	282.276	.000
GasVOL	503810.411	2	251905.206	16.473	.000
Design * GasVOL	135587.359	2	67793.680	4.433	.012
Error	8165967.600	534	15292.074		
Total	5.263×10^7	540			
Corrected Total	1.312×10^7	539			

Total mean square value, MS_{TOTAL} was calculated by dividing Corrected Total with df of the same row. The calculation was carried out using Microsoft Excel spreadsheet. Table B-108 tabulates the result.

Table B-108: Calculated MS_{TOTAL}

Corrected total	df	MS_{TOTAL}
1.31×10^7	539	24341.4

The new test-statistics, denoted by H, for each experimental factor, Design and ArtCompliance, was calculated by dividing the rank-transformed ANOVA's sum of square with MS_{TOTAL}.

The p-value then was obtained by using the Chi-Square distribution formula CHIDIST provided in the Microsoft Excel. The formula calculated the one-tail probability according to the test-statistics, H, and df (degree of freedom) value.

Table B-109 : The SRH test result. SS: Sum of Squares, df: degree of freedoms, H: test-statistics for SRH test

Source	SS	df	H	P-value
Design	4316589.63	1	177.3355	1.85×10^{-40}
GasVOL	503810.411	2	20.6977	3.20×10^{-5}
Design * GasVOL	135587.359	2	5.5702	0.062

B-2   Nemenyi Test

The post-hoc Nemenyi test is similar to Tukey Honest Significant Difference (HSD) test, used on non-parametric data. The origin of Nemenyi is an extension of Kruskal-Wallis test, which is for two or more groups with non-parametric data distribution. The post-hoc test can only be carried out if p-value of the experimental factor showed a significant difference.

The procedure/algorithm for Nemenyi test is as follows (Zar, 2010).

i.   Apply non-parametric Kruskal-Wallis test on the groups to compute the mean rank of each level.

ii.   The groups then are ranked according to the highest sum of ranks.

iii.   The standard error, *SE*, then is calculated using Eq. B-1, where *n* is the number of samples, while *k* is the number of groups.

$$SE = \sqrt{\frac{n(nk)(nk + 1)}{12}}$$
B-1

iv.   Pairwise comparison of the groups is conducted starting with the difference between the largest and the smallest rank sums, before proceeding to the next bigger rank sums. The test statistic, *q*, also known as Studentized range, is computed by dividing the difference between rank sums with the SE.

v.   The computed *q* value is compared to the critical value, q (*α, v, k*), where α: confidence level, set at 5 %, *v* = error degree of freedom appropriate to a statistical test, and k : number of groups. If the *q* > q(α, ∞, k), there is enough evidence to reject H_0, and accept the alternative hypothesis, H_1.

SPSS and Microsoft Excel software was used during the process.

An example of the Nemenyi test is presented; the data used was from the same dataset as B-1.

B-2-1   Example of Nemenyi Test

Table B-110 tabulates the result of Kruskal Wallis test for GasVOL experiment data with three levels.

Table B-110: Kruskal Wallis test result of each level's Mean Rank value

GasVOL		N	Mean Rank
CO	V20	180	237.14
	V25	180	310.94
	V30	180	263.42
	Total	540	

The order of the group was determined from sums of rank by multiplying the mean rank with the number of samples, N. The standard error, SE, was calculated using equation B-1.

Table B-111: The result of rank of each level and SE

Response Output	GasVol	N	Mean Rank	Sums of Rank	rank
CO	V20	180	237.14	42685.2	3
	V25	180	310.94	55969.2	1
	V30	180	263.42	47415.6	2
	Total	540			

$$k = 3$$
$$SE = 2093.347$$

Pairwise comparison was then computed. Since critical value $\alpha = 0.05$, $v = \infty$, and $k = 3$; the $q(0.05, \infty, 3)$ value is 3.314 (Zar, 2010). The comparison was conducted by subtracting the highest ranked group (Rb) with the lowest (Ra), and then with the second lowest, and so on. In this sample, the first two comparisons detected significant difference between groups involved, thus the * sign is tabulated in the Table B-112.

Table B-112: Nemenyi test result.

B	vs	A		vs		(Rb-Ra)	SE	q	q(0.05,∞,3)	Result	significant
1		3	V25		V20	13284	2093.35	6.346	3.314	Reject H_0	YES
1		2	V25		V30	8553.6	2093.35	4.086	3.314	Reject H_0	YES
2		3	V30		V20	4730.4	2093.35	2.260	3.314	Accept H_0	

B-3   Sample Size Calculation

Sample size for an experiment determines the power of the test involved whether the test would have enough sensitivity to detect any differences between means etc. In the case of two different populations with different standard deviation (SD) values, these equations were used.

$$N_1 = (U_\alpha + U_\beta)^2 \times \frac{\sigma_1 \, (\sigma_1 + \sigma_2)}{\delta^2} \qquad \text{B-2}$$

and

$$N_2 = (U_\alpha + U_\beta)^2 \times \frac{\sigma_2 \, (\sigma_1 + \sigma_2)}{\delta^2}. \qquad \text{B-3}$$

Where N_1 = sample size from the first population,

N_2 = sample size from the second population,

σ_1 = standard deviation of the first population

σ_2 = standard deviation of the first population

U_α = Normal distribution number for alpha risk (normally at 0.05 = 1.96)

U_β = Normal distribution number for beta risk (normally for 0.10 = 90% power is 1.282)

δ = important engineering increment that we want to observe, or the minimum change in the mean that would be useful/interesting.

An example of sample size calculation is given:

Since the main output response of interest is cardiac output (CO), the sample size calculation is as follows, where α = 0.05, β = 0.10, δ = 0.3 L/min (10% of 3.0 L/min for HF mode), σ_1 = 0.05 L/min, σ_2 = 0.2 L/min (assumed to be four times the value of σ_1).

For non-assisted flow:

$$N_1 = \left(U_\alpha + U_\beta\right)^2 \times \frac{\sigma_1 \, (\sigma_1 + \sigma_2)}{\delta^2}$$
$$N_1 = (1.960 + 1.282)^2 \times \frac{0.05(0.05 + 0.2)}{0.3^2}$$
$$N_1 = 1.45$$
$$N_1 \cong 2$$

Similar calculation for assisted flow yields:

$$N_2 = (1.960 + 1.282)^2 \times \frac{0.2(0.05 + 0.2)}{0.3^2}$$
$$N_2 = 5.84$$
$$N_2 \cong 6$$

From the results, the amount of sample size between non-assisted and assisted flow is different since the standard deviation between groups is unequal; if the intention is to be able to detect at least 10% changes of CO of the assisted flow, an overall sample size of 6 is enough. Higher sample

size allows for a better detection range. In Table B-113, sample sizes are shown to change according to the sensitivity to detect smaller mean differences:

Table B-113: Sample size of non-assisted (N1) and assisted flow (N2) according to the flow SD and δ level with power of test at 90%, (β = 0.10).

SD	δ	N1	N2
$\sigma_1 = 0.05$ $\sigma_2 = 0.2$	10 %	2	6
	5 %	6	24
	1 %	146	584
$\sigma_1 = 0.02$ $\sigma_2 = 0.04$	10 %	≈ 1	20
	5 %	≈ 3	79
	1 %	99	1962
$\sigma_1 = \sigma_2 = 0.1$	10 %	3	
	5 %	10	
	1 %	234	

If the SD is equal for both populations, set at SD = 0.3 L/min for CO, while δ is set at 5% (0.15 L/min), the minimum sample size is 85 for both of groups. Clearly the amount of sample size is different according to the nature of the experiment. From preliminary tests, it was found that most of the SD was very small (≈ 0.02 L/min) and CO's mean difference was at least 5% and greater. A decision to adopt sample size of 30 for both populations (non-assisted and assisted flow) was taken, since it would give good detection range at δ = 5%.

APPENDIX C – Statistical Analysis Result

C-1 TIMING
The statistical results for response outputs of TIMING experiment.

C-1-1 Cardiac Output

Table C-114: SRH test result for Cardiac Output of TIMING experiment

Source	SS	df	MS_{TOTAL}	H	P-value
Inflation	9204221.089	2		94.58	2.89×10^{-21}
Deflation	9227589.533	3		94.82	2.01×10^{-21}
Inflation × Deflation	4641448.156	6		47.7	1.36×10^{-21}
Corrected Total	105000000	1079	97312.3262		

C-1-1Left Coronary Artery Mean Flowrate

Table C-115: Levene's test result for data variance's equality

Levene's Test of Equality of Error Variances[a]			
Dependent Variable: QcorMean			
F	df1	df2	Sig.
21.813	11	1068	.000

Table C-116: SRH test result for LCA flowrate of TIMING experiment

Source	SS	df	MS_{TOTAL}	H	P-value
Inflation	1822695.117	2		18.73	8.57×10^{-5}
Deflation	16150000	3		165.96	9.48×10^{-36}
Inflation × Deflation	8260363.594	6		84.89	3.49×10^{-16}
Corrected Total	105000000	1079	97312.3262		

Table C-117: The rank for Inflation factor

Response Output	Inflation	N	Mean Rank	SumRank	rank
QcorMean	A	360	521.84	187862.4	2
	B	360	597.48	215092.8	1
	C	360	502.18	180784.8	3
	Total	1080		*k =*	3
				SE	5918.142

Table C-118: The rank result for Deflation factor

Response Output	Deflation	N	Mean Rank	Sum Rank	rank
QcorMean	G	270	473.17	127755.9	3
	H	270	575.93	155501.1	2
	I	270	720.04	194410.8	1
	J	270	392.86	106072.2	4
	Total	1080		*k =*	4
				SE =	5125.261

C-1-2 Aortic Systolic Pressure (AoPmax)

Table C-119: Levene's test for homogeneity of variance

Levene's Test of Equality of Error Variances[a]			
Dependent Variable: AoPmax			
F	df1	df2	Sig.
25.200	11	1068	.000

Table C-120: SRH test result for AoPmax of TIMING experiment

Source	SS	df	MS_{TOTAL}	H	P-value
Inflation	2553684.617	2		26.24	2.00×10^{-6}
Deflation	16540000	3		169.97	1.29×10^{-36}
Inflation × Deflation	6112216.82	6		62.81	1.21×10^{-11}
Corrected Total	105000000	1079	97312.3262		

Table C-121 : The rank result for Inflation factor

Response Output	Inflation	N	Mean Rank	SumRank	rank
AoPmax	A	360	496.48	178732.8	3
	B	360	608.25	218970	1
	C	360	516.77	186037.2	2
	Total	1080		*k =*	3
				SE	5918.142

Table C-122 : The rank result for Deflation factor

Response Output	Deflation	N	Mean Rank	Sum Rank	rank
AoPmax	G	270	644.51	174017.7	1
	H	270	604.27	163152.9	2
	I	270	583.67	157590.9	3
	J	270	329.54	88975.8	4
	Total	1080		$k =$	4
				$SE =$	5125.261

C-1-3 Aortic End-Diastolic Pressure (AoEDP)

Table C-123: SRH test result for AoEDP of TIMING experiment

Source	SS	df	MS_{TOTAL}	H	P-value
Inflation	246594.839	2		2.53	0.282
Deflation	613091.63	3		6.30	0.095
Inflation × Deflation	1258293.198	6		12.93	0.044
Corrected Total	105000000	1079	97312.3262		

Table C-124: The Levene's test for homogeneity of variance

Levene's Test of Equality of Error Variances[a]			
Dependent Variable: AoEDP			
F	df1	df2	Sig.
45.705	11	1068	.000

C-1-4 Correlation

Table C-125: Correlation of coefficient for dP and CO

Correlations				CO	dP
Spearman's rho	CO	Correlation Coefficient		1.000	.171[**]
		Sig. (2-tailed)		.	.000
		N		1080	1080
	dP	Correlation Coefficient		.171[**]	1.000
		Sig. (2-tailed)		.000	.
		N		1080	1080

**. Correlation is significant at the 0.01 level (2-tailed).

Table C-126: The correlation coefficient result for dP and QcorMean

Correlations

			dP	QcorMean
Spearman's rho	dP	Correlation Coefficient	1.000	.206[**]
		Sig. (1-tailed)	.	.000
		N	1080	1080
	QcorMean	Correlation Coefficient	.206[**]	1.000
		Sig. (1-tailed)	.000	.
		N	1080	1080

**. Correlation is significant at the 0.01 level (1-tailed).

C-2 Helium Gas Volume

C-2-1 Cardiac Output

Table C-127: Levene's test for homogeneity of data

Levene's Test of Equality of Error Variances[a]

Dependent Variable: CO

F	df1	df2	Sig.
19.402	5	534	.000

Table C-128: SRH test result for CO of Helium gas volume experiment

Source	SS	df	MS_{TOTAL}	H	P-value
Design	4316589.63	1		177.34	1.85×10^{-40}
GasVOL	503810.411	2		20.8	3.203×10^{-5}
Design × GasVOL	135587.359	2		5.57	0.062
Corrected Total	13120000	539	24341.3729		

Table C-129 : The ranks result for GasVol factor

Response Output	GasVol	N	Mean Rank	SumRank	rank
CO	V20	180	237.14	42685.2	3
	V25	180	310.94	55969.2	1
	V30	180	263.42	47415.6	2
	Total	540		$k =$	3
				$SE =$	2093.347

C-2-2 Left Coronary Artery Mean Flowrate (QcorMean)

Table C-130: Levene's test for Design & GasVol factors data

Levene's Test of Equality of Error Variances[a]			
Dependent Variable: QcorMean			
F	df1	df2	Sig.
21.541	5	534	.000

Table C-131: SRH test result for QcorMean of Helium gas volume experiment

Source	SS	df	MS_{TOTAL}	H	P-value
Design	2445816.6	1		100.48	1.196×10^{-23}
GasVOL	4964390.578	2		203.95	5.165×10^{-45}
Design × GasVOL	119590.178	2		4.91	0.086
Corrected Total	13120000	539	24341.3729		

Table C-132 : The ranks result for GasVol factor

Response Output	GasVol	N	Mean Rank	SumRank	rank
QcorMean	V20	180	145.1	26118	3
	V25	180	288.52	51933.6	2
	V30	180	377.88	68018.4	1
	Total	540		$k =$	3
				$SE =$	2093.347

C-2-3 Aortic Systolic Pressure (AoPmax)

Table C-133: Levene's test for equality for AoPmax response output

Levene's Test of Equality of Error Variances[a]			
Dependent Variable:AoPmax			
F	df1	df2	Sig.
21.353	5	534	.000

Table C-134: SRH test result for AoPmax

Source	SS	df	MS$_{TOTAL}$	H	P-value
Design	1125957.341	1		46.26	1.037×10^{-11}
GasVOL	554700.044	2		22.79	1.126×10^{-5}
Design × GasVOL	57065.304	2		2.34	0.31
Corrected Total	13120000	539	24341.3729		

Table C-135 : Kruskal-Wallis test result for the Mean Rank

Response Output	GasVol	N	Mean Rank	SumRank	rank
AoPmax	V20	180	292.66	52678.8	2
	V25	180	293.69	52864.2	1
	V30	180	225.14	40525.2	3
	Total	540		*k =*	3
				SE =	2093.347

C-2-4   *Aortic End-Diastolic Pressure (AoEDP)*

Table C-136 : The Levene's test for homogeneity of variance

Levene's Test of Equality of Error Variances[a]

Dependent Variable:AoEDP

F	df1	df2	Sig.
19.714	5	534	.000

Table C-137: SRH test result for AoEDP

Source	SS	df	MS$_{TOTAL}$	H	P-value
Design	332022.407	1		13.64	2×10^{-4}
GasVOL	1604911.944	2		65.93	4.82×10^{-15}
Design × GasVOL	334019.07	2		13.72	0.001
Corrected Total	13120000	539	24341.3729		

Table C-138 : The rank of each levels in GasVol factor

Response Output	GasVol	N	Mean Rank	SumRank	rank
AoEDP	V20	180	336.04	60487.2	1
	V25	180	272.91	49123.8	2
	V30	180	202.55	36459	3
	Total	540		*k =*	3
				SE =	2093.347

C-2-5   Correlation

Table C-139: Correlation between dP and CO

Correlations

			dP	CO
Spearman's rho	dP	Correlation Coefficient	1.000	.477[**]
		Sig. (2-tailed)	.	.000
		N	540	540
	CO	Correlation Coefficient	.477[**]	1.000
		Sig. (2-tailed)	.000	.
		N	540	540

[**]. Correlation is significant at the 0.01 level (2-tailed).

Table C-140: Correlation between dP and QcorMean

Correlations

			dP	QcorMean
Spearman's rho	dP	Correlation Coefficient	1.000	.705[**]
		Sig. (2-tailed)	.	.000
		N	540	540
	QcorMean	Correlation Coefficient	.705[**]	1.000
		Sig. (2-tailed)	.000	.
		N	540	540

[**]. Correlation is significant at the 0.01 level (2-tailed).

C-3   COMPLIANCE

The statistical results for response output of COMPLIANCE experiment are presented.

C-3-1   Cardiac Output

Table C-141: Levene's Test

Levene's Test of Equality of Error Variances			
Dependent Variable: CO			
F	df1	df2	Sig.
20.035	3	356	.000

Table 142: SRH test result for CO of COMPLIANCE experiment

Source	SS	df	MS$_{TOTAL}$	H	P-value
Design	1440708.54	1		133.03	8.91×10^{-31}
ArtCompliance	1065587.21	1		98.39	3.432×10^{-23}
Design × ArtCompliance	5953.6	1		0.55	0.458
Corrected Total	3887970	359	10830		

C-3-2   Left Coronary Artery Mean Flowrate (QcorMean)

Table C-143 : Levene's test for homogeneity of variance for the data.

Levene's Test of Equality of Error Variances[a]			
Dependent Variable:QcorMean			
F	df1	df2	Sig.
34.195	3	356	.000

Table C-144: SRH test result for QcorMean of COMPLIANCE experiment

Source	SS	df	MS$_{TOTAL}$	H	P-value
Design	250377.88	1		23.12	1.522×10^{-6}
ArtCompliance	2127669.38	1		196.46	1.237×10^{-44}
Design × ArtCompliance	39396.54	1		3.64	0.056
Corrected Total	3887970	359	10830		

C-3-3 Aortic Systolic Pressure (AoPmax)

Table C-145 : The Levene's test for homogeneity of data

Levene's Test of Equality of Error Variances[a]			
Dependent Variable: AoPmax			
F	df1	df2	Sig.
11.113	3	356	.000

Table C-146: SRH test result for AoPmax of COMPLIANCE experiment

Source	SS	df	MS_{TOTAL}	H	P-value
Design	62726.4	1		5.79	0.016
ArtCompliance	62199.511	1		5.74	0.016
Design × ArtCompliance	10627.6	1		0.98	0.322
Corrected Total	3887970	359	10830		

C-3-4 Aortic End-Diastolic Pressure (AoEDP)

Table C-147 : Levene's test for the homogeneity of data variance

Levene's Test of Equality of Error Variances[a]			
Dependent Variable: AoEDP			
F	df1	df2	Sig.
12.034	3	356	.000

Table C-148: The SRH test for AoEDP of COMPLIANCE experiment

Source	SS	df	MS_{TOTAL}	H	P-value
Design	71121.111	1		6.57	0.01
ArtCompliance	2157292.844	1		199.2	3.128×10^{-45}
Design × ArtCompliance	11244.844	1		1.04	0.308
Corrected Total	3887970	359	10830		

C-3-5   Correlation

Table C-149 : The data for correlation between CO and dP

Correlations

			CO	dP
Spearman's rho	CO	Correlation Coefficient	1.000	.684[**]
		Sig. (2-tailed)	.	.000
		N	360	360
	dP	Correlation Coefficient	.684[**]	1.000
		Sig. (2-tailed)	.000	.
		N	360	360

**. Correlation is significant at the 0.01 level (2-tailed).

Table C-150: Correlation result for dP and QcorMean

Correlations

			dP	QcorMean
Spearman's rho	dP	Correlation Coefficient	1.000	.557[**]
		Sig. (2-tailed)	.	.000
		N	360	360
	QcorMean	Correlation Coefficient	.557[**]	1.000
		Sig. (2-tailed)	.000	.
		N	360	360

**. Correlation is significant at the 0.01 level (2-tailed).

C-4   Heart Valve

The results of Heart Valve experiments are divided into two parts, MHV and BioProsthetic.

C-4-1   Mechanical Heart Valve (MHV)

The statistical results of MHV are presented here.

C-4-1-1   Cardiac Output

Table C-151: Levene's test for homogeneity of variance

Levene's Test of Equality of Error Variances[a]			
Dependent Variable: CO			
F	df1	df2	Sig.
27.229	5	534	.000

Table C-152: SRH test for CO

Source	SS	df	MS_{TOTAL}	H	P-value
ArtCompliance	8466024.067	1		347.80	1.275×10^{-77}
DeflationPoint	280436.411	2		11.52	0.003
ArtCompliance × DeflationPoint	236295.811	2		9.71	0.008
Corrected Total	13120000	539	24341.3729		

Table C-153: The rank result from for Deflation Point factor

Response Output	Deflation Point	N	Mean Rank	SumRank	rank
CO	BG	180	256.29	46132.2	2
	BI	180	302.66	54478.8	1
	BJ	180	252.55	45459	3
	Total	540		*k =*	3
				SE =	2093.347

C-4-1-2   Left Coronary Artery Mean Flowrate (QcorMean)

Table C-154: Levene's test for homogeneity of variance

Levene's Test of Equality of Error Variances[a]			
Dependent Variable: QcorMean			
F	df1	df2	Sig.
59.280	5	534	.000

Table C-155: SRH test result for QcorMean

Source	SS	df	MS$_{TOTAL}$	H	P-value
ArtCompliance	9590402.4	1		394.0	1.117×10^{-87}
DeflationPoint	1607569.6	2		66.04	4.56×10^{-15}
ArtCompliance × DeflationPoint	45233.911	2		1.86	0.395
Corrected Total	13120000	539	24341.3729		

Table C-156: Mean Rank result from Kruskal-Wallis test

Response Output	Deflation Point	N	Mean Rank	SumRank	rank
QcorMean	BG	180	222.57	40062.6	3
	BI	180	346.84	62431.2	1
	BJ	180	242.09	43576.2	2
	Total	540		$k =$	3
				$SE =$	2093.347

C-4-1-3   Aortic Systolic Pressure (AoPmax)

Table C-157: Levene's test for homogeneity of variance

Levene's Test of Equality of Error Variances[a]			
Dependent Variable: AoPmax			
F	df1	df2	Sig.
43.646	5	534	.000

Table C-158: SRH test result for AoPmax

Source	SS	df	MS$_{TOTAL}$	H	P-value
ArtCompliance	1818648.6	1		74.71	5.44×10^{-18}
DeflationPoint	1148335.544	2		47.18	5.7×10^{-11}
ArtCompliance × DeflationPoint	176530.9	2		7.25	0.027
Corrected Total	13120000	539	24341.3729		

Table C-159: Mean Rank result from Kruskal-Wallis test

Response Output	Deflation Point	N	Mean Rank	SumRank	rank
AoPmax	BG	180	286.15	51507	2
	BI	180	317.51	57151.8	1
	BJ	180	207.84	37411.2	3
	Total	540		$k =$	3
				$SE =$	2093.347

C-4-1-4　　　Aortic End-Diastolic Pressure (AoEDP)

Table C-160: Levene's test for homogeneity of data

Levene's Test of Equality of Error Variances[a]			
Dependent Variable: AoEDP			
F	df1	df2	Sig.
24.307	5	534	.000

Table C-161: SRH test result for AoEDP

Source	SS	df	MS$_{TOTAL}$	H	P-value
ArtCompliance	9414768.896	1		386.78	4.157×10^{-86}
DeflationPoint	530045.911	2		21.78	1.869×10^{-5}
ArtCompliance × DeflationPoint	25061.97	2		1.03	0.598
Corrected Total	13120000	539	24341.3729		

Table C-162: Mean Rank result from Kruskal-Wallis test

Response Output	Deflation Point	N	Mean Rank	SumRank	rank
AoEDP	BG	180	314.81	56665.8	1
	BI	180	249.04	44827.2	2
	BJ	180	247.65	44577	3
	Total	540		$k =$	3
				$SE =$	2093.347

C-4-1-5　　　Correlation

Table C-163: Correlation test result between dP and CO

Correlations				dP	CO
Spearman's rho	dP	Correlation Coefficient		1.000	.253[**]
		Sig. (2-tailed)		.	.000
		N		540	540
	CO	Correlation Coefficient		.253[**]	1.000
		Sig. (2-tailed)		.000	.
		N		540	540

[**]. Correlation is significant at the 0.01 level (2-tailed).

Table C-164: Correlation test result between

Correlations

			dP	QcorMean
Spearman's rho	dP	Correlation Coefficient	1.000	.447[**]
		Sig. (2-tailed)	.	.000
		N	540	540
	QcorMean	Correlation Coefficient	.447[**]	1.000
		Sig. (2-tailed)	.000	.
		N	540	540

**. Correlation is significant at the 0.01 level (2-tailed).

C-4-2 BioPHV

The statistical results of bio-prosthetic heart valve are presented here.

C-4-2-1   Cardiac Output

Table C-165: Levene's test for homogeneity of variance

Levene's Test of Equality of Error Variances[a]

Dependent Variable: CO

F	df1	df2	Sig.
1.543	5	534	.175

Table C-166: The normality result from Kolmogorov-Smirnov and Shapiro-Wilk test

Kolmogorov-Smirnov & Shapiro-Wilk P-value	BG		BI		BJ	
	K-S	S-W	K-S	S-W	K-S	S-W
C2.5	0.2	0.742	0.2	0.253	0.2	0.138
C1.25	0.2	0.477	0.2	0.046	0.2	0.175

(K-S: Kolmogorov-Smirnov, S-W: Shapiro-Wilk)

Table C-167: ANOVA result for CO of BioPHV experiment. The result was generated using SPSS program

Tests of Between-Subjects Effects

Dependent Variable : CO

Source	Type III Sum of Squares	df	Mean Square	F	Sig.
Corrected Model	1430.501[a]	5	286.100	81.919	.000
Intercept	17035.642	1	17035.642	4877.796	.000
ArtCompliance	828.044	1	828.044	237.093	.000
DeflationPoint	587.847	2	293.923	84.159	.000
ArtCompliance × DeflationPoint	14.610	2	7.305	2.092	.124
Error	1864.988	534	3.492		
Total	20331.131	540			
Corrected Total	3295.489	539			

a. R Squared = .434 (Adjusted R Squared = .429)

Table C-168: Post-hoc TukeyHSD test for CO factor that has three levels

Tukey HSD : Variable = CO

(I) DeflationPoint	(J) DeflationPoint	Mean Difference (I-J)	Std. Error	Sig.	95% Confidence Interval	
					Lower Bound	Upper Bound
BG	BI	1.7811[*]	.19699	.000	1.3181	2.2441
	BJ	2.4778[*]	.19699	.000	2.0149	2.9408
BI	BG	-1.7811[*]	.19699	.000	-2.2441	-1.3181
	BJ	.6967[*]	.19699	.001	.2338	1.1597
BJ	BG	-2.4778[*]	.19699	.000	-2.9408	-2.0149
	BI	-.6967[*]	.19699	.001	-1.1597	-.2338

Based on observed means.

The error term is Mean Square (Error) = 3.492.

*. The mean difference is significant at the .05 level.

C-4-2-2   Left Coronary Artery Mean Flowrate (QcorMean)

Table C-169: Levene's test of homogeneity of variance

Levene's Test of Equality of Error Variances[a]			
Dependent Variable : QcorMean			
F	df1	df2	Sig.
7.951	5	534	.000

Table C-170: SRH test result for QcorMean

Source	SS	df	MS$_{TOTAL}$	H	P-value
ArtCompliance	8052983.585	1		330.84	6.322×10^{-74}
DeflationPoint	3318147.344	2		136.32	2.507×10^{-30}
ArtCompliance × DeflationPoint	62251.181	2		2.56	0.278
Corrected Total	13120000	539	24341.3729		

Table C-171: The rank result of Deflation Point factor

Response Output	Deflation Point	N	Mean Rank	SumRank	rank
QcorMean	BG	180	376.44	67759.2	1
	BI	180	245.82	44247.6	2
	BJ	180	189.23	34061.4	3
	Total	540		$k =$	3
				$SE =$	2093.347

C-4-2-3   Aortic Systolic Pressure (AoPmax)

Table C-172: Levene's test for homogeneity of variance

Levene's Test of Equality of Error Variances[a]			
Dependent Variable: AoPmax			
F	df1	df2	Sig.
6.559	5	534	.000

Table C-173: SRH test result for AoPmax

Source	SS	df	MS$_{TOTAL}$	H	P-value
ArtCompliance	3734.074	1		0.15	0.695
DeflationPoint	7154452.3	2		293.92	1.5×10^{-64}
ArtCompliance × DeflationPoint	67936.604	2		2.79	0.247
Corrected Total	13120000	539	24341.3729		

Table C-174: The rank result for each level of Deflation Point

Response Output	Deflation Point	N	Mean Rank	SumRank	rank
AoPmax	BG	180	425.33	76559.4	1
	BI	180	236.64	42595.2	2
	BJ	180	149.53	26915.4	3
	Total	540		$k =$	3
				$SE =$	2093.347

C-4-2-4   Aortic End-Diastolic Pressure (AoEDP)

Table C-175: The Levene's test of homogeneity of variance

Levene's Test of Equality of Error Variances[a]			
Dependent Variable: AoEDP			
F	df1	df2	Sig.
42.794	5	534	.000

Table C-176: SRH test result for AoEDP

Source	SS	df	MS_{TOTAL}	H	P-value
ArtCompliance	6655560.185	1		273.43	2.034×10^{-61}
DeflationPoint	446518.633	2		18.34	01×10^{-4}
ArtCompliance × DeflationPoint	774469.915	2		31.82	1.233×10^{-7}
Corrected Total	13120000	539	24341.37		

Table C-177: Mean Rank result from Kruskal-Wallis test

Response Output	Deflation Point	N	Mean Rank	SumRank	rank
AoEDP	BG	180	275.81	49645.8	2
	BI	180	232.93	41927.4	3
	BJ	180	302.76	54496.8	1
	Total	540		$k =$	3
				$SE =$	2093.347

C-4-2-5   Correlation

Table C-178: Correlation test result between dP and CO

Correlations		CO	dP
CO	Pearson Correlation	1	.179[**]
	Sig. (2-tailed)		.000
	N	540	540
dP	Pearson Correlation	.179[**]	1
	Sig. (2-tailed)	.000	
	N	540	540

[**]. Correlation is significant at the 0.01 level (2-tailed).

Table C-179: Spearman's correlation test result for dP and QcorMean

Correlations

			dP	QcorMean
Spearman's rho	dP	Correlation Coefficient	1.000	.177[**]
		Sig. (2-tailed)	.	.000
		N	540	540
	QcorMean	Correlation Coefficient	.177[**]	1.000
		Sig. (2-tailed)	.000	.
		N	540	540

**. Correlation is significant at the 0.01 level (2-tailed).

APPENDIX D – Rapid Prototyping Machine

D-1   Types of machines

The rapid prototype machines used to construct the rigid body balloon pump are

1) Dimension Elite by Stratasys Inc. (MN, USA) (refer to Figure D-142) and

 2) Viper si2 SLA System by 3D Systems Inc. (SC, USA) (refer to Figure D-143).

The main difference between those machines lies in the material used to construct the model. The Dimension Elite (Stratasys Inc., USA) uses ABS*plus* which is a production-grade thermoplastic, and by heating the material in an extrusion head, thin layers are deposited on a modelling base gradually forming the 3D model. This is what termed as Fused Deposited Molding (FDM) technology.

Figure D-142: A rapid prototyping machine (Dimension Elite by Stratasys Inc.) using Fused Deposition Modeling (FDM®) technology.

The Viper si2 SLA System machine (3D System Inc., USA) uses an UV-curable photopolymer resin (Accura® 60). A laser ray is beamed onto a container filled with the UV-curable photopolymer, and that solidifies the photopolymer fluid. The thin layer is formed layer by layer.

The straight body (SB) balloon pump was made using the rapid prototyping machine FDM. Although the FDM material offers a good structural rigidity and strength, its porous body was

unsuitable. To ensure no Helium gas escapes to surrounding air during balloon activation the body was coated with several layers of super glue, primer paint and lacquer in that order. The coated balloon pump body was stronger, waterproof and gas impermeable.

Figure D-143: A rapid prototyping machine (VIPER si2™ SLA® System) to manufacture transparent housing body for balloon pump prototype.

D-2   Technical Drawing of Balloon Pump Prototype

The technical drawings of the CIMS balloon pump: standard body (SB) and compliant body (CB) are illustrated in Figure D-144 and Figure D-145.
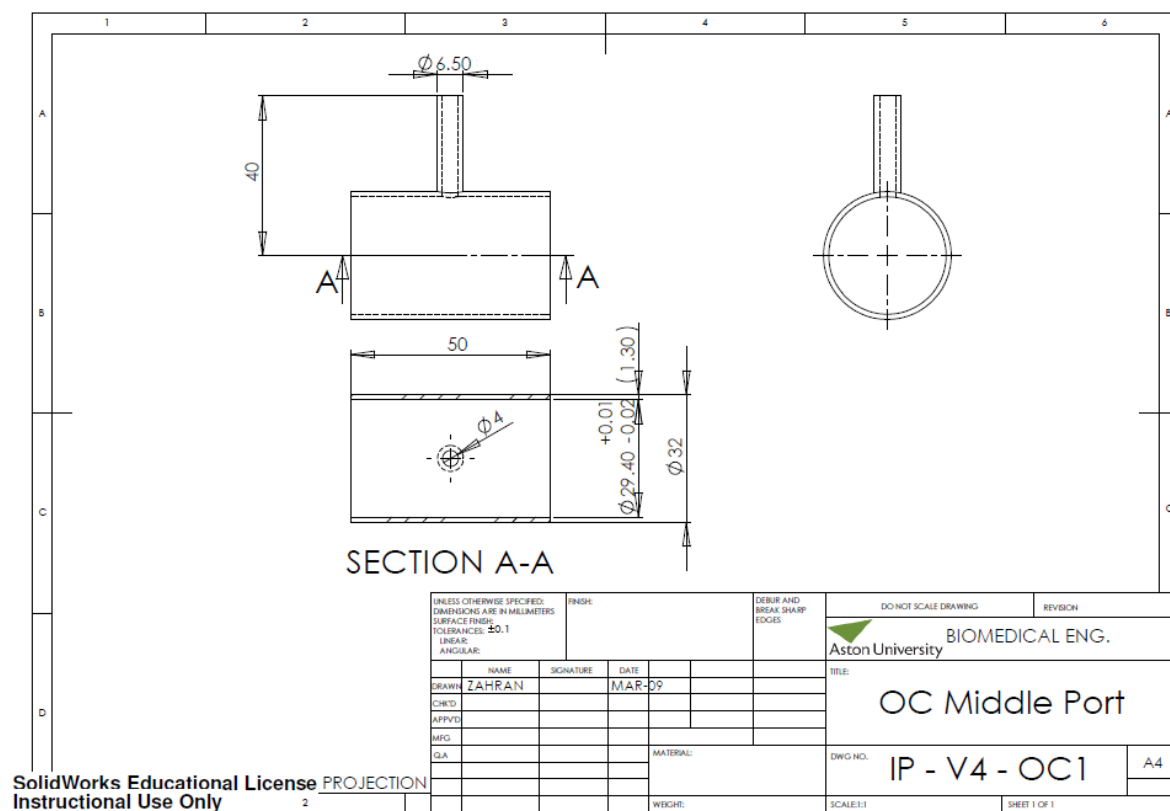
Figure D-144: Technical drawing for SB type balloon pump. OC : Outer Case
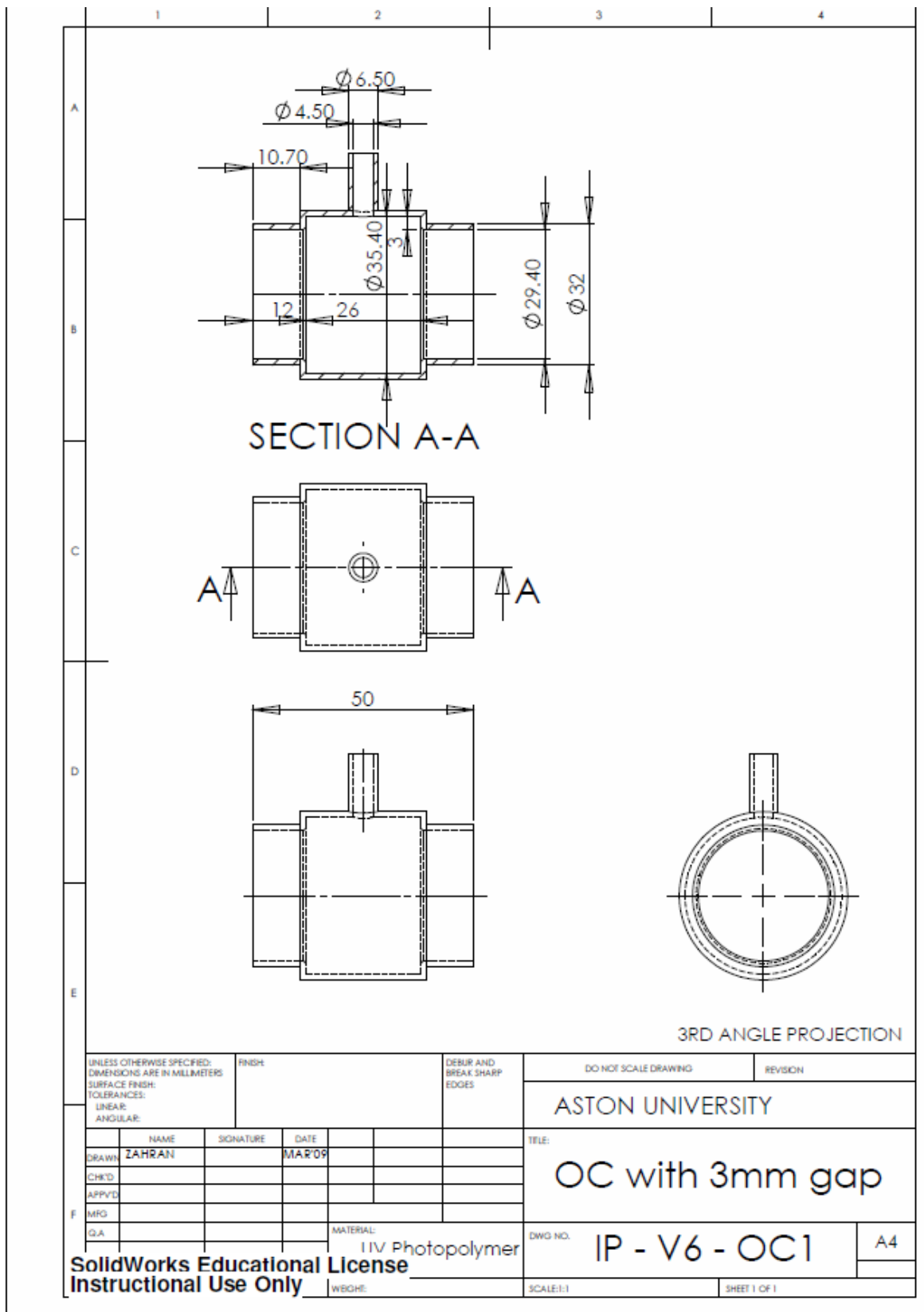
Figure D-145: Technical drawing for CB type balloon pump

D-3   Compliance Test Procedure

Blood vessel compliance is an important characteristic in arterial haemodynamics. A high compliance blood vessel expands more during systole, thus able to store more blood which later flows to peripheral arteries in diastole. A compliant blood vessel also keeps the pulse pressure moderate. Balloon pump compliance was measured by looking at the ratio between volumetric expansion and changes in pressure. The formula is presented as per Eq. 1.14, rewritten as:

$$C = \frac{\Delta V}{\Delta P} = \frac{dV}{dP} \ [\frac{mL}{mmHg}]$$

D −1

Three consecutive tests to determine the static compliance of the balloon pump were carried out by computing the reciprocal of the ratio between internal pressure increases against additional water injected into the balloon pump. The compliant body balloon pump was fixed between two aluminum blocks, each with a tap hole for a luer connector as per Figure D-146. A disposable pressure transducer[47] was connected to the luer connector at one end, while the other end was for a syringe. Distilled water was inserted into the centre of the balloon pump approximately 25 mL. After the pressure in the balloon pump was set to 0 mmHg by using a cable checker, then by using a syringe, one mL of water was injected into the rig and the pressure was recorded using National Instruments DAQ hardware, NI cDAQ-9172 and NI 9723. A simple Labview ™ program was used to display and record the pressure increase. Three consecutive tests were done. The text file of the pressure data was then opened and manipulated using Microsoft Office Excel spreadsheet program. The pressure increase was plotted against volumetric increase, and the slope was computed. The slope value is the elastance of the balloon pump; the SI unit is mmHg/mL. The compliance value can be easily calculated by getting the reciprocal value of the elastance:

$$C = \frac{1}{Elastance}$$

D − 2

---

[47] Similar model to the one used in the mock circulatory loop
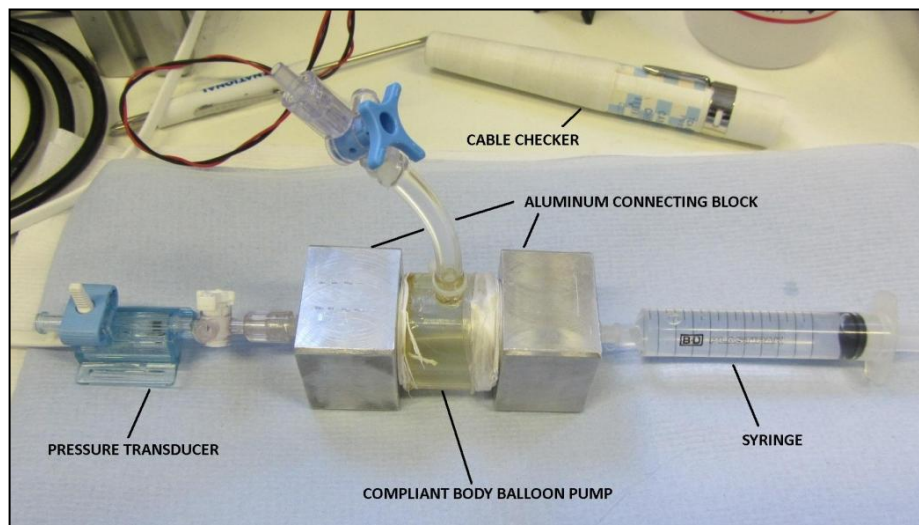
Figure D-146: The setting up for compliance testing for the CIMS balloon pump prototype

The static compliance value computed for the Compliant Body type balloon pump was 0.11 mmHg/mL.

There was another type of test conducted to determine the compliance of the CIMS balloon pump (SB & CB). A tube and a pressure transducer are connected to the balloon pump as illustrated in Figure D-147. A fixed amount of water of 20 mL was inserted using syringe for several times. Before and after insertion, the water column height and pressure were recorded, and then the amount of water raised was calculated. The results for both SB and CB are tabulated in Table D-180 and Table D-181.

Figure D-147: Balloon pump compliance test setting

Table D-180: Pressure of water column and increment of water height for SB type balloon pump

SB	P1	28.3	35.4	42.4	49.4	56.6
	P2	35.4	42.4	49.4	56.6	63.9
	ΔP	7.1	7	7	7.2	7.3
	ΔL	98	98	98	98	98

Table D-181: Pressure of water column and increment of water height for CB type balloon pump

CB	P1	13	20.3	27.1	36	43	49	56	65.5	72	79
	P2	20.3	27	34	43	50	56	63	72	79	85
	ΔP	7.3	6.7	6.9	7	7	7	7	6.5	7	6
	ΔL	98	96.5	96	96	96	96	95	95	94.5	94

In Figure D-148, the water column pressure is plotted against water column height. Compared to when SB type balloon pump, the CB type balloon pump exhibited different trend. The amount of water inserted is fixed at 20 mL, yet the height increment decreased over the increased pressure. This shows that the silicone membrane expanded with increasing pressure, which in this experiment, reached up to 85 mmHg. Compared this to the SB type balloon pump which exhibited no differences as per expected. This confirms the above experiment that CB type balloon pump

has an internal compliance with incorporation of flexible silicone membrane and the CB balloon pump design.
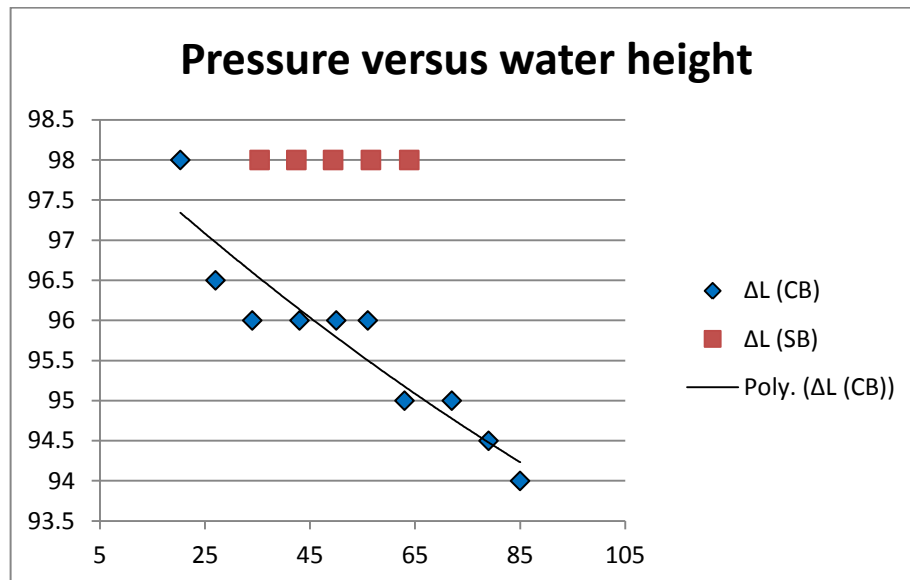
Figure D-148: Plot of water increment against water column pressure

APPENDIX E – Haemodynamics of the CIMS Balloon Pump

Raw data and statistical results of analysed data are presented here.

E – 1   Flow Visualisation

60 beats/min

Table E-182: Frame count for Non-Assisted and Assisted at 60 beats/min

60 bpm		LED On Period	Δt	Valve Open Period
Non-assisted	1	0.50	0.30	0.27
	2	0.50	0.30	0.30
	3	0.50	0.30	0.33
	4	0.50	0.30	0.33
	5	0.50	0.30	0.30
	6	0.50	0.30	0.30
	7	0.50	0.30	0.30
	8	0.50	0.30	0.30
	9	0.50	0.30	0.30
	10	0.50	0.30	0.30
	Mean	0.50	0.30	0.30
	SD	0.000	0.000	0.019
Assisted	1	0.50	0.17	0.43
	2	0.50	0.23	0.37
	3	0.50	0.20	0.40
	4	0.50	0.17	0.43
	5	0.50	0.27	0.33
	6	0.50	0.23	0.37
	7	0.50	0.17	0.40
	8	0.50	0.17	0.43
	9	0.50	0.23	0.37
	10	0.50	0.20	0.37
	Mean	0.50	0.20	0.39
	SD	0.000	0.037	0.035

Table E-183: Mann-Whitney test result for 60 beats/min experiment

	HR60_DeltaT	HR60_ValveOpeningT
Mann-Whitney U	.000	1.000
Wilcoxon W	55.000	56.000
Z	-4.065	-3.813
Asymp. Sig. (2-tailed)	.000	.000
Exact Sig. [2*(1-tailed Sig.)]	.000[a]	.000

54 beats/min

Table E-184: Frame count for 54 beats/min experiment

54 bpm		LED On Period	DeltaT	Valve Open Period
Non-assisted	1	0.50	0.33	0.27
	2	0.50	0.33	0.27
	3	0.50	0.33	0.30
	4	0.57	0.33	0.30
	5	0.57	0.37	0.27
	6	0.53	0.33	0.30
	7	0.53	0.33	0.30
	8	0.53	0.33	0.33
	9	0.60	0.37	0.30
	10	0.60	0.37	0.30
	Mean	0.54	0.34	0.29
	SD	0.039	0.016	0.021
Assisted	1	0.57	0.20	0.40
	2	0.60	0.23	0.40
	3	0.57	0.27	0.37
	4	0.57	0.23	0.40
	5	0.53	0.23	0.40
	6	0.53	0.27	0.37
	7	0.57	0.27	0.37
	8	0.60	0.27	0.40
	9	0.60	0.27	0.37
	10	0.53	0.23	0.37
	Mean	0.57	0.25	0.38
	SD	0.027	0.023	0.018

Table E- 185: Independent t-test for 54 beats/min experiment

	HR54_DeltaT	HR54_ValveOpeningT
Mann-Whitney U	.000	.000
Wilcoxon W	55.000	55.000
Z	-3.914	-3.897
Asymp. Sig. (2-tailed)	.000	.000
Exact Sig. [2*(1-tailed Sig.)]	.000[a]	.000[a]

APPENDIX F – Student T-test Result

The Student t-test results of all combinations carried out for this study. The * sign denotes p < 0.05.

F-1   TIMING EXPERIMENT

CO	DEFLATION											
INFLATION	G			H			I			J		
	1	2	3	1	2	3	1	2	3	1	2	3
A	*	*	*	*	*	*	*	*	*	*	*	*
B	*	*	*	*	*	*	*	*	*	*	*	*
C	*	*	*	*	*	*	*	*	*	*	*	*

*: p < 0.05

QcorMean	DEFLATION											
INFLATION	G			H			I			J		
	1	2	3	1	2	3	1	2	3	1	2	3
A	*	*	*	*	*	*	*	*	*	*	*	*
B	*	*	*	*	*	*	*	*	*	*	*	*
C	*	*	*	*	*	*	*	*	*	*	*	*

*: p < 0.05

AoPmax	DEFLATION											
INFLATION	G			H			I			J		
	1	2	3	1	2	3	1	2	3	1	2	3
A	0.09	0.41	0.39	0.3	0.13	0.08	*	*	0.32	*	*	*
B	*	*	*	*	*	0.18	*	0.1	*	*	*	*
C	*	0.15	*	*	0.23	0.26	0.12	*	*	*	*	*

*: $p < 0.05$

AoEDP	DEFLATION											
INFLATION	G			H			I			J		
	1	2	3	1	2	3	1	2	3	1	2	3
A	*	*	*	*	*	*	*	*	0.27	*	*	0.33
B	*	*	*	*	*	*	*	*	*	*	0.24	*
C	*	*	*	*	*	*	*	*	*	*	*	*

*: $p < 0.05$

F-2 Helium Gas Volume

CO	GasVol								
Device Design	20 mL			25 mL			30 mL		
	1	2	3	1	2	3	1	2	3
Straight Body	*	*	*	*	*	*	*	*	*
Compliant Body	*	*	*	*	*	*	*	*	*

*: $p < 0.05$

QcorMean	GasVol								
Device Design	20 mL			25 mL			30 mL		
	1	2	3	1	2	3	1	2	3
Straight Body	*	*	*	*	*	*	*	*	*
Compliant Body	*	*	*	*	*	*	*	*	*

*: $p < 0.05$

AoPmax	GasVol								
Device Design	20 mL			25 mL			30 mL		
	1	2	3	1	2	3	1	2	3
Straight Body	0.32	*	0.32	0.15	*	*	0.06	0.12	*
Compliant Body	*	*	*	0.25	*	*	0.14	*	0.09

*: $p < 0.05$

AoEDP	GasVol								
Device Design	20 mL			25 mL			30 mL		
	1	2	3	1	2	3	1	2	3
Straight Body	*	*	0.10	*	*	*	*	*	*
Compliant Body	*	0.18	0.18	*	0.19	*	0.30	*	0.07

*: $p < 0.05$

F-3   COMPLIANCE

CO	Balloon Pump Stiffness					
Arterial Compliance	Straight Body			Compliant Body		
	1	2	3	1	2	3
Soft (C2.5)	*	*	*	*	*	*
Stiff (C1.25)	*	*	*	*	*	*

*: $p < 0.05$

QcorMean	Balloon Pump Stiffness					
Arterial Compliance	Straight Body			Compliant Body		
	1	2	3	1	2	3
Soft (C2.5)	*	*	*	*	*	*
Stiff (C1.25)	*	*	*	*	*	*

*: $p < 0.05$

AoPmax	Balloon Pump Stiffness					
Arterial	Straight Body			Compliant Body		
Compliance	1	2	3	1	2	3
Soft (C2.5)	0.09	*	*	0.06	0.11	*
Stiff (C1.25)	*	0.05	*	0.37	0.11	*

*: $p < 0.05$

AoEDP	Balloon Pump Stiffness					
Arterial	Straight Body			Compliant Body		
Compliance	1	2	3	1	2	3
Soft (C2.5)	*	0.11	*	0.13	*	*
Stiff (C1.25)	*	*	*	*	*	*

*: $p < 0.05$

F-4   Heart Valve

F-4-1   Mechanical Heart Valve

CO	GasVol								
Device Design	Early (G)			Safe (I)			Late (J)		
	1	2	3	1	2	3	1	2	3
Soft (C2.5)	*	*	*	*	*	*	*	*	*
Stiff (C1.25)	*	*	*	*	*	*	*	*	*

*: $p < 0.05$

QcorMean	GasVol								
Device Design	Early (G)			Safe (I)			Late (J)		
	1	2	3	1	2	3	1	2	3
Soft (C2.5)	*	*	*	*	*	*	*	*	*
Stiff (C1.25)	*	*	*	*	*	*	*	*	*

*: $p < 0.05$

AoPmax	GasVol								
Device Design	Early (G)			Safe (I)			Late (J)		
	1	2	3	1	2	3	1	2	3
Soft (C2.5)	0.22	*	*	*	*	*	0.06	*	*
Stiff (C1.25)	*	*	*	*	*	*	0.13	*	*

*: $p < 0.05$

AoEDP	GasVol								
Device Design	Early (G)			Safe (I)			Late (J)		
	1	2	3	1	2	3	1	2	3
Soft (C2.5)	*	*	*	*	*	*	*	*	*
Stiff (C1.25)	*	*	*	*	*	*	*	*	*

*: $p < 0.05$

F-4-2 BioProsthetic Heart Valve

CO	GasVol								
Device Design	Early (G)			Safe (I)			Late (J)		
	1	2	3	1	2	3	1	2	3
Soft (C2.5)	*	*	*	*	*	*	*	*	*
Stiff (C1.25)	*	*	*	*	*	*	*	*	*

*: $p < 0.05$

QcorMean	GasVol								
Device Design	Early (G)			Safe (I)			Late (J)		
	1	2	3	1	2	3	1	2	3
Soft (C2.5)	*	*	*	*	*	*	*	*	*
Stiff (C1.25)	*	*	*	*	*	*	*	*	*

*: $p < 0.05$

AoPmax	GasVol								
Device Design	Early (G)			Safe (I)			Late (J)		
	1	2	3	1	2	3	1	2	3
Soft (C2.5)	0.31	*	*	*	*	*	*	*	*
Stiff (C1.25)	*	*	*	*	*	*	*	*	*

*: p < 0.05

AoEDP	GasVol								
Device Design	Early (G)			Safe (I)			Late (J)		
	1	2	3	1	2	3	1	2	3
Soft (C2.5)	*	*	*	*	*	*	*	*	*
Stiff (C1.25)	*	*	*	*	*	*	*	*	*

*: p < 0.05